

University of Kentucky

UKnowledge

Theses and Dissertations--Microbiology,
Immunology, and Molecular Genetics

Microbiology, Immunology, and Molecular
Genetics

2012

PRION CHARACTERIZATION USING CELL BASED APPROACHES

Vadim Khaychuk

University of Kentucky, vkhaychuk@gmail.com

[Right click to open a feedback form in a new tab to let us know how this document benefits you.](#)

Recommended Citation

Khaychuk, Vadim, "PRION CHARACTERIZATION USING CELL BASED APPROACHES" (2012). *Theses and Dissertations--Microbiology, Immunology, and Molecular Genetics*. 2.

https://uknowledge.uky.edu/microbio_etds/2

This Doctoral Dissertation is brought to you for free and open access by the Microbiology, Immunology, and Molecular Genetics at UKnowledge. It has been accepted for inclusion in Theses and Dissertations--Microbiology, Immunology, and Molecular Genetics by an authorized administrator of UKnowledge. For more information, please contact UKnowledge@lsv.uky.edu.

STUDENT AGREEMENT:

I represent that my thesis or dissertation and abstract are my original work. Proper attribution has been given to all outside sources. I understand that I am solely responsible for obtaining any needed copyright permissions. I have obtained and attached hereto needed written permission statements(s) from the owner(s) of each third-party copyrighted matter to be included in my work, allowing electronic distribution (if such use is not permitted by the fair use doctrine).

I hereby grant to The University of Kentucky and its agents the non-exclusive license to archive and make accessible my work in whole or in part in all forms of media, now or hereafter known. I agree that the document mentioned above may be made available immediately for worldwide access unless a preapproved embargo applies.

I retain all other ownership rights to the copyright of my work. I also retain the right to use in future works (such as articles or books) all or part of my work. I understand that I am free to register the copyright to my work.

REVIEW, APPROVAL AND ACCEPTANCE

The document mentioned above has been reviewed and accepted by the student's advisor, on behalf of the advisory committee, and by the Director of Graduate Studies (DGS), on behalf of the program; we verify that this is the final, approved version of the student's dissertation including all changes required by the advisory committee. The undersigned agree to abide by the statements above.

Vadim Khaychuk, Student

Dr. Glenn C. Telling, Major Professor

Dr. Charlotte S. Kaetzel, Director of Graduate Studies

PRION CHARACTERIZATION USING CELL BASED APPROACHES

Dissertation

A dissertation submitted in partial fulfillment of the requirements for the degree of
Doctor of Philosophy in the College of Medicine at the University of Kentucky

By

Vadim Khaychuk

Lexington, Kentucky

Director: Glenn C. Telling, Ph.D.

Professor of Microbiology, Immunology, and Molecular Genetics

Lexington, Kentucky

Copyright © Vadim Khaychuk 2012

ABSTRACT OF DISSERTATION

PRION CHARACTERIZATION USING CELL BASED APPROACHES

Prions are the causative agents of a group of lethal, neurodegenerative conditions that include sheep scrapie, bovine spongiform encephalopathy (BSE), and human Creutzfeldt-Jakob disease (CJD). Prions are derived from the conversion of a normal, primarily alpha-helical, cellular prion protein (PrP^C), to an infectious, beta sheet-rich conformer (PrP^{Sc}). Many unresolved issues surround the process of PrP conversion, and we know very little about cellular responses to these unique pathogens. Our lack of knowledge relates, in part, to the difficulty of infecting cells in vitro with prions. While expression of PrP^C is an absolute requirement for prion propagation, I show here that not all cells that express PrP^C are capable of propagating PrP^{Sc}. The goal of this thesis is to understand the role that host factors play in sustaining prion infection and to develop systems in which the cellular response to prion infection can be assessed. We hypothesize that cellular permissiveness to prion infectivity is co-dependent on unidentified additional cellular factors. To study the role of PrP^C expression in susceptibility to prion infectivity, and identify these cofactors in cell culture, we utilized cells which fail to express endogenous PrP^C, but become susceptible to prions following stable expression of PrP^C. Following transfection of a species specific PrP expression construct and isolation of single cell clones, we assessed PrP expression and susceptibility to prion infectivity by measuring accumulation of protease resistant PrP^{Sc}. Differential gene expression studies suggest significant transcriptional differences between susceptible and resistant clones. Using three independent gene expression databases our analyses suggest that the resistant transcriptional profile favors cell division/cycle and chromosomal regulation pathways, while the sensitive transcriptional profile is involved in protein homeostasis and quality control. The results of these studies will not only lead to a greater understanding of PrP cell biology and the mechanisms of prion pathogenesis, but should ultimately lead to sensitive and expedient methods for detecting and characterizing prion infectivity from a wide range of sources.

KEYWORDS: Prions; Cellular Permissiveness; Cellular PrP^C; Protease Resistant PrP^{Sc}; Transcriptional Differences

Vadim Khaychuk

March 16, 2012

PRION CHARACTERIZATION USING CELL BASED APPROACHES

By

Vadim Khaychuk

Glenn C. Telling, Ph.D.
Director of Dissertation

Charlotte S. Kaetzel, Ph.D.
Director of Graduate Studies

March 16, 2012
Date

DEDICATION

This dissertation is dedicated to my parents, brother and grandparents (Rita and Slava Khaychuk, Felix, Masha and David Khaychuk), who instilled in me the moral virtues of hard work and diligence, and who were unequivocally supportive throughout my scientific journey.

In Loving Memory Of My Dear Cousin Anton Khlevitt
1982-201

ACKNOWLEDGEMENTS

In completion of my graduate school career, I would like to express sincere gratefulness and appreciation to the many people helping me along the way. First and foremost, I would like to thank my mentor, Dr. Glenn C. Telling, for all of his guidance towards the completion of my project and keeping me focused on the primary task. Furthermore, I would like to thank him for always pushing me to achieve my best. Throughout this process, Dr. Telling became not just a mentor but also a great friend. I would also like to acknowledge and thank my committee; Dr. Alan Kaplan, Dr. Beth Garvy, Dr. Chongsuk Ryou and Dr. Hansruedi Büeler, for their dedication and commitment in helping me complete my graduate school career. I greatly appreciate the effort that was taken by Dr. Telling and my committee to help me seamlessly integrate into the graduate program upon my transfer from University of Rochester. Throughout my graduate career I have had the pleasure to work alongside wonderful lab members that I want to thank and acknowledge. To all of the Telling lab members (past and present), thank you for providing me with great friendship and assistance when I needed it. Specifically, I would like to thank Jifeng Bian, Hae-Eun Kang and Sehun Kim, Eri Saijo and Yuri Klyachkin for their friendship, technical support during critical experiments and providing me with the much-needed feedback about my research throughout the years. I would like to thank Dr. Arnold Stromberg, Dr. Peter Huggins, Dr. Anthony Athippozhy, Dr. Nigel Cooper and Xiaohong Li (Xiao) for dedicating the time, energy and effort to technically support and train me to conduct the microarray gene expression studies.

Finally, I want to thank my family and friends for the support they have provided me throughout my graduate school career. To my parents and grandparents, I am eternally grateful for their support in my career choice and willingness to try to understand my research. I would like to thank them for everything they sacrificed to leave our home country of Ukraine to bring my brother and I to this country, which ultimately provided me with this opportunity to succeed and become the person I am today. To my brother, Felix and his family, thank you for all of your support and friendship. Lastly, I would like to thank my dearest friends Vlad and Genna Mirochnik, Ilya Vaynshteyn, Alex Nesterenko and Irene Chernyak for always being there for me, no matter what.

TABLE OF CONTENTS

Acknowledgements.....	iii
List of Tables.....	vi
List of Figures.....	vii
Abbreviations.....	viii
Chapter 1: General Introduction to Prion Biology	
Introduction.....	1
Section I: General Introduction to Prion Biology.....	1
Section II: Experimental Approaches To Analyze Prions.....	27
Section III: PrP Interacting Molecules.....	38
Dissertation research.....	70
Chapter 2: Materials and methods.....	72
Chapter 3: Characterization of Prion Strains in Cell Culture Systems	
Introduction.....	93
Results.....	99
Section I: Prion Species Barriers, Interference and the Attempt to Propagate of Chronic Wasting Disease (CWD) in Cell Culture.....	99
Section II: Replication of Biologically Cloned Hyper (HY) and Drowsy (DY) Hamster-Adapted TME Prion Strains in Cell Culture.....	120
Discussion.....	131
Chapter 4: Identification Of Host Factors That Confer Susceptibility to Prions	
Introduction.....	138
Results.....	147
Section I: Identification and characterization of susceptible/resistant RK13 clones expressing murine PrPC (RKM).....	147
Section II The Identification of CWD susceptible and resistant RK13-Deer PrPC (RKD) clones.....	172
Discussion.....	193
Chapter 5: Discussion and Future Directions.....	256
References.....	274
Vita.....	330

LIST OF TABLES

Table 1.1, Human and animal prion diseases.....	8
Table 1.2, Cell culture models for prion replication <i>in vitro</i>	33
Table 1.3, Prion protein interacting molecules.....	56
Table 3.1, Prion strains used for cell culture infectivity analysis.....	104
Table 4.1, Summary of RML prion replication amongst cloned RKM cells using three distinct assays for assessment.....	155
Table 4.2, Transcripts identified by RDA in the prion susceptible RKM 7 clone.....	166
Table 4.3, Bioinformatic prediction analysis of RDA identified hypothetical proteins..	167
Table 4.4, Transcripts identified by RDA in the prion resistant RKM 78 clone.....	171
Table 4.5, Summaries of identified and annotated genes lists by microarray experiments.....	184
Table 4.6, Differentially down regulated gene expression in RKD-R cells as compared to the RKD-S cells.....	220
Table 4.7, Differentially up regulated gene expression in RKD-R cells as compared to the RKD-S cells.....	239
Table 4.8, Prion Disease Database (PDDb) cross-referenced RKD-R down regulated genes associated with published prion literature.....	242
Table 4.9, Prion Disease Database (PDDb) cross-referenced RKD-R upregulated genes associated with published prion literature.....	244
Table 4.10, Extrapolated gene list grouped by functional association.....	245

LIST OF FIGURES

Figure 1.1, Schematic representation of the human cellular prion protein (PrP ^C).....	13
Figure 1.2, Intracellular trafficking of PrP ^C	15
Figure 1.3, Models for prion replication.....	21
Figure 1.4, Schematic representation of the protein X hypothesis.....	42
Figure 1.5, Molecules associated with PrP interaction in the extracellular/plasma membrane space.....	50
Figure 1.6, Molecules associated with PrP interaction within intracellular space of the cell.....	67
Figure 3.1, The prion species barrier and PrP interference.....	97
Figure 3.2, Stable expression of cervid PrP ^C in the N2a cell culture model.....	102
Figure 3.3, Mouse N2a cells expressing cervid PrP ^C are not permissive to CWD prions.....	105
Figure 3.4, Characterization of CWD replication in the RK13 cell culture system.....	110
Figure 3.5, Quantification of CWD infectivity using the RKE cell line in a Cervid Prion Cell Assay (CPCA).....	114
Figure 3.6, Stable expression of cervid PrP ^C and assessment of CWD replication in HEK 293A Cells.....	118
Figure 3.7, Characterization of HY and DY prions in cell culture.....	123
Figure 3.8, Characterization of HY and DY prion replication cell-lifting assay.....	125
Figure 3.9, Transient replication of HY prions in RK13Gag-SHa-PrP ^C cells.....	129
Figure 4.1, RKM clonal variability towards PrP ^C expression and RML susceptibility.....	151
Figure 4.2, Accumulation of PK-resistant PrP and PrP ^C surface expression in RML susceptible and resistant RKM clones	157
Figure 4.3, RDA for the identification of differentially expressed genes in RKM subclones.....	160
Figure 4.4, Molecular characterizations of RKD subclones.....	175
Figure 4.5, Microarray statistical data analysis of differential gene expression in the 5E9 RKD CWD prion subclones	181
Figure 4.6, Bioinformatic analysis of the 1,375 RKD-R differentially expressed genes.....	188
Figure 4.7, Autophagy and PrP ^{Sc} Replication.....	218
Figure 4.8, RKD differentially expressed genes targeted for cell-surface presentation and intracellular transport.....	237
Figure 5.1 Generating a prion permissive susceptible cell line.....	271

Abbreviations

AD	Alzheimer's Disease
ADAM	A Disintegrin And Metalloproteinase
ALS	Amyotrophic Lateral Sclerosis
APLP	Amyloid Precursor Like Protein
AVs	Autophagic Vacuoles
BCA	Bicinchoninic Acid
Bcl-2	B-Cell CLL/Lymphoma Protein-2
BCIP	5-Bromo-4-Chloro-3'-Indolyphosphate p-Toluidine Salt
BH	Brain Homogenate
CerPrP ^{Sc}	Chronic Wasting Disease Associated Cervid Prion Protein Isoform
BSE	Bovine Spongiform Encephalopathy
CCT3	Chaperonin-Containing TCP-1 Subunit
CD	Circular Dichroism Spectroscopy
CerPrP ^C	Cervid Cellular Prion Protein
CerPrP ^{Sc}	Cervid-CWD Associated Isoform Of The Prion Protein
CFCA	Cell-Free Conversion Assay
CJD	Creutzfeldt Jacob disease
Ck2	Casein Kinase II
CLB	Cold Lysis Buffer
Co-IP	Co-immuno precipitation
CMA	Chaperone-Mediated Autophagy
CPCA	Cervid Prion Cell Assay
CSF	Cerebrospinal Fluid
CWD	Chronic Wasting Disease
DGC	Dystrophin-Glycoprotein Complex
DMEM	Dulbecco's Modified Eagle Medium
DNA	Deoxyribonucleic acid
dpi	Days Post Infection
DRM	Detergent Resistant Microdomain
DY	Drowsy Prion strain
EGF	Epidermal Growth Factor
ELISA	Enzyme Linked Immuno-Sorbent Assay
EM	Electron Microscopy
ER	Endoplasmic Reticulum
ESCRT	Endosomal Sorting Complex Required for Transport
EUE	Exotic Ungulate Spongiform Encephalopathy
FBS	Fetal Bovine Serum
fCJD	Familial Creutzfeldt Jacob disease
FCS	Fetal Calf Serum
FFI	Fatal Familial Insomnia
FGF	Fibroblast Growth Factor
FSE	Feline Spongiform Encephalopathy
GAG	Glycosaminoglycan
GFAP	Glial Fibrillary Acidic Protein

GITC	Guanidinium Thiocyanate
Grb2	Growth Factor Receptor-Bound Protein 2
GSS	Gerstmann-Straussler-Scheinker disease
HD	Huntington's Disease
HEK293	Human Embryonic Kidney cells
HIV	Human Immunodeficiency Virus
HMM	High Molecular Mass
Hsp	Heat Shock Protein
HSPG	Heparin Sulphate Proteoglycans
HuPrP	Human PrP ^C
IC	Intracerebrally Injection
HY	Hyper Prion Strain
iCJD	Iatrogenic Creutzfeldt Jacob disease
IGSF	Immunoglobulin Super Family
ITC	Isothermal Titration Calorimetry
LN	Laminin
LR	Mature 37-kDa/67-kDa Laminin Receptor
LRP	37-kDa-Laminin Precursor
mAb	Monoclonal Antibody
MHu2M	Chimeric PrP ^C (Human Sequence 96-167aa)
MMP	Matrix Metalloproteinase
MOI	Multiplicity Of Infection
mSCA	Modified-Scrapie Cell Assay
MVB	Multivesicular Bodies
NA	Nucleic Acid
N2a	Neuroblastoma 2a Cell line
NBT	Nitro-Blue Tetrazolium Chloride
NCAM	Neuronal Adhesion Molecule
NCBI	National Center for Biotechnology Information
nNOS	Nitric Oxide Synthase
NGB	Neuroglobin
NRAGE	Neurotrophin Receptor-Interacting MAGE Homolog
Nrf2	Nuclear Factor Erythroid 2-Like
ORF	Open Reading Frame
PBS	Phosphate Buffered Saline
PCR	Polymerase Chain Reaction
PD ¹	Parkinson's Disease
PD ²	Pick's Disease
PDGF	Platelet-Derived Growth Factor
Pint1	Prion Interactor-1
PIPLC	Phosphatidylinositol-Specific Phospholipase C
PK	Proteinase K
PLG	Plasminogen
PM	Plasma Membrane
PMCA	Protein Misfolded Cyclic Amplification
PMSF	Phenyl Methyl Sulfonyl Fluoride

POPG	1-palmitoyl-2-oleoylphosphatidylglycerol
PR	Retroviral Protease (<i>pro</i> ORF)
PrP	Prion Protein
PrP ^C	Cellular Isoform of the Prion Protein
PrP ^{Sc}	Disease-Associated Isoform of the Prion Protein
QuIC	Quacking-Induced Conversion Assay
Rab	RAS-Associated Protein
RDA	Representational Difference Analysis
RK13	Rabbit Kidney Epithelial cells
RML	Rocky Mountain Lab Strain of Mouse-Adapted Scrapie
RMA	Robust Multichip Average
RNA	Ribonucleic acid
rPMCA	Recombinant Protein Misfolding Cyclical Amplification
rPrP	Recombinant Prion Protein
RT-QuIC	Real-Time Quacking-Induced Conversion Assay
SCA	Scrapie Cell Assay
SHaPrP ^C	Syrian Hamster Cellular Prion Protein
SHa-TME	Syrian Hamster-Adapted Transmissible Mink Encephalopathy
SPR	Surface Plasmon Resonance
STI1	Stress Inducible Phosphoprotein 1
SSBP/1	Sheep Scrapie Brain Pool 1
TCP-1	T-Complex Protein 1
TME	Transmissible Mink Encephalopathy
Tg	Transgenic
TGF	Transforming Growth Factor
tPA	Tissue Plasminogen Activator Enzyme
TRiC	TCP1 Ring Complex
TSE	Transmissible Spongiform Encephalopathy
UniProt	Universal Protein Resource
uPA	Urokinase Plasminogen Activator
UPS	Ubiquitin Proteasome System
vCJD	Variant Creutzfeldt Jacob Disease
VEGF	Vascular Endothelial Growth Factor
Wt	Wild Type
w/v	Weight/Volume

Chapter 1

I: General Introduction to Prion Biology

I-A: Prion History

Transmissible spongiform encephalopathies (TSE's), which are commonly known as prion diseases, cause incurable, progressively fatal neurodegeneration in humans and animals. Biochemically, the propagative mechanism entails the conformational change of the cellular prion protein (PrP^{C}) into the pathogenic, more stable, and partially protease resistant scrapie prion protein (PrP^{Sc}). The prion (PrP^{Sc}) is considered to be the central component to TSE. Scrapie, the prototypic prion disease affecting sheep and goats, is prevalent worldwide and has been known in Europe for centuries (Cuillé and Chelle 1939). Other known animal prion diseases include bovine spongiform encephalopathy (BSE) affecting cattle, chronic wasting disease (CWD) of cervids, and transmissible mink encephalopathy (TME) affecting farmed raised mink. Human prion diseases include Creutzfeldt-Jacob disease (CJD), Gertsman-Straussler-Scheinker syndrome (GSS), fatal familial insomnia (FFI) and Kuru (Glatzel, Stoeck et al. 2005). Currently, there is no medical treatment in existence for these diseases.

Although cellular toxicity and neuronal death are universally shared features of protein misfolding neurodegenerative diseases such as Alzheimer's (AD), Parkinson's (PD^1) and Huntington disease (HD), prion diseases are unique because of their infectious transmission properties (Aguzzi and Calella 2009). Human prion diseases can be contracted through various sources. They can originate through exposure to contaminated source, for example variant CJD (vCJD) through the consumption of BSE, or iatrogenic

(iCJD). Genetic inheritance of an autosomal dominant mutation in the *PRNP* gene (familial form) also causes disease. Lastly, prion disease in humans can be sporadic with an unknown etiology (sCJD) (Mead 2006).

Early in the 20th century, sheep scrapie was described as a transmissible (Cuillé and Chelle 1939) disease that caused pathology in muscle (M'Gowan 1914; M'Fadyean 1918). The novel biochemical nature of this infectious agent began to emerge in the 1950's and 1960's. Specifically, filtration methodology and several denaturing techniques revealed that the infectious agent was small and proteinaceous (Wilson, Anderson et al. 1950; Alper, Haig et al. 1966; Alper, Cramp et al. 1967). Based on all the biochemical evidence gathered in 1967, Griffith, J.S. formulated the hypothesis that the infectious agent causing scrapie is a self-replicating protein (Griffith 1967). In the 1980's, Dr. Stanley Prusiner's biochemical experiments ultimately led to elucidating and characterizing the nature of the scrapie agent. Sifting for differences between the scrapie infected and uninfected brains, the endogenously expressed cellular prion protein was identified subsequent to purification and characterization of PrP^{Sc}, and subsequently demonstrated to have direct association with prion disease development. Additionally, because of the lack of nucleic acids and the proteinaceous properties of this infectious agent, Prusiner formulated the "protein only" hypothesis which defined the causative agent of scrapie to consist of "proteinaceous infectious particles lacking nucleic acids" or simply "prions"(Prusiner 1982).

I-B: Human Prion Diseases

Human prion diseases cause widespread neurodegeneration and share several important clinical features. The symptoms are multifaceted that effect both the cognitive

and motor functions (Collinge 2001). Common to all human prion diseases is the rapid progression of dementia, myoclonus, ataxia, vision loss, insomnia and final onset of akinetic mutism prior to death (Collinge 2001). CJD was described by two independent German doctors, neurologist Hans Gerhard Creutzfeldt and Alfons Maria Jacob (Creutzfeldt 1920; Jakob 1921). sCJD is the most common human prion disease. With an unknown etiology, sCJD occurs at rate of 1 person per million worldwide (Collinge 2001). This disease accounts for 85% of all human TSE's. fCJD, GSS and FFI are inherited through an autosomal dominant mutation in the *PRNP* gene, and account for 15-20% of all presented cases (Aguzzi and Calella 2009). The etiology of acquired CJD varies. The consumption of BSE contaminated meat from infected cattle was hypothesized to directly link with the etiology of vCJD (Collinge, Sidle et al. 1996). Accidental transmission of prions through iatrogenic methods that include direct exposure through contact with contaminated neurosurgical equipment, inoculation with contaminated human growth hormone and/or prion contaminated corneal graft treatment are all example sources for acquired human prion diseases (Job, Maillard et al. 1992; Martínez-Lage, Poza et al. 1994; Mitrova and Belay 1999; Croes, Roks et al. 2002). Recent findings provided evidence for direct iatrogenic transmission of human prions from a preclinical vCJD patient through blood transfusion to other individuals, suggesting that the risk to prion exposure is significantly higher than previously thought (Peden, Head et al. 2004; Panigaj, Brouckova et al. 2010). Finally, Kuru, which affected the indigenous people of the Eastern Highlands of Papua New Guinea was transmitted through cannibalistic rituals (Collinge 2001). Importantly, Kuru was the first human prion disease to be transmitted in laboratory animals (Gajdusek, Gibbs et al. 1966).

I-C: Animal Prion Diseases

Scrapie, was described in Europe in the 18th century that became the prototypic experimental agent in prion research two centuries later (M'Fadyean 1918). It is readily transmitted in sheep and goat, although the actual mechanism of dispersion is not completely understood (van Keulen, Bossers et al. 2008). Clinical and neuropathological characteristics vary amongst scrapie-infected animals. These differences have strong dependence on the genetic background of the infected animal and prion strains, which will be described in another section of this chapter in greater detail. The incubation time of ovine scrapie can range from 2 to 5 years, with death occurring within 6 months after the onset of clinical signs (Jeffrey and Gonzalez 2007). The most common clinical signs associated with scrapie is pruritus (itching), which leads to rubbing, scraping and the eventual loss of wool but other behavioral, and motor dysfunctional symptoms also exist (Jeffrey and Gonzalez 2007). Atypical scrapie in sheep and goats has recently been described, which differs from classical scrapie by its biochemical and neuropathological features (Benestad, Sarradin et al. 2003; Orge, Galo et al. 2004; Le Dur, Beringue et al. 2005; Everest, Thorne et al. 2006; Konold, Davis et al. 2007). Major neurological signs of atypical scrapie include ataxia and incoordination and the absence of pruritus (Benestad, Sarradin et al. 2003). Polymorphism in the *PRNP* gene is strongly correlated with the animal's susceptibility to contracting classical scrapie (Baylis and Goldmann 2004). While, atypical scrapie is prevalent in animals that have a polymorphism that is linked with resistance to classical scrapie (Benestad, Arsac et al. 2008).

BSE, also known as “Mad Cow” disease, emerged in the mid 1980's as a previously unknown epidemic in cattle of Great Britain. This epidemic ravaged the

agricultural industry, destroying cattle farms throughout Europe (Aguzzi and Calella 2009). The incubation time for classical BSE ranges between 2 to 8 years (Wells, Scott et al. 1987; Novakofski, Brewer et al. 2005). Transmission and biochemical studies revealed that classical BSE was a prion disease (Hope, Reekie et al. 1988; Collinge, Palmer et al. 1995). The disease peaked in the early 90's and declined to rare occurrences as the dietary supplementation of protein from rendered cattle became prohibited. Importantly, classical BSE is considered to be the direct causative agent of vCJD, which has been experimentally supported through biochemical and histopathological similarities (Collinge, Sidle et al. 1996; Bruce, Will et al. 1997; Scott, Will et al. 1999; Clewley, Kelly et al. 2009). Additionally, atypical BSE was identified through active BSE surveillance programs in Europe (Biacabe, Morignat et al. 2008; Ducrot, Arnold et al. 2008) and subdivided into two strains, L-type and H-type (Buschmann, Biacabe et al. 2004; Casalone, Zanusso et al. 2004). These BSE's differ by incubation times in cattle and in transmissions through transgenic mice expressing bovine PrP^C, glycopatterns of PK digested PrP^{Sc}, and neurohistological profiles (Buschmann, Gretzschel et al. 2006).

Chronic wasting disease (CWD) of elk, deer and moose is an emerging prion disease that is causing public concern. Originally described in the 1980's as a TSE in captive mule deer (Williams and Young 1980), the disease has spread to free ranging deer, elk and moose throughout North America and South Korea. Clinical signs in cervids include patchy coats, a lowered head with drooping ears, weight loss, ataxia along with behavioral alterations (Williams and Young 1980). Central nervous system (CNS) assessment of CWD infected cervids shows neuronal vacuolation, neuropil spongiosis, astrocytic hypertrophy, hyperplasia and amyloid plaques (Williams and Young 1980;

Bahmanyar, Williams et al. 1985). Even though CWD affects cervids, the zoonotic potential of this disease has not been well characterized.

Transmissible mink encephalopathy (TME) is a TSE of farmed mink first recognized in the Wisconsin and Minnesota mink farms in the late 1940's but described in 1965 (Burger and Hartsough 1965; Hartsough and Burger 1965). The origin of TME is unknown, but is hypothesized to have originated from rendered prion infected cattle used as protein source to feed the animals (Marsh, Bessen et al. 1991). Transmission studies of Stetsonville TME into cattle produced prion disease with an incubation time of 18.5 months, followed by back passaging the bovine TME into mink, which also resulted in the development of prion disease (Marsh, Bessen et al. 1991). Recent transmission studies compared TME, bovine passaged TME and 3 distinct natural BSE (classical, L-, H-type) in ovine PrP^C expressing transgenic mice (TgOvPrP4) (Baron, Bencsik et al. 2007). The results of this study, which included incubation time, lesion profiling and biochemical properties of the PK resistant materials demonstrated that TgOvPrP4 mice were susceptible to bovine passaged TME, classical BSE and L-Type BSE but not H-type BSE, suggesting that L-type BSE is the most likely related to TME (Baron, Bencsik et al. 2007). Clinical signs in mink include the progressive lack of grooming, weight loss, ataxia and incoordination, behavioral changes, curled tail and mutilation (Hartsough and Burger 1965). Neuropathology of TME includes spongiform degeneration and astrocytosis throughout the CNS (Hartsough and Burger 1965; Eckroade, ZuRhein et al. 1973; Guiroy, Marsh et al. 1993). Transmission studies of TME into the Syrian golden hamster led to the identification of two biologically distinct prion strains, Hyper (HY)

and Drowsy (DY) (Bessen and Marsh 1992; Bessen and Marsh 1992), which are described in greater detail below.

Other rare TSE's described in animals include the exotic ungulate encephalopathy (EUE) affecting exotic zoo ruminants, and feline spongiform encephalopathy (FSE) of domestic and captive wild cats. Both EUE and FSE are considered to be linked to BSE contaminated feed sources (Cunningham, Wells et al. 1993), <http://www.cfsph.iastate.edu>. Clinical and neurohistological data supports these diseases to be part of the TSE disease family (Pearson, Wyatt et al. 1992; Kirkwood, Cunningham et al. 1993). A brief overview of prion diseases is presented in table 1.

In summary, prions cause fatal, neurodegenerative disease that affects both humans and animals. Clinical manifestations of these diseases are complex which include both cognitive and muscle-motor deficits. The causative agent of the disease is the β -sheet rich, protease resistant and detergent insoluble, PrP^{Sc}, derived through conformational conversion process from the endogenously expressed and post-translationally modified PrP^C. Prion diseases have a broad etiological range that includes genetic predisposition through polymorphism in the *PRNP* gene, transmissibility by exposure to the infectious agent and/or through other ill-defined origins. The molecular mechanisms that govern the etiology of prion diseases are beginning to be better understood, which ultimately have much wider implications for our understanding of protein misfolding “conformational” diseases.

Table 1.1 Human and animal prion diseases

Disease	Host	Source
Kuru	Human	Ritualistic Cannibalism
Sporadic Creutzfeldt-Jacob disease (sCJD)	Human	Spontaneous or somatic mutation
Familial Creutzfeldt-Jacob disease (fCJD)	Human	<i>PRNP</i> mutations
Iatrogenic Creutzfeldt-Jacob disease (iCJD)	Human	Acquired accidentally from medical procedures
Variant Creutzfeldt-Jacob disease (vCJD)	Human	Acquired from BSE
Gertsmann-Straussler-Scheinker syndrome (GSS)	Human	<i>PRNP</i> Mutations
Fatal Familial Insomnia (FFI)	Human	<i>PRNP</i> haplotype 178N-129M
Scrapie	Sheep, Goats	Unknown
Transmissible Mink Encephalopathy (TME)	Mink	Infection from either sheep or cattle
Chronic Wasting Disease (CWD)	Cervid (Elk, Deer, Moose)	Unknown
Bovine Spongiform Encephalopathy (BSE)	Cattle	Unknown
Feline Spongiform Encephalopathy (FSE)	Cats	BSE
Exotic Ungulate Encephalopathy (EUE)	Nyala, Kudu, Oryx, bison	BSE

I-D: The Cellular Prion Protein

Unique biochemical properties associated with the infectious scrapie agent were crucial for the identification of the PrP^C. These distinguishing properties included resistance towards nucleic acid inactivation (scrapie agent remained infectious) but not towards protein denaturation (Prusiner 1982). The partial resistance to protease degradation and insolubility in detergents allowed for the identification of a unique protein that was associated with scrapie diseased hamster brains but not in the healthy counterparts (Prusiner, Groth et al. 1980). Further subcellular fractionation of scrapie infected hamster brains led to the purification of the protease resistant peptide that had a migration pattern on the SDS-PAGE yielding a size of approximately 27-30 kDa, designated as PrP27-30 (Prusiner, Bolton et al. 1982). The purification of PrP27-30 facilitated reverse sequencing of the amino terminal end of the polypeptide, enabling the identification of the host encoded gene for PrP (Oesch, Westaway et al. 1985) (Basler, Oesch et al. 1986). PrP^C was determined to be a host-encoded protein that is located on chromosome 20 in humans and chromosome 2 in mice (Sparkes, Simon et al. 1986). The PrP open reading frame (ORF) is confined within one exon and prior to processing and posttranslational modifications, the human prion protein is 253 amino acids in length (Kretzschmar, Stowring et al. 1986).

I-D-1: PrP^C Structure

PrP^C peptide has two signal sequence motifs: at the N-terminus (1-22aa) for targeting to the endoplasmic reticulum (ER) where the protein undergoes post-translational modification; and at the C-terminus, where the glycosylphosphatidylinositol (GPI) anchor is attached for cell surface presentation within lipid rafts on the plasma

membrane (Fig. 1.1A) (Stahl, Borchelt et al. 1987). The N-terminus of PrP spans the residues 23 to 124 aa and is primarily unstructured (Fig. 1.1A). This region of the protein contains octapeptide repeats that bind copper ions (Hornshaw, McDermott et al. 1995). The central portion of the protein consists of a hydrophobic core that overlaps the N-terminus, encompassing the amino acids residues 111 to 134. The hydrophobic core has a transmembrane tethering function (Lopez, Yost et al. 1990), which upon deletion causes spontaneous neurodegeneration in transgenic mice (Shmerling, Hegyi et al. 1998) (Chiesa, Piccardo et al. 1998) (Baumann, Tolnay et al. 2007). The C-terminus of PrP is the globular structured region that consists of three α -helices and two β -sheet strands (Fig. 1.1A) (Riek, Hornemann et al. 1996). As a glycoprotein, PrP^C can present itself in a di-, mono- or un glycosylated form. N-linked glycosylation occurs at Asn-180 and Asn-197 in humans (Kretzschmar, Stowring et al. 1986; Liao, Lebo et al. 1986; Bazan, Fletterick et al. 1987; Haraguchi, Fisher et al. 1989). Lastly, helices two and three of the prion protein are linked through an intramolecular disulfide bridge (Turk, Teplow et al. 1988).

I-D-2: PrP^C Trafficking and Membrane Topology

The GPI-anchor signal is the predominant localization motif that targets the protein to the plasma membrane, although two additional transmembrane topological designations exist (Yost, Lopez et al. 1990). These transmembrane topologies are for insertion into the lipid bilayer via the central hydrophobic core and are found in low-abundance (<10%). They present themselves with either the C-terminus or the N-terminus outwards facing the lumen while presenting the opposite end towards the cytoplasm, respectively designated as, CtmPrP and NtmPrP (Fig. 1.1B) (Hegde, Mastrianni

et al. 1998; Holscher, Bach et al. 2001; Stewart, Drisaldi et al. 2001). The C-terminus topologically oriented ^{Ctm}PrP retains both the N- and C-terminus signal motifs with predominant retention in the ER, ultimately targeting the protein for proteasomal degradation as demonstrated in cell culture models expressing a mutant PrP protein with ^{Ctm}PrP characteristics (Stewart, Drisaldi et al. 2001). While transgenic mice expressing a mutant PrP that mimics the ^{Ctm}PrP topology develop fatal neurodegeneration with significant neuronal loss in the cerebellum and the hippocampus (Stewart, Piccardo et al. 2005). Cultured neurons from these transgenic mice, localize ^{Ctm}PrP to the Golgi which differs from cell culture models that localize ^{Ctm}PrP to the ER (Stewart and Harris 2005). Therefore, ^{Ctm}PrP is hypothesized to be a toxic intermediate for neurodegeneration in prion disease through the induction of cellular stress pathways that ultimately cause apoptosis (Shi and Dong 2011). Both transmembrane proteins (^{Ntm}PrP and ^{Ctm}PrP) have been demonstrated to reduce bcl-2-Associated X protein activity (Bax) (Lin, Jodoin et al. 2008).

Synthesis and posttranslational modification of PrP^C occur in the ER. Once passed through the cell's protein quality control mechanisms, PrP^C is transported into the Golgi network where it is attached to lipid rafts via the GPI anchor and trafficked to the cell surface (Taraboulos, Raeber et al. 1992). Alternatively, improper folding of PrP^C triggers the protein quality control mechanisms that ultimately target the protein for degradation through the ubiquitin-proteasome system (UPS) (Fig. 1.2) (Ma and Lindquist 2001). Surface retention is short lived and the protein is internalized back into the cytosol where it is either recycled or degraded in lysosomes (Taraboulos, Raeber et al. 1992). Furthermore, internalization and trafficking of PrP^C appear to be mediated by both

clathrin-coated pits and/or caveolin mediated endocytic mechanisms (Harris, Huber et al. 1993; Shyng, Huber et al. 1993; Shyng, Heuser et al. 1994; Vey, Pilkuhn et al. 1996). Additionally, PrP^C existence as a secreted protein through enzymatic cleaving at the GPI-anchor has been reported (Hay, Prusiner et al. 1987). The intracellular trafficking process of PrP^C is presented in a schematic diagram of figure 1.2.

In summary, discovery of endogenously expressed PrP^C was a crucial step towards understanding the molecular basis of prion diseases. The unique biochemical properties of the infectious scrapie agent in combination with meticulous deductive biochemistry enabled the host-encoded gene for the prion protein to be identified (Prusiner, Bolton et al. 1982; Oesch, Westaway et al. 1985; Basler, Oesch et al. 1986). Additional experiments began to resolve the cellular biogenesis and structure of PrP^C, thus identifying the cellular localization and structural domains of this protein (Stahl, Borchelt et al. 1987; Lopez, Yost et al. 1990; Riek, Hornemann et al. 1996). These analyses laid the foundation towards characterizing the normal physiological functions of PrP^C, which remains an ongoing process, and more importantly its direct role as the etiological source/substrate for PrP^{Sc} conversion in prion diseases.

Figure 1.1 Schematic representations of the human cellular prion protein (PrP^C) and PrP^C's membrane topology. A. The prion protein consists of two signal sequences and three distinct domains. The N-terminal target sequence (yellow) is cleaved after amino acid 22 during the processing of the protein as it transits to the plasma membrane. The rest of the N-terminus is a charged, and primarily unstructured domain that contains the Cu²⁺-Octapeptide repeat binding motif (purple). The central domain consists of a hydrophobic core (HC, blue) and is associated with neurotoxicity. The C-terminal domain is structured and consists of three α -helices (H1, H2, and H3, orange) and two β -sheet motifs (B1 & B2, black) flanking the first helix. PrP^C undergoes post translational modification by glycosylation at asparagine residues (CHO, 181aa, 197aa). A stabilizing disulfide bridge forms between helices 2 and 3 (blue arrows, S-S). Finally, a GPI-anchor signal (green) that anchors the protein to the plasma membrane is at the C-terminus. **B.** PrP^C's three topological designations include the cell surface GPI-anchored PrP^C, and two transmembrane spanning PrP's presenting either the C- or the N- terminus to the surface, respectively designated ^{Ctm}PrP and ^{Ntm}PrP. Figure 1.1B has been adapted from a previously published review (Harris 2003).

Figure 1.1 Schematic representations of the human cellular prion protein (PrP^C) and PrP^C's membrane topology.

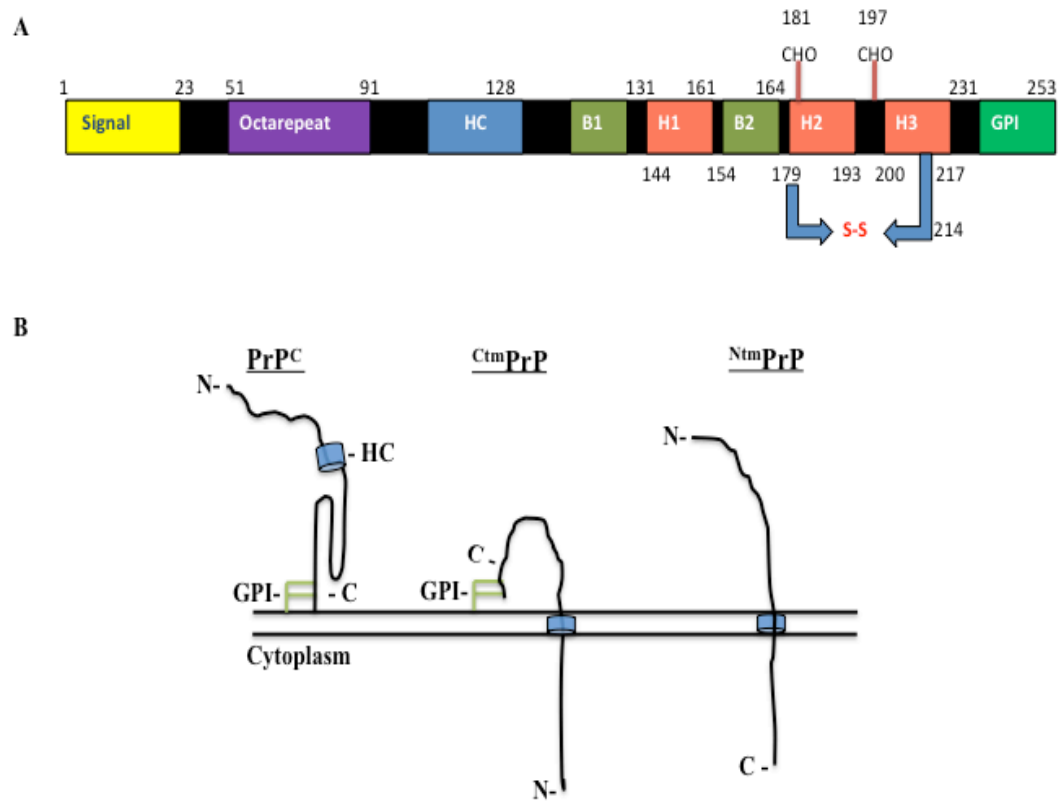
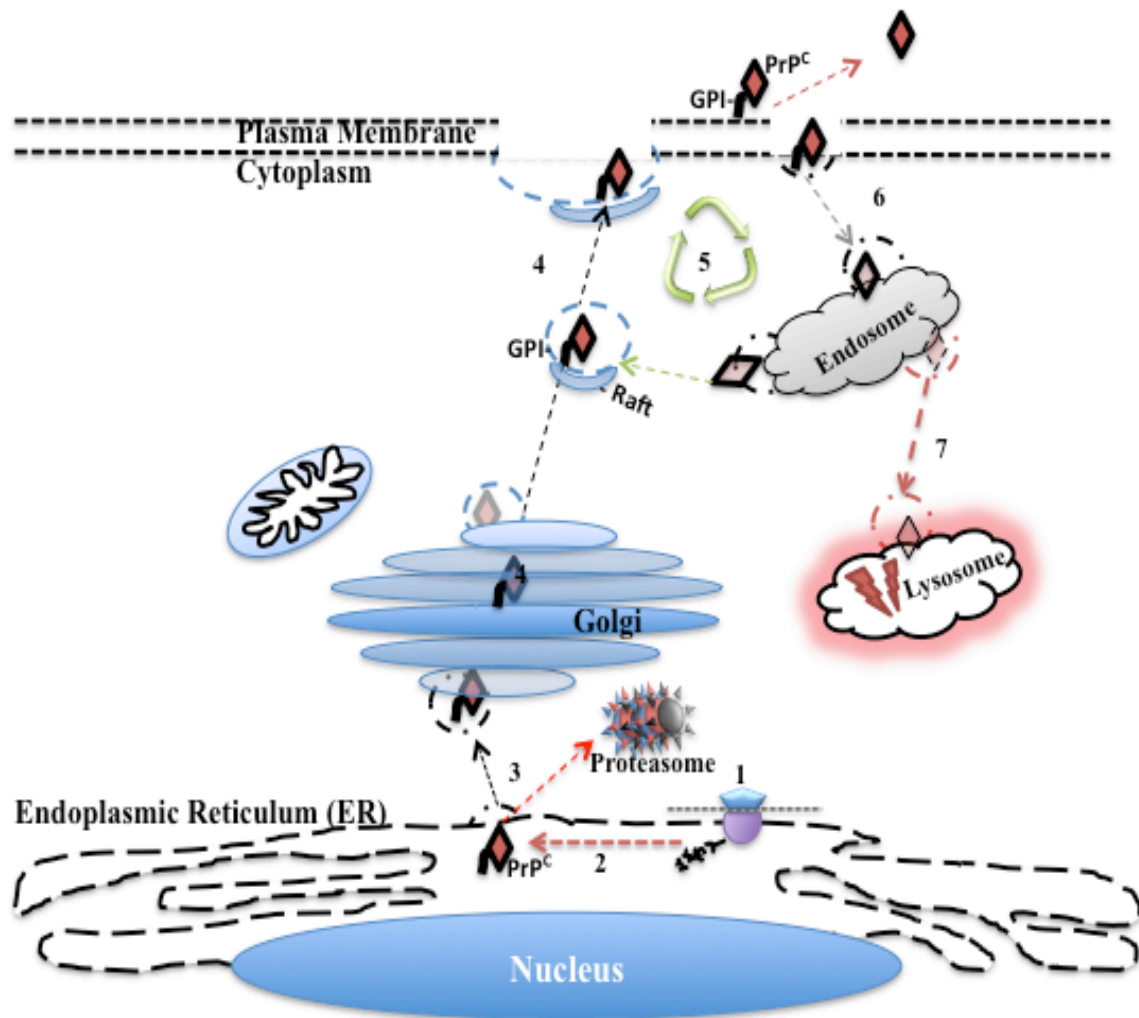


Figure 1.2 Intracellular trafficking of PrP^C. (1) PrP^C is translated and targeted to the endoplasmic reticulum (ER) by the N-terminal signal sequence. (2-3) In the ER, PrP^C undergoes proper folding and acquires post-translational modifications, where it is transported to the Golgi network for cell surface presentation in the lipid raft portion of the plasma membrane tethered by glycosylphosphatidylinositol (GPI) anchor. (3) Alternatively, subsets of newly synthesized PrP^C that does not attain proper conformational structure are passed through protein quality control mechanisms which target them for degradation in the ubiquitin-proteasome system (UPS). (4) Once in the Golgi, PrP^C is trafficked towards the cell surface in lipid-raft rich vesicles. (5) PrP^C presentation to the cell surface and internalization is a constitutively recycling process. (6) Endocytosis and trafficking of PrP^C is mediated through multiple endocytic mechanisms that include both the clathrin-coated pits and caveolae pathways. (7) Endocytosed PrP^C not destined for recycling is trafficked from late endosomal compartments into lysosome for proteolytic degradation.

Figure 1.2 Intracellular trafficking of PrP^C

Intracellular Trafficking of Cellular Prion Protein (PrP^C)



I-E: Prion Replication and Strain Diversity

Prion Replication

Because the novel properties of the scrapie agent distinguish it from viruses, plasmids, and viroids, a new term “prion” is proposed to denote a small *proteinaceous infectious* particle that is resistant to inactivation by most procedures that modify nucleic acids. Knowledge of the scrapie agent structure may have significance for understanding the causes of several degenerative diseases. (Dr. Stanley Prusiner, (Prusiner 1982))

Characterization of PrP^{Sc} replication and conversion is a biologically complex process that requires an experimentally combinatorial approach. Unlike the viral strain classification system, which is based on nucleic acid compositions and follows the central dogma of molecular biology, molecular classification of prion strains is based on the transfer of information through conformational changes in association with the “protein only” hypothesis (Fig. 1.3A). As earlier discussed, protein sequencing and reverse genetics facilitated the identification of the host encoded prion protein (PrP^C), which laid the supporting foundation for the “protein only” hypothesis regarding prion diseases (Griffith 1967; Prusiner 1982; Prusiner, Groth et al. 1984; Westaway and Prusiner 1986). This hypothesis postulated that PrP^C is the main substrate for the replication of the more stable, conformationally altered and partially protease resistant PrP^{Sc} lacking nucleic acids. Under this hypothesis, there are two central models for prion replication. The template-directed refolding model postulates that PrP^C to PrP^{Sc} conformational change requires the addition of an exogenous template to modulate PrP^C structure to a more stable isoform. This reaction is driven by the continuous addition of PrP^C substrate (Fig. 1.3B). In the second model, termed “the seeded nucleation” model, PrP^C and PrP^{Sc} are both present (Fig. 1.3C). PrP^{Sc} develops spontaneously although at an unfavorable

equilibrium as compared to PrP^C. The initial seeding of PrP^{Sc} is energetically unfavorable and extremely slow, but once PrP^{Sc} becomes ordered, the process begins to seed the formation of larger aggregates leading to the formation of infectious particles (Jarrett and Lansbury 1993). Protein Misfolding Cyclic Amplification (PMCA) has provided supporting evidence towards the “protein only” hypothesis by demonstrating the formation of infectious PK resistant protein aggregates in vitro (explained below) (Saborio, Permanne et al. 2001).

I-F: Prion Strains

Describing the diversity of prion strains and the transfer of conformational information lacking nucleic acids to transmit and cause disease has been challenging. The intrinsic difficulty of describing this diversity is based on our lack of understanding protein-mediated conformational transfer of information. It is hypothesized that PrP^{Sc} acts as the template to convert the PrP^C isoform (Prusiner 1982; Basler, Oesch et al. 1986; Büeler, Aguzzi et al. 1993). This process requires that both PrP isoforms maintain near identical primary structure for efficient transmission, thus explaining why interspecies prion transmission is generally less efficient than intraspecies transmission, (Scott, Groth et al. 1993; Telling, Scott et al. 1994).

At the molecular level, the diversity and specificity of individual prion strains is proposed to be associated with the different conformational states that the PrP molecule acquires. The evidence to support this hypothesis was experimentally investigated using biochemical and spectroscopic techniques (Safar, Wille et al. 1998; Kuczius and Groschup 1999; Wadsworth, Hill et al. 1999; Safar, Cohen et al. 2000). Moreover,

numerous PrP^{Sc} strains have been identified within mammalian prion diseases, which indicate that the selection process for these strains is co-dependent on several factors. The conformational selection model suggests that PrP^{Sc} replication is strongly dependent on host encoded PrP homology and thermodynamically favorable conformations of the outcompeting PrP^{Sc} (Collinge 1999; Collinge and Clarke 2007). Specifically, it is the competition between thermodynamically favorable PrP^{Sc} conformational states (Levinthal's paradox on protein folding estimates 10^{143} possible conformation a protein may take, (Zwanzig, Szabo et al. 1992)), structural similarity to the host encoded PrP^C, and the kinetic rate of conversion as compared to the rate of clearance that is mediated by the endogenous protein quality control mechanism that are designed to prevent aggregation.

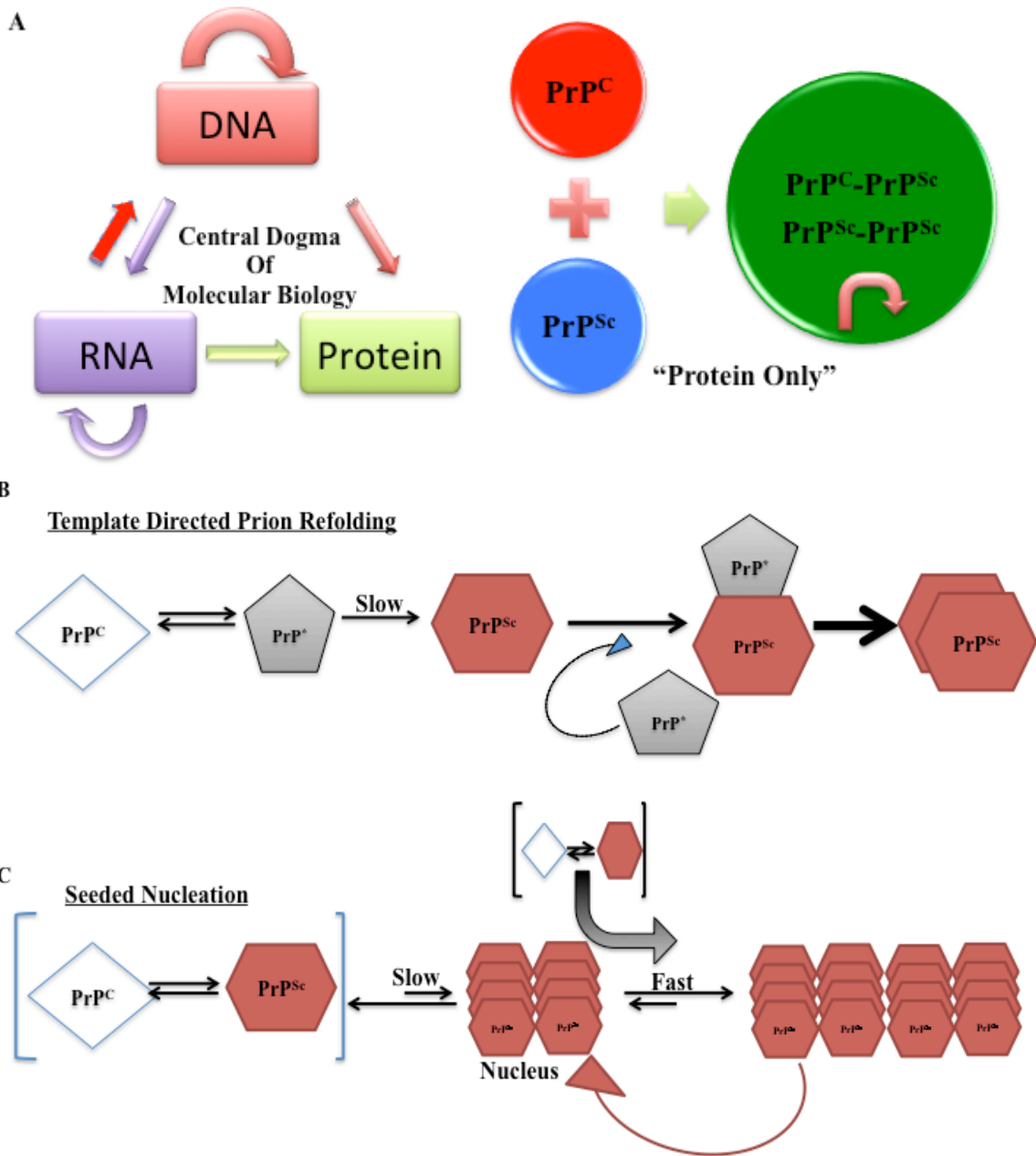
Evidence supporting conformational selection was experimentally validated using synthetic yeast (PSI+) prions derived from the Sup35 substrate protein, which can be used to adopt distinct infectious conformations in vitro (Tanaka, Collins et al. 2006). Using this yeast prion system, it was demonstrated that distinct conformations of the synthetically generated PSI+ prions had profound effects on the growth and division phases of prion particle formation and aggregation thus indicating that the variation in aggregate formation represents a mechanisms by which specific prion strain phenotype dominates selection (Tanaka, Collins et al. 2006). Significantly less is understood for the selection and replication mechanisms in animals.

Experimentally, prion strain properties are analyzed through transmission studies in animal models and subsequently assessed histologically and biochemically (Bruce, McBride et al. 1989). Biological prion strain characteristics are described using

incubation times in animal models, clinical signs at onset of disease, neuropathological analysis, and PrP deposition within brain sections (Bruce and Dickinson 1979; Bruce, McBride et al. 1989). Serial transmission and cloning of prion strains in the respective host is required to identify the specific phenotypic property of the infectious agent. These properties are influenced by the genetic background of the host and may alter upon interspecies transmission (Pattison 1965; Westaway, Goodman et al. 1987). Biochemically, prion properties are described using denaturing agents that break (denature) prions in a concentration dependent manner using conformational stability assay (Peretz, Scott et al. 2001). Protease digestion by proteinase K (PK), glycoform ratios and electrophoretic migration patterns on SDS-PAGE gels are characteristic properties used to distinguish prion strains as well (Collinge, Sidle et al. 1996). Furthermore, strain specificity has also been analyzed through conformational-dependent immuno assays and conformational alterations dictated through metal-ion occupancy binding assays (Safar, Wille et al. 1998; Wadsworth, Hill et al. 1999). Although the molecular complexities associated with prion strains are slowly being experimentally defined, many unanswered questions remain regarding prion prevalence and replication in naturally susceptible animals.

Figure 1.3 Models for prion replication. **A.** Schematic models comparing modes of information transfer between the central dogma of molecular biology, and protein only information transfer model. **B.** In template directed model, conversion of PrP^{C} (diamond) or an intermediate conformation PrP^* (pentagon) to PrP^{Sc} (hexagon) is slow and irreversible. **C.** In the seeded nucleation model, PrP^{Sc} formation is not rate limiting, but the accumulation of PrP^{Sc} into an ordered nucleus is slow, once formed, it acts as the seed to form larger aggregates. (Come, Fraser et al. 1993) (Brown, Goldfarb et al. 1991) (Griffith 1967) (Jarrett and Lansbury 1993)

Figure 1.3 Models for prion replication.



I-F-I: Scrapie Strains

Initial studies describing prion strain properties were through experimental transmission of sheep and goat scrapie (Pattison and Millson 1961; Pattison and Millson 1961). Two distinct phenotypes designated “drowsy” and “scratching” appeared in goats after inoculating them with sheep scrapie brain pool-1 (SSBP/1). The name designations were based directly on behavioral patterns (Pattison and Millson 1961). The two strains manifested distinctly different clinical syndromes that became more evident with continuous passage (Pattison and Millson 1961). The diversity of prion strains in goats has not been well defined although it would be predicted, based on the acquired data from natural goat scrapie samples, that multiple strains exist. Importantly, the European active TSE surveillance programs have identified both “atypical” scrapie and BSE in goats (Eloit, Adjou et al. 2005; Le Dur, Beringue et al. 2005).

Although the exact number of scrapie strains affecting sheep and goats remains to be determined, it is known that genetic polymorphism in *PRNP* of these animals greatly influences their susceptibility to disease (Hunter, Goldmann et al. 2000). Three polymorphic positions in sheep are particularly associated with susceptibility to scrapie: Valine/Alanine (V/A) at 136, Arginine/Histidine (R/H) at 154, and Glutamine/Arginine (Q/H) at 171 (Westaway, Zuliani et al. 1994; Cloucard, Beaudry et al. 1995; Foster, Wilson et al. 1996; Hunter, Foster et al. 1996). These polymorphisms have been ranked by their permissiveness towards scrapie. The VRQ/VRQ, ARQ/VRQ and ARQ/ARQ genotypes are considered to confer greatest susceptibility, while the AHQ and ARR genotypes confer strong resistance (Hunter, Foster et al. 1996; Dawson, Hoinville et al. 1998; Woolhouse, Matthews et al. 1999; Matthews, Coen et al. 2001; Baylis, Goldmann

et al. 2002). As previously mentioned, active surveillance for scrapie in Europe identified new scrapie strain termed “atypical” scrapie (Benestad, Sarradin et al. 2003; Everest, Thorne et al. 2006), which differs from classical scrapie in several aspects. Atypical scrapie distinguishable properties include increased incubation time (atypical scrapie found in older sheep), decreased neuropathological lesions, decreased biochemical stability of PrP^{Sc} and a notably lower electrophoretic migratory band representing ~12 kDa size fragment on a western immunoblots (Benestad, Sarradin et al. 2003; Luhken, Buschmann et al. 2007).

I-F-2: TME Prion Strains

TME transmission studies have provided evidence for biologically distinct prion strains. Transmission studies using Syrian golden hamsters model facilitated identification and characterization of the two TME prion strains called: HY and DY (Bessen and Marsh 1992; Bessen and Marsh 1992). As indicated by the name, the HY strain is biologically characterized through short lived hyperactive behavior in the infected animal that rapidly progresses to cause disease with a mean incubation time of ~60 days, whereas DY infected animals present themselves with lethargic behavior and a delayed onset of disease with a mean incubation time of ~165 days (Bessen and Marsh 1992). Biochemical analysis of PrP^{Sc} constituting HY and DY demonstrate strain-specific differences which are best described by their differential sensitivity to protease digestion and electrophoretic migration on sodium dodecyl sulfate polyacrylamide gel electrophoresis (SDS-PAGE) (Bessen and Marsh 1992). The source of TME is hypothesized to be bovine prions accidentally transmitted to farm raised mink through

contaminated feed (Marsh, Bessen et al. 1991; Robinson, Hadlow et al. 1994; Baron, Bencsik et al. 2007).

I-F-3: BSE Prions

In addition to the classical BSE prions described earlier, international surveillance efforts and careful analysis of prion infected cattle tissue has led to the identification of two additional BSE variants that until recently have remained unknown (Jacobs, Langeveld et al. 2007). The identification of the “atypical” BSE L- and H-type strains directly resulted from rigorous testing of aged, asymptomatic cattle in European slaughterhouses (Buschmann, Biacabe et al. 2004; Casalone, Zanusso et al. 2004). Analogous to the description of “atypical” scrapie, L- and H-type BSE differ from classical BSE. H-type BSE is characterized by a higher molecular weight but conventional glycoform migration pattern of PrP^{Sc} after PK digestion (Biacabe, Laplanche et al. 2004). PrP^{Sc} of L-type BSE has a lower molecular weight and distinctly different glycoform migration pattern (Casalone, Zanusso et al. 2004). Transmission studies in transgenic mice expressing bovine PrP using the three BSE strains revealed significant differences in incubation times and deposition of PrP^{Sc}, providing further evidence towards the existence of unique prion strains amongst cattle (Everest, Thorne et al. 2006). Furthermore, due to their identification in older, asymptomatic cattle, it has been hypothesized that the atypical BSE strains could be the result of naturally occurring sporadic TSE. Evidence supporting this hypothesis was provided from a 10-year-old BSE H-type positive cow with a mutation (E211K) correlating to a known substitution frequently associated with familial-CJD (Nicholson, Brunelle et al. 2008; Richt and Hall 2008). Lastly, the comparison of biochemical properties of PrP^{Sc} in BSE and vCJD linked

these two diseases, providing evidence for the abrogation of the species barrier between humans and domestic cattle through the ingestion of BSE contaminated food (Collinge 1996).

I-F-4: CWD Prions

The characterization of prion strain diversity in cervids has recently begun to unravel. As with other species-specific prion diseases, CWD susceptibility is dependent on the genetic background of the host and the polymorphisms in *PRNP* (Green, Browning et al. 2008). Using transgenic mice expressing cervid PrP^C, it was possible to successfully transmit CWD and characterize biological and biochemical properties of this infectious agent (Browning, Mason et al. 2004; LaFauci, Carp et al. 2006; Tamguney, Giles et al. 2006; Meade-White, Race et al. 2007). Recently, two novel CWD strains types, referred to as CWD1 and CWD2, were identified in natural elk field isolates in transgenic mice referred to as Tg(CerPrP)1536^{+/-} mice, expressing deer PrP^C (Angers, Kang et al. 2010). These studies demonstrated distinct strain differences based on incubation time and neuropathology that were composed of PrP^{Sc} with indistinguishable characteristics. In an attempt to understand these strain profile differences between deer and elk, it was hypothesized that the difference of a single amino acid in the primary structure of cervid PrP (deer PrP^C-Q226 and elk PrP^C-E226) dictates the selection and propagation stability of these CWD strains (Angers, Kang et al. 2010; Telling 2011).

Concluding Summary

Undoubtedly, understanding the underlying mechanisms that dictate protein-mediated conformational transfer of information in the context of protein misfolding diseases is important. The unique properties that allow prions to infect, propagate and

transfer their strain information to animal hosts without nucleic acids make them a tractable system in which to study general mechanisms of protein-misfolding diseases. Equally important to understand are the mechanisms that dictate the interactions, compatibility and species barriers in the selection process of a specific prion strain amongst a vast pool of conformationally distinct PrP^{Sc} molecules (Collinge 1999; Collinge and Clarke 2007). The mutability and diversity of prion strains among animals raises a greater concern for the zoonotic potential, as already seen with the BSE-vCJD connection in the mid 1990's (Collinge, Sidle et al. 1996; Bruce, Will et al. 1997; Collinge 1999). The uses of transgenic mouse models, cell culture models and in vitro prion conversion assays have greatly enabled us to address these fundamental questions.

II: Experimental Approaches To Analyze Prions

II-A: *Prnp*^{0/0} Knockout Mice & PrP^C Transgenic Mice

Transgenic animal models have become very important tools for studying prion biology. These models help identify and understand the physiological function of PrP^C. The cellular prion protein is highly conserved and has been identified in birds (Harris, Lele et al. 1993), reptiles (Simonic, Duga et al. 2000), amphibians (Strumbo, Ronchi et al. 2001) and fish (Gibbs and Bolis 1997), which would suggest significant biological importance. A commonly used method to elucidate the physiological function of a protein is to delete or mutate it, and to characterize the resulting phenotype(s) (Capecchi 1989). Although high PrP homology and conservation among animals would suggest a crucial physiological function, *Prnp*^{0/0} knockout mice were not embryonic lethal and demonstrated normal development with no gross-phenotypic abnormalities (Büeler,

Fischer et al. 1992). More importantly, these knockout mice were completely resistant to scrapie prion infection (Büeler, Aguzzi et al. 1993; Sailer, Bueler et al. 1994). Subsequent phenotypic characterization of *Prnp*^{0/0} mice suggested that PrP^C is functionally multifaceted. These functions include roles in circadian/sleep regulation (Tobler, Gaus et al. 1996; Tobler, Deboer et al. 1997), oxidative stress response and metal ion metabolism (Klamt, Dal-Pizzol et al. 2001; Wong, Liu et al. 2001; Brown, Nicholas et al. 2002; Singh, Kong et al. 2009), immune system signaling and phagocytosis (de Almeida, Chiarini et al. 2005; Ballerini, Gourdain et al. 2006), cell adhesion (Schmitt-Ulms, Legname et al. 2001; Malaga-Trillo, Solis et al. 2009), neuronal excitability and neuroprotection (Collinge, Whittington et al. 1994; Manson, Hope et al. 1995; Hoshino, Inoue et al. 2003; Gains, Roth et al. 2006), neurite outgrowth (Santuccione, Sytnyk et al. 2005) and behavior (Coitinho, Roesler et al. 2003; Nico, de-Paris et al. 2005). An interesting study utilizing a Cre-lox system to postnatally delete PrP^C in mice demonstrated reversal of neuropathology and improved motor and behavioral deficits post prion infection (Mallucci, Ratte et al. 2002; Mallucci, Dickinson et al. 2003). Neurological recovery and full restoration in the life span of these mice further confirm the importance PrP^C function *in vivo*.

The generation of the *Prnp*^{0/0} knockout mice facilitated the subsequent creation of other transgenic mouse models that express heterologous prion proteins from various species. These transgenic models enable scientists to address many of the unresolved prion biology questions, which include prion strain diversity, mechanisms of prion replication, species barriers and disease transmission (Scott, Foster et al. 1989; Hsiao, Scott et al. 1990; Telling, Scott et al. 1995; Weissmann, Fischer et al. 1998; Agrimi,

Nonno et al. 2008; Telling 2011). Specifically, PrP^C transgenesis in mice enabled to experimentally address the species barrier of BSE and the zoonotic potential of CWD using mice expressing human PrP^C (Collinge, Palmer et al. 1995; Bruce, Will et al. 1997; Kong, Zheng et al. 2008; Sandberg, Al-Doujaily et al. 2010). Moreover, transgenic mice expressing heterologous *PRNP* genes with polymorphic mutations have become functional models to assess spontaneously acquired prion diseases in humans (Telling, Haga et al. 1996; Mastrianni, Capellari et al. 2001; Nazor, Kuhn et al. 2005). Although transgenic mouse models are crucially important to understanding prion diseases and physiological functions of PrP^C, the complexities associated with multicellular organisms make it difficult to address the aforementioned unknowns at the cellular level.

II-B: Prion Cell Models

Cell culture models have helped characterize PrP^C processing, intracellular trafficking, localization within cellular compartments and likely interacting molecules (Harris, Lesko et al. 1993; Shyng, Huber et al. 1993; Shyng, Heuser et al. 1994; Shyng, Lehmann et al. 1995; Pauly and Harris 1998; Taylor and Hooper 2007; Hooper 2011). Furthermore, cell models simplify the analysis of PrP^{Sc} conversion mechanisms by reducing the complexity of the system from animal tissue to monolayer cells (mouse brain contains ~ 7.5e7 neurons, 2.3e7 glia, 7.0e6 endothelial cells, 3~4e6 misc. cells (data derived from the mouse brain library database, <http://www.mbl.org/>)). Analysis of PrP^{Sc} replication in cell culture supports the identification of cellular factors that enhance/promote infectivity, enabling the use of these cells for anti-prion drug screening.

The development of the Scrapie Cell Assay (SCA) for mouse-adapted prion strains was the “proof of principle” that demonstrates the utility of cell culture systems

for rapid prion titer calculation *in vitro*, albeit that particular assay did not include natural field prion isolates (Mahal, Demczyk et al. 2008). Recent improvements in this assay using a different cell model, validated titer calculations in CWD derived from field isolates, further supporting the multiple advantages cell culture models provide for prion analysis (Bian, Napier et al. 2010).

Initial cell culture models for scrapie replication were developed and described in the 1970's. These cells were produced by cultivating explants from scrapie-infected mouse brains which became known as SMB cells (Clarke and Haig 1970). Although these cells sustain chronic infectivity, the absence of uninfected controls was a drawback. The use of pentosan-sulfate to “cure” SMB cells solved this issue (Birkett, Hennion et al. 2001). While extensive attempts have been made to infect various cell lines with prions, only a handful demonstrate the ability to replicate prions and accumulate PrP^{Sc} (Table 1.2). These cell lines break down into two key categories: their origin (neuronal/ non-neuronal) and their ability to replicate heterologous (not of same genetic background) prion strains.

II-B-1: Cell Culture Models Permissive to Experimentally Adapted Mouse Prions

The mouse neuroblastoma (N2a) and the immortalized hypothalamic neuron (GT1) cell lines, both of neuronal origin, have been demonstrated to be highly permissive to mouse-adapted scrapie prion replication (Butler, Scott et al. 1988; Schätzl, Laszlo et al. 1997). Sub-cloning N2a cells led to the identification of clonal populations that vary in susceptibility (Bosque and Prusiner 2000). Typical infection of N2a cells (ScN2a) with mouse-adapted PrP^{Sc} results in a fraction of cells that sustain chronic infectivity amongst the total population (<2%), which can be enriched through sub-cloning for susceptibility

(~90%) (Race, Fadness et al. 1987; Butler, Scott et al. 1988; Race, Caughey et al. 1988; Bosque and Prusiner 2000; Mahal, Baker et al. 2007). Furthermore, the sub-cloning process of a susceptible N2a cell (N2a-PK1) leads to clones that show preferential susceptibility towards particular prion strains (Mahal, Baker et al. 2007; Browning, Baker et al. 2011). Recent findings using the N2a cells to replicate heterologous CWD PrP^{Sc}, suggests that these cells maintain the complete repertoire of cellular factors necessary to maintain infectivity from various sources (Pulford, Reim et al. 2010).

GT1 cells are highly differentiated gonadotropin-releasing hormone neurons which have also shown enhanced susceptibility towards replicating mouse-adapted prions (Table 1.2) (Schätzl, Laszlo et al. 1997). These cells express elevated amounts of PrP^C and demonstrate enhanced sensitivity compared to N2a cells (Nishida, Harris et al. 2000). Furthermore, the GT1 cells do not require additional cloning for producing chronically infected prion cultures. The permissiveness of GT1 cells has made them a tractable tool for analyzing mouse-adapted prion strains in culture (Arima, Nishida et al. 2005) and have been reported to replicate mouse-adapted human derived CJD PrP^{Sc} (Nishida, Katamine et al. 2005).

II-B-2: Cell Line Permissive to Heterologous Prions: RK13 Cells

The propagation of natural sheep scrapie prion isolates was first demonstrated using transgenically modified epithelial rabbit kidney cells (RK13) expressing ovine PrP^C (VRQ variant)(Vilette, Andreoletti et al. 2001). RK13 cells do not express endogenous rabbit PrP^C, making them the cell culture equivalent of the *Prnp*^{0/0} knockout mouse. Subsequent work using these cells have shown them to be permissive towards both natural and mouse-adapted prion strains (Vilette, Andreoletti et al. 2001; Paquet, Sabuncu

et al. 2004; Paquet, Daude et al. 2007; Courageot, Daude et al. 2008; Bian, Napier et al. 2010). RK13 cells co-expressing HIV-1 Gag and heterologous elk PrP^C showed enhanced CWD prion replication (Leblanc, Alais et al. 2006; Bian, Napier et al. 2010). This enhancement was subsequently used for the cervid prion cell assay (CPCA) to titer CWD prions in vitro, a technique modeled after the previously described SCA for mouse-adapted prions (Bian, Napier et al. 2010). Additional data characterizing these cells is described in the subsequent chapters of this thesis. Despite all of these developments for replicating PrP^{Sc} in cell culture systems, cells capable of replicating naturally derived human prions remain to be identified.

II-C: In Vitro PrP^{Sc} Conversion Assays

In vitro methods for detecting PrP^{Sc} are unconventional compared to other infectious agents. Standard polymerase chain reaction (PCR) assays cannot be used for the detection of prions because they lack nucleic acids (Prusiner 1982). Furthermore, standard immunological assays, such as the ELISA, cannot easily differentiate PrP^{Sc} from PrP^C. Nonetheless, several in vitro assays have been developed for the detection of prions and studying the conversion PrP^{Sc} process. These conversion assays rely on methods that utilize PrP^C as the substrate in a reaction to amplify PrP^{Sc}. The semi-quantitative analysis of PrP^C to PrP^{Sc} conversion *in vitro* using these assays provides a tractable means to calculate conversion PrP^{Sc} kinetics. Moreover, these assays accelerate species barrier adaptation of PrP^{Sc}, which otherwise requires multiple transmissions in bioassays (Green, Castilla et al. 2008). Lastly, these conversion assays may enable the elucidation of cofactors that participate in the replication and conversion process.

Table 1.2 Cell culture models for prion replication *in vitro*.

Cell Type	Origin/cell type	Species	Prion Strain	Reference
N2a	Neuroblastoma	Mouse	Chandler, Fukuoka-1, RML	(Race, Fadness et al. 1987; Butler, Scott et al. 1988; Bosque and Prusiner 2000; Enari, Flechsig et al. 2001)
N2a #58	Neuroblastoma	Mouse	Chandler, 139A, 22L	(Nishida, Harris et al. 2000)
C-1300	Neuroblastoma	Mouse	Chandler	(Butler, Scott et al. 1988)
NIE-115	Neuroblastoma	Mouse	Chandler	(Markovits, Mutel et al. 1985)
N2a-PK1	Neuroblastoma	Mouse	RML, 22L	(Mahal, Baker et al. 2007; Mahal, Browning et al. 2010; Browning, Baker et al. 2011)
N2a-R33	Neuroblastoma	Mouse	22L	(Mahal, Baker et al. 2007; Mahal, Browning et al. 2010; Browning, Baker et al. 2011)
GT1	Hypothalamic cells	Mouse	Chandler, ^a SY-CJD, ^b FU-CJD, RML, 22L, Fukuoka-1	(Rubenstein, Carp et al. 1984; Schätzl, Laszlo et al. 1997; Milhavet, McMahon et al. 2000; Nishida, Harris et al. 2000; Arjona, Simarro et al. 2004; Arima, Nishida et al. 2005; Nishida, Katamine et al. 2005)
SMB	Scrapie Mouse Brain cells	Mouse	139A, Chandler, 22F, 79A	(Clarke and Haig 1970; Birkett, Hennion et al. 2001; Kanu, Imokawa et al. 2002)
CAD5	CNS catecholaminergic cell line	Mouse	RML, 22L, ME7, 301C	(Mahal, Baker et al. 2007; Mahal, Browning et al. 2010; Browning, Baker et al. 2011)
PC12	Pheochromocytoma	Mouse	139A	(Rubenstein, Carp et al. 1984)
SN56	Septal neuronal cells	Mouse	Chandler, ME7, 22L	(Baron, Magalhaes et al. 2006)
NSC	Neuronal stem cells	Mouse	RML, 22L	(Giri, Young et al. 2006; Milhavet, Casanova et al. 2006)

MSC80	Schwann like cells	Mouse	Chandler	(Follet, Lemaire-Vieille et al. 2002)
HpL3-4	Hippocampal cells	Mouse	22L	(Maas, Geissen et al. 2007)
NIH/3T3, L929	Fibroblasts	Mouse	22L, ME7, RML	(Vorberg, Raines et al. 2004)
MG20	Microglial	Mouse	Chandler, mouse BSE, ME7	(Iwamaru, Takenouchi et al. 2007)
C2C12	Myoblasts	Mouse	22L	(Dlakic, Grigg et al. 2007)
HaB	Brain cells	Hamster	Hamster prions	(Taraboulos, Serban et al. 1990)
MovS	Schwann like from Dorsal Root Ganglia (DRG)	Mouse	Natural sheep scrapie	(Archer, Bachelin et al. 2004)
MDB	Fibroblast	Deer	CWD	(Raymond, Olsen et al. 2006)
CGN^{ov}	Neuronal primary cultures	Mouse	Natural sheep scrapie	(Cronier, Laude et al. 2004)
moRK13	Epithelial rabbit kidney cells (RK13)	Rabbit	Chandler, Fukuoka-1, 22L, M100	(Vella, Sharples et al. 2007; Courageot, Daude et al. 2008)
voRK13	Epithelial rabbit kidney cells (RK13)	Rabbit	Vole adapted BSE	(Courageot, Daude et al. 2008)
ovRK13	Epithelial rabbit kidney cells (RK13)	Rabbit	Natural sheep scrapie	(Vilette, Andreoletti et al. 2001)
RKE21⁺	Epithelial rabbit kidney cells (RK13)	Rabbit	Elk isolate CWD	(Bian, Napier et al. 2010)
RKD	Epithelial rabbit kidney cells (RK13)	Rabbit	Deer isolate CWD	Unpublished
RK13-SHa-PrP^C	Epithelial rabbit kidney cells (RK13)	Rabbit	Syrian golden hamster adapted Hyper TME	Unpublished

^aSY, mouse-adapted sporadic CJD (sCJD)

^bFU, mouse-adapted Fukuoka-1 (Familial GSS)

The first assay developed and described to convert PrP^C to PrP^{Sc} was the Cell-Free Conversion Assay (CFCA) (Kocisko, Come et al. 1994). This assay-utilized brain derived PrP^{Sc} as seed and radioactively labeled PrP^C, which, under the conditions described in the paper, created partially protease-resistant PrP molecules. The lack of exogenous energy sources to drive this assay is a key feature that makes it unique from all of the subsequently described assays. The assay was shown to be specific in recapitulating prion transmission barriers and strain properties (Bessen, Kocisko et al. 1995; Kocisko, Priola et al. 1995). Yet the primary limitation of the assay is detection and sensitivity due to the inherent difficulty of distinguishing newly generated PrP^{Sc} from initially seeded material (Hill, Antoniou et al. 1999). Although recent data has been described using this assay to identify disease specific low-density subcellular fractions composed of cell membrane and cytoplasmic proteins that enhance prion protein misfolding (Graham, Agarwal et al. 2010).

Protein misfolding cyclic amplification (PMCA) was the next in vitro conversion assay developed to amplify PrP^{Sc} (Saborio, Permanne et al. 2001). This reaction utilizes crude brain extract as PrP^C substrate in combination with PrP^{Sc} seed molecules, which are amplified through multiple cycles of sonication. Performing sequential rounds of PMCA enhances the sensitivity of the assay (Castilla, Saa et al. 2005), facilitating the detection of PrP^{Sc} from various biological and environmental sources (Castilla, Saa et al. 2006; Nichols, Pulford et al. 2009). This conversion assay has successfully been adapted to amplifying PrP^{Sc} from various animal species (Soto, Anderes et al. 2005; Kurt, Perrott et al. 2007; Murayama, Yoshioka et al. 2007; Green, Castilla et al. 2008; Thorne and Terry 2008).

PMCA and other in vitro conversion assays, provide an approach to validate the prion hypothesis. Utilizing PMCA, several groups have provided evidence that exogenous cofactors participate in prion conversion (Geoghegan, Valdes et al. 2007; Kim, Cali et al. 2010; Wang, Wang et al. 2010). PMCA was used to identify the three minimal components required to generate infectious recombinant prions, which were recombinant PrP (rPrP), POPG (1-palmitoyl-2-oleoylphosphatidylglycerol) and RNA (Wang, Wang et al. 2010). Concurrently, others reported the production of infectious prions using prion-seeded bacterially-derived recombinant protein misfolding cyclical amplification (rPMCA) in the absence of any co-factors (Kim, Cali et al. 2010). They go on to support this claim through bioassay experiments using hamsters, showing that at primary passage the rPMCA-produced prions display variable attack rates but stabilize upon second passage. Finally, PMCA was used to systematically analyze potential cofactors involved in prion conversion within various tissue sources and the effects of nucleic acid depletion in the conversion process (Abid, Morales et al. 2010). This study provided evidence that cellular cofactors for prion conversion that localize to the lipid raft fractions and cytoplasmic membranes are present within all major mammalian organs, but are absent in lower organisms such as yeast, bacteria and flies (Abid, Morales et al. 2010). Additionally, treatments to deplete major classes of chemical molecules did not alter conversion activity, which suggests that cellular cofactors that enable prion conversion are numerous and diverse (Abid, Morales et al. 2010). There are several caveats that must be taken into account when using the PMCA assay. This is an in vitro assay, which cannot fully recapitulate the phenomenon of PrP^C-PrP^{Sc} conformational switching that is associated with living organisms. The specific limitations of the assay

include the use of sonication to break aggregates of PrP^{Sc}, which does not recapitulate the cellular conversion mechanism. Moreover, this assay utilizes detergents, and cell extracts which are removed from the environment in which PrP^C is converted.

Finally, the Quaking-Induced Conversion Reaction (QuIC) and the real-time Quaking-Induced Conversion Reaction (RT-QuIC) are additional in vitro conversion assays utilized for identifying cellular cofactors that facilitate PrP^{Sc} conversion. This assay was first described in 2008, and differs from other conversion assays by methods used to amplify PrP^{Sc} (Atarashi, Wilham et al. 2008). In QuIC, periodic shaking replaces sonication. Like PMCA, QuIC can successfully discriminate between infected and uninfected biological samples (Atarashi, Wilham et al. 2008; Orru, Wilham et al. 2009; Bessen, Shearin et al. 2010). Additionally, the QuIC was improved with supplementation of thioflavin T (ThT) and the use of a temperature-controlled fluorescence plate reader, to continuously monitor of newly produced PrP^{Sc} in real time (Wilham, Orru et al. 2010). Due to its sensitivity, high throughput, real-time quantitation and relatively low costs, the QuIC assay is highly advantages for studying prion conversion in vitro.

In summary, the approaches used for examining PrP biology have significantly improved our understanding the mechanisms that govern prion replication and disease. More generally, prion research models aid in the understanding of other conformational diseases such as AD and PD. The transmissibility of prions in transgenic mice expressing heterologous PrP^C on a *Prnp*^{0/0} background recapitulates prion disease that can be assessed on multiple levels, this is generally not the case for AD or PD animal models. Moreover, transgenic animal models enable characterization of natural prion isolates, and model the risks associated with their transmission to other species, including humans. In

vivo PrP^{Sc} conversion can also be analyzed in vitro using cell culture models and cell-free conversion assays (Castilla, Saa et al. 2006; Green, Castilla et al. 2008; Bian, Napier et al. 2010; Wang, Wang et al. 2010; Goold, Rabbanian et al. 2011; Nunziante, Ackermann et al. 2011). Cell culture models have been useful for understanding the fundamental cellular biology of PrP^C and for identifying cellular compartments crucial for PrP^{Sc} conversion (Shyng, Heuser et al. 1994; Vey, Pilkuhn et al. 1996; Pauly and Harris 1998; Goold, Rabbanian et al. 2011), while in vitro conversion assays provide a facile system for detecting, converting and generating novel PrP^{Sc} molecules (Wong, Xiong et al. 2001; Castilla, Saa et al. 2005; Deleault, Geoghegan et al. 2005; Castilla, Saa et al. 2006; Kurt, Perrott et al. 2007; Green, Castilla et al. 2008; Mays, Yeom et al. 2011).

III: PrP Interacting Molecules

The specific cellular mechanisms that support and sustain prion replication remain undefined. The inherent difficulty of generating infectious prions *in vitro* without exogenously added cellular components strongly argues towards the requirement of endogenous host factors (Supattapone, Deleault et al. 2008; Wang, Wang et al. 2010; Piro, Harris et al. 2011). Cellular host factors have been shown to be essential components for other invading pathogens, which act to enhance factors such as infectivity, replication and/or protection. For example, the HIV retrovirus requires the CD4 cell surface receptor parallel with other co-receptors for efficient entry into the host cell (Doms and Moore 2000), Mycobacterium tuberculosis utilizes lipid raft micro domains to gain entry into both phagocytic and non-phagocytic cells (Munoz, Rivas-Santiago et al. 2009), and bacteria utilize several different adhesion molecules that recognize the host cell surface for internalization (Pizarro-Cerda and Cossart 2006).

Although the infectious entities described above, vary in composition and life cycle, they follow the central dogma of molecular biology (Fig. 1.3A). To explain and characterize the infectious protein only (PrP^C-PrP^{Sc}) replication process in the cell, several important concepts were proposed.

Initial experiments were designed to characterize the normal biogenesis and life cycle of PrP^C, and to identify interacting proteins. Evidence that PrP^C endocytosis was mediated through clathrin-coated pit internalization indicated that other proteins are involved (Shyng, Heuser et al. 1994). PrP^C protein is predominantly GPI-anchored at the cell surface (Fig 1.1B) lacking a cytoplasmic domain, which suggests that active internalization via clathrin-coated pit endocytic mechanism could only occur if there was direct interaction with an extracellular domain of a proximal transmembrane protein (Shyng, Heuser et al. 1994).

Other experimental evidence using chimeric-PrP molecules in vivo suggested that a species-specific cellular chaperone termed “Protein X” was required to for prion replication (Telling, Scott et al. 1995). Nuclear magnetic resonance (NMR)-derived structural data demonstrated variation in the putative “Protein X” binding site, implying that structural constraints of PrP^C are also important for efficient prion conversion (Gossert, Bonjour et al. 2005). Additional approaches have been utilized to identify cellular proteins that facilitate PrP^{Sc} replication. This ongoing exhaustive search for interacting molecules has already helped identify both extracellular and intracellular proteins/molecules alongside metal ions (Brown 1999), nucleic acids (DNA/RNA) (Weiss, Proske et al. 1997) and glycosaminoglycans (GAG) (Priola, Caughey et al. 1994) that interact with PrP.

III-A: Protein X

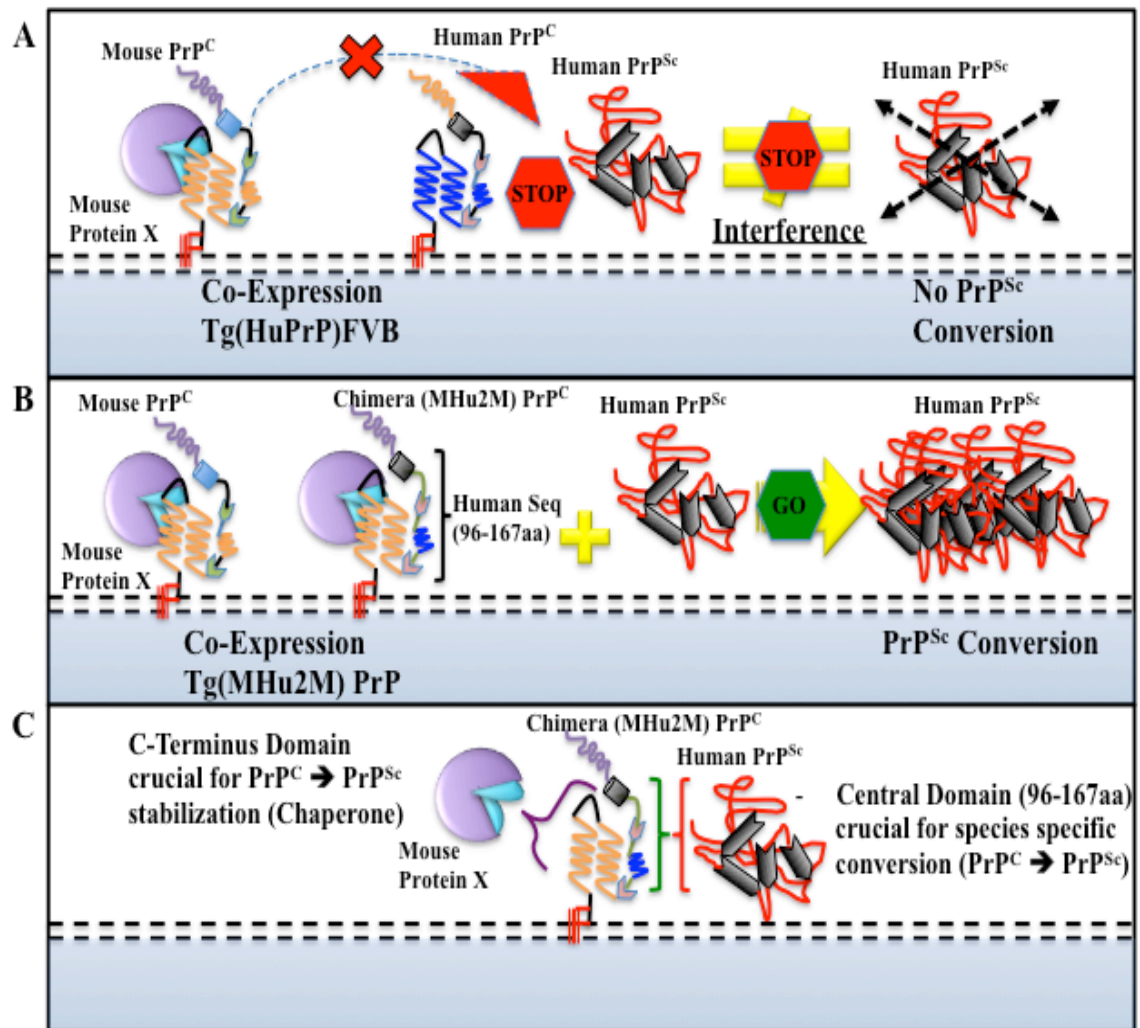
Transmission studies in transgenic mice provided evidence for the involvement of a third molecule termed protein X in the replication process. Initial experiments in cell culture to identify PrP^C's structural domains contribution towards PrP^{Sc} conversion provided indications that the first 66aa of the N-terminus and the GPI-anchor sequence of the C-terminus were unnecessary (Rogers, Yehiely et al. 1993). Additionally, prion infectivity data using transgenic mice supported the protein X model. The prion species barrier data using transgenic mice expressing human PrP^C on both wild type FVB and *Prnp*^{0/0} mice, indicated that endogenously expressed mouse PrP^C in mice co-expressing human PrP^C (Tg(HuPrP)FVB) inhibited the replication of human PrP^{Sc} (Fig. 1.4A) (Telling, Scott et al. 1995). While, expression of a human/mouse chimera PrP^C (MHu2M, 96-167aa human sequence) in transgenic mice exhibited efficient replication of human but not mouse PrP^{Sc} in Tg(MHu2M)*Prnp*^{0/0} although both PrP^{Sc} replicated in Tg(MHu2M)FVB wt mice (Fig. 1.4B) (Telling, Scott et al. 1994; Telling, Scott et al. 1995). These data suggested that two domains in the PrP^C sequence were required for prion replication, including the central domain of PrP^C (96aa-167aa) for PrP^C-PrP^{Sc} direct interaction, and the C-terminal domain which binds the predicted protein X to stabilize/chaperone the replicative process (Fig. 1.4C) (Telling, Scott et al. 1994; Telling, Scott et al. 1995). Protein X was suggested to have enhanced affinity for endogenous mouse PrP^C compared to overexpressed heterologous PrP^C.

Following the prediction that protein X binds the C-terminus of PrP^C, mutations were introduced at positions 214 and 218 of the human/mouse chimera PrP, to assess their role in PrP^{Sc} formation (Kaneko, Zulianello et al. 1997). These two specific residues

were predicted to protrude from α -helix 3 and form a discontinuous epitope with residues 167 and 171, a region suggested to be crucial for PrP^C-PrP^{Sc} replication (Donne, Viles et al. 1997; James, Liu et al. 1997; Kaneko, Zulianello et al. 1997). Using the ScN2a cell culture model to assess PrP^{Sc} replication (Table 1.2), it was demonstrated that these mutations inhibited PrP^{Sc} formation, suggesting that these amino acid form an epitope for protein X and facilitate PrP^{Sc} conversion (Kaneko, Zulianello et al. 1997). Moreover, NMR analysis of residues connecting β -sheet 2 with α -helix 2 (166-175aa, Fig. 1.1A) demonstrates variation in structural definition amongst species within that region ranging from highly structured to unstructured, which coincidentally includes the residues predicted to interact with C-terminal positions 214 and 218 (Gossert, Bonjour et al. 2005). Although it is hypothesized that PrP^C regions encompassing residues 166-175aa, 215aa and 218aa are crucial for the formation of the disease related epitope protein X, the identification of protein X has not been possible (Telling, Scott et al. 1995; Riek, Hornemann et al. 1996; James, Liu et al. 1997; Kaneko, Zulianello et al. 1997; Gossert, Bonjour et al. 2005).

Figure 1.4 Schematic representation of the protein X hypothesis. A. Over expression of human PrP^C in an FVB wt mouse referred to as Tg(HuPrP)FVB does not facilitate the replication and conversion of human PrP^{Sc}, while expression of human PrP^C on a *Prnp*^{0/0} background results in prion disease (not shown in figure). These findings indicate that endogenously expressed mouse PrP^C interferes in the replication of human prions. **B.** Inoculation of human prions into mice expressing mouse/human chimeric PrP^C protein in a wt FVB mouse, referred to as Tg(MHu2M)FVB produces PrP^{Sc} and recapitulates prion disease. The chimeric PrP^C was designed by replacing the central region of the mouse PrP protein with human sequence 96-167 aa, encompassing the hydrophobic core, β -sheet 1, α -helix 1 and β -sheet 2 (see Figure 1.1A for schematic details). **C.** The replication of human prions in Tg(MHu2M)FVB mice indicates that a third molecule, termed protein X, facilitates replication through a chaperoning/stabilizing mechanism. Hence, two domains are deemed crucial for PrP^{Sc} replication; the central domain, which dictates the compatibility between the infecting PrP^{Sc} and the endogenously expressed PrP^C; the C-terminal domain (α -helices 2 and 3) dictate the interactions with protein X. (Telling, Scott et al. 1994; Telling, Scott et al. 1995)

Figure 1.4 Schematic representation of the protein X hypothesis



III-B: PrP^C Binding Partners

The surface of the plasma membrane and endosomal compartment trafficking pathways are implicated as the primary locations for conversion of PrP^C-PrP^{Sc} (DeArmond, Qiu et al. 1996; Marijanovic, Caputo et al. 2009; Sarnataro, Caputo et al. 2009; Goold, Rabbanian et al. 2011; Nunziante, Ackermann et al. 2011). Many of the proteins that interact with PrP^C are located in these cellular compartments. Table 1.3 represents the majority of proteins that have been determined to interact with PrP^C, while figures 1.5 and 1.6 schematically depict these interactions. The proteins described thus far have been experimentally validated as binding partners through multiple biophysical and immune-based assays. Recent studies using large-scale proteomic analysis identified additional PrP^C interacting proteins but are not described in this section because validation to ascertain relevance in prion biology is lacking (Satoh, Obayashi et al. 2009; Zafar, von Ahsen et al. 2011). Experimentally validated evidence suggests that PrP^{Sc} replication includes cell-surface receptors, along with other chaperone proteins which are present at the surface, to support the stabilization and internalization of the PrP^C-PrP^{Sc} complex, leading towards intracellular accumulation of infectious PrP^{Sc} with the aid of intracellular proteins (Table 1.3).

III-B-1 Extracellular Interactors

The extracellular/plasma membrane molecules identified to associate with PrP include receptor proteins, adhesion proteoglycans with glycosaminoglycan (GAG) moieties, chaperone proteins, zymogen proteolytic enzymes, metal ions and other aggregating peptides. These are listed in Table 1.3 and schematically presented in Figure 1.5. These associations implicate PrP's involvement in internalization and endocytic

trafficking, intracellular signal cascade activation, survival, and ion homoeostasis. Evidence for these functions include cell explant data demonstrating PrP^C neuroprotective signaling potential through a cAMP/PKA-dependent pathway (Chiarini, Freitas et al. 2002) and conversely activating signaling cascades that induce cell death in vivo (Solforosi, Criado et al. 2004). These, and other observations subsequently described, suggests that PrP is a multifaceted protein involved in many cellular processes.

III-B-2: PrP Internalization and Signaling From The Cell Surface

As mentioned in previous sections, the predominant GPI-anchorage of PrP to lipid rafts of the PM and subsequent endocytosis using either the clathrin-coated pit- (Shyng, Heuser et al. 1994) and/or caveolin-mediated mechanisms (Vey, Pilkuhn et al. 1996) strongly advocates direct interaction with a surface receptor. Yeast two-hybrid (Y2H) studies revealed strong interaction between the 37-kDa laminin receptor precursor (LRP) and PrP^C, which were subsequently confirmed in higher order eukaryotic cells. These studies suggested that LRP was act as the receptor and/or co-receptor for PrP^C (Rieger, Edenhofer et al. 1997). Additional studies confirmed that both LRP and the mature 37-kDa/67-kDa laminin receptor (LR) interact with PrP^C and PrP^{Sc} at the cell surface, and in endosomal compartments during the internalization process (Table 1.3) (Fig. 1.5A) (Shmakov, Bode et al. 2000; Gauczynski, Peyrin et al. 2001; Baloui, von Boxberg et al. 2004; Nikles, Vana et al. 2008; Kolodziejczak, Da Costa Dias et al. 2010). Furthermore, the use of anti-LRP/LR specific antibodies, single-chain fragment antibodies and polysulfated glycans inhibited prion replication in vivo (Gauczynski, Nikles et al. 2006; Zuber, Knackmuss et al. 2008; Zuber, Mitteregger et al. 2008; Vana, Zuber et al. 2009).

Collectively, these findings indicate that interactions between PrP and LRP/LR are functionally relevant.

Several additional studies have revealed other transmembrane receptors proteins that interact with PrP, which possibly induce endosomal internalization mechanisms and/or initiate intracellular signaling cascades. Dystroglycan, is a transmembrane protein associated with the dystrophin-glycoprotein complex (DGC) that exhibited strong binding interaction with PrP (Keshet, Bar-Peled et al. 2000). The DGC modulates the activity of nitric oxide synthase (nNOS), which subsequently synthesizes nitric-oxide (Bredt and Snyder 1994), a neurotransmitter with crucial functions in muscle and CNS (Kobzik, Reid et al. 1994; Keshet, Ovadia et al. 1999). Although the exact function for PrP in the DGC has not been established, a protective role associated with presynaptic neuroprotection has been hypothesized (Keshet, Bar-Peled et al. 2000). Conversely, the p75 neurotrophin receptor's affinity towards recombinant PrP peptides caused internalization, which subsequently induced cytotoxic effects (Fig. 1.5A, described in the next section) (Della-Bianca, Rossi et al. 2001). Recent experimental findings have revealed binding association of amyloid- β to PrP^C, designating PrP^C as a receptor that mediates cytotoxic signaling (Fig. 1.5A) (Lauren, Gimbel et al. 2009; Resenberger, Winklhofer et al. 2011). In addition to transmembrane receptors, internalization of PrP^C has also been demonstrated using Cu²⁺ and other positively charged metal ions (Hornshaw, McDermott et al. 1995; Pauly and Harris 1998; Stockel, Safar et al. 1998; Wadsworth, Hill et al. 1999; Brazier, Davies et al. 2008; Li, Dong et al. 2009; Liu, Jiang et al. 2011; Stellato, Spevacek et al. 2011).

III-B-3: Outgrowth/Adhesion and Neuroprotection Functions

In situ cross-linking experiments using N2a cells led to the identification of high molecular mass (HMM) protein complexes (200-225 kDa), which included the presence PrP^C (Schmitt-Ulms, Legname et al. 2001). Proteomic analyses of these HMM protein complexes revealed the presence of neuronal adhesion molecules (N-CAM's). Subsequent binding studies using N-CAM peptide-library indicated that PrP^C's N-terminus and α -helix bound to the membrane attachment site of N-CAM (Schmitt-Ulms, Legname et al. 2001). Comparable levels of PrP/N-CAM complexes were identified in both N2a and ScN2a cells (Schmitt-Ulms, Legname et al. 2001). To ascertain the functional role of this PrP^C-N-CAM interaction, N-CAM-deficient mice were challenged with scrapie prions, which resulted in prion disease with incubation time of ~122 days (Schmitt-Ulms, Legname et al. 2001). Elimination of N-CAM molecules in transgenic mice did not alter prion disease incubation time compared to control mice. Thus, the interaction between these two molecules indicates a physiological function not associated with PrP^{Sc} conversion (Schmitt-Ulms, Legname et al. 2001). Additional evidence for PrP^C's interactions with N-CAM's has implicated a physiological role in neurite outgrowth and adhesion (Santuccione, Sytnyk et al. 2005). These findings provide direct evidence of PrP interaction with N-CAM at the neuronal surface, activating N-CAM mediated signaling through Fyn kinase activation (Santuccione, Sytnyk et al. 2005). The disruption of this interaction using neurons deficient in N-CAM's or PrP^C, and/or use of anti-PrP antibodies, arrested neurite outgrowth (Santuccione, Sytnyk et al. 2005). Additional experimental evidence has associated the extracellular matrix protein, Vitronectin, as another protein capable of binding PrP to induce axonal growth and neurite development (Hajj, Lopes et al. 2007; Hajj, Santos et al. 2009). Collectively,

these data strongly support a physiological role for PrP in neuronal outgrowth/adhesion through cooperative interaction with the N-CAM signaling receptors and extracellular matrix proteins (Fig. 1.5B).

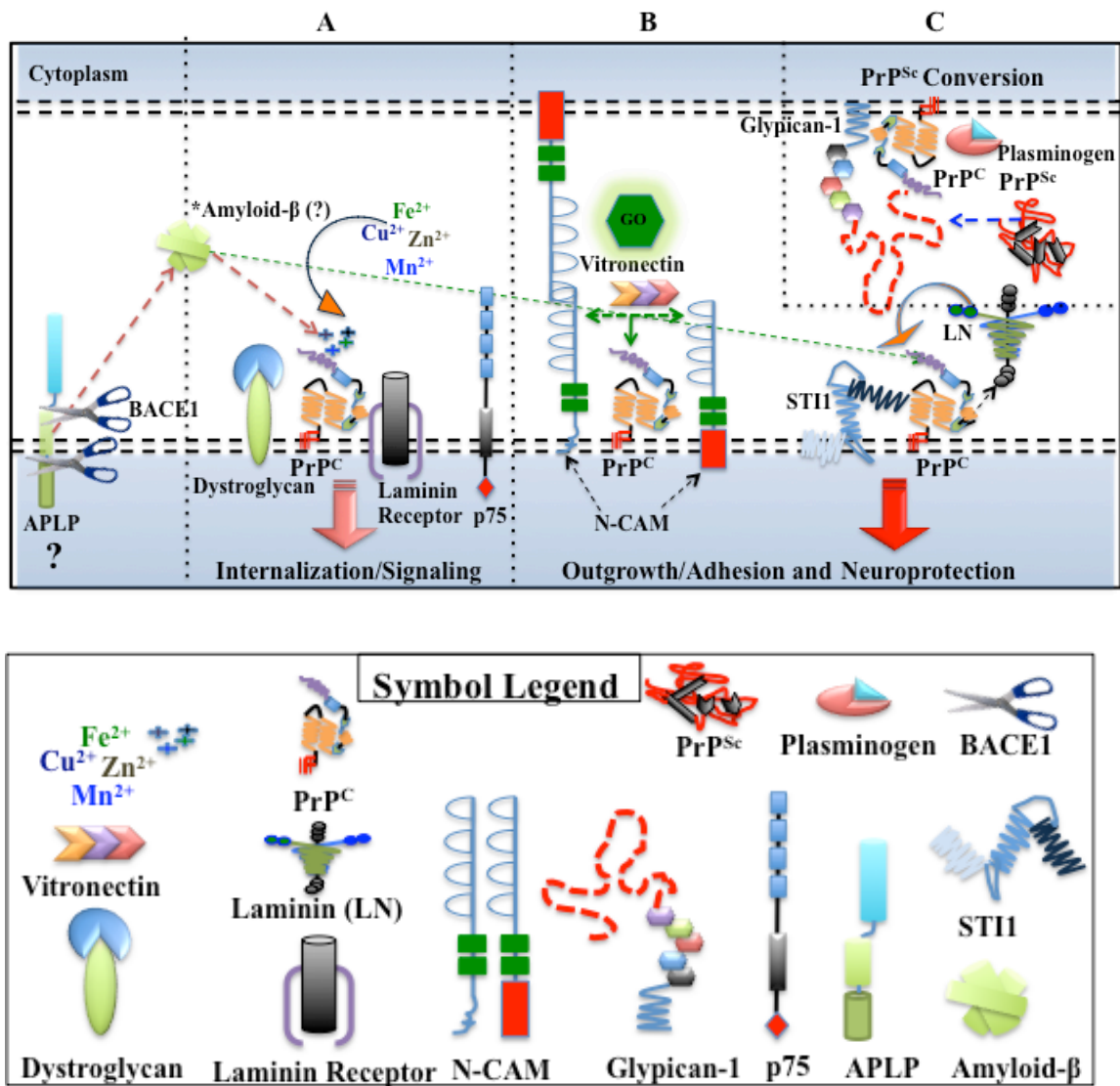
PrP^C's role in neuroprotection is mediated through the interaction with several proteins at the cell surface and other subcellular locations. The extracellular matrix protein, laminin (LN), triggers cellular responses through direct interactions with cell-surface receptors such as integrins, to promote neurite outgrowth, regeneration and neuroprotection (Tomaselli and Reichardt 1988; Tashiro, Sephel et al. 1989). To address PrP^C's role in neuronal development and neuroprotection, binding assays and cell culture experiments were utilized to identify LN's interaction with PrP^C (Graner, Mercadante et al. 2000). These studies demonstrated that PrP^C binds LN with high affinity with epitope specificity towards the C-terminus of the γ -1 chain (Graner, Mercadante et al. 2000). Interestingly, several studies have specified the role of the γ -1 chain in neurite outgrowth in neocortical and hippocampal neurons (Liesi, Narvanen et al. 1989; Hager, Pawelzik et al. 1998). PC12 cells (Table 1.2) and explant rat-neuronal cell culture models provide additional data supporting the direct interaction between PrP^C and LN to promote neuritogenesis, demonstrating direct reduction of growth in the cells upon addition of anti-PrP antibodies (Graner, Mercadante et al. 2000). Although these experimental observations support PrP^C's role as a receptor for LN to promote neuritogenesis, the signaling cascades governing these interactions have not been identified. It is important to remember that the ablation of the *Prnp* gene in mice does not inhibit CNS development (Bueler, Fischer et al. 1992), suggesting signal pathway redundancy that regulates these important functions. Interestingly, LN has also been shown to bind

amyloid-precursor protein (APP) and amyloid- β (Narindrasorasak, Lowery et al. 1992), which very recently was associated to directly interact with PrP^C (Fig. 1.5B) (Lauren, Gimbel et al. 2009; Kessels, Nguyen et al. 2010; Resenberger, Winklhofer et al. 2011).

PrP^C has been reported to interact with the stress-inducible protein 1 (STI1) at the PM to induce neuroprotective signaling. Cell-surface binding studies, co-IP and binding assays confirmed these interactions, which showed that PrP^C (epitope mapped residues 113-128aa) bound STI1 with high affinity (K_d of 10^{-7} M) to a mapped region designated for neuroprotective signaling (Fig. 1.5B) (Zanata, Lopes et al. 2002). These interactions were confirmed using retinal explant cultures from neonatal rats and, while hypothesis driven interactions of PrP^C, LN and ST1 to form a macromolecular complex in the extracellular space/cell-surface to provide cytoprotective functions were suggested but the exact mechanisms of the interactions were not defined (Zanata, Lopes et al. 2002).

Figure 1.5 Molecules associated with PrP interaction in the extracellular/plasma membrane space. Extracellular and cell surface molecules that demonstrate physical interaction with PrP are predicted to modulate functions associated with PrP^C and/or PrP^{Sc} conversion process. These associated functions include **(A)** Internalization of PrP into the endocytic trafficking pathways (Clathrin coated pit- and/or Caveolin mediated mechanisms) and/or direct association with transmembrane proteins to perform receptor-type functions (Signaling), **(B)** Outgrowth/adhesion and/or neuroprotection of neurons, and **(C)** Protein molecules associated with the conversion process of PrP^C to PrP^{Sc}. The details of specific interactions between these molecules and PrP (PrP^C, PrP^{Sc}), which include mode of interaction/binding, location specificity and references describing the findings, are summarized in Table 1.3. The question marks (?) in the schematic represent an unknown interaction/function. The asterisk (*) before Amyloid- β represents its direct binding with PrP^C with undefined mechanisms and/or functions associated with the interaction. **Abbreviations:** Neuronal cell-adhesion molecule (N-CAM), Amyloid precursor like protein 1 (APLP1), Stress-induced Phosphoprotein (STI1), β -secretase 1 (BACE1), Laminin (LN), Cellular prion protein (PrP^C), Scrapie prion (PrP^{Sc}), Iron (Fe), Copper (Cu), Zinc (Zn), Manganese (Mn).

Figure 1.5 Molecules associated with PrP interaction in the extracellular/plasma membrane space.



III-B-4: PrP^C-PrP^{Sc} Conversion At The Cell Surface

The cell surface is hypothesized to be the predominant location for PrP^{Sc} conversion (Goold, Rabbanian et al. 2011). A recently identified cell surface protein correlated with prion conversion is Glypican-1. Glypican-1 is a PM associated, GPI-anchored, heparin sulfate containing proteoglycan co-localized with PrP^C to lipid rafts (Fig. 1.5C) (Cheng, Lindqvist et al. 2006). Also, the addition of Cu²⁺ ions stimulates endocytosis of PrP^C, which co-internalizes Glypican-1 from the cell surface (Cheng, Lindqvist et al. 2006). In cell culture models, heparin was shown to displace PrP^C from lipid rafts, directly inducing endocytosis, suggesting that heparin acts as a direct competitor with endogenous heparin sulphate proteoglycans (HSPG) for PrP^C binding (Taylor, Whitehouse et al. 2009). Likewise, the depletion of glypican-1 displaced PrP^C from lipid rafts triggering internalization into endosomal compartments. Additional co-localization and co-immuno precipitation (co-IP) assays confirmed the interaction between glypican-1 and PrP^C (Taylor, Whitehouse et al. 2009). The relevance of these interactions to PrP^{Sc} conversion was confirmed in ScN2a cells (Table 1.2), where down regulation of glypican-1 showed significant reduction in PrP^{Sc} formation (Taylor, Whitehouse et al. 2009). Interestingly, previously published data using heparin and glycosaminoglycans (GAG) have exhibited an inhibitory effect on prion conversion in both cell culture and animal models (Kimberlin and Walker 1986; Caughey and Raymond 1993; Beringue, Adjou et al. 2000; Adjou, Simoneau et al. 2003). In contrast GAGs promote the conversion process in cell-free systems (Wong, Xiong et al. 2001; Deleault, Geoghegan et al. 2005).

GAG's are sulfated polysaccharides that maintain a net negative charge. These molecules were shown to be present in amyloid plaques in CJD, GSS, and Kuru (Snow, Kisilevsky et al. 1989). To clarify the relationship of GAG's with amyloid aggregates, functional studies were conducted to assess their role in PrP^{Sc} conversion. Like other HSPG's found on the cell surface, Glypican-1 is competed out by the addition of exogenous GAG's (Taylor, Whitehouse et al. 2009). Inhibition of PrP^{Sc} conversion occurs through an obstructive mechanism, which directly inhibits contact of cellular HSPG's with PrP^C. It suggests that these molecules function as direct scaffolds to promote interaction between PrP^C and PrP^{Sc} to enhance conversion (Hooper 2011). Finally, siRNA depletion of glypican-1 in ScN2a cells reduced but did not completely inhibit PrP^{Sc} conversion (Taylor, Whitehouse et al. 2009), which suggests that PrP^{Sc} conversion is dependent on multiple cellular cofactors (Fig 1.5C). Although the exact mechanisms that govern these interactions require more experimental characterization, the effect of GAG's on PrP^{Sc} conversion provides additional insight towards the global complexity PrP^{Sc} replication process.

Another cellular factor exhibiting association with PrP^{Sc} conversion is plasminogen (PLG). Plasminogen (PLG) is a zymogen precursor to plasmin, a serine protease that functions to dissolve fibrin blood clots (Forsgren, Raden et al. 1987). The activation and conversion of PLG is mediated by the tissue plasminogen activator enzyme (tPA) and/or urokinase plasminogen activator (uPA) (Silverstein, Leung et al. 1984). Interaction studies analyzing potential binding partners of PrP^C have identified plasminogen as one of the key proteins that interacts with both PrP^C and PrP^{Sc} (Fig. 1.5C) (Fischer, Roeckl et al. 2000; Maissen, Roeckl et al. 2001; Ryou, Prusiner et al. 2003).

Screening human and mouse serum for prion binding factors showed that plasminogen was capable of binding disease-associated PrP but not PrP^C, which suggested that the interaction was conformation specific (Fischer, Roeckl et al. 2000). PrP devoid of bound copper was shown to interact with both tPA and PLG, which caused PLG activation in a copper-dependent manner (Ellis, Daniels et al. 2002). This PrP mediated activation of PLG together with copper levels was suggested to be an indicators for the kinetics of PrP^{Sc} conversion, therefore linking PLG as a cellular cofactor (Ellis, Daniels et al. 2002). In studies designed for identifying “protein X”, phage display cDNA expression library methods were used to establish PrP^C interaction with kringle domains (Ryou, Prusiner et al. 2003). These kringle domains consist of ~80aa that have three intra-disulfide bonds between cysteine residues (Castellino and McCance 1997). PLG has five of these kringle domains originating in the N-terminus (Castellino and McCance 1997). Thus, an unbiased forward genetic screen confirmed interaction of PrP^C with PLG (Ryou, Prusiner et al. 2003). Recent data using PMCA supported the role of PLG in a concentration-dependent manner to accelerate the PrP^{Sc} conversion process (Mays, Yeom et al. 2011). However, plasminogen-deficient (Plg^{-/-}) mice infected with scrapie revealed no major effect on the survival of these infected mice (Salmona, Capobianco et al. 2005). Collectively, the biochemical data indicates that plasminogen is an important cofactor for PrP^{Sc} conversion. However, its exact role in prion disease remains to be characterized.

In summary, the interaction of PrP^C with protein molecules at the cell surface is multidimensional, (Fig. 1.5) suggesting that PrP^C has several important physiological functions that remain to be fully validated. These functions may include the activation of

intracellular signaling cascades, which promote neuritogenesis, neuroprotection and/or other intracellular roles that have not yet been defined.

III-C: Intracellular Interactors

PrP^C intracellular trafficking and continuous recycling to- and -from the PM (Fig. 1.2) suggests that PrP^C-PrP^{Sc} conversion is not limited to the cell surface. The specific intracellular compartments where this conversion occurs have not been specifically identified but experimental evidence supports the importance for endosomal, lysosomal and exosomal compartments in this process (Taraboulos, Serban et al. 1990; Borchelt, Taraboulos et al. 1992; Taraboulos, Raeber et al. 1992; Gilch, Winklhofer et al. 2001; Aguib, Heiseke et al. 2009; Nunziante, Ackermann et al. 2011). PrP^C has been shown to interact with proteins that mediate cell survival pathways (Kurschner and Morgan 1995), internalization and vesicle trafficking (Borchelt, Taraboulos et al. 1992; Taraboulos, Raeber et al. 1992), aggregation/chaperone/protein folding responses (Fernandez-Funez, Casas-Tinto et al. 2009; Nunziante, Ackermann et al. 2011) and other proteins which have not been specified with a PrP-interacting function (Strom, Diecke et al. 2006) . A comprehensive list of the proteins shown to interact with PrP^C within intracellular compartments is presented in Table 1.3 and schematically depicted in Figure 1.6.

Table 1.3 Prion protein interacting molecules. All data presented is formulated and adapted from previously published reviews (Lee, Linden et al. 2003; Fasano, Campana et al. 2006; Nieznanski 2010)

PrP ^C Interacting Molecules	PrP Type/Technique	Cellular Location	Function
Extracellular/Cell Surface/Plasma Membrane			
Plasminogen (PLG) (Fischer, Roeckl et al. 2000; Maissen, Roeckl et al. 2001; Ellis, Daniels et al. 2002; Mays and Ryou 2010)	PrP ^C -PrP ^{Sc} /Y2H, Cells, PMCA	Extracellular /Raft	Zymogen (Plasmin Precursor), Proteolytic enzyme
Laminin (LN) (Graner, Mercadante et al. 2000; Musinova, Lisitsyna et al. 2011)	rPrP ^C -PrP ^C /Cells and cell free	Plasma Membrane (PM)/Cell Surface	Neurite Outgrowth
Laminin Receptor/Precursor (Rieger, Edenhofer et al. 1997; Gauczynski, Peyrin et al. 2001; Hundt, Peyrin et al. 2001; Gauczynski, Nikles et al. 2006; Nikles, Vana et al. 2008; Kolodziejczak, Da Costa Dias et al. 2010)	PrP ^C /Y2H, Cell lines	Plasma Membrane	Internalization
Dystroglycan (Keshet, Bar-Peled et al. 2000)	PrP ^C /co-IP, co-Localization, co-Fractionate	Plasma Membrane	Copper Homeostasis/Unknown
Vitronectin (Hajj, Lopes et al. 2007; Hajj, Santos et al. 2009)	PrP ^C / Overlay, co-Localization, Binding & Competition Assay, Pull-Down	Plasma Membrane	Axonal Growth
Neuronal cell adhesion molecule (N-CAM) (Schmitt-Ulms, Legname et al. 2001; Santuccione, Sytnyk et al. 2005)	PrP ^C /Cell lines	Plasma Membrane, Caveolae	Neurite outgrowth/ Internalization
Glypican-1 (Taylor, Whitehouse et al. 2009; Hooper 2011)	PrP ^C -PrP ^{Sc} /cell models, Co-IP	Lipid Rafts, Plasma Membrane	PrP ^{Sc} conversion, Cell division/growth Regulation
Metalloproteinases; A Disintegrin And	PrP ^C -PrP ^{Sc} /Cell-Culture models	Plasma Membrane	PrP Cleavage

Metalloproteinase (ADAM), Matrix Metalloproteinase (MMP) (Vincent, Paitel et al. 2001; Mange, Beranger et al. 2004; Parkin, Watt et al. 2004; Cisse, Sunyach et al. 2005; Hooper 2005; Taylor, Parkin et al. 2009)			
Amyloid precursor like protein 1 (APLP1) (Yehiely, Bamborough et al. 1997)	rPrP ^C fragment/cDNA library screen	Plasma Membrane	Unknown
Stress-Induced Phosphoprotein (STI1) (Chiarini, Freitas et al. 2002; Zanata, Lopes et al. 2002; Hajj, Santos et al. 2009)	PrP ^C	Plasma Membrane	Neuroprotection
p75 (Della-Bianca, Rossi et al. 2001)	PrP ^C /Cell Culture	Plasma Membrane, Caveolae	Apoptosis, Internalization, Transport
Tetraspanin-7 (CD231) (Guo, Huang et al. 2008)	PrP ^C /Y2H, Co-localization, IP	Plasma Membrane	Internalization
Glycosaminoglycan (GAG) (Priola, Caughey et al. 1994; Wong, Xiong et al. 2001; Pan, Wong et al. 2002)	PrP ^C /Cell Culture, Y2H	Plasma Membrane	
Clusterin (Xu, Karnaukhova et al. 2008)	PrP ^C /Y2H, co-IP, CD	Plasma Membrane, Cytosol, ER	Chaperone
Amyloid-β (Lauren, Gimbel et al. 2009; Balducci, Beeg et al. 2010; Kessels, Nguyen et al. 2010; Resenberger, Winklhofer et al. 2011; Tofoleanu and Buchete 2012)	PrP ^C /Aβ-Biotin in cell culture, SPR	Plasma Membrane, Extracellular	Transcytosis, Undefined
β-secretase 1 (BACE1) (Parkin, Watt et al. 2007; Griffiths, Whitehouse et al. 2011) (Parkin, Watt et al. 2007; Griffiths, Whitehouse et al. 2011)	PrP ^C / Co-IP, ELISA, SPR	Plasma Membrane, Endosomes	Proteolytic enzyme cleaves APP
Metal Ions (Cu, Mn, Fe, Zn) (Brazier, Davies et al.	rPrP ^C , PrP ^C /Cyclic-	Extra-, Intra cellular	Ion homeostasis, Internalization

2008; Zhu, Davies et al. 2008; Li, Dong et al. 2009; Singh, Mohan et al. 2009; Liu, Jiang et al. 2011; Martin, Anantharam et al. 2011; Pushie, Pickering et al. 2011; Stellato, Spevacek et al. 2011; Younan, Klewpatinond et al. 2011)	Voltammetrics, UV- Spectroscopic, ITC, CD		
Intracellular Interacting Molecules			
Aβ-Crystallin (Sun, Guo et al. 2005)	PrP ^C /Y2H, cDNA Library, co-localization, SPR	Cytosol	Undetermined
Heat-Shock 60-KD Protein 1(HSPD1/HSP60) (Stockel and Hartl 2001; Satoh, Onoue et al. 2005; Alexeeva, Valieva et al. 2011)	rPrP, PrP ^C /cDNA Library Screen, Cell Free	Plasma Membrane	PrP Aggregation
Caveolin-1 (Mouillet- Richard, Ermonval et al. 2000; Vana, Zuber et al. 2007; Schneider, Pietri et al. 2011)	rPrP ^C /Cell lines	Caveolae Rafts	Signaling
Nuclear factor erythroid 2-like2 (Nrf2) (Yehiely, Bamborough et al. 1997)	rPrP/Phage screen of expression library from brain cDNA	Cytosol, Nucleus	Unknown
Synapsin 1b (Spielhaupter and Schatzl 2001)	rPrP, PrP ^C / Y2H, co-IP, co- fractionation	Cytosol, Vesicles	Signaling, Internalization
Growth factor receptor- bound protein 2 (Grb2) (Spielhaupter and Schatzl 2001; Lysek and Wuthrich 2004)	rPrP, PrP ^C , PrP ^{Sc} /Y2H, co- IP, co- fractionation	Cytosol, Nucleus, Vesicles	Internalization
Prion interactor-1 (Pint1) (Spielhaupter and Schatzl 2001)	rPrP ^C , PrP ^C /Y2H, cell culture	Unknown	Signaling, Internalization, Transport
Casein Kinase II (Ck2) (Meggio, Negro et al. 2000; Negro, Meggio et al. 2000)	rPrP, PrPC/ pull- down, overlay, SPR, co-IP	Cytosol, Nucleus, Extracellula r Matrix	Kinase Activity, Internalization
B-cell CLL/Lymphoma	rPrP,	Cytosol	Loss of Bcl-2

(Bcl-2) (Kurschner and Morgan 1995; Rambold, Miesbauer et al. 2006; Lisitsyn 2010)	cytoPrP/Y2H, co-IP, Affinity		function, induction of Apoptosis
Glial Fibrillary Acidic Protein (GFAP) (Oesch, Teplow et al. 1990; Dong, Wang et al. 2008)	rPrP, PrP ^C , PrP ^{Sc} / Pull-Down, Overlay, co-IP	Cytosol	Unknown
Heat-Shock 70-KD Protein 5 (HSPA5/Bip) (Jin, Gu et al. 2000)	PrP ^C , Mutant PrP/Cell Lines	Endoplasmic Reticulum (ER)	Chaperoning
Nucleic Acids (Cordeiro, Machado et al. 2001; Derrington, Gabus et al. 2002; Deleault, Lucassen et al. 2003; Silva, Vieira et al. 2011)	PrP ^C /Cell Culture, Cell Free, PMCA	Nucleus	Chaperoning and Aggregation
14-3-3 protein (Satoh, Onoue et al. 2005; Mei, Li et al. 2009)	rPrP, PrP ^C , PrP ^{Sc} / Pull-Down, Overlay, co-IP	Cytosol	Unknown
Neuroglobin (NGB) (Lechauve, Rezaei et al. 2009)	rPrP/Affinity	Cytosol	Aggregation
Tubulin (Brown 1998; Brown 2000; Nieznanski, Nieznanska et al. 2005; Nieznanski, Podlubnaya et al. 2006; Dong, Shi et al. 2008; Giorgi, Di Francesco et al. 2009; Osiecka, Nieznanska et al. 2009)	rPrP, PrP ^C , PrP ^{Sc} / Pull-Down, Overlay, co-IP, co-Fractionation, Cross-Linking, Affinity	Cytosol	Oligomerization, Aggregation, Inhibition of Microtubule Assembly
Tau (Tomoo, Yao et al. 2005; Han, Zhang et al. 2006; Wang, Dong et al. 2008)	rPrP, PrP ^C , PrP ^{Sc} / Pull-Down, co-IP	Cytosol	Reduction of binding to tubulin
Aldolase C (Strom, Diecke et al. 2006)	rPrP, PrP ^C /Overlay	Cytosol	Unknown
Neurotrophin receptor-Interacting MAGE Homolog (NRAGE) (Bragason and Palsdottir 2005)	rPrP, PrP ^C , cytoPrP/Pull-Down, Y2H, co-IP	Cytosol	Aggregation, Mitochondrial Potential
Mahogunin (Chakrabarti and Hegde 2009)	cytoPrP, ctmPrP/Pull-Down, Affinity	Cytosol	Aggregation, Neurodegeneration
Flotillins (Solis, Malaga-	rPrP, PrP ^C /Y2H,	Rafts,	Signaling, Raft

Trillo et al. 2010; Wang, Zhou et al. 2011)	Cell Culture	Vesicles	Carrier
RAS-Associated Protein (Rab4, 6a, 7a) (Beranger, Mange et al. 2002; Zafar, von Ahsen et al. 2011)	PrP ^C /MS/MS, co-IP, co-localization	Cytosol, Vesicles	Intracellular trafficking
Ferritin (Mishra, Basu et al. 2004; Sunkesula, Luo et al. 2010)	PrP ^{Sc} /Co-IP, Co-localization, EM	Phagosome, Vesicles, Cytoplasm	Ion transport

III-C-1: Cell Survival and Apoptosis

Initial PrP^C binding studies using the Y2H system established selective binding of the B-cell lymphoma 2 (Bcl-2) protein to PrP^C, suggesting that PrP^C could have anti-apoptotic function (Kurschner and Morgan 1995). The Bcl-2 protein is localized to the mitochondrial membrane with a predominant function to regulate apoptotic pathways (Hockenbery, Nunez et al. 1990). Thus direct binding of PrP^C to Bcl-2 would imply an intracellular regulatory function modulating cell survival pathways (Fig. 1.6A). Targeting PrP^C to various cellular compartments exhibited specific cytotoxicity in the cytosol (Rambold, Miesbauer et al. 2006). Pull-down assays confirmed that the cytosolic PrP selectively bound the Bcl-2 protein thus causing it to co-aggregate and be sequestered from its anti-apoptotic function (Rambold, Miesbauer et al. 2006). Interestingly, the addition of cytosolic chaperones (Hsp70 and Hsp40) interfered in the PrP/Bcl-2 aggregation and reduced cell death (Rambold, Miesbauer et al. 2006). In contrast, other lines of evidence argue that cytosolic PrP is not cytotoxic in primary human neurons, but rather protects cells against Bax-mediated (Bcl-2 binding protein) apoptosis (Roucou, Guo et al. 2003).

The p75 receptor was previously discussed in the context of cell surface interaction with PrP^C, but its main role as the signal transducing receptor to activate apoptosis in neurons has relevance for the intracellular PrP discussion. The neurotrophin receptor interacting melanoma antigen (MAGE) homolog (NRAGE) directly interacts with the cytosolic region of p75 to activate the JNK-mediated mitochondrial apoptotic pathway (Fig. 1.6A,C) (Salehi, Xanthoudakis et al. 2002). Interestingly, using the Y2H system and PrP^C as bait, NRAGE was identified as an interactor and subsequently

confirmed to bind PrP (Bragason and Palsdottir 2005). Proteins that interact with NRAGE in the cytosol ultimately activate apoptotic pathways (Salehi, Xanthoudakis et al. 2002). Although the relevance of PrP binding to either p75 and/or NRAGE must be functionally determined, the coincidental affinity for both molecules that regulate cell survival pathways should not be disregarded.

III-C-2: Internalization and Signaling

Several proteins within the endosomal recycling compartments are of interest as PrP interactors and as cofactors that enable/enhance the PrP misfolding process. These proteins include the Ras-related GTP-binding protein family (Rab), which predominantly regulates vesicular trafficking in cells (Davies, Cotter et al. 1997). Experiments using dominant-negative GTPase Rab4 and Rab6a proteins exhibited increased amounts of PrP^{Sc} in infected cells through the inhibition of the plasma membrane recycling process (Beranger, Mange et al. 2002). The reduction of the Rab7a protein in cell culture by gene silencing methods caused PrP^C accumulation in Rab9 positive endosome compartments, therefore implying direct interaction between the Rab proteins and PrP^C (Zafar, von Ahsen et al. 2011). Lastly, systematic impairment of protein trafficking in PrP^{Sc} infected cells, while quantitating the distribution of PrP^C and PrP^{Sc} strongly designates the endosomal recycling compartments as the most likely site for prion conversion (Marijanovic, Caputo et al. 2009), providing additional evidence towards intracellular mechanisms governing PrP interaction and conversion process.

Additional proteins have been described to interact with PrP inside the vesicle trafficking compartments. These proteins include the synapsin 1b adaptor-like phosphoprotein and growth factor receptor-bound protein 2 (Grb2), both involved in

signal transduction. They bind PrP^C with high affinity, as determined with the Y2H system (Spielhauer and Schatzl 2001). An additional protein identified in the complex with PrP^C, synapsin and Grb2 was the prion-interactor 1 protein (Pint1), but the function of this protein remains undefined (Fig. 1.6B) (Spielhauer and Schatzl 2001).

As briefly alluded to earlier, PrP^C has been implicated as a receptor with signal transduction capabilities. Since PrP^C is GPI-anchored protein, which lacks a cytoplasmic tail to transduce signals intracellularly. Any signal transduction pathways that are activated upon ligand interaction with PrP^C must involve an intermediate protein. Initial evidence for GPI-anchored cell surface proteins ability to transduce a signal was first demonstrated using antibody-mediated cross linking of various GPI-linked cluster of differentiation (CD) proteins on leukocytes, which subsequently activated protein tyrosine kinases (Stefanova, Horejsi et al. 1991). Applying similar experimental approach and logic, PrP^C exhibited activation of the tyrosine kinase Fyn signal transduction pathway through an intermediating caveolin-1 protein (Fig. 1.6B) (Mouillet-Richard, Ermonval et al. 2000). In vivo, antibody-mediated crosslinking of PrP^C induced neuronal apoptosis in the hippocampus (Solfrosi, Criado et al. 2004). Additionally, these antibody-mediated cross-linking techniques have revealed a spatial link between PrP^C and microdomain-forming protein, flotillin-1 and -2, which collectively contribute towards PrP signaling capabilities (Solis, Malaga-Trillo et al. 2010). Interestingly, casein kinase 2 (Ck2), a phosphorylating enzyme involved in signal transduction pathways, was experimentally validated to bind PrP^C and moreover phosphorylate it at the serine 154 position of bovine PrP (Meggio, Negro et al. 2000; Negro, Meggio et al. 2000).

III-C-3: The Interaction with Chaperones and Intracellular Aggregation

The implication for a host chaperone protein to mediate PrP^{Sc} conversion relates back to the transgenic data, which led to the protein X hypothesis (Telling, Scott et al. 1995). Cellular chaperones play a crucial role in modulating the normal folding process of PrP^C and subsequently become up regulated through the induction of the unfolded protein response (UPR) that occurs when misfolded protein induces ER stress (Martins, Graner et al. 1997; Shyu, Harn et al. 2002; Fernandez-Funez, Casas-Tinto et al. 2009; Luo, Li et al. 2010; Wilkins, Choglay et al. 2010; Shorter 2011). Cell culture models were used to demonstrate active binding of the ER chaperone heat shock protein 70-kDa (Hsp70/Bip/HSPA5) to PrP^C thereby reducing cytosolic aggregate formation by selectively targeting these proteins for proteasomal degradation (Fig 1.6C) (Jin, Gu et al. 2000). Subsequent in vitro data revealed that GroEL, a bacterial homolog to the heat shock protein 60-kDa (Hsp60) binds PrP (recombinant) and actively catalyzes aggregate formation of chemically denatured and/or folded rPrP^C (Stockel and Hartl 2001). This data, collectively suggests that chaperones are crucial modulators for PrP's intracellular fate. Although functionally undefined, Hsp60 was also discovered to form a molecular complex with PrP^C and the 14-3-3 proteins both in cell culture models and in reactive astrocytes of human brains (Satoh, Onoue et al. 2005). The 14-3-3-protein family is a group of ubiquitously expressed regulatory molecules throughout eukaryotic cells, which have been shown to bind and interact with signaling proteins (Nielsen 1991; Xiao, Smerdon et al. 1995). Although unrelated to this topic, 14-3-3 proteins have been shown to be present in elevated levels in the cerebrospinal fluid (CSF) of CJD patients (Takahashi, Iwata et al. 1999). Furthermore, biochemical and biophysical analyses in combination with the initial Y2H screen revealed that clusterin, a chaperone

glycoprotein, also interacts with PrP^C (Xu, Karnaukhova et al. 2008). These Y2H binding analyses facilitate the identification of interacting proteins through mutual affinity without providing insight in their function, which is the case for several proteins linked to PrP by affinity binding experiments (Fig. 1.6D).

III-D: Other Interacting Molecules Implicated In PrP^{Sc} Conversion

III-D-1: Nucleic Acids

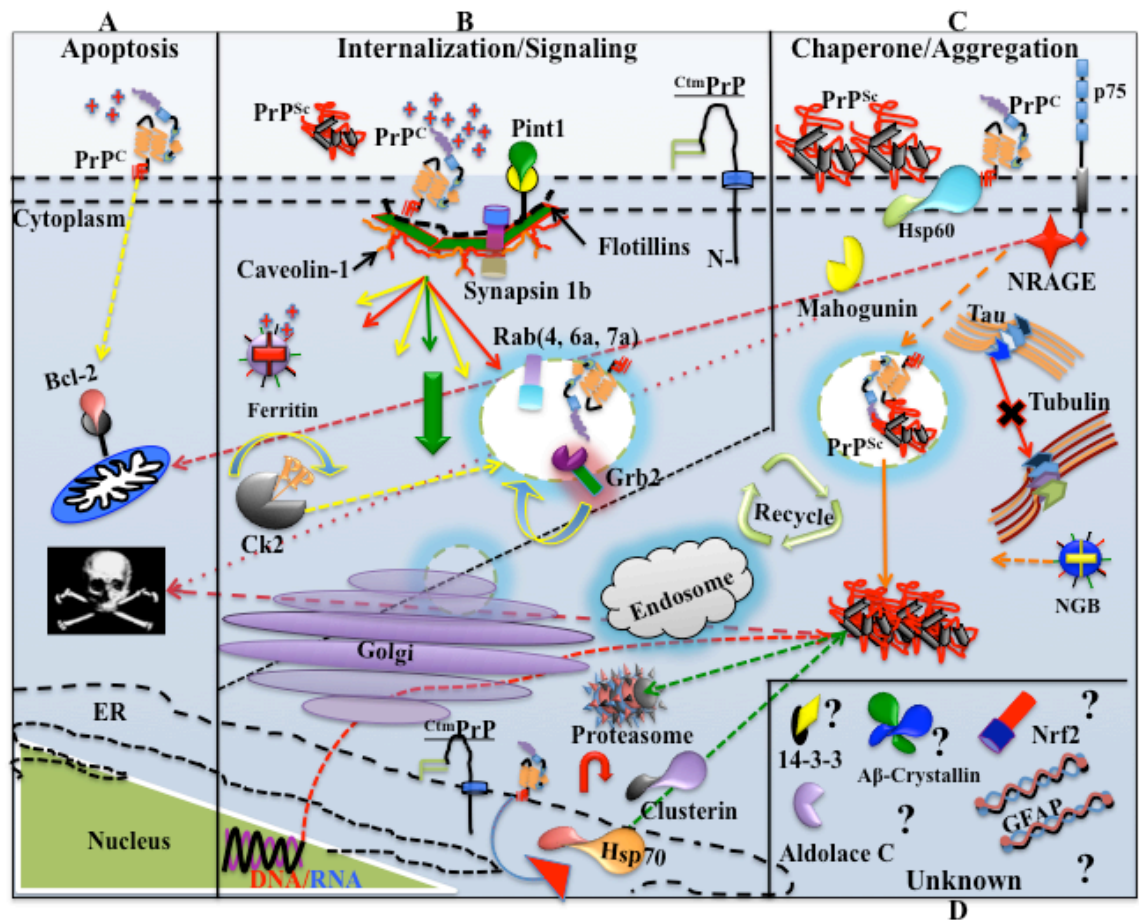
Nucleic acids (NA) and glycosaminoglycans (GAG) molecules have longstanding experimental evidence to link them to the prion conversion process (Cordeiro, Machado et al. 2001; Deleault, Lucassen et al. 2003; Cordeiro and Silva 2005; Deleault, Geoghegan et al. 2005; Lima, Cordeiro et al. 2006; Gomes, Millen et al. 2008; Silva, Lima et al. 2008; Marques, Cordeiro et al. 2009). Early hypotheses suggested that nucleic acids were potential interacting partners for PrP^C, and helped facilitate its conversion to PrP^{Sc} (Weissmann 1991). *In vitro* experiments have validated a physiological relevance between PrP^C and NA (Cordeiro, Machado et al. 2001). Recently, studies have shown that the N-terminal domain of the prion protein interacts with DNA and/or RNA molecules to form toxic aggregates (Fig. 1.6) (Cordeiro, Machado et al. 2001; Gomes, Cordeiro et al. 2008). Moreover, the deletion of the N-terminal domain (23-90aa) in PrP^C inhibited RNA binding, and aggregate formation in N2a cells (Cordeiro, Machado et al. 2001; Gomes, Cordeiro et al. 2008). Highly structured (shs)RNA binds recombinant human prion protein (hrPrP) with high affinity, inducing the formation of a protease resistant complex between these molecules (Adler, Zeiler et al. 2003). Together, these studies indicate that nucleic acids cofactors function in a chaperone-type mechanism that potentially enhances the PrP^{Sc} conversion process. This

chaperone mechanism could entail a biochemical process that reduces the activation barrier for PrP^{Sc} conformational switching, upon NA binding to PrP^C. Conversely, *in vitro* conversion assays provide evidence that certain DNA/RNA aptamers inhibit the formation of PrP^{Sc} (Sayer, Cubin et al. 2004; Sekiya, Nishikawa et al. 2005; King, Safar et al. 2007). The molar range affinities nucleic acids bind PrP implicate the possibility for an unexplored regulatory function between these molecules, which is still to be defined.

Figure 1.6 Molecules associated with PrP within the intracellular space of the cell.

Various experimental approaches have identified intracellular proteins that interact with PrP. These approaches include direct/indirect-binding analyses that include biophysical affinity calculations and co-localizations within intracellular organelle compartments. The studies reveal that PrP interacts with proteins that modulate cell survival (A), followed by proteins that initiate signaling cascades along with regulating endocytic/exocytic and intracellular trafficking utilizing vesicle transport mechanisms (B). Moreover, cell-fractionations and pull-down affinity studies have facilitated the identification of proteins that associate with the PrP^{Sc} aggregation/stabilization/chaperoning process (C)). While, other proteins identified to interact with PrP remain without defined association in function (D). The details of specific interactions between these molecules and PrP (PrP^C, PrP^{Sc}), which include mode of interaction/binding, location specificity and references describing the findings, are summarized in Table 1.3. **Abbreviations:** Heat-Shock 60-Kda Protein (Hsp60), Heat-Shock 70-Kda Protein (Hsp70), Nuclear factor erythroid 2-like 2 (Nrf2), Growth factor receptor-bound protein 2 (Grb2), Prion interactor-1 (Pint1), Casein kinase II (Ck2), B-cell CLL/Lymphoma (Bcl-2), Glial fibrillary acidic protein (GFAP), Neuroglobin (NGB), Neurotrophin receptor-interacting MAGE homolog (NRAGE), RAS-Associated protein (Rab7a), Cellular prion protein (PrP^C), Scrapie prions (PrP^{Sc}), Transmembrane-topological C-terminus cellular prion protein (^{Ctm}PrP).

Figure 1.6 Molecules associated with PrP interaction within intracellular space of the cell.



Concluding Summary

Significant amounts of data have been collected in recent years in an attempt to define the physiological function of PrP^C and the cellular cofactors this protein interacts with. The biogenesis and localization of GPI-anchored PrP^C would strongly implicate function by association with interacting proteins (Figs. 1.1, 1.2, 1.5 and 1.6). Localization of PrP^C to lipid rafts would advocate towards a signaling/regulatory function as observed with other proteins that co-localize to this highly ordered plasma membrane domain (Staubach and Hanisch 2011). Moreover, precedence for GPI-anchored proteins to activate signal transduction pathways has been demonstrated (Stefanova, Horejsi et al. 1991). Therefore the absence of a cytoplasmic tail would again indicate mandatory interaction with intermediate proteins. Furthermore, as PrP is endocytosed through clathrin- and/or caveolin mediated mechanism, more opportunity is provided to interact with intracellular proteins that could assume functional roles or stabilize/enhance PrP^C-PrP^{Sc} conversion (Fig. 1.5, 1.6B). The aforementioned experimental data supplies additional evidence to support both of these hypotheses (Marijanovic, Caputo et al. 2009; Goold, Rabbanian et al. 2011; Zafar, von Ahsen et al. 2011). Lastly, besides understanding the normal function of PrP, the interacting proteins that have already been identified (Table 1.3) and others yet to be discovered, will also provide insight towards the mechanisms that govern PrP^{Sc} conversion, aggregation and ultimately disease.

Dissertation Research

The main objective of my research is to gain an understanding of prion replication at the cellular level, and to identify host factors associated with this process. **My overarching hypothesis is that permissiveness to prion replication is dependent on unidentified, endogenous factors that act in concert with PrP^C.** By establishing novel cell culture systems that express heterologous PrP^C from different species, I set out to identify and describe these factors. We utilized these cell culture models to answer the following questions:

Question 1: Can prion strain diversity be characterized using in vitro cell culture models?

Our initial studies describe the behavior of prion strains in cell culture using three different cell lines (Chapter 3). RK13 cells do not express endogenous PrP^C, making them the ideal *in vitro* knockout model for genetic manipulation that is analogous to the *Prnp*^{0/0} mouse background used to create transgenic mouse models for bioassay analyses (Bueler, Fischer et al. 1992; Browning, Mason et al. 2004). Furthermore, unlike other cell culture systems used in prion studies that replicate only experimentally adapted mouse prions (Race, Fadness et al. 1987), RK13 cells are capable of replicating heterologous prions from different species (Chapters 3 & 4). I describe the RK13 cell's capability to replicate CWD prions (Chapter 3), mouse prions, and TME, Hyper (HY) and Drowsy (DY) (Chapter 3). Finally, I describe the production and partial characterization of susceptible cells expressing genetically removable PrP^C using the Cre-lox system (Chapter 5).

Question 2: Do endogenous host factors mediate the susceptibility and/or resistance to prions?

I show that cloning of RK13 cells facilitated the identification of subclones with wide-ranging susceptibility to PrP^{Sc} replication. Despite evidence from *in vivo* studies (Westaway, Mirenda et al. 1991; Carlson, Ebeling et al. 1994; DeArmond and Prusiner 1996; Fischer, Rulicke et al. 1996; Telling, Haga et al. 1996), susceptibility and/or resistance to prion replication in cells was not solely dependent on PrP^C expression levels (Chapter 4). To identify the molecular differences between the sensitive and resistant cells, we utilized representational difference analysis (RDA) and microarray technologies to distinguish unique genes and pathways associated with these respective phenotypes (Chapter 4).

Chapter 2

Materials and Methods

Cell Cultures: N2a, HEK293A and RK13 cells were freshly obtained from the American Type Culture Collection (ATCC, Manassas, VA) and maintained in 5 % CO₂ at 37°C in Dulbecco's modified Eagle's medium (DMEM) (Gibco Life Technologies, Grand Island, NY) with 10 % fetal bovine serum (FBS) (Gibco Life Technologies, Grand Island, NY) and Penicillin/Streptomycin (P/S) (Gibco Life Technologies, Grand Island, NY). Cell clones were derived by limited dilution in 96-well plates (BD Falcon, Franklin Lakes, NJ) seeded with 100 µl of cell suspension containing 0.3 cells. Cells were cured of PrP^{Sc} by treatment with dextran sulfate-500 (DS-500) (100 ng/ml) (Sigma-Aldrich, St. Louis, MO), prepared in distilled water and sterilized by passage through a 0.22 µm filter

Genomic DNA Extraction: Homogenization of Brain tissue was homogenized in buffer (100mM NaCl, 10mM Tris HCl pH 8.0, 25 mM EDTA, 0.5% sodium dodecyl sulphate (SDS), 0.1mg/ml Proteinase K concentration). Twelve ml of buffer was added per gram of tissue and incubated overnight at 50°C. The sample was extracted with one volume of phenol/chloroform (1:1), the phenol having been previously saturated with water or buffer. The aqueous layer was removed, and 0.5 volume of 5M-ammonium acetate and two volumes of 100 % ethanol was added. The DNA was precipitated and recovered by centrifugation at 5000 rpm for 5 min. The DNA in the pellet was dissolved and resuspended in 2ml of TE (10mM Tris, 1mM EDTA, pH 8.0)

Expression Constructs: The mouse, hamster, deer and elk PrP coding sequences were PCR amplified with primers containing *AflIII* and *EcoRI* restriction endonuclease

recognition sites. Digested amplicons were inserted into pIRESpuro3 vector (Clontech, Mountain View, CA). The PrP ORF was sequenced in the recombinant vector and transfected into N2a, RK13 and HEK293A cells (empty vector to produce RKV cells). RKE, RKD and RK13-SHaPrP^C cells were further transfected with pcDNA3-gag expressing HIV-1 GAG precursor protein, generating RKE-, RKD-, and RK13-SHaPrP--Gag cells. Transfected cells were grown in complete medium containing 1 µg/ml puromycin (Sigma-Aldrich, St. Louis, MO). Co-transfected RK13 cells expressing both PrP and HIV-1 Gag genes were supplemented with 1 µg/ml puromycin (Sigma-Aldrich, St. Louis, MO) and 1 mg/ml neomycin (Sigma-Aldrich, St. Louis, MO). Selection medium was changed every 3 days.

Cell Transfection: Cells were grown to 75-80 % confluence in 6-well cell culture plates (BD Falcon, Franklin Lakes, NJ) and maintained in 5 % CO₂ at 37°C in DMEM (Gibco Life Technologies, Grand Island, NY) with 10% FBS (Gibco Life Technologies, Grand Island, NY) and 1% Penicillin/streptomycin (PS) (Gibco Life Technologies, Grand Island, NY). Transfection DNA solution was made by combining 5 µl of Lipofectamine reagent (Invitrogen, Life Technologies, Grand Island, NY) diluted in 100 µl Opti-MEM (Gibco Life Technologies, Grand Island, NY) with 2.6 µg of plasmid DNA diluted in 100 µl Opti-MEM. The 200 µl combined solution was gently mixed and allowed to incubate at room temperature for 30 min upon which 800 µl of Opti-MEM was added to bring the volume of the solution to 1.0 ml. Cells were washed 2x with 5.0 ml Opti-MEM. Each well to be transfected received 1ml of transfection solution and incubated in 5% CO₂ at 37°C for 5 h. The cells were supplemented with 1.0 ml of complete Opti-MEM solution (20% FBS, 2% PS) and replaced into the incubator for overnight (O/N) incubation in 5 %

CO₂ at 37°C. On the following day, cells were detached from plates by trypsinization and scaled up to a 10-cm cell culture dish (BD Falcon, Franklin Lakes, NJ). Selection of transfected cells was completed with the addition of puromycin (1µg/ml), neomycin (1mg/ml) or a combination of both.

Preparation Of Brain Homogenates: Brain tissues from sacrificed mice were stored frozen at -80°C. Ten % brain homogenizates was made in PBS lacking Ca²⁺ and Mg²⁺ on ice by repeated passage through 18-, 23-, and 26-gage needles.

Infection Of Transgenic Mice: Isoflurane anesthetized mice were inoculated intracerebrally (IC) with 1 % elk or mouse brain homogenate. Inocula from cell cultures were prepared by washing confluent monolayers 2x with cold PBS, collecting cells in PBS by scraping, followed by three -80°C freeze and thaw cycles. Mice were inoculated with infected brain and cell culture preparations (infected & uninfected) containing equivalent amounts of PrP^{Sc} quantified by Western blot analysis. Mice were monitored weekly. Inoculated mice were diagnosed with prion disease displaying at least three clinical signs, the time from inoculation to the onset of definitive clinical signs being referred to as the incubation time.

Cell infections: Cells (2×10^5) were plated into 6 well plates one day before prion infection. Ten % brain homogenates diluted in Opti-MEM medium to 0.2 -2% were added to cell monolayers, 1.0 ml per well. After 5 h, 2.0 ml of Opti-MEM medium containing 15 % fetal calf serum (FCS) (Gibco Life Technologies, Grand Island, NY) was added. Cell lysates were harvested at passage 3 for Western blotting.

Analysis Of PrP^C And PrP^{Sc} By Western Blotting: For cell culture, confluent cells were lysed with cold lysis buffer (50 mM Tris, pH 8.0, 150 mM NaCl, 0.5% sodium

deoxycholate, 0.5% Igepal CA-630) and total protein concentration was determined by bicinchoninic acid (BCA) assay (Pierce Biotechnology Inc., Rockford, IL). Lysates and brain extracts (w/v 2 % sarkosyl) were either untreated or treated with 40 µg/ml proteinase K (PK) (Pierce Biotechnology Inc., Rockford, IL) for 1 hr at 50°C and the reaction was terminated with 4 mM phenyl methyl sulfonyl fluoride (PMSF). PrP^{Sc} in cell culture lysates was purified by centrifugation for 1 h at 100,000 \times g at 4°C. Proteins were separated by SDS-PAGE using discontinuous 12 % Tris-Glycine gels, and transferred to PVDF-FL membranes (Millipore, Billerica, MA). Membranes were blocked in Tris buffered saline, 0.05 % Tween (TBS-T) and 5% non-fat milk, incubated with the primary anti-PrP (mAb) 6H4 (Prionics AG, Schlieren-Zurich), 3F4 mAb (Covance, Cat. No. SIG-39600) or 9E9 (Telling lab) or total protein control antibody Pan-Actin mAb-5 (Lab Vision Corporation, Fremont, CA), followed by HRP-conjugated sheep α -mouse IgG secondary antibody. Membranes were developed using ECL-plus (GE Healthcare Biosciences, Pittsburgh, PA), and analyzed with a FLA-5000 scanner (Fuji/ GE Healthcare Biosciences, Pittsburgh, PA).

Cell Lifting Assay And Blot Development: Three passages after prion infection, cells were subpassaged 1:10 in a 6-well plate, which contains cell culture cover slips (25 mm diameter, Cat. No. 174985) (NUNC, Rochester, NY). Confluent coverslips were washed 2x with cold PBS, and placed cell side down on nitrocellulose paper (0.45 µm, Whatman, Cat. No. 10485375) soaked in cold lysis buffer, backed with similarly soaked blotting paper (Bio-Rad, Hercules, CA). Coverslips were pressed firmly for 1 min, and removed. Membranes were air dried for 2 h. Membranes are rewetted with cold lysis buffer, and incubated in cold lysis buffer containing 5 µg/ml PK for 90 min at 37°C with constant

shaking. PK digestion was terminated with PMSF (2 mM) for 20 min. Membranes were rinsed 4x with dH₂O, and immersed in 3M guanidine isothiocyanate/10 mM Tris-HCl, pH 8.0 for 10 min, then rinsed 4x with dH₂O. Membranes were blocked in TBS-T and 5% non-fat milk, incubated with anti-PrP for 2h at room temperature, shaking. The membranes are then washed 3x with TBS-T, followed by the addition of HRP-conjugated sheep α -mouse IgG secondary antibody with 1h incubation at room temperature and shaking. Membranes were washed 3x with TBS-T and developed using ECL-plus (GE Healthcare Biosciences, Pittsburgh, PA). The blots were exposed to X-ray film and developed.

Protein Level Evaluation by Densitometry Using The ImageJ Software: Western blot PrP^C protein levels and cell-lifting PK resistant PrP^{Sc} was assessed using the densitometry function of the ImageJ software bundle (Abramoff 2004). The uploaded JPEG image file of respective membrane blots were normalized with a background correction function (ImageJ \rightarrow Process tab \rightarrow Subtract Background). The total density of each sample (lane or PK resistant circle from cell lift) was individually measured using the measure function (ImageJ \rightarrow Analyze tab \rightarrow Measure). Empty lanes/blot circles were used as background to calculate density (density value = background density value – sample density value).

Histopathological studies: Brains were immersion fixed in 10% buffered formalin. Tissues were embedded in paraffin and 10 mm thick coronal microtome sections were mounted onto positively charged glass slides. Immunohistochemistry (IHC) was performed as previously described using anti-PrP mAb 6H4 as primary antibody and

IgG1 biotinylated goat anti-mouse secondary antibody (Southern Biotech). Detection was with Vectastain ABC reagents and slides were developed with diaminobenzidine.

Cervid Prion Cell Assay (CPCA): Susceptible Elk21- cells in 96 well plates were exposed to serial dilutions of Elk CWD brain homogenates ranging from 10^{-2} to 10^{-5} in 100 μ l per well. Cell cultures were split 3x, first passage cells were split at 1:4 and thereafter at 1:7. Inclusion of RK13 cells stably transfected with empty vector (RKV cells) were used as negative controls. At final passage, 20,000 cells were filtered onto Multiscreen IP 96-well 0.45- μ m filter plates (Elispot plates, Millipore, Billerica, MA), or AcroWell 96-well 0.45- μ m BioTrace filter plates (Pall, East Hills, NY). Cells were subjected to PK digestion and denaturation with guanidiniumthiocyanate (3 M in 10 mM Tris-HCl, pH 8). CerPrP^{Sc}-producing cells were detected by ELISPOT using anti-PrP mAb 6H4, followed by AP-conjugated secondary anti-mouse IgG, and developed with nitro-blue tetrazolium chloride/ 5-bromo-4-chloro-3'-indolylphosphate p-toluidine salt (NBT/BCIP). Images were scanned with CTL ELISPOT equipment, and spot numbers were determined using ImmunoSpot3 software (Cellular Technology Ltd, Shaker Heights, OH). Statistical analyses were performed using GraphPad Prism 5.0 for Mac OS X software (San Diego California USA, www.graphpad.com).

Modified Scrapie Cell Assay: Cells were infected with 0.2% (w/v) prion infected brain homogenate and passaged three times. At final passage, 20,000 cells were filtered onto Multiscreen IP 96-well 0.45- μ m Elispot plates (Millipore, Billerica, MA), or AcroWell 96-well 0.45- μ m BioTrace filter plates (Pall, East Hills, NY). Cells were subjected to PK digestion and denaturation with guanidiniumthiocyanate (3 M in 10 mM Tris-HCl, pH 8). PrP^{Sc}-producing cells were detected by Elispot analysis using anti-PrP mAb 6H4,

followed by AP-conjugated secondary anti-mouse IgG and developed with nitro-blue tetrazolium chloride/ 5-bromo-4-chloro-3'-indolyphosphate p-toluidine salt (NBT/BCIP). Images were scanned with CTL ELISPOT equipment, and spot numbers were determined using ImmunoSpot3 software (Cellular Technology Ltd, Shaker Heights, OH). Statistical analyses were performed using GraphPad Prism 5.0 for Mac OS X software (San Diego California USA, www.graphpad.com).

Transduction of Cells Expressing lox-P Flanked PrP^C With Adeno-Cre-recombinase

Viral Vector: Cells were plated in 6-well tissue culture plates (BD Falcon, Franklin Lakes, NJ) and grown to confluence. Cells were washed 2x with PBS, trypsinized (200µl) and placed into 37°C + 5 % CO₂ incubator for 5 min. Cell were resuspended in 1.0 mL serum free DMEM. One of the 6 wells was used as the representative for counting. The cells from this well were saved as time point 0 prior to Adeno-Cre-GFP viral transduction (Vector Biolabs, Philadelphia, PA) at multiplicity of infection (MOI) of 15. Adeno-Cre-GFP virus was suspended in Opti-MEM for a total of 0.6 ml per plate. Regular growth media (DMEM + 10% FBS + 1% P/S) was aspirated and diluted Ad-Cre virus (MOI 15) in 0.1 ml serum-free medium per well was added. The transduction reaction was incubated for 90 minutes in a 37°C + 5 % CO₂ incubator with occasional rocking (every 20 to 30 min). At completion of the incubation 2ml DMEM media with 2.0 % serum was added. Cell lysates were collected at designated time points (12h, 24h, 36h, 48h and 72h). Lysates were analyzed by Western blotting

Flow Cytometry: Single-cell suspensions of RK13 cells were generated by incubating the cells in PBS/4 mM EDTA at 37°C for 15 min. Cells were washed in FACS buffer (PBS, 2% heat-inactivated FBS), incubated for 10 min on ice in 100 µl primary antibody diluted

in FACS buffer (SAF-32 anti-PrP; 4 µg ml⁻¹, Cayman Chemical, Cat. No. 189720, Ann Arbor, MI), washed in FACS buffer, incubated for 10 min on ice in 100 µl FITC-conjugated secondary antibody diluted in FACS buffer (anti-mouse-FITC at 1:200) and washed in FACS buffer; twenty µl propidium iodide (50 µg /ml) was added before analysis.

Representational Difference Analysis (RDA): mRNA isolation out of the RK13-MoPrP cells was accomplished using the Invitrogen Dynabeads mRNA Direct Kit. The basis of this kit is to simplify purification of total mRNA using oligo(dT)₂₅ residues that have been covalently coupled to the surface of Dynabeads. The Dynabeads are uniform, super paramagnetic beads, stable in the pH range of 4-13. Physical characteristics of beads are as follows; diameter 2.8 µm ± 0.2 µm (C.V. max 5%); Surface area: 3-7 m²/g; Density: Approx. 1.6 g/cm³ ; Magnetic mass susceptibility: 120±25×10⁻⁶m³/kg. RK13-MoPrP cells grown to 90% confluence in 10-cm cell culture dishes were washed three times with 5.0 ml of cold (4°C) phosphate-buffered saline (PBS, Gibco). Upon the completion of washing the cells, 1.0 ml of Trypsin EDTA (Gibco) was added and placed for 5 min in 37°C + 5.0% CO₂ incubator to allow cells to detach from the surface. Detached cells were gently resuspended in PBS and pelleted in 4°C, 250xg refrigerated centrifuge for 5 min. The supernatant was decanted and the cell pellet was gently resuspended in 5.0 ml of PBS. The cell pellet is resuspended in 1.25 ml of Lysis/Binding buffer (100mM Tris-HCl (pH 7.5), 500 mM LiCl, 10 mM EDTA (pH 8.0), 1 % LiDS, 5 mM dithiothritol (DTT)) and pipetted several times to obtain full resuspension. Cellular DNA was sheared by passing lysate 3-5x through a 21-gauge needle in 2.0 ml syringe on ice. Dynabeads Oligo(dT)₂₅ was thoroughly resuspended and 250 µl was transferred to 1.5 ml RNase

free microcentrifuge tube. The tubes were placed onto a DynaMag magnet for 30 sec until the Dynabead suspension was clear. The beads were washed in an equal volume of lysis/binding buffer and removed using the magnet. Cell lysate was added to the prepared Dynabeads, completely resuspended and incubated with continuous mixing for 5 min at room temperature. The lysate/bead mixture was placed on the magnet and incubated for 2 min, until the solution became clear. The supernatant was removed and the beads are washed twice with 1.5 ml Washing Buffer A (10 mM Tris-HCl (pH 7.5), 0.15 M LiCl, 1 mM EDTA, 0.1 % LiDS) at room temperature. The magnet was used in between steps to separate phases. The beads were washed twice with 1.5 ml Wash Buffer B (10 mM Tris-HCl (pH 7.5), 0.15 M LiCl, 1 mM EDTA). Finally, the beads were washed once in 5x First-strand Reaction Buffer (Invitrogen, cat #11917-010).

RDA Double-Stranded cDNA Synthesis: Double stranded cDNA for the RDA was synthesized using the Superscript Double-Stranded cDNA Synthesis kit (Invitrogen, Cat no.# 11917-010). Bead-primed mRNA and 9 µl of DEPC-treated H₂O was heated to 70° C for 10 min and quickly chilled on ice. The samples were briefly centrifuged and 4 µl of 5X First-strand reaction Buffer, 2 µl 0.1M DTT and 1 µl 10mM dNTP mix were added. Samples were briefly vortexed and centrifuged. The tubes were placed at 45°C for two min. Three µl of Superscript II Reverse transcriptase was added, mixed and incubated at 45°C for 1 h. The reaction was stopped by transfer to ice. Second strand cDNA synthesis was completed by adding 91 µl DEPC-H₂O, 30 µl 5X second-strand reaction buffer, 3 µl 10mM dNTP mix, 1 µl *E.coli* DNA ligase (10U/µl), 4 µl *E.coli* DNA Polymerase I (10U/µl), and 1 µl *E.coli* RNase H (2U/ µl) in the respective order. This was mixed and incubated for 2h at 16°C. Two µl (10 units) of T4 DNA Polymerase were added,

followed by further incubation for 5 min. The tubes were placed on ice and 10 µl of 0.5 M EDTA was added. Samples were cleaned and purified by addition of 160 µl phenol: chloroform: isoamyl alcohol (25:24:1), and centrifuged at room temperature for 5 min at 14,000 x g. One hundred and forty µl of the top aqueous phase was placed into a new 1.5 ml tube. Seventy µl of 7.5 M NH₄OAc was added followed by 0.5 ml of ice-cold absolute ethanol. The samples were mixed and centrifuged for 20 min at 14,000 x g at room temperature. The supernatant was removed and the pellet was washed in 0.5 ml of ice-cold 70 % ethanol and centrifuged for 2 min at 14,000 x g at room temperature. The cDNA pellet was dried at 37°C for 10 min and resuspended in DEPC-H₂O.

Representational Difference Analysis (RDA): The RDA described in these methods is adapted from the following (Lisitsyn Iu 1992; Lisitsyn, Rosenberg et al. 1993; Lisitsyn, Leach et al. 1994). All procedures utilize RNase/DNase free water. Primers were synthesized by Integrated DNA Technologies Inc. The primers were de-salted and HPLC purified. All primers were resuspended in water at 62pmol/ µl concentration.

RDA Primers:

Representation:

24-mer: **R-Bgl24** – 5'-AGCACTCTCCAGCCTCTCACCGCAA-3'

12-mer: **R-Bgl12** – 5'- GATCTGCGGTGA-3'

Odd cycle:

24-mer: **O-Bgl24** – 5'-ACCGACGTCGACTATCCATGAACAA-3'

12-mer: **O-Bgl12** – 5'-GATCTGTTCATG-3'

Even cycle:

24-mer: **E-Bgl24** – 5'-AGGCAACTGTGCTATCCGAGGGAAA-3'

12-mer: E-Bgl12 – 5'-GATCTTCCCTCG-3'

Preparation of amplicons and representation: Tester and driver double-stranded (ds) cDNA (5 µg) synthesized from RK13 sensitive and resistant cells, clone 7 and clone 78 respectively, were digested using 10 U DpnII restriction enzyme per microgram of ds cDNA (New England Biolabs (NEB)) in a total volume of 400 µl per reaction. The digested tester and driver samples were extracted and purified using 1 volume of phenol (400 µl) followed by 1 volume of phenol: chloroform: isoamyl alcohol (400 µl). Ethanol precipitation was performed using 1/10 volume 3M Sodium Acetate (pH 5.2), 2.5 volume 100% ice-cold ethanol, and 20 µg glycogen and centrifuged at 4°C for 20 min. The pellet was washed once with 70% ethanol and air dried. The pellet was suspended was done using TE buffer (10mM Tris-Cl, pH 8.0, 1mM EDTA, pH 8.0) at a concentration of 0.1 µg/µl.

Ligation Of Adapters Onto Tester And Driver ds-cDNA: In 30 µl volume, a mixture of 2 µl H₂O, 3 µl 10x Ligase buffer (NEB), 7.5 µl 12-mer R-primer, 7.5 µl 24-mer R-primer, and 10 µl (1µg) ds-cDNA tester/driver digest was established in a PCR tube. The tubes were placed in a thermo cycler at 55°C with gradual temperature decrease to 4°C over 1 h. One µl of 400 U/ µl T4 DNA ligase (NEB) was added, gently mixed and incubated for 16 hours at 14°C. Samples were then transferred to 1.5ml DNase/RNase free microfuge tubes and resuspended with 970ul of TE buffer (1 ng/µl ds-cDNA).

PCR-Amplification Of Driver And Tester Amplicons: A master mix was set up based on the following PCR reaction; 280 µl water, 40 µl 10x *Taq* Polymerase buffer (NEB), 32 µl dNTP chase solution (4 mM (each) dGTP, dATP, dTTP, dCTP), 8 µl 24-mer R-primer. Generally, two tester and twelve driver reactions were established. Forty µl of adapter

ligated DNA was added per reaction. The mix was held at 72°C in a thermal cycler for two min. Three µl of 5 U/µl *Taq* DNA polymerase was added to each reaction prior to thermo cycling initiation. PCR parameters were as follows; **step 1**: 5 min incubation at 72°C, **step 2**: 20 cycles of 1 min denaturation at 95°C followed by 3 min extension at 72°C, and **step 3**: final step of 10 minute extension at 72°C. Upon completion, all samples were combined respectively and extracted as previously described. Amplicons are precipitated using 1 volume of isopropanol with 20 µg glycogen followed by two 70% ethanol washes. Driver and tester amplicons were resuspended in TE buffer at 0.2 to 0.4 µg/µl concentration.

Linker Removal: One hundred and fifty µg of driver and 15 µg of tester DNA was digested using 10 U Bgl (NEB) restriction endonuclease in a 400 µl total volume. The samples was extracted and purified using ethanol as previously described and resuspended in 125 µl TE buffer. Concentration was measured in comparison with lambda DNA (NEB) standards on a 2% agarose gel.

Adapter Change On Tester Amplicons: Five µg of tester amplicon was loaded on a 1% agarose gel and electrophoresed to separate DNA in the range from 150 base pair (bp) to 1500bp. Within the described range using a clean and sterile razor blade, two full slits were made in the gel and a 24-mm GF/C glass microfiber filter and a 6,000- to 8,000-MWCO dialysis tubing are inserted using blunt ended forceps. Electrophoresis was resumed until the DNA had migrated past the filter/dialysis inserts. A collection apparatus was setup by puncturing a hole in the bottom of a 0.5 ml PCR tube with an 18-gage needle and placed into a 1.5 ml microfuge tube. The filter/dialysis samples were

placed into the apparatus and spun at 8,000 rpm at room temperature for 5 min. The PCR tubes with filter/dialysis were discarded and the samples were resuspended in 400 µl water. The amplicons were extracted and purified, dissolved in 30 µl TE buffer, and the concentration was determined. One µg of tester amplicon DNA was ligated with the O-primer set following the same protocol as described above. Upon extraction and clean up, the pellet was resuspended at 10 ng/µl concentration in TE.

Subtractive/kinetic enrichment:

Tester: Driver ratio

Round 1: 1:50, **Round 2:** 1:500, **Round 3:** 1:1000

Eighty µl driver amplicon digest (0.5 µg/µl) and 80 µl tester amplicon digest (10 µg/µl) DNA were combined and mixed. Followed by extraction with 160 µl phenol: chloroform: isoamyl alcohol. Ethanol precipitation with ammonium acetate; 30 µl of 10 M ammonium acetate, 300 µl ice-cold 100% ethanol, 1 µl glycogen (20µg), for 10 min, centrifuged at 13,000 rpm for 20 min. The pellet was washed with 1.0 ml 70% ethanol and air dried. Four µl of 3 X EE hybridization buffer (30 mM 4-(2-hydroxyethyl)-1-piperazinepropanesulfonic acid (EPPS). pH 8.0, 3 mM EDTA) was added to pellet, resuspended and incubated at 37°C for 5 min, followed by 2 min of vortexing and a short centrifugation at maximum speed to collect sample. In a PCR tube, the resuspended samples were mixed with 1 µl of 5 M NaCl (preheated to 95°C). The mixture was incubated for 1 min at 95°C and centrifuged, followed by the addition of 35 µl mineral oil to overlay the samples. The tubes were incubated for an additional 4 min at 95°C for, followed by a 30 h incubation at 67°C to hybridize complementary strands.

Selective Amplification: Mineral oil was removed and the samples were gradually diluted to 0.1 µg/ µl through the sequential addition of 8 µl of 5 µg/ µl glycogen in TE, 23 µl TE, and 364 µl TE mixing and vortexing between each step. The adapter ends were filled in by mixing 275 µl water, 40 µl 10x PCR buffer (NEB) and 32 µl dNTP chase solution with 40 µl of diluted hybridized DNA and incubated at 72°C. Three µl of Taq DNA polymerase (NEB) was added with an additional 5 min incubation at 72°C. Ten µl of 24-mer O-primers was added and the complete mixture was amplified using the following parameters; step 1: 10 cycles of 1 min denaturation at 95°C followed by 3 min extension at 72°C, step 2; final extension at 72°C for 10 min. The samples were extracted, and isopropanol precipitated, and the pellet was dissolved in 40 µl water. Single stranded templates were digested using Mung bean nuclease (MBN, NEB); 14 µl water, 4 µl 10x MBN buffer, 20 µl amplified difference product and 2 µl 10 U/ µl Mung bean nuclease were mixed and incubated at 30°C for 30 min. One hundred and sixty µl of 50 mM Tris-Cl, pH 8.9 was added to each sample and incubated at 98°C for 5 min to inactivate the MBN. A PCR mixture as described in the initial tester/driver amplification step was set up using the 24-mer O-primer and 40 µl of MBN treated difference product. The addition of Taq polymerase and thermal cycling steps are as described in the initial PCR setup.

Adapter Change On The Difference Product: PCR samples were extracted and isopropanol precipitated. Pellets were dissolved in 80 µl TE and the concentration determined. Five µg of difference product was digested using BglII restriction endonuclease in 200 µl total volume. Samples were brought to 400 µl total volume, phenol/chloroform extracted and ethanol precipitated. The DNA pellet was resuspended

at 0.1 $\mu\text{g}/\mu\text{l}$ in TE. One μg of DNA solution was ligated to E-primer set in a 30 μl volume. The ligated product was diluted to 1.25 $\text{ng}/\mu\text{l}$ in TE.

Subsequent Subtraction/Kinetic Enrichment: The difference products were enriched in subsequent subtraction rounds following the described protocol with a change in ratio of tester: driver concentrations.

Cloning RDA Products And Sequencing: Following 3 rounds of RDA enrichment, the difference product was run out on a 1% agarose gel. Observed bands were excised and purified with the Promega Wizard SV gel and PCR clean up system kit (Catalog # A9280). Excised bands were dissolved in membrane binding solution (4.5 M guanidine isothiocyanate, 0.5 M potassium acetate (pH 5.0) and incubated at 65°C for 10 min. Dissolved samples were transferred to the SV Minicolumn, held for 1 min prior to centrifugation at 16,000 x g. The columns were washed with Membrane Wash Solution (10 mM potassium acetate (pH 5.0), 80% ethanol, 16.7 μM EDTA (pH 8.0)) twice. Samples were eluted from the columns with nuclease free water and collected in a 1.5 ml microcentrifuge tubes. Eluted RDA difference product was ligated into the pGEM-T vector (Promega, Madison, WI). Ligation was setup accordingly; 5 μl 2x Rapid Ligation Buffer, T4 DNA ligase, 1 μl pGEM-T vector (50 ng), 2 μl RDA product, 1 μl T4 DNA Ligase and 1 μl water. The mixture was incubated at room temperature for 1 h.

Transformation Of pGEM-T Ligated Difference Product: Two μl of ligated product was added to 50 μl of competent XL10 bacterial cells, on ice. The cells were kept on ice for 30 min. Heat shock was done at 42°C for 45 sec and immediately transferred to ice for an additional 2 min. Two hundred and fifty μl of LB (10g Tryptone, 5g Yeast extract, 10g NaCl for 1 liter production) was added to each transformation tube and incubated for

1 h shaking at 37°C. One hundred µl of transformed product was spread on to LB/ampicillin (100µg/ml) agar plates and incubated overnight at 37°C. Colonies were individually picked and grown in 3ml LB/ampicillin (100ug/ml) medium. Each identified and expanded clone was subsequently purified by alkaline lysis plasmid isolation and silica column purification using the Qiagen plasmid mini prep kit (cat.no. 19064).

DNA Sequencing Of Cloned RDA Plasmids: Purified clones were sequenced using the Beckman Coulter Ceq 8000 DNA Sequencer and The GenomeLab™ DTCS Quick Start Kit (cat.no. 608120). Sequencing reactions were setup as follows; 9 µl dH₂O, 1 µl pGEM-T-RDA product plasmid were mixed in 0.2 ml thin wall tubes and incubated in 96°C for 1 min. Samples were collected by quick centrifugation, chilled on ice and 2 µl of T7 forward primer (1.6 µM) and 8 µl DTCS Quick Start Master mix were added. Thermal cycling conditions were as follows; 30 cycles of: 96°C for 20 sec, 50°C for 20 sec and 60°C for 4 min; samples were held at 4°C. For ethanol precipitation; 5 µl of stop solution is applied to each sample (2 µl 3M Sodium Acetate (pH 5.2), 2 µl 100 mM Na₂-EDTA (pH 8.0) 1 µl glycogen (20 mg/ml). Sixty µl of cold 95% ethanol was added and immediately spun at 14,000 rpm at 4°C for 15 min. Pellets were washed twice with 200 µl 70% ethanol followed by 5 min centrifugation at 14,000 rpm at 4°C. Pellets were air dried and resuspended in 40 µl Sample Loading Solution (DTCS kit). Resuspended samples were loaded on to sequencing 96-well plate (P/N 609801) and placed into the Beckman Coulter Ceq 8000 DNA Sequencer. Consumables placed into the sequencer were;

- GenomeLab DNA Separation Capillary Array 33cm x 75um (P/N 608087)
- GenomeLab Separation Gel LPA-1 (P/N 609010 10mL for CEQ 8000; P/N

391438 20 ml for CEQ 8800)

- GenomeLab Sequencing Separation Buffer (P/N 608012)

- Sample Microtiter Plates (P/N 609801)

- 96 Well Plates for sequencing buffer (P/N 609844)

Sequenced data were analyzed using CEQ8000 Genetic Analysis System software, and nucleotide blasted against all known sequences in the National Center for Biotechnology Information Data Base (NCBI).

Microarray Studies:

The format of the microarray chip is designated as a 4x44K system, which essentially contains four distinct arrays on a single chip with 43,803 rabbit probes represented per array (<http://www.genomics.agilent.com>). To reduce technical variance, all of the RNA samples were treated, reverse transcribed, Cy-3 labeled and hybridized simultaneously. The data acquisition and feature extraction was performed using the Agilent's microarray scanner and software.

RNA Isolation: RNA was isolated using the Qiagen RNeasy mini kit (cat. No. 74124). Six RK13-DeerPrP (RKD) sensitive and six resistant clones were grown to 90% confluence on a 10cm cell culture plates. Cells were washed twice with PBS and trypsinized to detach them from the plates. The cells were resuspended in 9 ml of PBS and pelleted at 300 x g for 5 min at 4°C. The pellets were washed twice more with PBS. Pellets were then dissolved and lysed with RLT buffer (RNeasy kit). The lysates were passed through a blunt 20-gauge needle 5 times. One volume of 70% ethanol was added and mixed by pipetting. Samples were then transferred to the RNeasy spin column and centrifuged at 14,000 rpm for 30 sec. Seven hundred µl of RW1 buffer was added to each

column and centrifuged. The columns were then washed twice with 500 µl of RPE buffer and centrifuged once for 15 sec and the second time for 2 min at 14,000 rpm. The RNA was eluted with 50 µl RNase-free water and by placing the columns into new nuclease free 1.5 ml microcentrifuge tubes.

Total RNA Integrity Analysis: The integrity of the isolated RNA was measured using the Agilent's 2100 Bioanalyzer (p/n G2938A) and the RNA 6000 Nano Assay Kit (p/n 5067-1511). Parts required and used in this experiment were: Chip priming station (p/n 5065-4401), 16-pin bayonet electrode cartridge (p/n 5065-4413) and the IKA- Vortex mixer (model MS2-S8). RNA was quantified using the NanoDrop ND-1000 UV-VIS Spectrophotometer (Thermo Scientific).

One-Color (Cy3) Labeling RNA: Agilent one-color spike in master mix (p/n 5188-5282) was developed based on Agilent's protocol (<http://www.chem.agilent.com/Library/usermanuals/Public/5188-5977.pdf>), two hundred ng of total RNA (1.5 µl) was used in the labeling reaction. Two µl of diluted Spike in mix was added. Low input quick amp labeling kit, one color (p/n 5190-2305) was used. T7 primer (1.8 µl) was added and denatured at 65°C for 10 min followed by a 5 min incubation on ice. cDNA master mix ((4.7 µl) 2 µl 5x First Strand buffer, 1 µl 0.1 M DTT, 0.5 µl 10 mM dNTP mix, 1.2 µl Affinity Script RNase Block Mix) was added per reaction and incubated at 40°C for 2 h followed by 15 min incubation at 70°C. Samples were transferred and held on ice. Six µl of transcription mix (0.75 µl water, 3.2 µl 5X transcription buffer, 0.6 µl 0.1 M DTT, 1 µl NTP mix, 0.21 µl T7 RNA Polymerase blend, 0.24 µl Cyanine 3-CTP) was added per reaction and incubated at 40°C for 2 h. The

labeled cRNA was purified using Qiagen RNeasy mini spin columns. Eighty-four µl nuclease free water was added to each reaction, 350 µl of Buffer RLT (cat. no. 79216) was added and mixed followed by 25 µl 100% ethanol. The total volume was transferred to the RNeasy spin column and centrifuged at 13,000 rpm for 30 sec at 4°C. The columns were washed twice with 500 µl buffer RPE (cat. No. 1018013). The cRNA was eluted with 30 µl nuclease free water. cRNA quantification was performed using the microarray measurement tab within the NanoDrop ND-1000 UV-VIS Spectrophotometer. The following measurements were recorded: Cyanine 3 dye concentration (pmol/µl), RNA absorbance (260nm/280nm), cRNA concentration (ng/µl). cRNA yield (µg) was determined as follows: ((concentration of cRNA) x 30 µl (elution volume))/1000

Cyanine 3 incorporation was calculated: ((concentration of Cy3)/(concentration of cRNA))x 1000 = pmol Cy3 per µg cRNA.

Hybridization: Agilent's Gene Expression Hybridization Kit (p/n 5188-5242) was used. Blocking agent (10x) (p/n 5188-5281) was prepared by the addition of 500 µl nuclease free water and mixing. Fragmentation mix was prepared in a 55 µl total volume; 1.65 µg Cy3 labeled cRNA, 11 µl 10X blocking agent, 2.2 µl 25X fragmentation buffer, nuclease free water brought to 52.8 µl. Samples were incubated at 60°C for 30 min and cooled on ice for one min. The fragmentation reaction was stopped with the addition of 55ul 2X GEx Hybridization Buffer HI-RPM and mixing, being careful not to introduce bubbles into the solution. Samples were centrifuged for one min at room temperature 13,000 rpm. 100 µl of hybridization sample was applied to the loaded Agilent SureHyb chamber assembly (cat.No. G2534A)/gasket (p/n G2534-60011) and gently placed with the Rabbit Gene Expression Microarray, 4x44K array (cat. No. G2519F-020908). The complete

hybridization assembly was placed into the hybridization rotator (p/n G2530-60029) and transferred to the hybridization oven (p/n G2545A) set to 65°C. The hybridization was set up to run for 17 hours. The arrays were washed with GE Wash Buffer 1 for one min at room temperature, and a second wash with pre-warmed (37°C) GE Wash Buffer 2 for one min (Gene Expression Wash Buffer Kit p/n 5188-5327). Each slide was scanned using the Agilent Microarray Scanner (p/n G2565BA). Agilent Feature Extraction (FE) Software was used to extract scanned data from each chip.

Microarray Data Analysis:

JMP Genomics Software: JMP Genomics was utilized for manipulation of extracted raw microarray data, statistical analysis, and hierarchical data clustering to ascertain gene significance of microarray data. Total overview of this software can be found at: <http://www.jmp.com/software/genomics/index.shtml>

The Database for Annotation, Visualization and Integrated Discovery (DAVID): National Institute of Allergy and Infectious Disease (NIAID) bioinformatic database used for functional enrichment of identified genes. This database was used to identify biological themes and processes by uploading the microarray gene lists deemed statistically significant by the t-test, p-value of 0.05, and a fold cutoff set to 1.5.

DAVID website address: <http://david.abcc.ncifcrf.gov>

Protein Analysis Through Evolutionary Relationships (PANTHER): Gene Ontology Reference Genome Project - <http://www.pantherdb.org/> PANTHER classification database is supported by the National Institute of General Medical Sciences and maintained by the Thomas lab at the University of Southern California. The database provides functional comparison and classification of up loaded genes using published

scientific experimental evidence and evolutionary relationships to predict function in the absence of direct experimental evidence. Classifications are based according to:

Additional Bioinformatic Websites and Databases Used For Data Analysis:

Literature Search: PubMed - <http://www.ncbi.nlm.nih.gov/pubmed>

Image Analysis: ImageJ - <http://rsb.info.nih.gov/ij/index.html>

Gene Sequence Identity, Homology, Protein Sequence Analysis, Secondary Structure

Prediction and Subcellular Localization:

ENTREZ Cross-Database Search - <http://www.ncbi.nlm.nih.gov/sites/gquery>

NCBI BLAST- <http://blast.ncbi.nlm.nih.gov/Blast.cgi>

ENSEMBL Genome Browser - <http://uswest.ensembl.org/index.html>

GeneCards Database - <http://www.genecards.org>

Universal Protein Resource (UniProt) - <http://www.uniprot.org>

Protein Data Bank (PDB) - <http://www.pdb.org/pdb/home/home.do>

SIB Bioinformatics Resource Portal (ExPASy) - <http://expasy.org>

- YASPIN (Hidden Neural Network) secondary structure prediction

- <http://www.ibi.vu.nl/programs/yaspinwww>

Center For Biological Sequence Analysis (CBS) - <http://www.cbs.dtu.dk/services>

TargetP (predicts the subcellular location of eukaryotic proteins)

ProtFun (Prediction of cellular role, enzyme class and Gene Ontology category)

MiniMotif Miner - <http://mnmm.engr.uconn.edu/MNM/SMSSearchServlet>

Protein Structure Classification - <http://www.cathdb.info>

Copyright © Vadim Khaychuk 2012

Chapter 3

Characterization of Prion Strains in Cell Culture Systems

Introduction

The molecular characterization of prion strain properties is challenging. It is the proteinaceous nature of prions that distinguishes them from viruses, bacteria and other known disease causing agents. This “protein only” molecular composition of prions utilizes atypical methods to replicate that differ from the standard dogma of molecular biology (Fig. 1.3). The absence of nucleic acids is central to the prion strain classification challenge. Evidence suggests that prion strain diversity relies on conformational differences PrP^{Sc} can acquire (Chapter 1, Section I) (Telling, Parchi et al. 1996; Wadsworth, Hill et al. 1999). In addition to these conformational differences, the structural homology between PrP^C and PrP^{Sc} is also a crucial determinant of replication, which underlies the fundamental concept of the prion species barrier (Fig. 3.1) (Scott, Groth et al. 1993; Telling, Scott et al. 1994; Collinge, Palmer et al. 1995; Telling, Scott et al. 1995). It is the combination of these findings that dictates the conformational selection hypothesis for prion strain selection and diversity (Collinge 1999; Collinge and Clarke 2007).

Prion Species Barrier: The parameters controlling interspecies prion transmission is not completely understood. The prion species barrier is influenced by the host's PrP^C primary structure homology to the PrP^{Sc} infectious agent (Fig. 3.1A-B) (Scott, Foster et al. 1989; Telling, Scott et al. 1995). The prion species barrier may not be absolute, since partial interspecies transmission have been demonstrated in experimental animals, subsequently

leading to total barrier abrogation upon serial transmission (Scott, Foster et al. 1989; Bessen and Marsh 1992; Bruce, Will et al. 1997; Baron, Bencsik et al. 2007; Agrimi, Nonno et al. 2008; Sandberg, Al-Doujaily et al. 2010). The transmission of BSE to humans in the form of vCJD is another example of a partial species barrier (Bruce, Will et al. 1997; Collinge 1999; Scott, Will et al. 1999). Understanding the molecular determinants of prion species barriers, and factors that regulate interspecies transmission are crucial for disease prevention in humans and other animals.

PrP^C Interference Effect: The interference of endogenously expressed mouse PrP^C to production of human PrP^{Sc} in Tg(HuPrP)FVB mice co-expressing mouse and human PrP was discovered during transmission of human prions to these mice (Fig. 3.1C) (Telling, Scott et al. 1995). Earlier studies using Tg mice co-expressing hamster and mouse PrP^C did not exhibit similar interfering effects, since these mice inoculated with hamster prions succumbed to disease (Scott, Foster et al. 1989). Although the differences in susceptibility for heterologous prions between these studies remains to be fully explained, it is hypothesized that primary structure homology between mouse and hamster PrP^C is closer than that of mouse and human PrP^C.

Heterologous PrP^{Sc} In Cell Culture: Methods used to characterize strains include incubation time in animals, clinical signs at the onset of disease, and neuropathological profiling of PrP^{Sc} (Bruce and Dickinson 1979; Bruce, McBride et al. 1989). Biochemically, strains may be characterized by analyzing their glycoform ratios of PrP^{Sc}, protease sensitivity of PrP^{Sc}, migration of PrP^{Sc} in SDS-PAGE, and conformational stability of PrP^{Sc} following treatment with denaturing agents.

Current methods used for CWD prion analysis consists of bioassays and/or *in vitro* PMCA conversion assays (Green, Castilla et al. 2008). Developing robust cell-culture models will provide additional insights into CWD prions at the cellular level. The studies described in this chapter aim to characterize and enhance *in vitro* cell culture models for prion strain analysis. Upon prion challenge, we attempt to isolate cells with capability to chronically sustain CWD. The prion strains used for these analyses are designated in table 3.1. The cells that were utilized include the rabbit kidney epithelial cells (RK13), mouse Neuroblastoma N2a cells and the human embryonic kidney 293 cells. Besides identifying cells capable of interspecies prion replication, these cell culture model studies recapitulated the prion species barrier and PrP^C interference effects previously demonstrated using transgenic animal models (Scott, Groth et al. 1993; Telling, Scott et al. 1995).

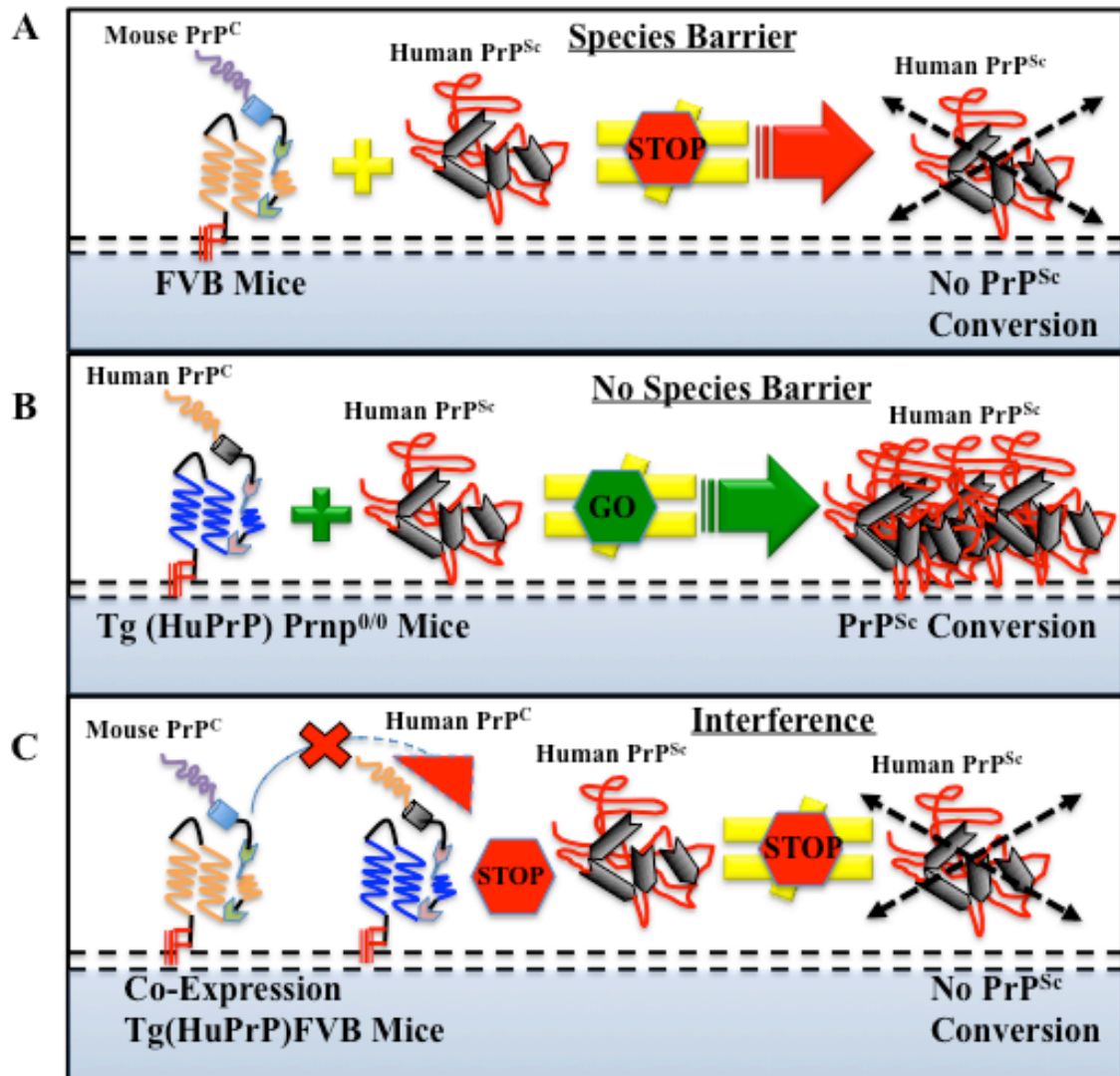
The neuroblastoma (N2a) cell line replicates experimentally adapted RML mouse-scrapie prions (Race, Fadness et al. 1987; Butler, Scott et al. 1988). Detailed characterization revealed that a subset of cells within the total culture efficiently replicate prions (<2%) (Race, Fadness et al. 1987; Race, Caughey et al. 1988; Bosque and Prusiner 2000). Clonal selection of N2a cells sensitive to prion replication enhanced PrP^{Sc} production by 80-90% (Race, Caughey et al. 1988). Through clonal selection and transgenesis of the N2a cells, we aimed to create cells that are sensitive towards natural prion isolates.

RK13 cells do not express endogenous rabbit PrP^C, therefore making them the *in vitro* cell culture model analogous to the well-established PrP^C knock out (*Prnp*^{0/0}) mouse (Büeler, Fischer et al. 1992; Büeler, Aguzzi et al. 1993). The absence of endogenous PrP^C

in these cells can be applied towards genetic modulation and infectivity analyses using heterologous PrP^s. The replication of naturally derived prion isolates without adaptation in mice was achieved using the RK13 cells (Vilette, Andreoletti et al. 2001). Genetic modulation of the RK13 cells to express ovine PrP^C resulted in chronic propagation of scrapie directly derived from sheep (Vilette, Andreoletti et al. 2001).

Figure 3.1 The prion species barrier and PrP interference. (A) Inoculation of wild type FVB mice with human prions does not cause disease, demonstrating a prion species barrier between mouse and human. (B) Expression of human PrP (HuPrP) on a *Prnp*^{0/0} background, replicates the heterologous human prions and recapitulates disease. Thus, expression of human PrP in Tg mice abrogates the species barrier between the two species. (C) Co-expression of human and mouse PrP does not facilitate human prion replication, demonstrating interference by the endogenously expressed mouse PrP^C. (Telling, Scott et al. 1995)

Figure 3.1 The prion species barrier and PrP interference.



RESULTS

Section I: Prion Species Barriers, Interference and the Attempt to Propagate

Chronic Wasting Disease (CWD) in Cell Culture

N2a Cells Recapitulate The Prion Species Barrier And Demonstrate The PrP Interference Effect

N2a cells were single-cell cloned using limited dilution. Individual clones were infected with mouse-adapted RML scrapie prions and PrP^{Sc} accumulation was assessed (Chapter 4, Fig. 4.2B). N2a sub-clone #2 exhibited high sensitivity for RML replication. The uninfected counterpart of this clone was selected for the subsequent transfection with deer and elk PrP^C. Transfection of the eukaryotic expression vector (pIRESpuro) genetically engineered to express elk or mule deer PrP^C resulted in stable expression of these proteins in the N2a clone (Fig. 3.2). Expression of cervid specific PrP^C was determined using the 9E9 monoclonal antibody (mAb). The 9E9 mAb was developed and epitope mapped within our lab (unpublished, Telling lab). Figure 3.2 exhibits 9E9 mAb specific recognition of elk and mule deer PrP^C but not the endogenously expressed mouse PrP^C in the un-transfected N2a sub-clone #2. Actin expression is used as a control for total protein (Fig. 3.2).

To determine N2a cell susceptibility to CWD, we infected elk and deer expressing cells with CWD isolates (Table 3.1). Each isolate used in the study was bioassayed and sub-passaged in transgenic mice expressing cervid PrP^C (Tg(deerPrP)1536^{+/-} and Tg(elkPrP)5037^{+/-}) (Fig. 3.3). The cell-lift assay was used to rapidly detect production of PrP^{Sc}. This assay is ~150-fold more sensitive for identifying prion infected cells than

standard cell lysate analysis by western immuno blotting (Bosque and Prusiner 2000). Figures 3.3A-F represents scanned x-ray film images obtained from the cell-lifting assay.

The positive and negative controls for the experiments are shown in figures 3.3C and 3.3F. N2a cells were either mock infected with PBS (negative control) or infected with RML prions (positive control). N2a cells co-expressing elk or deer PrP^C were also infected with RML. The sharp dark signal exhibited by the RML infected cells (positive controls) depicts the normal signal intensity of PrP^{Sc} replicating cells (Fig. 3.3C and 3.3F). The mock-infected negative controls demonstrated complete absence of PK positive material, confirming the uncontaminated purity of the parental N2a cell line (Fig. 3.3 C, F). RML infected cells showed robust production of PrP^{Sc}, confirming the highly sensitive phenotype of the parental sub-clone. Of interest, co-expression of cervid PrP^C did not alter the sensitivity to RML prion replication (Fig. 3.3 C, F).

The heightened sensitivity of these cells for RML prions indicates that the cellular machinery for replication are present and operational. We therefore hypothesized that these cofactors would facilitate CWD replication in the cervid PrP^C over-expressing cells. N2a cells expressing mule deer (N2aD-PrP) or elk PrP^C (N2aE-PrP) were infected with 0.2% (w/v) CWD brain homogenates obtained from Tg(deerPrP)1536^{+/-} (Fig. 3.3A and 3.3D) or Tg(elkPrP)5037^{+/-} (Fig. 3.3B and 3.3F) infected mice (Table 3.1). N2aD-PrP cells failed to replicate CWD prions (Table 3.1). The lack of PK resistant PrP^{Sc}, as analyzed by the cell-lifting assay, confirmed these findings (Fig. 3.3A-B). N2aE-PrP cells also exhibited resistance towards CWD prions. These cells did not demonstrate PrP^{Sc} conversion after CWD infection with isolates passaged in Tg(deerPrP)1536^{+/-} mice (Fig. 3.3D). Select CWD isolates derived from Tg(elkPrP)5037^{+/-} mice showed a weakly

positive PrP^{Sc} signal in N2aE-PrP cells (Fig. 3.3E). These CWD isolates include 73784, CWD pool, 012-09442, and 012-02212, which were originally derived from diseased elk (Table 3.1). The PrP^{Sc} positive N2aE-PrP cells were expanded for further analysis. Total cell lysates were processed for western blotting. The results revealed no detectable PrP^{Sc} after PK digestion within the expanded cell populations (Fig. 3.3G). N2aE-PrP cells demonstrate CWD resistance similar to N2aD-PrP. We conclude that N2aE-PrP and N2aD-PrP cells are resistant to CWD infection and that clonal selection was not sufficient to render N2a cells susceptible to CWD (Fig. 3.3). The data gathered using these cells recapitulate the originally described in vivo observations that demonstrate the prion species barrier using transgenic mice (Telling, Scott et al. 1995). Similar to mice, the murine cell line readily replicates mouse-adapted prions, irrespective of the presence of over-expressed heterologous PrP^C protein. Conversely, over-expression of the heterologous PrP^C is not sufficient to replicate prions that are homologous to that species. Our data indicate that the endogenous mouse PrP^C hinders the replication of heterologous CWD prions by CerPrP^C.

Figure 3.2 Stable expression of cervid PrP^C in N2a cells. N2a cells were transfected with pIRESpuro-elk PrP^C/mule deer PrP^C using lipid-based methods. Transfected cells were grown in selection media and assessed for cervid PrP^C expression by western blotting. The cervid specific 9E9 mAb (Telling *et al.*, unpublished) was used to detect cervid PrP^C. Actin expression is used for total protein control (Pan-Actin mAb-5, Lab Vision Corporation, Fremont, CA).

Figure 3.2 Stable expression of cervid PrP^C in N2a cells.

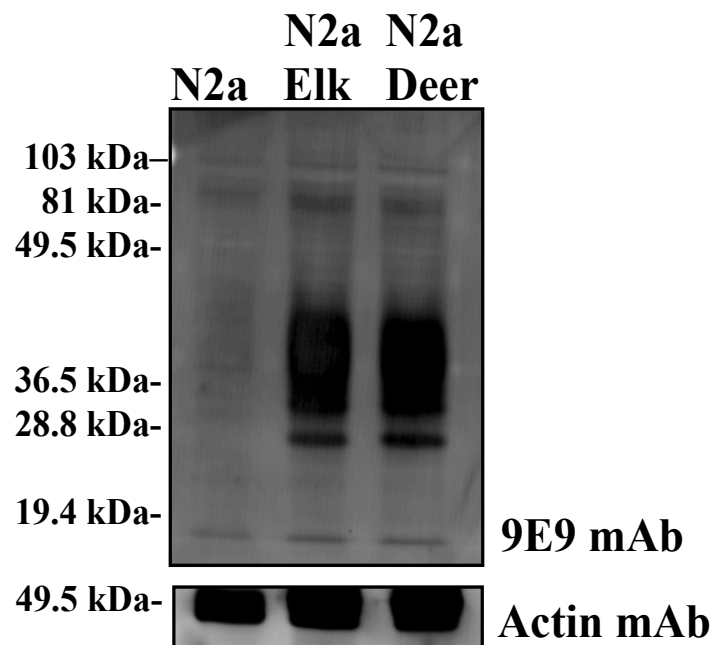
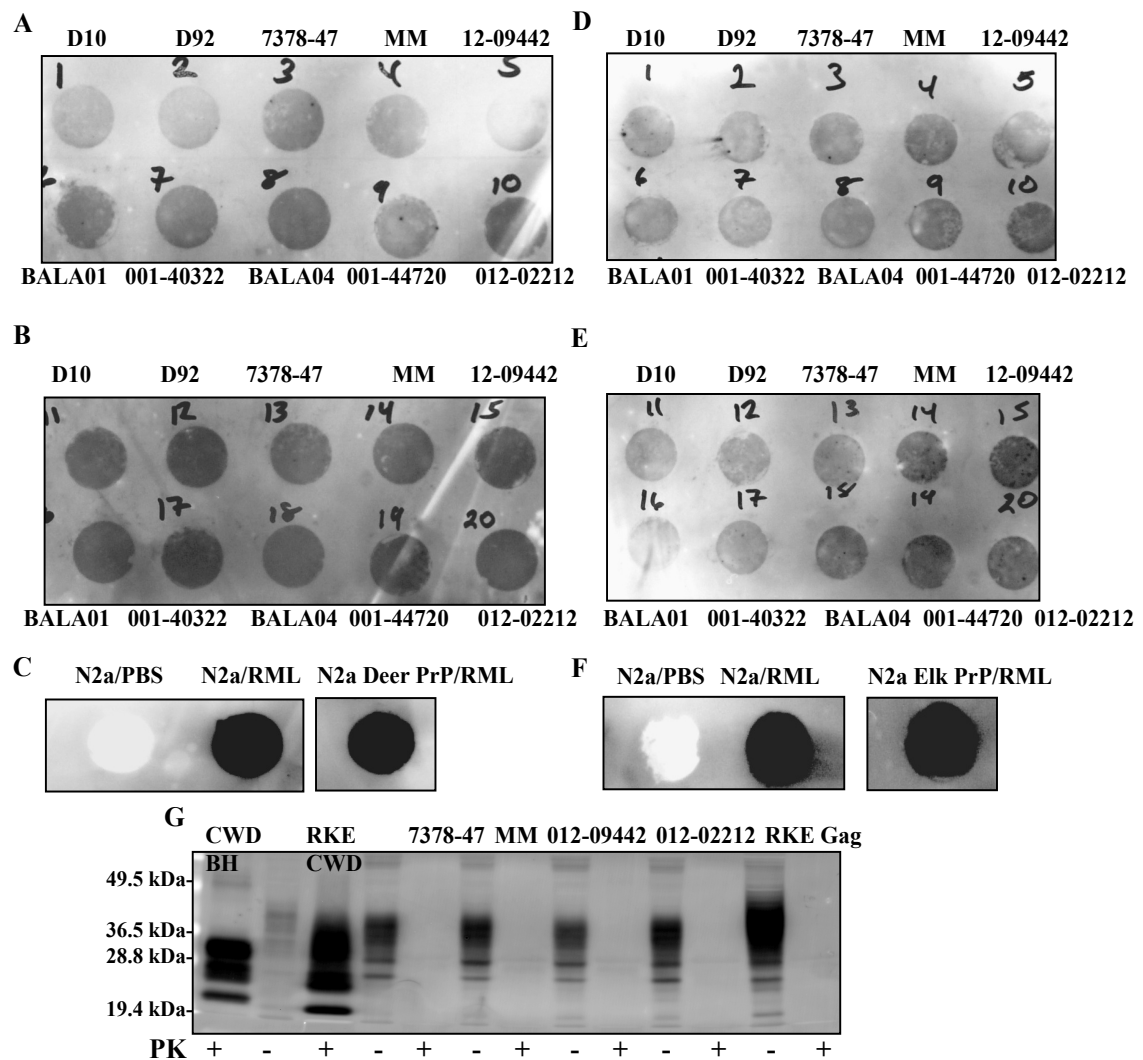


Table 3.1 Prion strains used for cell culture infectivity analysis.

Prion Strain	Origin	Host - Source	Species Adapted
Chronic Wasting Disease (CWD)			
D10	Colorado	Mule deer	Tg(deerPrP)1536 ^{+/-} & Tg(elkPrP)5037 ^{+/-} mice
D92	Colorado	Mule deer	Tg(deerPrP)1536 ^{+/-} & Tg(elkPrP)5037 ^{+/-} mice
73784-7	Wyoming	Elk	Tg(deerPrP)1536 ^{+/-} & Tg(elkPrP)5037 ^{+/-} mice
CWD Pool	Colorado	Mule Deer	Tg(deerPrP)1536 ^{+/-} & Tg(elkPrP)5037 ^{+/-} mice
012-09442	Colorado	Elk	Tg(deerPrP)1536 ^{+/-} & Tg(elkPrP)5037 ^{+/-} mice
BALA-01	Canada	Elk	Tg(deerPrP)1536 ^{+/-} & Tg(elkPrP)5037 ^{+/-} mice
001-403022	Colorado	Elk	Tg(deerPrP)1536 ^{+/-} & Tg(elkPrP)5037 ^{+/-} mice
BALA-04	Canada	Elk	Tg(deerPrP)1536 ^{+/-} & Tg(elkPrP)5037 ^{+/-} mice
001-44720	Colorado	Elk	Tg(deerPrP)1536 ^{+/-} & Tg(elkPrP)5037 ^{+/-} mice
012-02212	Colorado	Elk	Tg(deerPrP)1536 ^{+/-} & Tg(elkPrP)5037 ^{+/-} mice
Hamster-Adapted Transmissible Mink Encephalopathy (TME)			
Hyper (HY)	Wisconsin	Mink	Syrian golden hamster
Drowsy (DY)	Wisconsin	Mink	Syrian golden hamster
Mouse-Adapted Scrapie			
Rocky Mountain Laboratories (RML) Scrapie	Montana	Sheep	Mouse

Figure 3.3. Mouse N2a cells expressing cervid PrP^C are not permissive to CWD prions. N2a cells expressing deer PrP^C were infected with 0.2% (w/v) natural CWD isolates (D10, D92, 7378-47, CWD pool, 012-09441, BALA01, 001-40322, BALA04, 001-44720, 012-02212) adapted to (A) Tg1536^{+/-} mice expressing deer PrP^C or (B) Tg5037^{+/-} mice expressing elk PrP^C, and assessed for infectivity after three passages in 6-well cell culture plates by cell lifting assay. On third passage, cells were grown to confluence on NUNC cell culture cover slips (25mm diameter, Cat. No. 174985). The cells were directly transferred to cold lysis buffer soaked nitrocellulose membranes. The membrane was treated with PK (5 µg/ml), denatured with 3M guanidine isothiocyanate, immunoprobed with 9E9 mAb (A,B,D,E,G) or 6H4 mAb (C, F) and signal visualized with X-ray film. (C,F) Cell lift assay control samples demonstrated lack of prion contamination (mock infected with PBS) and N2a sensitivity to mouse adapted RML prions. The N2a cells expressing Elk PrP^C were infected with 0.2% (w/v) natural CWD isolates (D10, D92, 7378-47, CWD Pool, 012-09441, BALA01, 001-40322, BALA04, 001-44720, 012-02212) adapted to (D) Tg1536^{+/-} mice expressing deer PrP^C or (E) Tg5037^{+/-} mice expressing elk PrP^C. G. PrP^{Sc} positive cells within the N2a-ElkPrP^C cells were expanded, sub-passaged and screened for PK resistant material by Western blotting using the 9E9 mAb. PK +/- designates digested samples (+) or un-digested (-). RKE cells are RK13 cells expressing elk-PrP^C which maintain chronic CWD infectivity (described in Fig. 2.4).

Figure 3.3. Mouse N2a cells expressing cervid PrP^C are not permissive to CWD prions



Breaking the Prion Species Barrier: RK13 Cells (RKE21⁺) Expressing Elk PrP^C

Replicate Natural CWD Prions

To enhance their propensity to replicate prions, we genetically engineered RK13 cells to stably co-express HIV-1 Gag protein concurrently with PrP^C. The basis for the addition of HIV-1 Gag came from earlier published data providing evidence of positive enhancement for scrapie prion infectivity upon retroviral infection (Leblanc, Baas et al. 2004; Leblanc, Alais et al. 2006). The molecular mechanisms that govern retroviral enhancements of PrP^{Sc} replication remain to be defined. The following CWD replication studies with genetically modulated RK13 cells were conducted in cooperation with Dr. Jifeng Bian (Bian, Napier et al. 2010).

Two separate cell line were created that over-express elk PrP^C. The two stably transfected cell lines were designated as RKE (expressing elk PrP^C only) and RKE-Gag (co-expressing elk PrP^C and HIV-1 Gag) (Fig. 3.4). The CWD elk isolate designated 012-09442 (Table 3.1), was used to infect and serially passage both cell lines. CerPrP^{Sc} accumulation was assessed by PK treatment and subsequent western blotting and/or cell lift assay (Fig. 3.4A-B). RKE cells showed diminishing amounts of CerPrP^{Sc} replication by passage five, which was lost completely by passage seven, shown by the left western blot in figure 3.4A. Conversely, the RKE-Gag cells continued to accumulate and replicate CerPrP^{Sc} for over 67 passages (Fig. 3.4A). Direct comparison of cervid PrP^{Sc} replication by western blotting and cell lifting suggests that there is an approximate ~2 fold increase of CerPrP^{Sc} in the RKE-Gag cells (Fig. 3.4B). These results suggest that HIV-1 Gag is modulating the cells to efficiently replicate prions. The CWD chronically infected RKE-Gag cell line is referred to as Elk21⁺.

Elk21⁺ cells were cured of CWD prions by treatment with DS-500, a method that has previously been described in use for other cell lines (Ladogana, Casaccia et al. 1992; Caughey and Raymond 1993). The cured cells are referred to as Elk21⁻. These Elk21⁻ cells remained CerPrP^{Sc} negative for the remaining passages. Cured Elk21⁻ cells demonstrated sensitivity to CWD replication upon reinfection (Fig. 3.4I).

After 58 passages Elk21⁺ cells were further cloned by limited dilution. The process of cell cloning generated 3 CerPrP^{Sc} positive clones and 11 negative clones. Re-challenging negative cloned cells with CWD prions resulted in 10 of the 11 clones being re-infected (Fig. 3.4I).

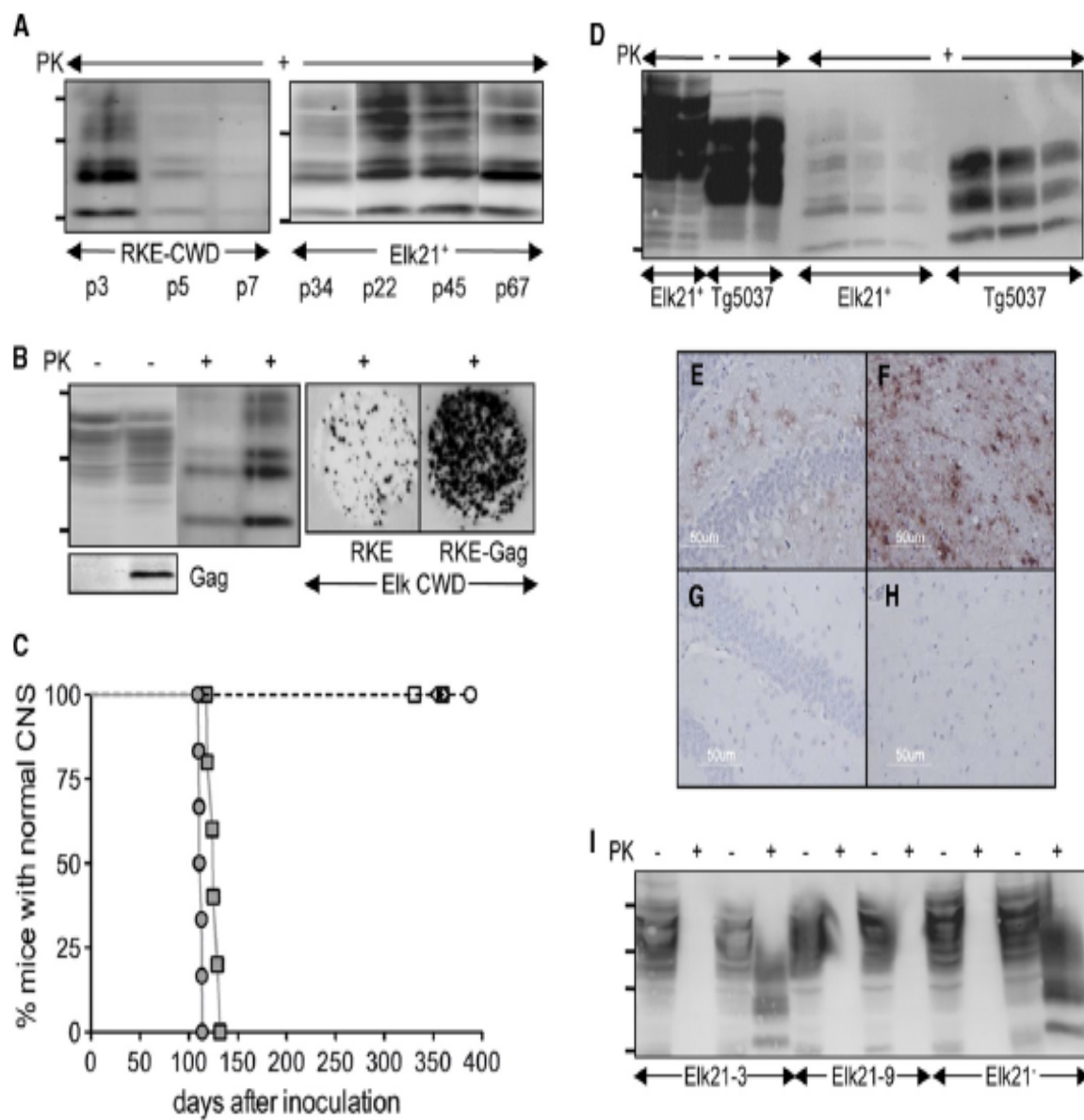
Strain stability in cell culture was determined by bioassay. Cell extracts from chronically infected Elk21⁺ cells passaged twenty-five consecutive rounds were used to confirm strain stability of the CWD 012-09442 isolate. CWD infected cell extracts from Elk21⁺ were ic injected into Tg(elkPrP)5037^{+/-} mice. The natural elk CWD isolate 012-09442 was used as a positive control. Elk21⁺ cell extract injected mice developed prion disease with a mean incubation time of 112±1 days, while the natural isolate produced disease with a mean incubation time of 126±2 days (Fig. 3.4C). Negative controls for the bioassay included uninfected RKE-Gag cell extract, Elk21⁻, and Elk21 subclones 3 and 9 (Fig. 3.4C). The cured cell extract controls of the bioassay confirmed the dextran sulfate-500 treatment cured cells of prions infectivity.

Cell extract preparations used in the bioassay were normalized for total protein equivalents by the bicinchronic acid (BCA) protein assay (Thermo Fischer-Scientific, Rockford, IL). Western blot analysis revealed that the glycosylation and electrophoretic migration patterns between Elk21⁺ cell lysate and Tg(elkPrP)5037^{+/-} brain homogenate

differed (Fig. 3.4D). Histopathological analysis of brain sections from mice inoculated with Elk21⁺ cell extract demonstrated diffuse and granular deposition of CerPrP^{Sc} (Fig. 3.4E-F), which is similar to previously published reports (Angers, Seward et al. 2009). The negative control, RKE-Gag cell extract injected mice displayed a disease free histopathological profile (Fig. 3.4G-H).

Figure 3.4 Characterization of CWD replication in RK13 cells. **A.** RK13 cells expressing Elk-PrP^C (RKE) did not sustain CWD infectivity (Elk isolate 012-09442) as compared to the RKE cells co-expressing HIV-1 Gag (Elk21⁺), which subsequently became chronically infected. **B.** Enhanced Cervid PrP^{Sc} replication was demonstrated in Elk21⁺ cells by both Western blotting and cell lifting, HIV-1 Gag expression indicates a ~2 fold increase in PrP^{Sc}. **C.** After 25 passages, the Elk21⁺ cells were bioassayed in Tg5037^{+/-} mice expressing elk PrP. The Elk21⁺ cell extract is represented by filled circles, Elk CWD 012-09442 in Tg5037 are filled squares, uninfected RKE-Gag cells are open circles, cured Elk21⁻ cells with DS-500 treatment after 13 passages (open triangles) and after 30 passages (filled triangles), Elk21 subclone 3 are open diamonds and subclone 9 are filled squares. **D.** Western blot representing CerPrP (100µg and 50µg total protein), CerPrP^{Sc} (200µg, 100µg, and 50µg total protein) generated in Elk21⁺ cells and Tg5037 mice inoculated with Elk21⁺ cell extract. **E-H.** Representation of CerPrP^{Sc} deposition in the hippocampus (**E,G**) and the thalamus (**F,H**) of Tg5037 mice that were inoculated with Elk21⁺ extract (**E,F**) or RKE-Gag (**G,H**) uninfected control. **I.** The susceptibility to CWD prions (isolate 012-09442), upon reinfection to individual clonal cells derived from the cured Elk21⁺ cells (clone 3, clone 9 and Elk21⁻) was assessed by western blotting. For each analyzed cell line, the first two lanes represent mock infection with PBS treatment and the second two lanes represent infection through exposure to CWD brain homogenate. Molecular mass markers represent 37, 25 and 20 kDa, top to bottom.

Figure 3.4 Characterization of CWD replication in the RK13 cell culture system.



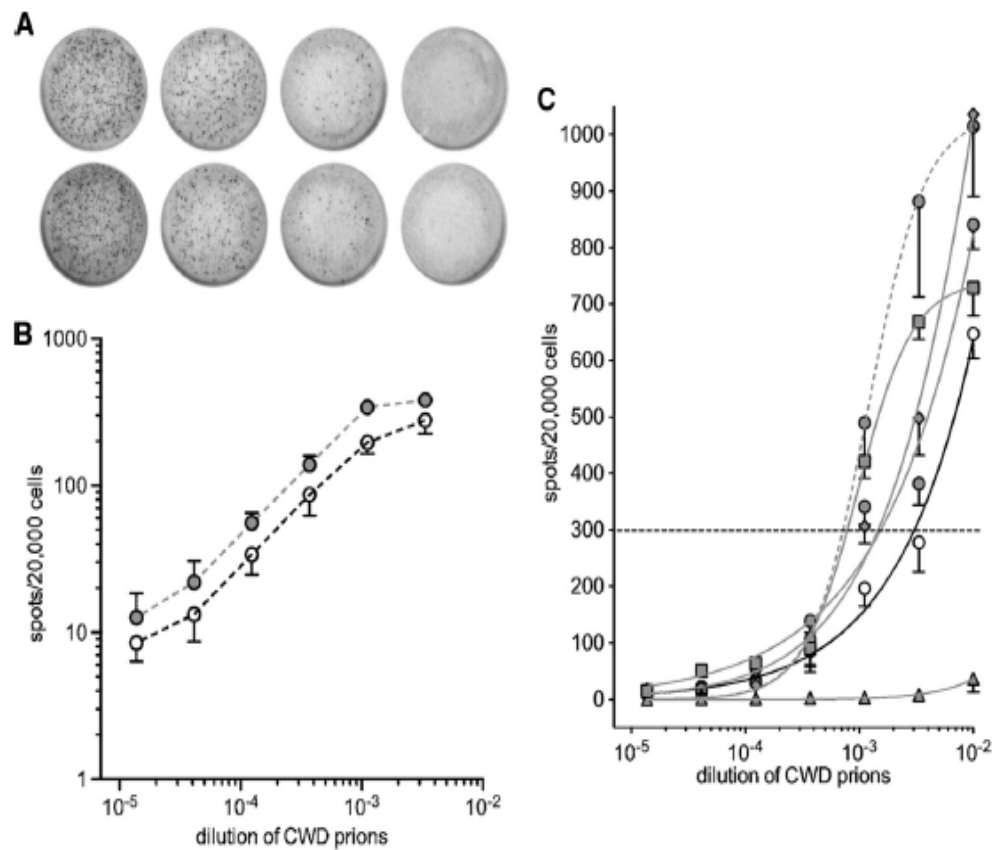
The sensitivity of Elk21⁺ cell to CWD prions facilitated the development of an *in vitro* cell assay for prion titer determination, which call the cervid prion cell assay (CPCA). Similar to the commonly used viral plaque assay for viral titer determination (Dulbecco and Vogt 1953), the CPCA calculates PrP^{Sc} accumulation on an individual cell basis using a dilution range of the PrP^{Sc} inoculum. The CPCA methodology is adapted from earlier described scrapie cell assay (SCA) that is used to calculate mouse-adapted scrapie prion titers with highly susceptible N2a clones (Klohn, Stoltze et al. 2003; Mahal, Demczyk et al. 2008). The major limitation of the SCA is the inability to use natural prion isolates, therefore making the CPCA a unique assay for its utility in calculating natural CWD isolates without the murine adaptation prerequisite (Klohn, Stoltze et al. 2003; Bian, Napier et al. 2010).

The basis of the assay is to infect cells with serially diluted increments of infectious prion material, in a 96-well format. The cells are passaged for three consecutive rounds. At confluence of the third passage, the cells are counted and transferred to a 96 well, 0.45µm filter-ELISPOT plate (Millipore, Billerica, MA) where they are fixed to the plate membrane. These plates are then PK digested and treated with guanidinium thiocyanate (GITC) denaturation, followed by an enzyme linked immune-sorbent assay-like (ELISA) developing procedure. The plates are scanned and quantified using the CTL-ELISPOT plate reader and the ImmunoSpot3 software (Cellular Technology, Ltd, Shaker Heights, OH). Figure 3.5A illustrates a representative read out of positive and negative wells upon final development.

The dose response relationship in Elk21⁺ cells to CWD prions was determined using elk CWD prions titrated in transgenic mice (Browning, Mason et al. 2004; Angers, Seward et al. 2009). Infected Elk21⁺ cells were assessed for titer infectivity at the dilution range of 10⁻² to 10⁻⁵ (Fig. 3.5B-C). The double logarithmic plots in figure 3.5B, demonstrates a linear response to the dilutions ranging from 10⁻³ to 10^{-4.4}. Positive cell count, representing CerPrP^{Sc}-producing cells, is reflective of prion titers. Furthermore, an increased dose-response for CWD passaged in the Tg(elkPrP)5037^{+/-} versus the CWD passaged in Tg(deerPrP)1536^{+/-}, signify higher titers in the former samples. Different CWD isolates were used to infect Elk21⁺ cells to determine and compare CPCA prion titers to previously acquired bioassay data (Fig. 3.5C). In our calculations, we estimate that 100 µl of 10^{-2.5} dilution of elk CWD pool yields 300 spots in the well of an ELISPOT plate, which is the reference point used to determine the response index in the SCA (Mahal, Baker et al. 2007). This calculated reference point corresponds to 10^{6.0} CPCA units/g. The titers calculated using the CPCA with various elk CWD inocula provided values of 10^{6.3}, 10^{6.3} and 10^{6.6} units/g of brain (Fig. 3.5C). The CPCA titration data was less than one log difference compared to the previously published bioassay titers (Browning, Mason et al. 2004; Angers, Seward et al. 2009). Consequently the CPCA is a viable *in vitro* alternative to the bioassay for calculating prion infectivity titers, which could reduce animal use and costs associated with these studies.

Figure 3.5 Quantification of CWD infectivity using the RKE cell line in a Cervid Prion Cell Assay (CPCA). **A.** Representation of developed wells in the Millipore ELISPOT plates of the CPCA. **B.** Demonstration of the double logarithmic plot of spot number versus brain homogenate dilution. CPCA using the Elk21⁺ cells has a linear response to pooled elk CWD brain homogenate (open circles) and CWD passaged in Tg mice (filled circles). Data representative of 6 separate experiments. **C.** Plots of PrP^{Sc} positive cells as a function of log dilution of CWD prion inocula. The numerical counts of positive cells reflect the prion titer. Three-hundred counted spots is the point used to determine the response index which corresponds to 10^{6.0} CPCA units/g brain.

Figure 3.5 Quantification of CWD infectivity using the RKE cell line in a Cervid Prion Cell Assay (CPCA).



Heterologous PrP^C Expression On a PrP-null Background Does Not Guarantee Prion Sensitivity: HEK293A Cells Resist CWD Replication

The human embryonic kidney-293 cells (HEK293A) were derived from the transformation of normal human embryonic kidney cells and are a commonly used cell line for various molecular analyses (Graham, Smiley et al. 1977). Similar to the RK13 cells, we found that HEK293A cells do not express detectable levels of endogenous PrP^C (Fig. 3.6A) (Ramljak, Asif et al. 2008). Therefore, we hypothesized that the introduction and over-expression of a heterologous PrP^C on a PrP-null background would permit prion. We also reasoned that attaining chronic CWD infectivity with 293 cells could aid in the identification of human-specific cellular components involved in interspecies transmission. Consequently, the HEK293A cells could provide an *in vitro* model to ascertain the zoonotic potential of CWD.

Stably transfected 293 cells were created with using the pIRESpuro-deer PrP^C open reading frame (ORF) expression vector. Stable expression of deer PrP^C in 293 cells was assessed using western immuno-blotting with mAb 9E9 (Fig. 3.6A). HEK293A-Deer-PrP^C cells were infected with the deer CWD D92 isolate (Table 3.1). The cells were infected using the standard 0.2% (w/v) CWD mixture and serially passaged four times prior to PrP^{Sc} assessment. Collected cell lysates were PK treated and electrophoretically separated on a 12%-SDS-PAGE. HEK293A-Deer-PrP^C cells did not produce detectable PrP^{Sc} implicating resistance towards prion replication (Fig. 3.6B). In addition, HEK293A-Deer-PrP^C cells were shown to be resistant to other CWD and 293 cells

expressing Mouse PrP^C were also found to be resistant to mouse RML prions (data not shown).

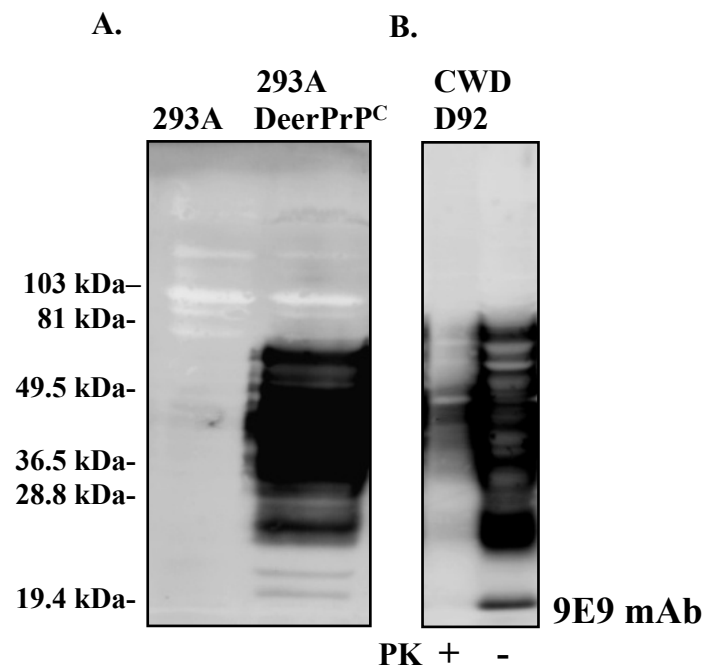
Section Summary: Three distinct cell lines were used to characterize and generate in vitro prion cell models. The N2a cell line has been well characterized for its ability to replicate mouse-adapted scrapie prions (Table 1.2). Through clonal selection of cells sensitive to prion replication, we reasoned that genetic modulation to introduce cervid-PrP^C could permit the replication of heterologous CWD-CerPrP^{Sc}. However, N2a cells remained resistant to CWD prions, while maintaining their sensitivity for RML prions. Our results indicate that the molecular basis for this resistance maybe an interference effect by mouse PrP on CWD prion conversion of CerPrP^C, as observed in Tg mouse models (Fig. 3.1) (Telling, Scott et al. 1995).

RK13 cells permitted replication of CWD prions after modifications to express elk-PrP^C. The absence of endogenous PrP^C in RK13 cells allows over-expression of species-specific PrP^C similar to Tg mice on a *Prnp*^{0/0} background. In addition to elk-PrP^C, introduction of HIV-1 Gag was shown to enhance PrP^{Sc} replication. In this way, we created a cell line chronically infected with CWD prions, called Elk21⁺ cells (Bian, Napier et al. 2010). CWD prion production in Elk21⁺ cells was confirmed by bioassay in Tg mice.

Finally, the lack of endogenously expressed PrP^C in the HEK293 cells was not sufficient to facilitate CWD prion replication upon stable expression of cervid PrP^C, indicating that PrP^C expression is not the only determining factor for cells to replicate foreign prions. Our results suggest that sensitivity of cells to prions is co-dependent on PrP^C expression and endogenously expressed factors.

Figure 3.6 Stable expression of cervid PrP^C and assessment of CWD replication in HEK 293A Cells. **A.** HEK 293A cells were stably transfected with the pIRESpuro-Deer PrP^C ORF expression vector. **B.** HEK293A cells were infected with CWD deer isolate D92 and passaged for four consecutive rounds. PrP^{Sc} replication in HEK293A-DeerPrP^C cells was assessed following PK digestion, SDS-PAGE separation and Western blotting. Monoclonal antibody 9E9 was used to probe Western blot for PK resistant material. PK +/- nomenclature designates digested samples (+) or un-digested (-).

Figure 3.6 Stable expression of cervid PrP^C and assessment of CWD replication in HEK 293A Cells.



Section II: Replication of Biologically Cloned Hyper (HY) and Drowsy (DY)

Hamster-Adapted TME Prion Strains in Cell Culture

Transmissible mink encephalopathy (TME) prion strains, Hyper (HY) and Drowsy (DY) were derived from ranch-raised mink in Stetsonville, Wisconsin and sub-passaged in Syrian golden hamsters. These prion strains have been well described and biologically cloned (Bessen and Marsh 1992; Bessen and Marsh 1992). These two prion strains differ in disease incubation times, histopathological deposition of PrP^{Sc}, behavioral phenotypes (HY –highly active, hyper, DY-lethargic, slow) and biochemically (protease sensitivity, glycoform migration patterning) (Bessen and Marsh 1992). In accordance with *in vivo* data, HY prions have rapid replication kinetics as compared to DY, yielding high titers (Bessen and Marsh 1992). The end stage titers of HY and DY, were $10^{9.5}$ LD₅₀/g and $10^{7.4}$ LD₅₀/g, respectively (Bessen and Marsh 1992). We used the RK13 cells to create an *in vitro* model to study the molecular characteristics that define HY and DY.

Expression Of Hamster PrP^C In RK13 And N2a Cells: Genomic DNA extracted from Syrian golden hamster (SHa) brain tissue was used to isolate, sequence and clone the SHa PrP ORF into the pIRESpuro expression vector. RK13 cells and N2a cells were stably transfected, and bulk populations expressing SHaPrP^C were created (Fig. 3.7A). Monoclonal antibody 3F4 was used to detect SHaPrP^C expression. In addition, site-directed mutagenesis was used to generate the L42 epitope (W144Y) within the SHaPrP ORF. The specific epitope for L42 occurs in human, cattle, sheep, goat, dog, cat, mink, rabbit and guinea pig PrP, but not hamster, mouse or rat PrP (Vorberg, Buschmann et al.

1999). By generating this epitope in the SHaPrP ORF, we aimed to measure *de novo* prion replication in cell cultures (Fig. 3.7A).

To assess susceptibility to HY and DY, RK13-SHaPrP cells were infected with 0.2% (w/v) HY and DY Syrian golden hamsters. RK13-SHaPrP cells were permissive for HY replication, but not the DY strain (Fig. 3.7A). Of interest, the electrophoretic migration patterns of CerPrP^{Sc} in Elk21⁺ cells (Fig. 3.4) and HY-PrP^{Sc} differ when compared to CWD- or HY-PrP^{Sc} derived from brain homogenates (Fig. 3.7B). The HY- and DY- from infected hamster brains were used as positive controls on Western blots (Fig. 3.7B) (Bessen and Marsh 1992).

Continuous passage of HY-infected RK13-SHaPrP cells resulted in the loss of PK resistant PrP^{Sc} in later passages. The capacity of RK13-SHaPrP cells to replicate HY-prions was confirmed using the cell-lifting assay (Fig. 3.8B). Repeated infectivity experiments using these prion strains produced consistent results. HY PrP^{Sc} consistently became undetectable between the seventh and ninth passage, while DY infected cells remained PrP^{Sc} free throughout the studies (Fig. 3.7B & 3.8B). These cell culture studies demonstrate differences in susceptibility of RK13-SHaPrP cells to HY and DY strains.

N2a cells expressing SHa-PrP^C were also infected with HY and DY prions. Unlike RK13 cells, the N2a cells did not replicate HY or DY prions (Fig. 3.7C and 3.8A). Although signal can be seen in PK⁺ lanes of the infected cells in figure 3.7C, incomplete protease digestion is the likely cause of this signal. The more sensitive cell-lifting assay confirms the lack of PrP^{Sc} in N2a SHa-PrP cells (Fig. 3.8A). In contrast, N2a SHa-PrP cells were capable of replicating RML prions (Fig. 3.8A). Using mAb 6H4, we show

robust accumulation of PrP^{Sc} in RML-infected N2aSHa-PrP cells, but not RK13SHa-PrP cells (Fig. 3.7D & 3.8B).

Figure 3.7 Characterization of HY and DY prion replication in cell culture. **A.** Stable expression of Syrian hamster PrP^C (SHa-PrP^C, Accession number K02234.1) in RK13 and N2a cells. Both cell lines were transfected with the pIRESpuro-SHa-PrP^C expression vector (Clontech Laboratories, Inc) and verified using the hamster/human PrP^C specific mAb 3F4 (Covance, Cat. No. SIG-39600). Actin expression is used for total protein control (Pan-Actin mAb-5, Lab Vision Corporation, Fremont, CA). Bulk selected **(B)** RK13 cells and **(C)** N2a cells expressing SHa-PrP^C were infected with 0.2%(w/v) HY and/or DY brain homogenate. Accumulation of PrP^{Sc} was assessed after three passages by Western blotting using mAb 3F4. **D.** RK13 and N2a cells expressing SHa-PrP^C were infected with 0.2% (w/v) mouse adapted RML scrapie brain homogenate and passaged three consecutive rounds: PrP^{Sc} was detected by Western blotting using mAb 6H4. The L42 designation in the figures represents the cell line expressing SHa-PrP^C with a site directed mutation at the 144 amino acid residue position (W144Y).

Figure 3.7 Characterization of HY and DY prion replication in cell culture.

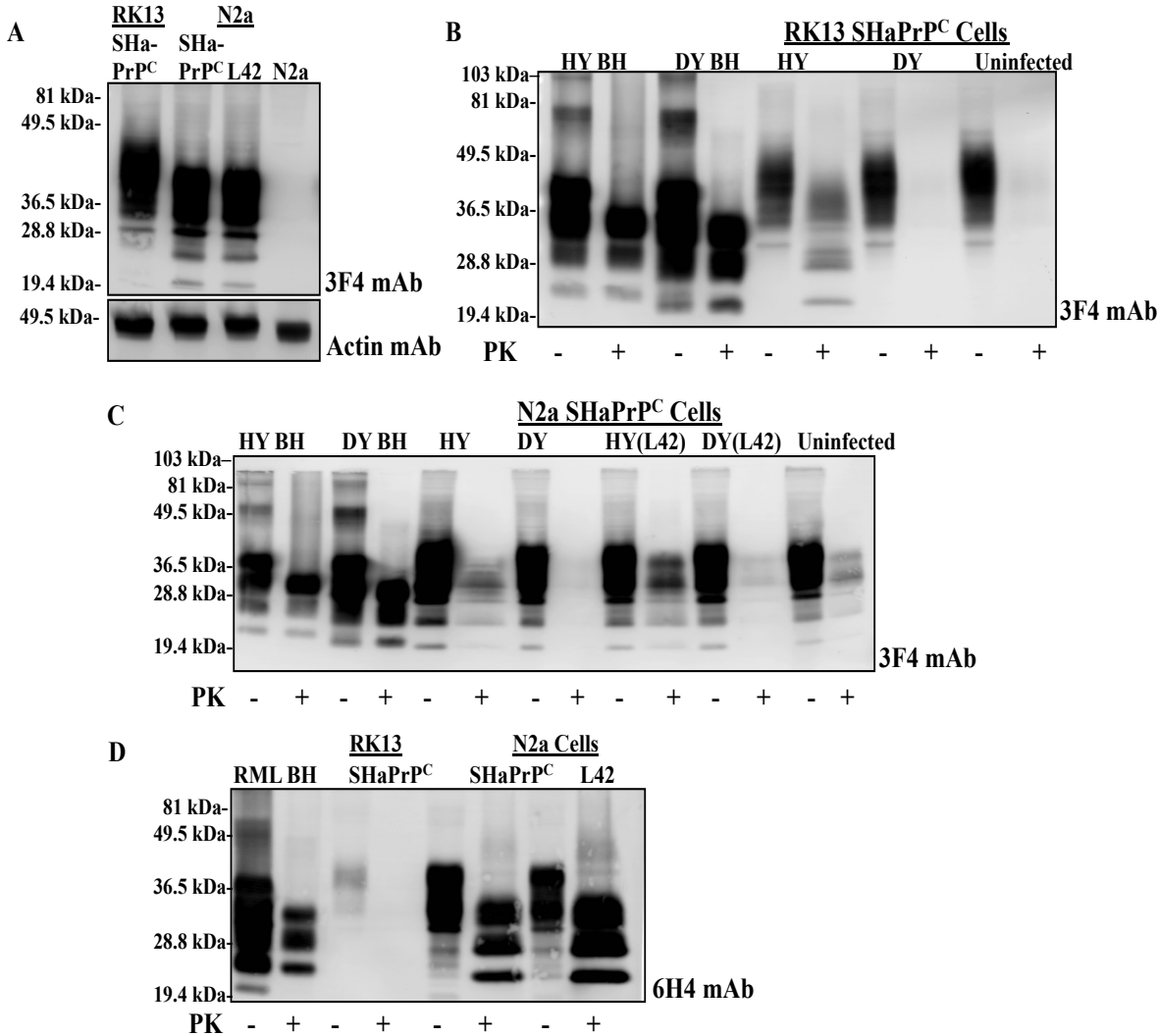
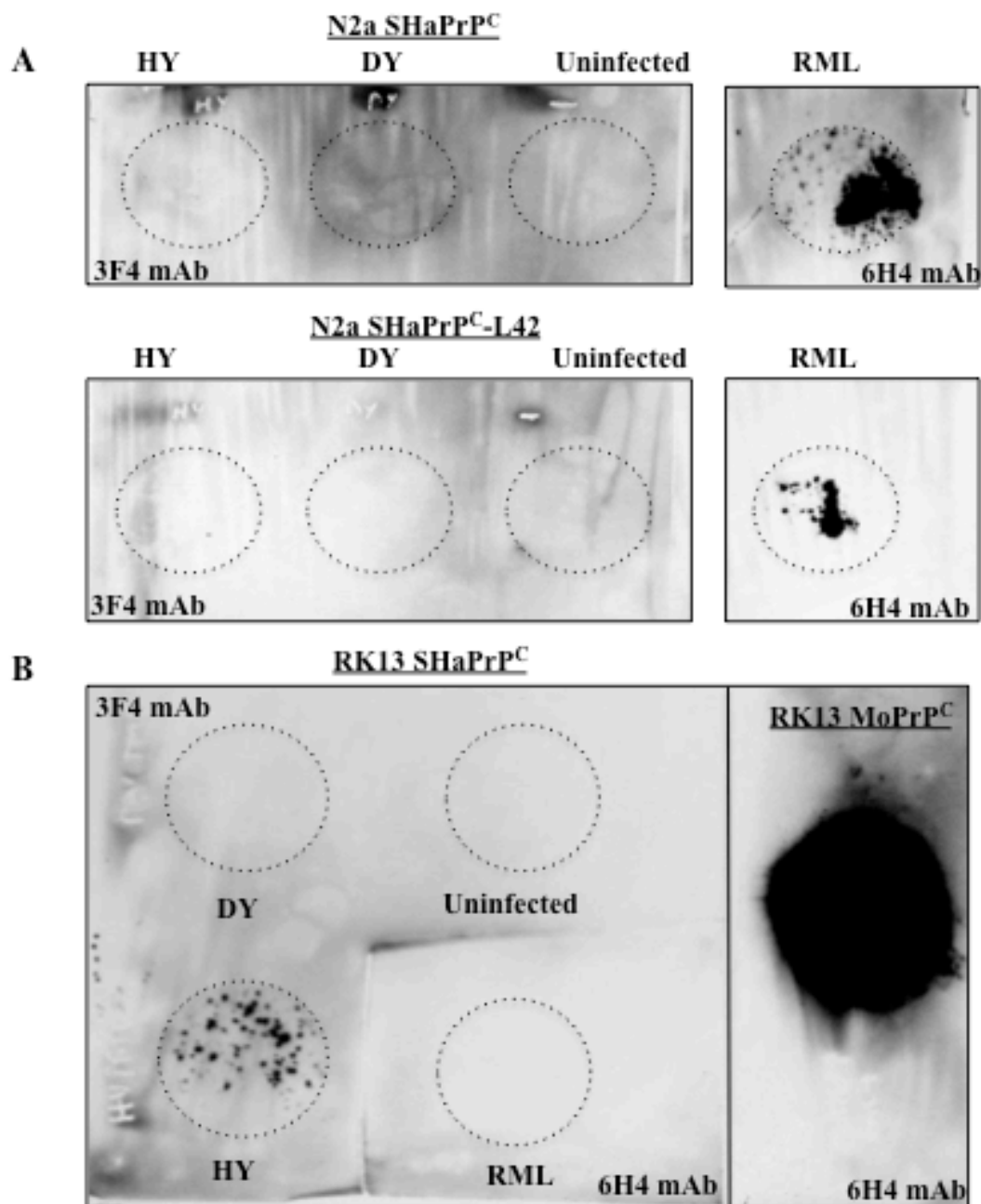


Figure 3.8 Characterization of HY and DY prion replication by cell-lifting assay. (A) N2a-SHaPrP^C/ N2a-SHaPrP^C-L42 and (B) RK13SHaPrP^C were infected with 0.2%(w/v) HY, DY prions, or mouse adapted RML prions and assessed for infectivity after three passages in 6-well cell culture plates by cell lifting assay. On third passage, cells were grown to confluence on cell culture cover slips. The cells were directly transferred to cold lysis buffer soaked nitrocellulose membrane. The membrane was treated with PK (5µg/ml), denatured with 3M-guanidine isothiocyanate, immunoprobed for the accumulation of PrP^{Sc} with mAb 3F4 or mAb 6H4 antibodies(Bosque and Prusiner 2000)(Bosque and Prusiner 2000)(Bosque and Prusiner 2000)(Bosque and Prusiner 2000)(Bosque and Prusiner 2000)(Bosque and Prusiner 2000). Dotted lines represent the boundaries of the coverslip.

Figure 3.8 Characterization of HY and DY prion replication by cell-lifting assay.



Production and Characterization of RK13 Cells Co-Expressing SHa-PrP^C & HIV-1 Gag

RK13SHa-PrP cells were transfected with HIV-1 Gag. After selection of stable HIV-1 gag expression, cells were infected with 0.2% (w/v) HY or DY infected brain homogenates and passaged for three rounds. At third passages the bulk-infected cell population was single-cell cloned by limited dilution. Individual clones were identified and consolidated to seven, 96-well cell culture plates, creating a total population of 672 clones (Fig. 3.9A). Of these 672 clones, 23 clones (3.4%) infected with HY exhibited a positive signal for PrP^{Sc}, while all 672 clones from the DY infection remained PrP^{Sc} negative (Fig. 3.9A).

A modified-scrapie cell assay was used to rapidly determine and identify PrP^{Sc} positive clones (Fig. 3.9B). Confluent clones grown in the 96-well cell culture plates were counted and 20,000 cells were transferred to the 96 well, 0.45µm filter-ELISPOT plates. Unlike the CPCA or the SCA (Mahal, Demczyk et al. 2008; Bian, Napier et al. 2010), this approach does not utilize log dilutions of infectious material. Equal amounts of the infectious agent were used (0.2% w/v HY or DY brain homogenate).

All 23 PrP^{Sc} positive clones infected with HY prions were expanded by serial passage to larger culture conditions for assessment of PrP^{Sc} production. Western immuno-blotting was used in subsequent analyses. At fifth passage, 8 out of 23 (35%) RK13SHaPrP^C-HY infected clones lost detectable PrP^{Sc} (Fig 3.9C top blots). By the tenth passage, none of the clones exhibited detectable PK resistant PrP^{Sc} (Fig 3.9C, middle blots). We continued to passage the 23 RK13SHaPrP^C-HY clones for 10 more passages, but PrP^{Sc} remained absent in all 23 clones after the 20th passage (Fig. 3.9C, lower blots).

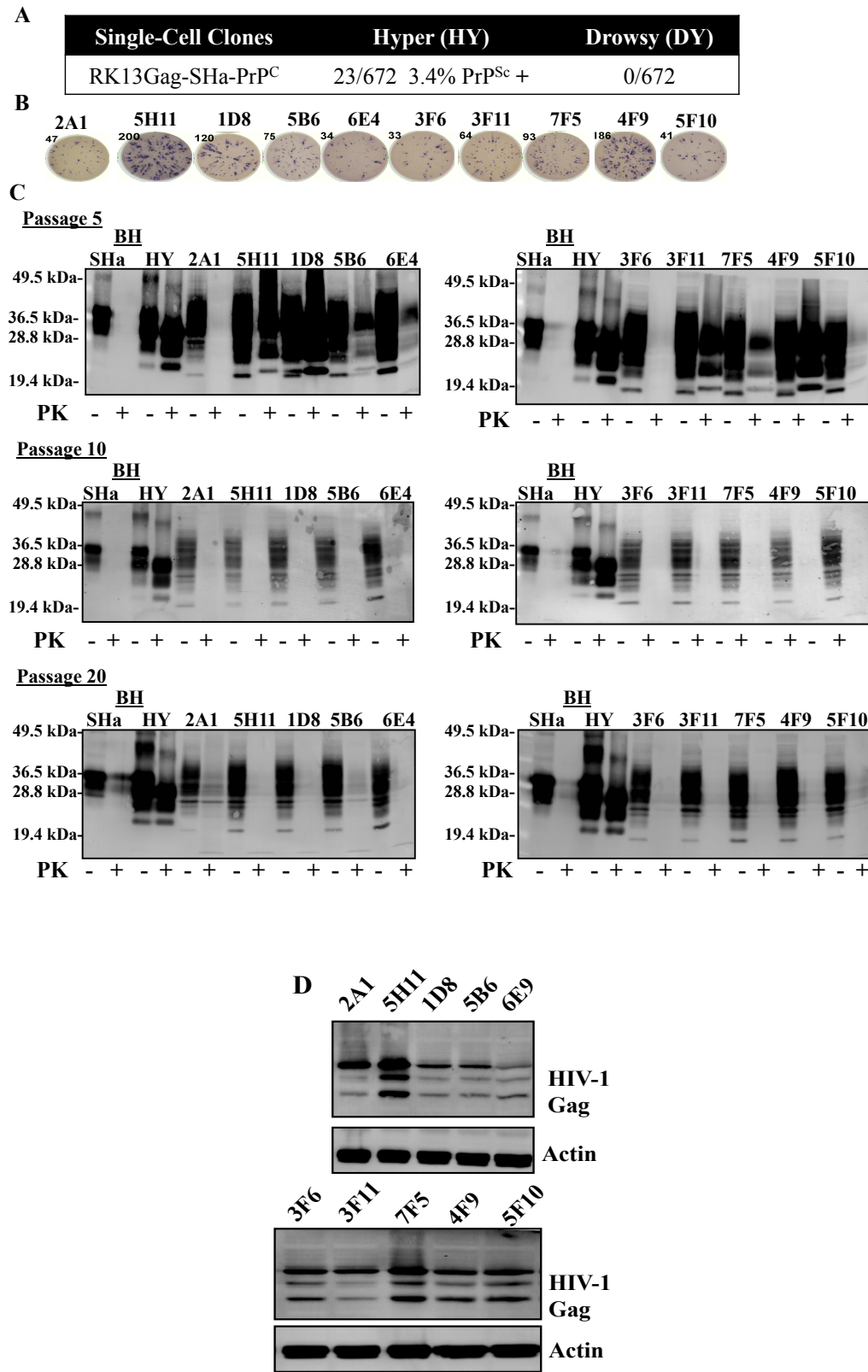
We hypothesized the eventual loss of HY-PrP^{Sc} in the 23 RK13 SHa-PrP^C-Gag clones was due to reduced expression of HIV-1 Gag. Expression of HIV-1 Gag was assessed for each clone through Western blotting using the p24 mAb (MAB880-A; Chemicon, Cat. No. 9876543). While expression of HIV-1 Gag varied between clones, it did not correlate with HY-PrP^{Sc} replication (Fig. 3.9D).

Section Summary: The results from this section show the versatility of RK13 cells to support replication of various prions from different species. Engineering of the RK13 cells to express hamster PrP^C permitted replication of HY- but not DY- prions, thus providing the means to differentiate these strains cell culture techniques. Our data indicate that cloning is a crucial step for identifying individual cells expressing the appropriate cellular co-factors for prion replication.

N2a cells demonstrate a similar resistant phenotype towards HY and DY as described in the CWD infection studies (Chapter 3, section I). In addition, the co-expression of hamster PrP^C in N2a-SHaPrP cells did not hinder the replication of mouse-adapted RML prions. In this respect, these results differ from the behavior of Tg mice expressing SHa and mouse PrP, which are capable of replicating SH prions (Scott, Foster et al. 1989).

Figure 3.9 Transient replication of HY prions in RK13Gag-SHaPrP cells. **A.** Single-cell RK13 clones co-expressing SHa-PrP^C and HIV-1 Gag, infected with 0.2% (w/v) HY or DY prions, assayed by a modified Scrapie cell assay. **B.** Wells representing PrP^{Sc} positive wells (clones) selected for further expansion and continuous passage. **C.** RK13-SHaPrP^C cells positively identified for HY replication by the SCA were expanded and serially passaged. The clones replicated HY for ten passages post infection. Immunoblots were assessed using mAb 3F4. **D.** Expression of HIV-1 Gag was assessed for each clone along with actin expression for total protein control. A total of 23 PrP^{Res} positive clones were identified. Upon expansion of these clones, some lost PrP^{Sc}. Ten of the 23 clones analyzed are represented.

Figure 3.9 Transient replication of HY prions in RK13Gag-SHaPrP cells.



Discussion

To summarize our findings: (i) Expression of cervid PrP^C in human 293 and N2a cells was not sufficient to sustain CWD replication. (ii) N2a cells co-expressing cervid PrP^C remained susceptible to mouse-adapted RML scrapie prions. (iii) RK13 cells engineered to express elk PrP^C (RKE-cells) transiently replicated CWD prions. (iv) RKE cells (Elk21⁺) were enhanced to sustain CWD prion replication co-expression of HIV-1 Gag and cloning. (v) Expression of SHa PrP^C and subsequent infection HY and DY prions in RK13 cells resulted in the transient replication of HY but not DY prions. (vi) N2a cells expressing SHa-PrP^C did not replicate HY or DY prions but replicated mouse-adapted scrapie RML prions.

Prion Replication and The Prion Species Barrier In Cell Culture: All analyzed cells in these studies ectopically expressed heterologous PrP^C. The stable over-expression of PrP^C did not necessarily confer sensitivity to prions, even within cells that are known for their prion replication capabilities. Previously published data support the notion that PrP^C expression alone is not sufficient for effective prion replication (Graham, Smiley et al. 1977; Telling, Scott et al. 1995; Raeber, Sailer et al. 1999; Bosque and Prusiner 2000). In vivo data implies that the efficiency of PrP^{Sc} replication is strongly influenced by its structural homology to PrP^C, which is the underlying basis for the prion species barrier (Fig. 3.1) (Telling, Scott et al. 1995). RK13 cells expressing Elk PrP^C sustained CWD prion replication, following the addition of HIV-1 Gag (Fig. 3.4). RK13 cells expressing SHa-PrP^C were susceptible to HY-prions (Fig. 3.9), thus abrogating another species barrier in cell culture. Both the N2a and the RK13 cells have previously been shown to

efficiently replicate prions (Race, Fadness et al. 1987; Vilette, Andreoletti et al. 2001). Expression of endogenous PrP^C is the marked difference between N2a and RK13 cells, which is present in the former and undetectable in the latter. This absence of endogenous PrP^C in RK13 cells and their ability to propagate prions from different species produces a system that is analogous to the Tg-mouse model (Fig. 3.1) (Telling, Scott et al. 1995). However, ectopic expression of PrP^C on a null background does not guarantee susceptibility to prions, which was established with the HEK293A cells inability to replicate CWD (Fig. 3.6)

Endogenous PrP Interference In Cell Culture: In addition to the structural homology prerequisites of the PrP molecules, the presence of two different (species) PrP^C proteins could sometimes impose an interfering effect on PrP^{Sc} replication (Scott, Foster et al. 1989; Telling, Scott et al. 1995). The selection of an N2a clonal population that is highly sensitive to mouse-adapted RML does not guarantee replication of prion strains derived from other species. Similar to the Tg-mice data (Telling, Scott et al. 1995), over-expression of cervid- or hamster- PrP^C in the presence of endogenous mouse PrP^C does not permit the replication of prions that are structurally homologous to the over-expressed transgene, indicating that endogenous PrP^C is interfering in the conversion process. More importantly, the interfering effect is unidirectional because cells over-expressing the heterologous PrP^C transgene continue to maintain full susceptibility for RML, which depends on conversion of mouse PrP^C to PrP^{Sc} (Fig. 3.3 and Fig. 3.7). Selection of N2a cells that lack endogenous PrP^C expression, was shown to enable CWD prion replication upon ectopic cervid PrP^C expression, thus further supporting the PrP interfering effect (Pulford, Reim et al. 2010).

A species-specific molecule, termed protein X, is hypothesized to act as cofactor that selectively binds and chaperones the PrP^C-PrP^{Sc} conversion (Fig. 1.4) (Telling, Scott et al. 1995). Thus, protein X's preferential binding for endogenous PrP^C could effectively sequester it from interacting with the heterologous PrP^C-PrP^{Sc} conversion process, consequently making the cells resistant (Fig. 3.3 and Fig. 3.7). Though hamster prion infectivity studies using Tg-mice co-expressing both murine- and hamster-PrP^C efficiently replicated PrP^{Sc} and succumbed to prion disease (Scott, Foster et al. 1989), N2a-SHa-PrP^C cells did not recapitulate these observations (Fig. 3.7 and Fig. 3.9). One possible explanation for these discrepancies is the difference in hamster prion strain used in previous work (Sc237 comparable to HY and DY here). Also, PrP interference was not a factor in these studies because hamster-PrP expressing mice on wt-background did replicate hamster PrP^{Sc} (Scott, Foster et al. 1989). The mechanisms governing these observations are not fully understood but were hypothesized to be related by close homology of murine and hamster PrP^C sequence.

Ectopic Expression of PrP^C is Not Sufficient for PrP^{Sc} Conversion: In transgenic mice, the inactivation of the endogenous *Prnp* gene with subsequent introduction of a heterologous PrP^C abrogates the prion species barrier (Telling, Scott et al. 1995). Furthermore, an inverse relationship exists between the expression level of PrP^C and incubation time of prion disease in mice (Westaway, Mirenda et al. 1991). While PrP^C is absolutely necessary for prion replication (Büeler, Aguzzi et al. 1993), the ectopic expression of PrP^C in certain tissues/cells of *Prnp*^{0/0} mice is not sufficient to sustain PrP^{Sc} (Raeber, Sailer et al. 1999). Likewise, cell culture data exhibit discernable variances towards PrP^{Sc} replication that is unrelated to endogenous PrP^C expression levels (Race,

Caughey et al. 1988; Bosque and Prusiner 2000). Besides the PrP requirement, this data collectively implies that additional cofactors are involved in the prion replication process. Both RK13 and HEK293A cells lack endogenous PrP^C expression, but only one of these cells has the ability to replicate the prions tested here (Fig. 3.4 and Fig. 3.6). Ectopic over-expression of cervid-PrP^C did not facilitate conversion of CerPrP^{Sc} in HEK293. In fact, the HEK293A cells demonstrated complete resistance towards CWD and RML prion replication. The RK13 cells do replicate CWD prions but only after clonal selection and the effect of HIV-1-Gag. In addition to CWD prion replication, we show here that RK13 cells also replicate hamster prions (HY), which suggests that the cellular factors are universally applicable to the PrP^{Sc} replication process.

Enhancement of PrP^{Sc} Replication by HIV-1 Gag: The retroviral element, HIV-1 Gag enhanced the susceptibility of RK13 cells to CWD infection (Bian, Napier et al. 2010). Earlier studies have shown that retroviral infection of cells enhanced scrapie infectivity and extracellular release of PrP^{Sc} by the accelerated formation of Gag-recruited detergent resistant microdomain (DRM)/lipid raft vesicles within the endosomal trafficking compartments (Leblanc, Alais et al. 2006). Coincidentally, PrP^C traffics and co-localizes to the same cellular compartments that the retrovirus uses for assembly and release (Fig. 1.2) (Shyng, Moulder et al. 1995; Vey, Pilkuhn et al. 1996; Ott 1997; Cimorelli and Darlix 2002; Demirov and Freed 2004; Fevrier, Vilette et al. 2004; Pelchen-Matthews, Raposo et al. 2004).

The Gag-polyprotein primary function is to direct viral-particle assembly and budding release using a non-lytic pathway, keeping the host cell viable for continuous viral production (Demirov and Freed 2004). This polyprotein consists of four structural

components that become part of the mature virus. These components consist of matrix protein (MA), capsid (CA), nucleocapsid (NC) and p6 (Gottlinger 2001). Each component has a distinct role in the assembly process. The matrix protein (MA) is a guided target for the plasma membrane, while the CA manages the protein-protein interactions of the assembly process (Gottlinger 2001). The role of NC is to guide and couple the newly generated RNA to the assembling virus (Gottlinger 2001). These three components are shared among all identified retroviruses, while p6 is a unique C-terminus domain found only in primate retrovirus (HIV-1) (Demirov and Freed 2004). The p6 domain's core function is to recruit cellular proteins to assist the budding and release of the newly formed virus (Yu, Matsuda et al. 1995). In addition to the recruitment process of cellular proteins, the p6 domain is vital for releasing the budding virus from the cell surface (Gottlinger, Dorfman et al. 1991). The exact mechanism that p6 uses to achieve this process is not fully understood but the highly conserved sequence motifs of p6 domain indicate a close functional connection to the ubiquitin proteasome system (UPS) (Patnaik, Chau et al. 2000; Schubert, Ott et al. 2000; Strack, Calistri et al. 2000). The components of Gag are activated by proteolytic cleavage of the polyprotein in the late stages of viral assembly and collectively function by recruiting cellular factors, modulating the intracellular trafficking mechanisms and distorting the plasma membrane (Demirov and Freed 2004), all of which are implicated in the PrP^C-PrP^{Sc} conversion process (Caughey, Raymond et al. 1991; Borchelt, Taraboulos et al. 1992; Taraboulos, Raeber et al. 1992; Shyng, Heuser et al. 1994; Peters, Mironov et al. 2003; Fevrier, Vilette et al. 2004; Sarnataro, Caputo et al. 2009; Taylor, Whitehouse et al. 2009; Solis, Malaga-Trillo et al. 2010; Goold, Rabbanian et al. 2011).

Thus, HIV-1 Gag's enhancement of PrP^{Sc} replication could be a multifaceted process involving several cellular mechanisms/pathways. At the cell surface, the distortion of the plasma membrane (PM) by Gag could accelerate PrP^{Sc} conversion by modulating the physical surface area of contact for PrP^C-PrP^{Sc}. Recent reports have suggested that conversion of PrP^{Sc} predominantly occurs at the cell-surface and very rapidly, within one minute of exposure (Goold, Rabbanian et al. 2011). Besides PM modulation, the release of empty buds/vesicles mediated by Gag could accelerate dispersion of newly formed PrP^{Sc} to uninfected neighboring cells by exocytosis (Campbell, Crowe et al. 2001; Fevrier, Vilette et al. 2004; Pelchen-Matthews, Raposo et al. 2004). Furthermore, because PrP^{Sc} conversion can also occur intracellularly, it is probable that Gag partakes within those sites of conversion as well (Borchelt, Taraboulos et al. 1992; Shyng, Huber et al. 1993; Shyng, Heuser et al. 1994; Vey, Pilkuhn et al. 1996; Beranger, Mange et al. 2002; Peters, Mironov et al. 2003; Vella, Sharples et al. 2007). Of potential interest to the PrP^{Sc} conversion process is the role of the p6 domain. In addition to potentially being the direct PrP interacting protein during the vesicle recruitment and formation process, this domain also modulates proteasome degradation pathways (Patnaik, Chau et al. 2000; Schubert, Ott et al. 2000; Strack, Calistri et al. 2000). This interaction of p6 and the UPS could indirectly skew the protein homeostasis machinery in favor of the PrP^C-PrP^{Sc} misfolding process.

The deregulation of UPS from correcting conformationally misfolded proteins by p6 could enhance PrP^{Sc} formation by several mechanisms. During normal biogenesis of PrP^C, misfolded PrP protein is delivered to the proteasome system for refolding or degradation (Ma and Lindquist 2001; Yedidia, Horonchik et al. 2001). The induction of

ER-stress and proteasomal dysfunction causes the cell to accumulate and aggregate PrP molecules (Ma, Wollmann et al. 2002). It has been shown that ER stress and proteasomal inhibition leads to the accelerated accumulation of PrP^{Sc} (Nunziante, Ackermann et al. 2011). Therefore, p6's hijacking of the UPS could produce a scenario where, in addition to the introduction of exogenous PrP^{Sc} from an infectious inoculum source, the cell is also accumulating its own, spontaneously generated aggregated-PrP molecules. Of course this would be a rare event, which would explain why clonal selection is so crucial for identification of cells that become chronically infected with CWD prions. Conversely, preoccupying the UPS could also simply distract the cellular protein aggregation defense mechanisms to give PrP^{Sc} free range on all available PrP^C substrate without interference. These Gag enhancement mechanisms have not been experimentally addressed, but could differ based on the prion strain used in the infection analysis. An example demonstrating the difference would be the RK13-SHaPrP^C-Gag cells inability to chronically replicate HY prions.

Concluding Remarks: The development of these cell culture models facilitates prion infectivity analysis in more depth. Many questions in prion biology remain unanswered. Molecular prion strain properties are difficult to characterize using complex organisms such as mice. Thus, analysis of prion infectivity at the cellular level reduces this complexity and allows characterization of PrP^{Sc} replication in better detail. Furthermore, besides identifying the mechanisms that dictate PrP^{Sc} replication, cell culture models will help pinpoint cofactors that contribute to this process. Of the three cell lines described in this chapter, RK13 cells show promise as a universal cell model for PrP^C-PrP^{Sc} conversion studies. The ability of these cells to replicate prions from different sources can

be used to generate cell based screening assays, elucidate cellular differences between strains and identify cofactors responsible for the permissiveness to convert PrP^C to PrP^{Sc}. It is clear from our work, and previous studies that sensitivity towards prions clonally varies between clones from the same parent cell. In the subsequent portion of this thesis, the phenotypic differences that dictate cellular permissiveness to prion replication begin to be addressed using genomic transcriptional analysis approaches.

Chapter 4

Identification Of Host Factors That Confer Susceptibility to Prions

Introduction

Prion Replication In Vivo: The proposal of a proteinaceous infectious agent that replicates without nucleic acids (Alper, Cramp et al. 1967; Griffith 1967) was substantiated with the identification of PrP^{Sc} and its normally expressed isoform, PrP^C (Fig. 1.3) (McKinley, Bolton et al. 1983; Oesch, Westaway et al. 1985; Barry, Kent et al. 1986; Basler, Oesch et al. 1986). Strong evidence to support the notion that conformational conversion of PrP^C to PrP^{Sc} causes prion disease was provided with the creation of *Prnp*^{0/0} knockout mice (Büeler, Fischer et al. 1992). Mice lacking PrP^C did not generate PrP^{Sc} and were resistant to prion disease (Büeler, Aguzzi et al. 1993). In addition, *Prnp*^{0/0} knockout mice did not exhibit any obvious developmental or behavioral abnormalities (Büeler, Fischer et al. 1992). The ablation of the gene and lack of gross phenotypic abnormalities in the *Prnp*^{0/0} knockout mice indicated that (i) PrP^C is not an embryonic lethal gene and (ii) PrP^C loss-of-function is not the cause of neuronal death in prion diseases (Büeler, Fischer et al. 1992). In contrast, over expression of this PrP in mice accelerates prion replication (Westaway, Mirenda et al. 1991). Finally, ectopic expression of species specific PrP^C on the *Prnp*^{0/0} background permitted numerous studies that improved our understanding of prion species barriers, replication kinetics in vivo, PrP^{Sc} tissue distribution/tropism and neurological deficits (Telling, Scott et al. 1995; Telling, Haga et al. 1996; Bruce, Will et al. 1997; Asante, Linehan et al. 2002; Browning, Mason et al. 2004; Tamguney, Giles et al. 2006; Green, Castilla et al. 2008; Angers, Seward et al. 2009; Angers, Kang et al. 2010). However, while animal models tell us that

PrP^C is required for disease, identification of additional cofactors that are involved in this process is more challenging. Furthermore, not all tissues/cells derived from *Prnp*^{0/0} mice have the ability to replicate prions upon ectopic expression of PrP^C, additional proof towards cofactor requirements (Raeber, Sailer et al. 1999).

Prion Replication In Vitro: Expression of PrP^C is not sufficient to sustain chronic prion infectivity in cell culture without additional, unidentified factors (Bosque and Prusiner 2000; Courageot, Daude et al. 2008; Lawson 2008; Bian, Napier et al. 2010). N2a cells, which are known to replicate mouse-adapted RML prions, vary in their susceptibility, regardless of expressed PrP levels (Bosque and Prusiner 2000). Studies characterizing N2a infectivity have demonstrated that only 1 out 144 or roughly 0.7% cells sustain chronic infectivity (Race, Fadness et al. 1987; Race, Caughey et al. 1988). This strongly implies that cellular permissiveness to prion replication is co-dependent on unidentified host factors for catalytic transformation of PrP^C into PrP^{Sc} to occur.

We hypothesize that ectopic clones of RK13 cells would vary in susceptibility to prion infection, and that susceptible and resistant clones would vary in levels of expression of required genes.

Transcriptional analysis to elucidate host factors involved in prion replication:

Identifying clonally distinct phenotypes (susceptible/resistant towards prion replication) amongst RK13 cells permits molecular level investigations to elucidate transcriptional differences that confer these phenotypes. We utilized two transcription-profiling approaches to elucidate these phenotypic differences, namely the representational difference analysis (RDA), and full genome microarray transcription scanning. RDA is a subtractive hybridization based method that provides insights into the transcriptional

differences between clonal populations. On the other hand, microarray analyses provide a global perspective of transcriptional differences between the sensitive and resistant clones. Both approaches are subsequently described in greater detail.

Transcription Profiling Using Subtractive Hybridization Methods: Representational Difference Analysis (RDA): In an attempt to identify specific transcriptional differences between sensitive and resistant clones, the first approach we used was the RDA (Vinnik and Lisitsyn 1993; Lisitsyn, Leach et al. 1994). The benefit of using this approach is its unbiased ability to identify unique transcripts without specific or known primers to initiate the search. The technique becomes advantageous when applied towards the RK13 system and its poorly annotated rabbit genome. RDA is a PCR based technique that uses subtractive hybridization to remove homologous transcripts shared between two DNA sources, referred to as “tester” and “driver” DNA. Total RNA is purified from two compared populations and mRNA is sub-purified for reverse transcription to cDNA. Generally, the “driver” DNA is supplied at various ratios in excess of the “tester” DNA to remove as many homologous transcripts as possible, leaving only the non-homologous transcripts for identification. By using this technique we aimed to identify and characterize unique transcripts in sensitive and resistant RK13 sub-clones.

Transcription Analysis Using DNA Microarray Technology: DNA microarrays, also known as DNA chips or gene chips, are essentially a large collection of oligonucleotide probes that have been attached to a solid surface. The attached oligonucleotide probes vary in length, which depends on target DNA source to be hybridized. Moreover, the probes used for the chips represent different aspects of genetic information from a target organism. This experimental design for the microarray chip can target expression level

variations, detect single nucleotide polymorphisms (SNP's), genotype and identify mutations in specific tissue sources (Churchill 2002; Oleksiak, Churchill et al. 2002). The microarray's sizeable probe capacity facilitates high-throughput investigations (Churchill 2002).

The primary principle of microarray technology is based on the hybridization of a fluorescently labeled target sample (cDNA, cRNA) to probe immobilized oligonucleotide sequences. The typical microarray experiments begin with RNA isolation from target tissue/cell source. The RNA is then quantified and analyzed for purity. Pure RNA is reverse transcribed and fluorescently labeled by sequential enzymatic reactions to produce microarray hybridizing nucleic acids for detection. The target sample is hybridized to the chips and put through stringency washes to remove poorly hybridized samples. Finally, a scanner is used to read the chips and quantitatively calculate the total strength of the hybridized signal intensity.

There are several challenges associated with the microarray methodology and the bioinformatic analysis of the data. These challenges come up for consideration prior to-, during- and post- experiments. They include: the biological complexity of the experimental design and the statistical significance that has to be attained to gain valid conclusions; standardization of the protocol for consistency of data acquisition; statistical analysis of the large data sets, which include normalization methods to remove background noise and identification of statistical significance; accuracy and precision of the hybridized probe, and the gene it matches; lastly, the handling and distribution of data, which is a major bottleneck for microarray experimentation due to a lack of standardized bioinformatic platforms and extremely large data sets that require immense

storage capacity and significant computing power (Simon 2009; Kim, Zakharkin et al. 2010).

Prion Disease Transcription Profiling: Initial transcription profiling of prion diseases utilized subtractive cloning of single stranded cDNA libraries derived from scrapie-infected mouse and/or hamster brains. These studies identified three specific transcripts that were present in abundance, the transcripts identified were the glial fibrillary acidic protein, metallothionein II, and the B chain of α -crystallin (Wietgreffe, Zupancic et al. 1985; Duguid, Rohwer et al. 1988). The follow up studies using a similar approach confirmed the original findings and in addition, identified transferrin and sulfated glycoprotein-2 (clusterin) (Duguid, Bohmont et al. 1989). Subsequently, differential gene expression of transferrin, sulfated glycoprotein-2, glial fibrillary acidic protein and metallothionein were also detected in hippocampal regions of Alzheimer's disease (AD) and Pick disease (PD²) (Duguid, Bohmont et al. 1989), thus linking these genes with other known neurodegenerative diseases (Duguid, Bohmont et al. 1989). The search for specific genes associated with neurodegeneration during the progression of prion disease continued with an improved technique of the time called the "mRNA differential display" method. This technique helped identify five more genes missed by previous analyses that include cathepsin S, the C1q B-chain of complement, apolipoprotein D, and scrapie-responsive genes ScRG-1 and ScRG-2 (Dandoy-Dron, Guillo et al. 1998).

Improvement in gene expression technology expanded and improved the studies searching for gene-specific changes associated with prion diseases. A high-throughput analysis using cDNA microarray chips identified 158 differentially expressed genes in the CNS of prion-infected mice (Booth, Bowman et al. 2004). These microarrays

facilitated analysis of gene expression changes throughout the progression of the disease that include early, middle (preclinical) and late (clinical) stage time points. The gradual gene expression data collected over the described stages of disease link biological processes with progression of neurodegeneration on a transcriptional level (Booth, Bowman et al. 2004). Similar studies using these profiling techniques reported additional genes that were associated with inflammation and stress response (Brown, Webb et al. 2004; Riemer, Neidhold et al. 2004; Xiang, Windl et al. 2004). Expression analysis of prion infected but preclinical (170 days post infection (dpi)) mouse hippocampus revealed 78 novel genes to be differentially expressed, specific that region of the brain (Brown, Rebus et al. 2005). These novel genes were reported to associate with perturbation of ER, up regulation of glycosylation enzymes, chaperones, protein trafficking and cellular degradation machinery.

In addition to the newly identified genes that associate with preclinical phase of prion disease in mice, the stringent mathematical conditions (fold change >1.5 and $p\text{-value} < 0.01$) applied towards microarray data set signal processing confirmed differential expression of genes that have been reported in previous studies (Brown, Rebus et al. 2005). These findings therefore validate transcription profiling as a viable technique to monitor molecular changes during prion pathogenesis (Duguid, Rohwer et al. 1988; Dandoy-Dron, Guillo et al. 1998; Booth, Bowman et al. 2004; Brown, Webb et al. 2004).

A recent study compared gene expression differences from mice infected with three different mouse-adapted scrapie prion strains (ME7, 22L & RML), therefore taking a global perspective of molecular events that occur in prion diseases (Skinner, Abbassi et

al. 2006). The results from those studies revealed a total of 400 genes differentially regulated during the symptomatic (clinical) stage and 22 genes during the preclinical stage, averaged out between all three prion strains. Significant differences of gene expression were reported within each prion strain as well (Skinner, Abbassi et al. 2006). These expression profiling studies were expanded for natural prion diseases, which include gene expression analysis in cattle post BSE infection (Khaniya, Almeida et al. 2009; Almeida, Basu et al. 2011; Panelli, Strozzi et al. 2011), natural scrapie in sheep (Filali, Martin-Burriel et al. 2011; Gossner, Foster et al. 2011), and human CJD (Baker, Martin et al. 2002; Sugaya, Nakamura et al. 2002; Baker and Manuelidis 2003; Xiang, Windl et al. 2005; Mead, Poulter et al. 2009; Medina, Hatherall et al. 2009).

In vitro experiments analyzing the transcriptional response to prion infection have thus far produced sub-optimal results that lack the consistency *in vivo* data exhibited (Doh-ura, Perryman et al. 1995; Satoh and Yamamura 2004; Greenwood, Horsch et al. 2005; Julius, Hutter et al. 2008). Initial cell culture experiments analyzing gene expression differences between infected (ScN2a) and un-infected N2a cells utilized cDNA library subtractive-hybridization techniques as described for the *in vivo* studies (Doh-ura, Perryman et al. 1995). Five specific genes with altered mRNA expression were identified in the ScN2a cells that included: chromogranin B, intracisternal-A particle envelope, ornithine decarboxylase antizyme, heat shock protein 70 and one gene not previously described (Doh-ura, Perryman et al. 1995). The identified transcripts were present in both cell types (ScN2a & N2a) and did not indicate a unique association with scrapie infection of the cells.

A different approach was used on cells that do not express endogenous PrP^C. To assess the effect ectopic expression of PrP has on a non-PrP expressing cell, HEK293 cells were genetically modified to express PrP and then transcriptionally profiled (Satoh and Yamamura 2004). Microarray screen revealed 33 genes to be differentially expressed after PrP over-expression. These genes were linked with various neuronal functions that might be associated with undefined PrP^C-mediated neurodegeneration mechanisms (Satoh and Yamamura 2004).

Large-scale gene expression analysis to identify differences between infected and uninfected neuroblastoma cells (ScN2a/N2a) and hypothalamic neuronal cells (GT1) revealed inconclusive results that were based on transcriptional variation of infected and uninfected cells derived from different neuronal sources (Greenwood, Horsch et al. 2005). Likewise, the absence of a universal transcriptional response to persistent prion infection within three murine cell lines led to the conclusion that prion infection does not induce transcriptional alterations in an *in vitro* setting, which implicate that genes that render the cells susceptible to prion replication are present prior to exposure (Julius, Hutter et al. 2008). Collectively, these studies examined differential gene expression that compared differences before and after prion infection and the effect PrP^C imposed on cells that do not normally express this gene (Doh-ura, Perryman et al. 1995; Satoh and Yamamura 2004; Greenwood, Horsch et al. 2005; Julius, Hutter et al. 2008). A mechanistic perspective towards prion replication and endogenous gene expression to identify cofactors was not considered.

In our study, we compare clonal cells derived from a common parental cell, that phenotypically differ in the susceptibility to replicating prions. Our primary aims are to identify genetic variance that distinguish these phenotypes.

RESULTS

Section I: Identification and Characterization of Susceptible/Resistant RK13 Clones

Expressing Murine PrP^C (RKM)

RKM Clonal Selection: We stably transfected RK13 cells with an expression vector containing the murine PrP^C ORF, using the pIRESpuro expression vector. Individual clones were generated by limited dilution cloning. Seventy-eight single cell RK13 (RKM) clones were identified. Clonal populations were expanded and passaged onto 10-cm cell culture plates. PrP^C expression in the RKM clones was assessed by Western immuno-blotting using mAb 6H4 (Fig. 4.1A). RKM clones exhibited differential expression and processing of PrP^C (Fig. 4.1A). PrP^C protein levels were evaluated by densitometry analysis (Fig. 4.1E), using ImageJ image analysis software (Abramoff 2004). The intensity of each protein band on the Western blot was measured and recorded (Table 4.1).

The variation of PrP^C expression is represented in figure 4.1E. To address whether PrP^C expression levels correlated with prion infectivity in cell culture, the cloned RKM cells were infected with mouse-adapted RML scrapie prions.

RKM/N2a Clone Infection With RML Scrapie:

The RKM's tolerance toward prion replication was assessed using the cell-lift assay and mSCA (described in chapter 3). Individual RKM clones were infected with 0.2% (w/v) mouse-adapted RML scrapie diseased-BH in a 48-well cell culture format. The cells were passaged for three consecutive rounds, and analyzed for PK resistant PrP^{Sc} by the cell-lifting assay. The RKM clones exhibited various levels of cellular permissiveness to prion replication, ranging from robust infectivity to complete resistance (Fig. 4.1B and Fig. 4.1F). Of the 78 RKM clones infected with RML, 8 (10%) were resistant, 15 (19%) were partially resistant (show weak signal), 18 (23%) were moderately sensitive, and were 37 (47%) are highly sensitive (Fig. 4.1B). PK resistant signals from the cell lifting membranes were evaluated using densitometry analysis, which is graphically and numerically presented in figure 4.1F and table 4.1.

Limited dilution cloning was used to identify 14 N2a single-cell clones, which were subject to similar experimental approaches used on the RKM cell. The RML infected N2a (ScN2a) clones were segregated based on susceptibility: 4 (29%) completely resistant sub-clones, 5 (36%) partially resistant sub-clones and 5 (36%) highly susceptible sub-clones (Fig. 4.1C). The dotted lines in figures 4.1B and 4.1C were added to represent the location of individual clones that demonstrated resistance towards PrP^{Sc} replication, exhibited by the absence PK resistant material.

The mSCA was used to confirm the cell lifting data and semi-quantify the results. The 78 RKM clones were infected with 0.2% RML using the mSCA format (described in chapter 3) and passaged three consecutive rounds in a 96-well cell culture plate post infection. These RML-infected cells were transferred (20,000 total cells) to the 96-well ELISPOT plate and developed. Figure 4.1D represents the individual well readout using

the mSCA, while figure 4.1G graphically demonstrates the susceptibility of cells to RML based on the averaged spot counts. The positive control used for the mSCA were RKM cells chronically infected with RML and designated with a plus sign (+) in Fig. 4.1D. The negative control was RK13 cells transfected with an empty expression vector referred to as RKV and designated by a negative sign (-) in Fig. 4.2C. The clones were infected in triplicate to establish an average spot count (Fig. 4.1D). Quantitation of PrP^{Sc} production using the mSCA was determined by counting individual spots from each well, which is presented by a numerical value directly above the well (Table 4.1). The averaged numerical data of the mSCA and of the cell lifting densitometry data was statistically applied to ascertain correlation between PrP^C expression level and clonal susceptibility to replicating RML prions.

PrP^C expression levels did not correlate with prion susceptibility in the RKM cell culture model. RKM clones 41 and 47 do not express PrP^C and have no detectable levels of PrP^{Sc} (Figs. 4.1A-B, 4.1E-G)(Table 4.1), while RKM clones 8 and 18 express low levels of PrP^C and exhibit moderate production of PrP^{Sc} (Figs. 4.1A-B, 4.1E-G). RKM clones 1, 5, 61, 76 and 78 exhibit robust expression of PrP^C by Western blot, however they did not accumulate PrP^{Sc} (Fig. 4.1A and 4.1B) (Table 4.1).

The coefficient of determination (R^2) was assessed using linear regression to calculate the correlation between PrP^C expression and PrP^{Sc} positive clones (Fig. 4.1H and Fig. 4.1I). Comparing the correlation between the evaluated densities of PrP^C (Fig. 4.1A) and PrP^{Sc} (Fig. 4.1B) resulted in a R^2 value of 0.01317 (Fig. 4.1H), which strongly suggests the absence of a relationship between cellular PrP expression levels and susceptibility for sustaining chronic prion infectivity. The RKM clone sensitivity by cell

lifting assay (Fig. 4.1B) was confirmed using the mSCA (Fig. 4.1D, exemplary representation of the assay). Specifically, RKM clones 7, 18, 19, 35, 36, 37, 38, 43, 51, 52, 60, 62, 65, 68 and 75 reveal increased RML susceptibility, while RKM clones 5, 8, 41, 47, 69 and 78 remained mostly PrP^{Sc} negative (Fig. 4.1B & 4.1D). The correlation comparison of PrP^C expression to mSCA averaged PrP^{Sc}-positive cell counts generated the R² value of 0.003517 (Fig. 4.1I). Collectively, our data suggests that PrP^C expression levels in the RKM clones do not dictate cellular susceptibility for RML, and although PrP^C expression is required for infectivity, supplementary host factors are also involved in the PrP^{Sc} replication process.

Figure 4.1 RKM clonal variability towards PrP^C expression and RML susceptibility.

A. 78 clones were identified through limited dilution single-cell cloning. PrP^C expression was assessed by western blotting using mAb 6H4. Actin expression in the lower panel represents total protein control. Single cell **(B)** RKM subclones and **(C)** N2a subclones were infected with 0.2% (w/v) mouse-adapted RML scrapie prions diseased mouse brain homogenate (BH), and assayed for prion susceptibility in 24-well cell culture plates by the cell lifting assay. The cells were grown to confluence on cell culture cover slips. Confluent cells were transferred to cold lysis buffer soaked nitrocellulose membrane. The membrane was treated with PK (5µg/ml), denatured with 3M guanidine isothiocyanate, immunoprobed mAb 6H4. The dark circles represent PK resistant material. **D.** Representation of the semi-quantitative modified scrapie cell assay to assess prion replication in the RKM subclones (examples include clones 1,7,8,9,18,19 &20). RKV (vector only) and chronically infected RKM cells represent the negative (-) and positive controls (+), respectively. The clones were seeded to 96-well cell culture plates (20,000 cells/well) and infected with 0.2% (w/v) mouse-adapted RML scrapie prions. On third passage after infection, the cells were trypsinized and counted. Twenty thousand cells were transferred to the 96-well ELISPOT filter plates. The plates were treated with PK (5µg/ml), denatured with 3M guanidine isothiocyanate, immunoprobed with mAb 6H4 primary and an Alkaline-Phosphatase (AP)-conjugated anti-mouse secondary antibody. The combination of NBT (nitro-blue tetrazolium chloride) and BCIP (5-bromo-4-chloro-3'-indolyphosphate p-toluidine salt) was used to detect PrP^{Sc} positive cells. Each 96-well plate was scanned using the CTL-ImmunoSpot plate reader and quantification of positive signal was achieved with the ImmunoSpot Software. **(E-F).** Western blot PrP^C expression

levels (**E**) and PK resistant PrP^{Sc} from cell lifting membranes (**F**) were quantified using the ImageJ analysis software package. The y-axis represents the densitometric value subtracted from the background of the scanned membrane. The densitometry values used for the bar graphs are listed in Table 4.1. The x-axis represents the 78 RKM clones in order from left to right (1...78). PrP^C expression does not correlate with susceptibility towards replicating RML prions. Linear regression was used to calculate the coefficient of determination (R^2) between PrP^C expression (x-axis) to (**H**) cell-lifting PK resistant PrP^{Sc} (y-axis) and (**I**) modified scrapie cell assay PrP^{Sc}-spot counts from infected clones (y-axis). GraphPad Prism Software was used to graph data points (Table 4.1) and calculate R^2 .

Figure 4.1 RKM clonal variability towards PrP^C expression and RML susceptibility.

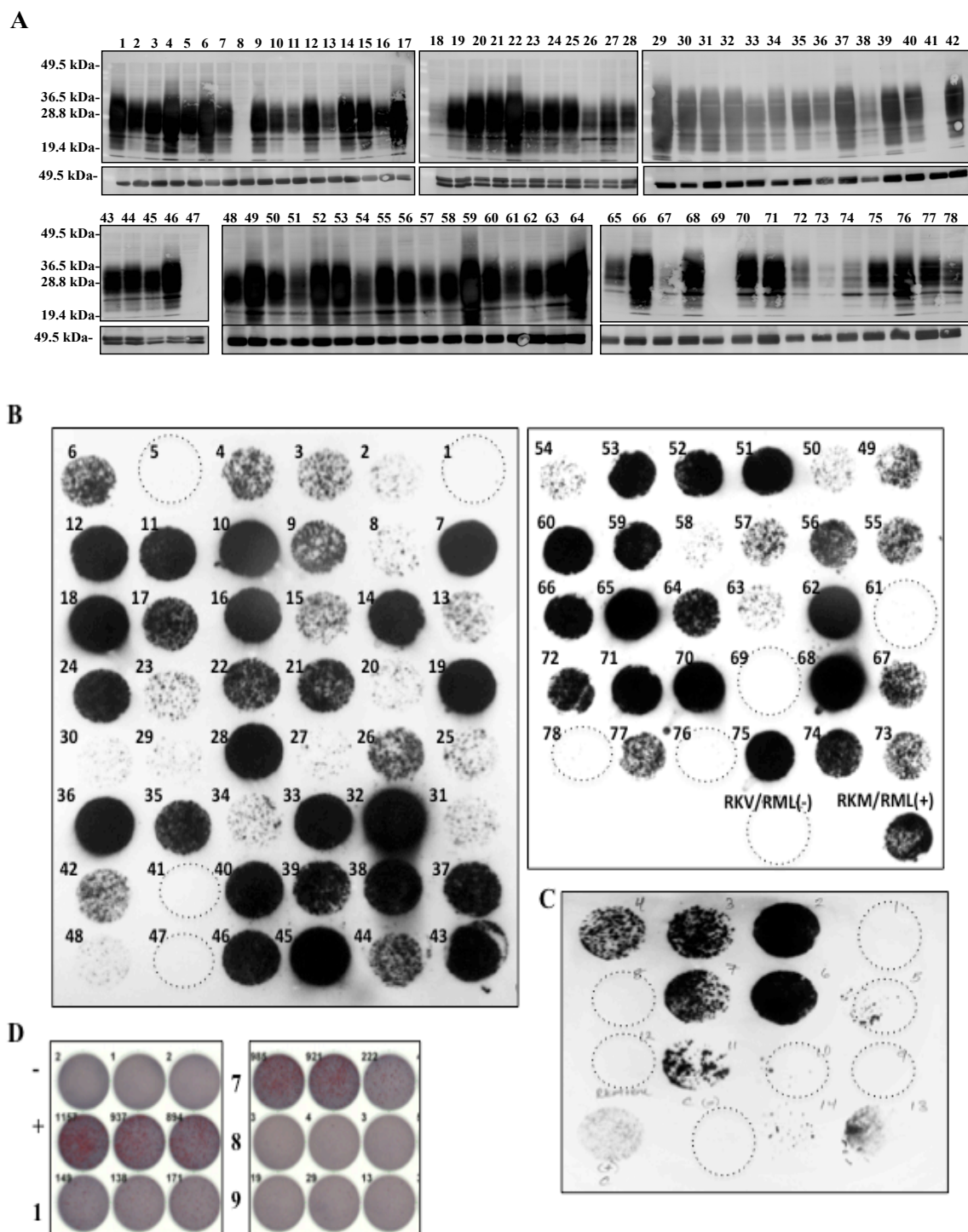


Figure 4.1 RKM clonal variability towards PrP^C expression and RML susceptibility

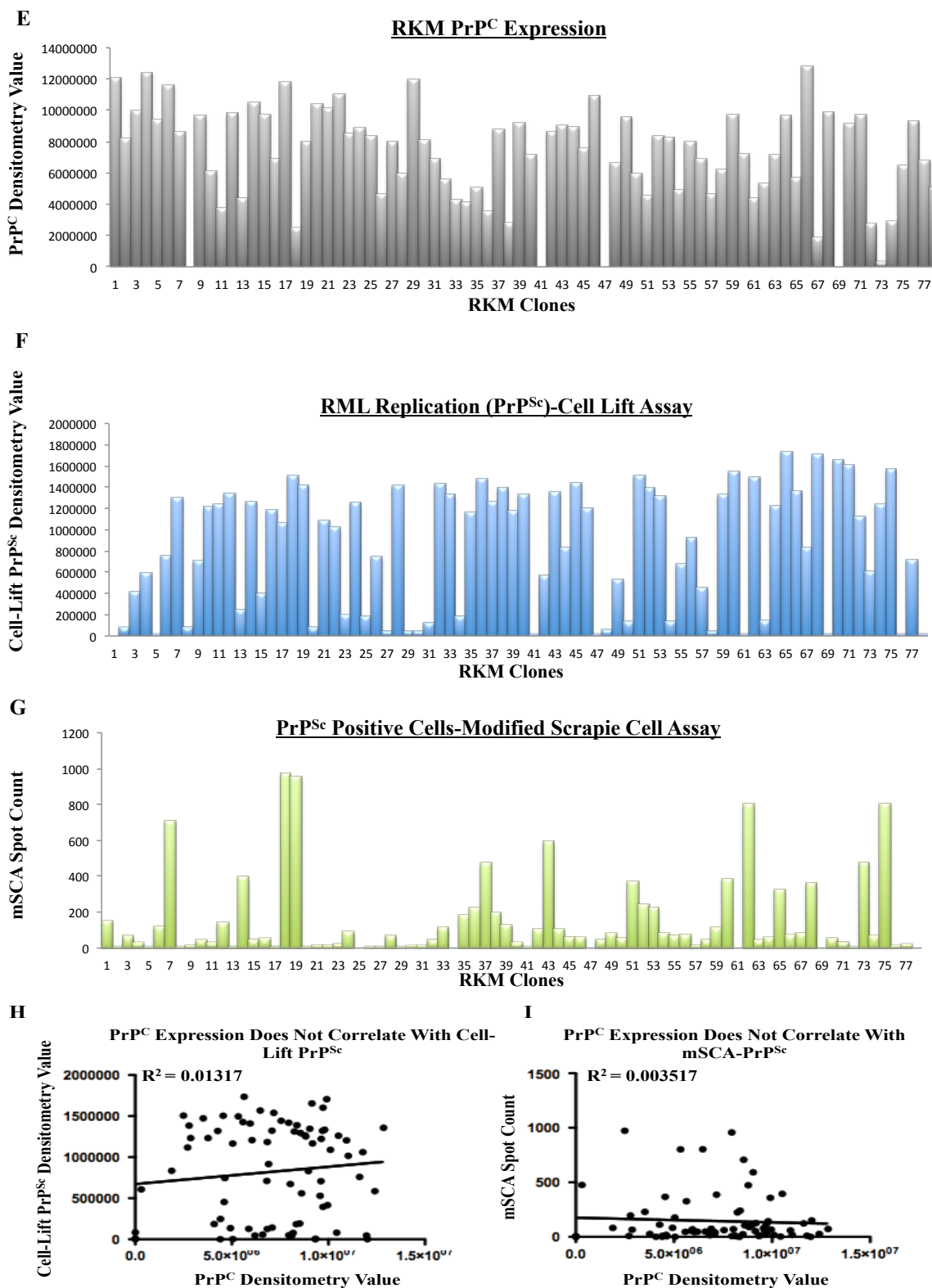


Table 4.1 Summary of RML prion replication amongst cloned RKM cells using three distinct assays for assessment (Abramoff 2004)

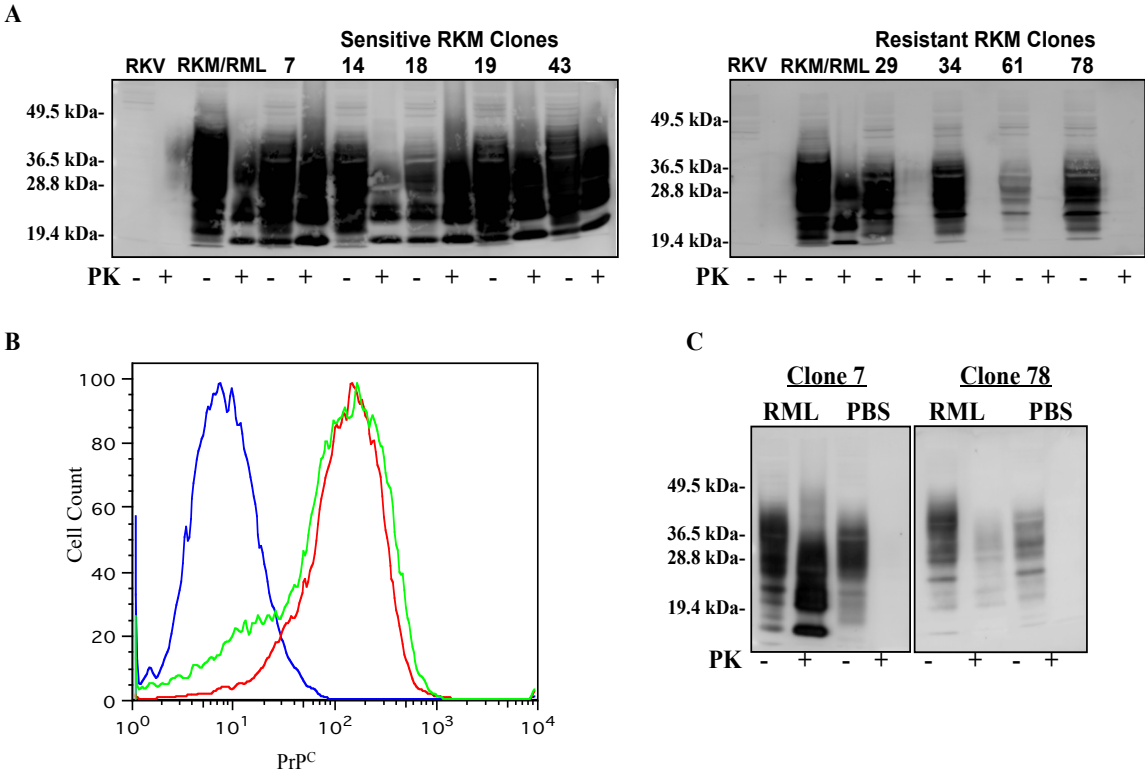
RKM clone	PrP ^C	PK+ Cell Lift	PK+ SCA	RKM clone	PrP ^C	PK+ Cell Lift	PK+ SCA	RKM clone	PrP ^C	PK+ Cell Lift	PK+ SCA
1	1.2E+07	0.0E+00	150.67	31	6.8E+06	1.3E+05	14.67	61	4.4E+06	9.8E+02	0
2	8.2E+06	7.7E+04	5	32	5.6E+06	1.4E+06	45.67	62	5.3E+06	1.5E+06	801.67
3	1.0E+07	4.2E+05	66.5	33	4.3E+06	1.3E+06	112.33	63	7.1E+06	1.4E+05	41.67
4	1.2E+07	5.9E+05	27.16	34	4.1E+06	1.9E+05	0	64	9.6E+06	1.2E+06	58.67
5	9.3E+06	5.8E+03	6.5	35	5.0E+06	1.2E+06	177.33	65	5.6E+06	1.7E+06	326.67
6	1.2E+07	7.6E+05	122.5	36	3.5E+06	1.5E+06	229	66	1.3E+07	1.4E+06	71.67
7	8.6E+06	1.3E+06	706.83	37	8.8E+06	1.3E+06	473	67	1.9E+06	8.3E+05	81.67
8	0.0E+00	8.5E+04	2.5	38	2.8E+06	1.4E+06	195.66	68	9.9E+06	1.7E+06	358
9	9.6E+06	7.1E+05	17.83	39	9.2E+06	1.2E+06	125.66	69	0.0E+00	1.3E+02	0
10	6.0E+06	1.2E+06	43.5	40	7.1E+06	1.3E+06	28.33	70	9.1E+06	1.7E+06	52.67
11	3.8E+06	1.2E+06	27.17	41	0.0E+00	5.7E+03	5.33	71	9.7E+06	1.6E+06	32
12	9.8E+06	1.3E+06	142.83	42	8.6E+06	5.6E+05	105	72	2.7E+06	1.1E+06	8.67
13	4.4E+06	2.5E+05	9.83	43	9.0E+06	1.3E+06	591.66	73	3.1E+05	6.1E+05	475.67
14	1.1E+07	1.3E+06	394.5	44	9.0E+06	8.3E+05	104.66	74	2.9E+06	1.2E+06	65.34
15	9.7E+06	3.9E+05	47.83	45	7.6E+06	1.4E+06	62.33	75	6.5E+06	1.6E+06	802.67
16	6.8E+06	1.2E+06	51.5	46	1.1E+07	1.2E+06	59.33	76	9.3E+06	1.1E+03	15
17	1.2E+07	1.1E+06	10.5	47	0.0E+00	8.9E+03	0	77	6.8E+06	7.1E+05	19.67
18	2.5E+06	1.5E+06	972.5	48	6.6E+06	5.7E+04	47.66	78	5.1E+06	3.0E+03	0
19	7.9E+06	1.4E+06	956.83	49	9.6E+06	5.3E+05	79.33				
20	1.0E+07	8.1E+04	3.5	50	5.9E+06	1.3E+05	55.33				
21	1.0E+07	1.1E+06	16.83	51	4.6E+06	1.5E+06	366.33				
22	1.1E+07	1.0E+06	16.83	52	8.4E+06	1.4E+06	241				
23	8.5E+06	1.9E+05	23.83	53	8.2E+06	1.3E+06	224.33				
24	8.8E+06	1.3E+06	89.67	54	4.9E+06	1.4E+05	83.66				
25	8.3E+06	1.8E+05	0	55	8.0E+06	6.7E+05	70				
26	4.6E+06	7.5E+05	5.16	56	6.9E+06	9.2E+05	74				
27	8.0E+06	4.9E+04	7.16	57	4.6E+06	4.5E+05	17.66				
28	5.9E+06	1.4E+06	69.16	58	6.2E+06	4.5E+04	47.33				
29	1.2E+07	4.6E+04	0.16	59	9.7E+06	1.3E+06	110.33				
30	8.1E+06	4.5E+04	11.16	60	7.2E+06	1.5E+06	386.66				

To ascertain chronic replication of RML prions, certain RKM clones were chosen for expansion and continuous passage. RKM clones 7, 14, 18, 19 and 43 were chosen for their sensitivity and RKM clones 29, 34, 61 and 78 were selected for their resistance to RML. Each clone was passaged 20 times and assessed for sustained production of PK resistant PrP^{Sc}. The RML sensitive clones (7, 14, 18, 19 and 43) chronically sustained a steady state of PK resistant PrP^{Sc}, whereas the resistant RKM clones (29, 34, 61 and 78) exhibited no detectable PK resistant PrP^{Sc} (Fig. 4.2A).

To address whether the sensitive/resistant phenotypes of cells reflect differences in cell surface presentation of PrP^C, two clones with similar PrP^C expression levels and distinct prion susceptibility (sensitive/resistant) were selected for cell surface presentation comparison analysis. The two RKM clones selected for the study were clone 7 (RML sensitive) and clone 78 (RML resistant) (Figs. 4.1 and 4.2A). Surface expression of PrP^C was analyzed in both clones by flow cytometry. The mAb SAF-32 targeted to the octapeptide-repeat region located at the N-terminus of the PrP^C (Fig. 1.1A) was utilized for this purpose. The flow cytometric data reveal no differences in cell surface expression of PrP^C between the two clones (Fig. 4.2B).

Figure 4.2 Accumulation of PK-resistant PrP and PrP^C surface expression in RML susceptible and resistant RKM clones. **A.** RML sensitive (7, 14, 18, 19, & 43) and resistant (29, 34, 61 & 78) clones cell lysates were PK digested and analyzed by Western immuno blotting after 20 passages. RKV (vector only) and chronically infected RKM cells represent the negative (-) and positive controls (+), respectively. PrP^{Sc} was detected using mAb 6H4. **B.** PrP^C cell surface expression was assessed in RML sensitive (RKM clone 7, green line) and resistant (RKM clone 78, red line) and compared to the non-PrP^C expressing RK13 control (blue line) by flow cytometry. The SAF-32 mAb was used for cell surface detection of PrP^C. The y- and x-axis of the histogram represents the cellular counts and the mean fluorescent intensity (MFI) of PrP^C, respectively. **(C)** Subsequent RML-susceptibility analyses of uninfected RKM clones (7 & 78) revealed RKM-78 (Resistant) ability to replicate low-levels of PK resistant PrP^{Sc}. The Western blot represents cell lysate analysis after 12 passage rounds. PrP was detected using mAb 6H4.

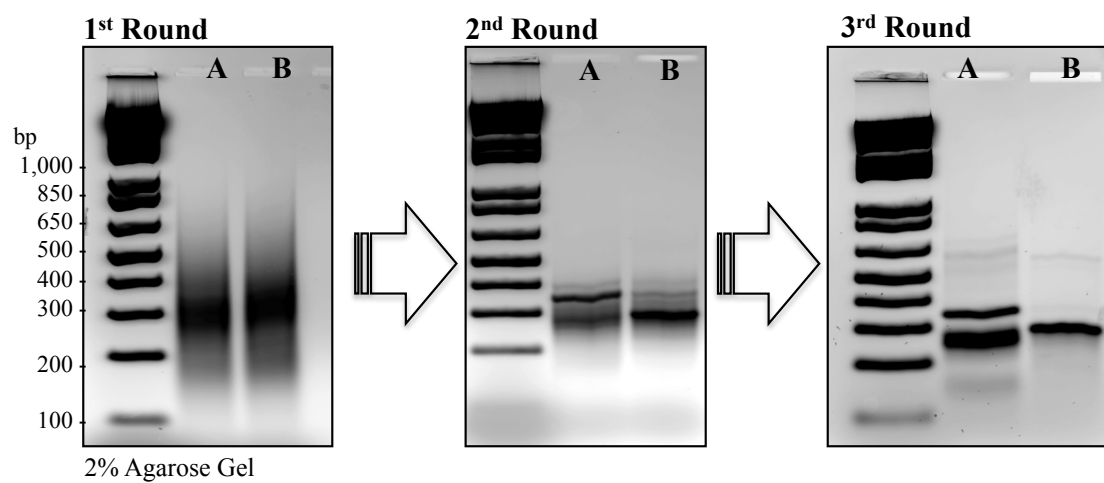
Figure 4.2 Accumulation of PK-resistant PrP and PrP^C surface expression in RML susceptible and resistant RKM clones.



Transcriptional Profiling By RDA: RKM clones 7 and 78 were utilized as the representative clones for transcriptional profiling by RDA. The two clones were subjected to three successive rounds of subtractive hybridization and amplification. The stringency of hybridization was increased with each round (Fig. 4.3). The final enriched PCR products of RKM 7 and RKM 78 were separated using 2% agarose DNA gel electrophoresis (Fig. 4.3). Distinct PCR bands were identified for both subtractive reactions and exhibited specific migration patterns in the range of 150 bp - 400 bp (Fig. 4.3). These DNA bands were carefully excised, purified and cloned into the pGEM-T vector. The cloned products were transformed into competent bacterial cells and grown on antibiotic selective agar plates. A total of 98 individual colonies were picked between the two clonal RDA products. Plasmids were purified from these colonies and subsequently sequenced to identify specific transcripts. A total of eight unique non-homologous transcripts were recognized between the susceptible and resistant clones (Table's 4.2 and 4.3).

Figure 4.3 RDA for the identification of differentially expressed genes in RKM subclones. The 2% agarose gels represent sequential subtractive hybridization coupled to PCR-mediated enrichment for differentially expressed transcripts in susceptible (RKM7) and resistant (RKM78) clones. Representation of two nearly identical DNA pools is generated in round 1, followed by subtractive/kinetic enrichment for distinct difference product in rounds 2 and 3. For each round, lane (A) represents RKM 7 (susceptible) clone as the tester (cDNA limited) cDNA amplifying non-homologous sequences unique to that cell that is subtracted by RKM 78 (resistant) clone driver (cDNA added in excess). Lane (B) is the subtractive/kinetic enrichment in reverse order of (A). The tester:driver stringency ratios were increased for each subtractive round as follows: Round 1: 1:50, Round 2: 1:500, Round 3: 1:1000

Figure 4.3 RDA for the identification of differentially expressed genes in RKM subclones.



RDA Identified Transcripts From RKM Clone 7 (Sensitive): Four specific transcripts were identified in RKM clone 7 by RDA profiling. Three of these four transcripts are either hypothetical and/or conserved hypothetical sequences. Thus, they completely lack functional data to support their existence. The criteria used by the National Center for Biotechnology Information (NCBI) to categorizes identified sequences as hypothetical proteins are based on one of two factors. The protein is deemed hypothetical if its sequence is homologous to genes of unknown function in the NCB database and/or no known homologs exist (Sivashankari and Shanmughavel 2006). All three proteins were derived from the *Oryctolagus cuniculus* (rabbit) genomic sequences annotated using the gene prediction method, GNOMON and supported by EST evidence. The GNOMON gene prediction method is used to predict and annotate genes from poorly unannotated genomes. A complete overview of GNOMON and the NCBI eukaryotic gene prediction tool is available on the NCBI website (<http://www.ncbi.nlm.nih.gov/projects/genome/guide/gnomon.shtml>).

The hypothetical protein with accession number XM_002722317 has not been characterized (Table 4.2). The NCBI nucleotide database search indicates that this predicted protein is 343 amino acids in length and has an approximate molecular weight of 37-kDa (Table 4.3). This novel protein has orthologs throughout mammalian species but has not been functionally analyzed in any of them. The Homo sapiens (human) ortholog is 351 amino acids long and belongs to the uncharacterized protein family 0692 (UPF0692). The Universal Protein Resource (UniProt) database analysis of this protein indicates that it exists at the protein level (subsection of protein attributes descriptor), is found on human chromosome 19, has three potential splice variants and is

posttranslationally modified with the attachment of a phosphate at a serine residue in the c-terminus of the peptide (316 aa, phosphorylated) (Gerhard, Wagner et al. 2004; Grimwood, Gordon et al. 2004; Ota, Suzuki et al. 2004; Dephoure, Zhou et al. 2008). In addition to the UniProt data mining, structure and localization prediction analyses were done using the ExPASy bioinformatic resource portal (<http://expasy.org/tools/>). TargetP (<http://www.cbs.dtu.dk/services/TargetP/>), a bioinformatic tool used to predict subcellular location of eukaryotic proteins indicates that this protein could localize to the mitochondria (mitochondrial targeting sequence) and/or vesicles of the secretory pathways (by signal sequence) (Emanuelsson, Nielsen et al. 2000). YASPIN secondary structure prediction tool (<http://www.ibi.vu.nl/programs/yaspinwww/>) predicts that this hypothetical protein is predominantly coiled due to a proline-rich composition (Lin, Simossis et al. 2005). In addition to the overall coiled structure, 7 α -helices and 8 β -sheets are predicted to span the entire protein (Table 4.3). Thus, although the protein has not been experimentally analyzed, the predicted attributes (evolutionary conservation, phosphorylation site, and highly structured) suggest that it has a physiological function that has yet to be defined. Moreover, as a unique transcript identified in RKM clone 7, this peptide could be one of the unidentified cofactors that are responsible for the prion susceptibility phenotype.

The second hypothetical protein recognized by the RDA has the accession number of XM_002723849 (Table 4.2). Like the above-mentioned hypothetical protein, this transcript has not been described and has not been shown to exist at the protein level. Additional bioinformatic database searches indicate that all data collected in regards to this protein is predicted and preliminary (Di Palma F. 2009). If this protein does exist, it

would be 533aa (488aa predicted) in length and have an approximate mass of 54.3-kDa (Table 4.3) (UniProtKB sequence analysis, <http://www.uniprot.org/uniprot/G1TFK2>). TargetP analysis indicates that this protein would localize to the mitochondria (Emanuelsson, Nielsen et al. 2000). YASPIN secondary structure prediction analysis indicates that this protein is predominantly unstructured but does have one short α -helix domain (~6aa) at the N-terminus and two short β -sheet domains (13aa and 4aa) at the C-terminus (Lin, Simossis et al. 2005). Furthermore, NCBI BLASTp analysis reveals that the C-terminus of this novel protein is homologous (7% of total protein) to a human integral membrane transporter protein with an accession number of CAB81951. This protein is also categorized as hypothetical but has more descriptors that indicate its primary function is involved with anti-apoptotic signaling (Liu 2000).

The third predicted transcript identified by RDA is categorized as a conserved hypothetical protein, meaning that its sequence is homologous to proteins that already have designated biological function. This protein is identified in the NCBI database by the accession number of XM_002723594 (Table 4.2) and is predicted to function as a signal transducer with kinase activity (<http://www.ncbi.nlm.nih.gov/protein/291414786>). UniProt analysis extrapolates this protein to have serine/threonine kinase activity, signal transducing activity and ATP binding affinity (<http://www.uniprot.org/uniprot/G1TSK1>). This hypothetical protein is large, it spans for 1,295aa and has molecular weight of 139.7-kDa (Table 4.3)(Di Palma F. 2009). The protein is predicted to have the PAS domain that contains serine/threonine kinase activity. PAS domains are evolutionary conserved signaling domains found in proteins which tend to function by associating with specific

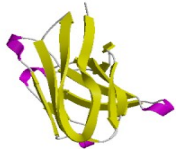
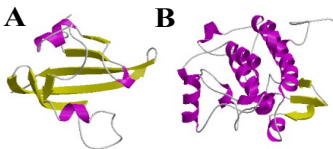
cofactors (Ponting and Aravind 1997). Structurally, this protein is predicted to have 25 α -helices and 37 β -sheets (Lin, Simossis et al. 2005).

The fourth unique transcript identified by the RDA in the RKM 7 susceptible clone is the rabbit MT-2 processed gene for metallothionein (accession number X07791.1). Described as a pseudogene without associated function, the transcript belongs to the family of low molecular weight (7 kDa), heavy metal-binding proteins with high cysteine content (Table 4.2). Metallothionein proteins generally localize to the Golgi and are assumed to confer protection against oxidative stress regulating metal homeostasis in the cell (Blindauer and Leszczyszyn 2010).

Table 4.2 Transcripts identified by RDA in the prion susceptible RKM 7 clone

Accession #	Susceptible RKM 7	Function
XM_002723849	hypothetical protein LOC100353326	Not characterized, novel protein. Partially homologous to an integral membrane transporter protein [Homo sapiens]. Associated with anti-apoptosis signaling
XM_002723594	PAS domain containing serine/threonine kinase (LOC100338542), mRNA	PAS domains regulate the function of many intracellular signaling pathways in response to both extrinsic and intrinsic stimuli
XM_002722317	hypothetical protein LOC100338446	Not characterized, novel protein
X07791.1	Rabbit MT-2 processed gene for metallothionein	Pseudogene, family of low molecular weight, heavy metal-binding proteins characterized by a high cysteine content

Table 4.3 Bioinformatic Prediction and Analysis Of RDA Identified Hypothetical Proteins

<u>Predicted Structure</u>	LOC100338446 – XM_002722317	LOC100338542 – XM_002723594	LOC100353326 – XM_002723849
			No Predicted Structure
	XM_002722317	XM_002723594	XM_002723849
Predicted Residues	1-113aa, 114-222aa	(A)1-114, (B)47-131, 132-321, 322-364	NA
Size (AA/kDa)	343aa/37-kDa	1,295aa/139.7-kDa	533aa/54.3-kDa
Functional Category	Biosynthesis of Cofactors/ Translation	Purines/Pyrimidines, Biosynthesis of Cofactors, Central Intermediary Metabolism	Translation
Enzyme-Class	Enzyme-Lyase	Enzyme-Ligase/ Hydrolase	Non-enzyme
Gene Ontology	Transcription/ Growth Factor	Structural Protein, Transcription Regulation, Growth Factor	Transcription-Regulation
Secondary Structure Prediction	(7) α -helix, (8) β -sheet	(25) α -helix, (37) β -sheet	Unstructured
Domains	Extracellular, Tyrosine-Protein-Kinase Receptor-like, Titin-like, IGSF-like Fibronectin-like, Tenascin-X, Filamin-like	PAS, MAPK-like, Protein Kinase, Tyrosine-Protein-Kinase-Fyn, Serine/ Threonine protein kinase	No Predicted Domains
Notable Motif	Binds EVH1(WH1), WW(PR40 & Fe65), SH3, Endothiapepsin, Rhodopsin, Protein Modification Targets, Phosphorylation Sites	Binds NAD, NADP, FAD, Cullin, Ubiquitin, SH3, Rhodopsin, Ankrin B, eIF4E, Protein Modification Targets, Phosphorylation Sites	Binds ATP, NADP, DNA Proteolysis by Furin, Modification Signals (Phosphorylation, Trafficking to ER, Endocytosis) Protein Binding

***Databases employed for analysis: Minimotif Miner 3.0, ProtFun 2.2, CATH v3.4, YASPIN, BLAST (Lin, Simossis et al. 2005; Balla, Thapar et al. 2006; Di Palma F. 2009; Rajasekaran, Balla et al. 2009; Mi, Merlin et al. 2012)**

RDA Identified Transcripts From RKM Clone 78 (Resistant): Similarly to RKM clone 7, RDA transcription profiling of RKM clone 78 (resistant) identified four unique transcripts (Table 4.4). These transcripts were unrelated to the transcripts identified in RKM clone 7. The transcripts unique to RKM clone 78 have enzymatic functions, which are associated with protein degradation, chaperone protein folding and endogenous retroviral elements.

A transcript homologous to the rabbit endogenous retrovirus H (RERV-H) (accession number AF480925) was identified using RDA in RKM clone 78. PCR screening of human tissue led to the identification of RERV-H, considered to be a novel human retrovirus (Griffiths, Venables et al. 1997). Subsequent cloning studies revealed the correct origin of RERV-H to originate from European rabbits (Griffiths, Voisset et al. 2002). This endogenous retrovirus is genome encoded and maintains highly conserved ORF for the *gag*, *pro* and *pol* retroviral elements (Griffiths, Voisset et al. 2002). Although functional characterization is still absent for this endogenous retrovirus, in vitro analysis has revealed that the RERV-H viral protease (PR, *pro* ORF) is active if recombinantly generated (Voisset, Myers et al. 2003). Retroviral proteases are functionally classified in the aspartic protease enzyme family (Wlodawer and Gustchina 2000), and have been identified in a wide range of living organisms (Davies 1990; Hill and Philip 1997).

The chaperonin-containing TCP-1 subunit gamma (CCT3), a transcript identified in RKM clone 78, belongs to the molecular chaperone complex called the TCP1 ring (TRiC) (Table 4.4). The predominant function of this chaperonin is to facilitate actin and tubulin folding (Kubota, Hynes et al. 1994). This 60kDa protein is an evolutionary

conserved member of a heat shock/chaperonin family with strong relation to Hsp60 (Kubota, Hynes et al. 1995). The CCT complex has been shown to promote activation of the anaphase-promoting complex (APC/C) by directly interacting with cell-division cycle protein 20 (Cdc20), a regulator of cell division (Camasses, Bogdanova et al. 2003). The direct interaction of CCT with Cdc20 positively regulates cell division, causing the cell cycle to progress (Camasses, Bogdanova et al. 2003).

The plasma alpha-1-antiprotease S-1 protein (accession number D16104.1) and mannose-binding protein associated serine protease-3 (MASP-1/3) (accession number XM_002716369.1) were two proteins identified in RKM clone 78 and associated with enzyme regulatory activity. Plasma alpha-1-antiproteases are glycoproteins that inhibit serine proteases, which include trypsin, chymotrypsin, elastase and plasmin (Travis and Salvesen 1983; Potempa, Watorek et al. 1986). Unlike other plasma alpha-1-antiproteases, the rabbit alpha-1-antiprotease S-1 has been characterized to protect trypsin from inactivation by other protease inhibitors (Saito and Sinohara 1993). While, MASP-1/3 is a serine protease that is involved in the lectin pathway activation complex of complement (Stover, Lynch et al. 2003). The function of this protease has not been determined but the related MASP-1 has been determined to cleave C3 and C2, while MASP-2 cleaves C4 and C2 complement components to produce the C3 convertase, C4BC2B (Matsushita, Thiel et al. 2000). Complement is an indispensable constituent of the innate immune response. Furthermore, complement activation has been demonstrated to facilitate prion infection *in vivo* (Klein, Kaeser et al. 2001) with a converse effect upon depletion (Mabbott, Bruce et al. 2001).

Section Summary: RK13 cells expressing mouse PrP^C were individually cloned from a bulk selected cell culture population. The individual clones were assessed for PrP^C expression level and susceptibility to replicating RML scrapie prions (Fig. 4.1). Although required, the variability of PrP^C expression amongst clonally selected RKM cells was the only determining factor for prion susceptibility (Fig. 4.1), and there was no correlation between PrP^C expression levels and PrP^{Sc} accumulation (Fig. 4.1). Several RKM clones were isolated that conferred the susceptible or resistant phenotype for RML prions (Fig. 4.2). These clones were continuously passaged to determine their ability to sustain chronic infectivity. PrP^C cell-surface presentation was assessed in individual clones bestowing the RML sensitive or resistant phenotypes (Fig. 4.2), but no difference in PrP^C surface presentation was observed. We applied RDA assay to assess transcriptional differences between these clones. A total of eight unique transcripts were identified between the sensitive and resistant clones (Tables 4.2 & 4.4). In the midst of the RDA analysis, it was discovered that RKM-78 (resistant clone) had the ability to replicate low-levels of PK resistant PrP^{Sc} (Fig. 4.2C).

Table 4.4 Transcripts identified by RDA in the prion resistant RKM 78 clone

Accession #	Resistant RKM 78	Function
AF480925	rabbit endogenous retrovirus H	Contains Functional gag, pro & pol
XM_002715377	chaperonin-containing TCP-1 subunit gamma (CCT3) mRNA	molecular chaperone called TCP1 ring complex (TRiC) plays a role in actin and tubulin folding
D16104.1	mRNA for plasma alpha-1-antiproteinase S-1, complete cds	Protects Trypsin from inactivation
XM_002716369.1	mannose-binding protein associated serine protease-3 (MASP-1/3), mRNA	Serine protease involved in complement activation

Section II: The Identification of CWD Susceptible and Resistant RK13-Deer PrP^C (RKD) Clones

Isolation And Characterization Of Sensitive And Resistant Clones: RKD clonal cells were generated using the multi-step stable transfection process to co-express deer PrP^C and HIV-1 Gag (Fig. 4.4A). CWD sensitivity of clones was determined. RKD cells were cloned by limited dilution and infected with 0.2% (w/v) CWD isolate 012-09442 passaged through Tg(deerPrP)1536^{+/-} mice (Table 3.1). RKD6 clone demonstrated susceptibility to CWD but could not sustain chronic replication of CWD prions. RKD6 cells were re-transfected with HIV-1 Gag , and the resulting RKD6-Gag cells were re-infected with CWD isolate 012-09442 and cloned by limited dilution. This resulted in the isolation of the 5E9 clonal cell line, which chronically replicates CWD prions (Fig. 4.4A). Subsequently, the 5E9 RKD clone was cured of CWD prions by single cell cloning, which enabled the identification of sub-clones that were either resistant or susceptible to CWD prions (Fig. 4.4A). A total of 20 5E9 sub-clones were identified using this procedure (10 susceptible and 10 resistant). Of those 20, 12 5E9 RKD sub-clones (6 sensitive and 6 resistant) were chosen for subsequent confirmation of susceptibility and microarray transcriptional profiling.

Confirmation of Susceptibility In RKD Subclones: Confirmation of CWD prion susceptibility was a prerequisite to transcriptional profiling. Twelve clones were re-infected with CWD prions and passaged three rounds. At passage three, Western blotting was used to assess PrP^{Sc} accumulation. Six chosen 5E9 RKD-resistant (RKD-R) clones remained free of PK resistant CerPrP^{Sc} material (Fig. 4.4B, left blot), while the sensitive 5E9 RKD cells (RKD-S) reconfirmed their ability to accumulate PK resistant CerPrP^{Sc}

(Fig. 4.4B, right blot). Equal amount of total protein was used throughout the experiment (Fig. 4.1B & C). PrP density measurements showed similar amount of PrP^C expression among the twelve RKD clones with only RKD-S cells replicating CWD prions.

The twelve CWD prion infected 5E9 RKD clones were continuously passaged to monitor prion replication in later passages. At the 12th passage, the sub-clones were re-screened for PK resistant CerPrP^{Sc} accumulation by Western blotting (Fig. 4.4C). RKD-R cells remained CerPrP^{Sc} negative, (Fig. 4.4C, left blot). However, RKD-S3 and RKD-S6 sub-clones became CerPrP^{Sc} negative by the 12th passage (Fig. 4.4C, right blot), raising the possibility for a cellular phenotype that supports incomplete expression of the necessary host factors required for CWD prion susceptibility (Fig. 4.4C).

Microarray Transcription Profiling: Previous data suggests there is no change in differential gene expression in cell cultures pre- and post- prion exposure (Julius, Hutter et al. 2008), indicating that endogenous prion host factors are always present. Total RNA was isolated from RKD sub-clones prior CWD prion re-infection. Microarray analysis was not initiated until the susceptibility phenotypes were reconfirmed. Isolated RNA was reversed transcribed, Cy-3 labeled, and hybridized to microarray chips for gene expression analysis, after CWD prion susceptibility confirmation.

Statistical Analysis of Microarray Data: The rabbit 4x44K chip used in these studies is shown in figure 4.5A. Acquired expression data from RKD clonal cells was Log2 transformed and normalized using robust multichip average (RMA) normalization method (Bolstad, Irizarry et al. 2003; Smyth, Yang et al. 2003; Kerr and Churchill 2007). Log2 transformation of microarray spot intensities and ratios is a prerequisite to data normalization processing. The transformation creates independence between intensity

variation and absolute magnitude of the data set (Smyth, Yang et al. 2003). Taking base 2 log of all spot intensity data from microarray scans completes this transformation. Normalization of microarray data removes background noise from nonspecific binding of fluorophores and reduces variances introduced by physical flaws of the printed chips. These normalization methods produced smoothed gene expression data sets that could be used in statistical analyses. The smoothed data sets were analyzed for mathematical stringency to determine significance.

Figure 4.4 Molecular characterizations of RKD subclones. **A.** Schematic of molecular characterization steps used to identify CWD prion susceptible and resistant RKD clonal cells. Western blot analysis representing RKD-R and RKD-S cells infected with 0.2 % (w/v) CWD prion brain homogenate, isolate CWD 012-09442 passaged through Tg1536^{+/-} mice, post **(B)** 3 and **(C)** 12 passages. The total protein amount used for analysis was 15µg for PK(-) lanes and 1000µg for PK(+) lanes. The mAb 9E9 was used to detect PrP signal. The designation of each clone goes by the letter indicating it's phenotype; resistant (R) or sensitive (S), and by a number indicating individual subclones (R1...R6, S1....S6). **(D)** Western blot PrP^C and PK resistant CerPrP^{Sc} expression levels were quantified using the ImageJ analysis software package The y-axis represents numerical densitometry value subtracted from the background of the scanned membrane. The x-axis represents the resistant (R) and sensitive (S) RKD clones. Blue bars represent total PrP^C expression without PK treatment. Red bars represent the density of PK⁺ material CerPrP^{Sc}.

Figure 4.4 Molecular characterizations of RKD subclones.

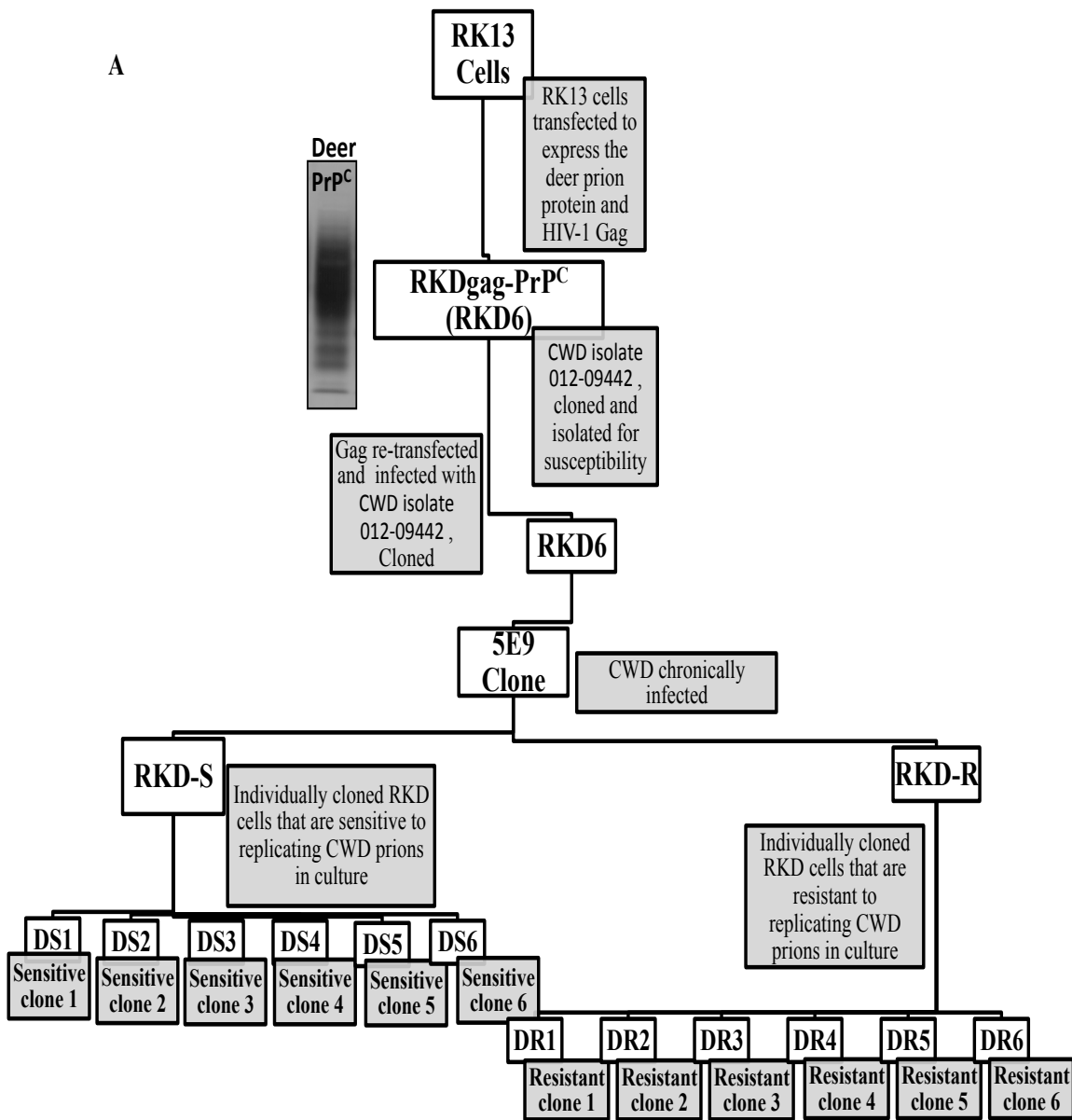
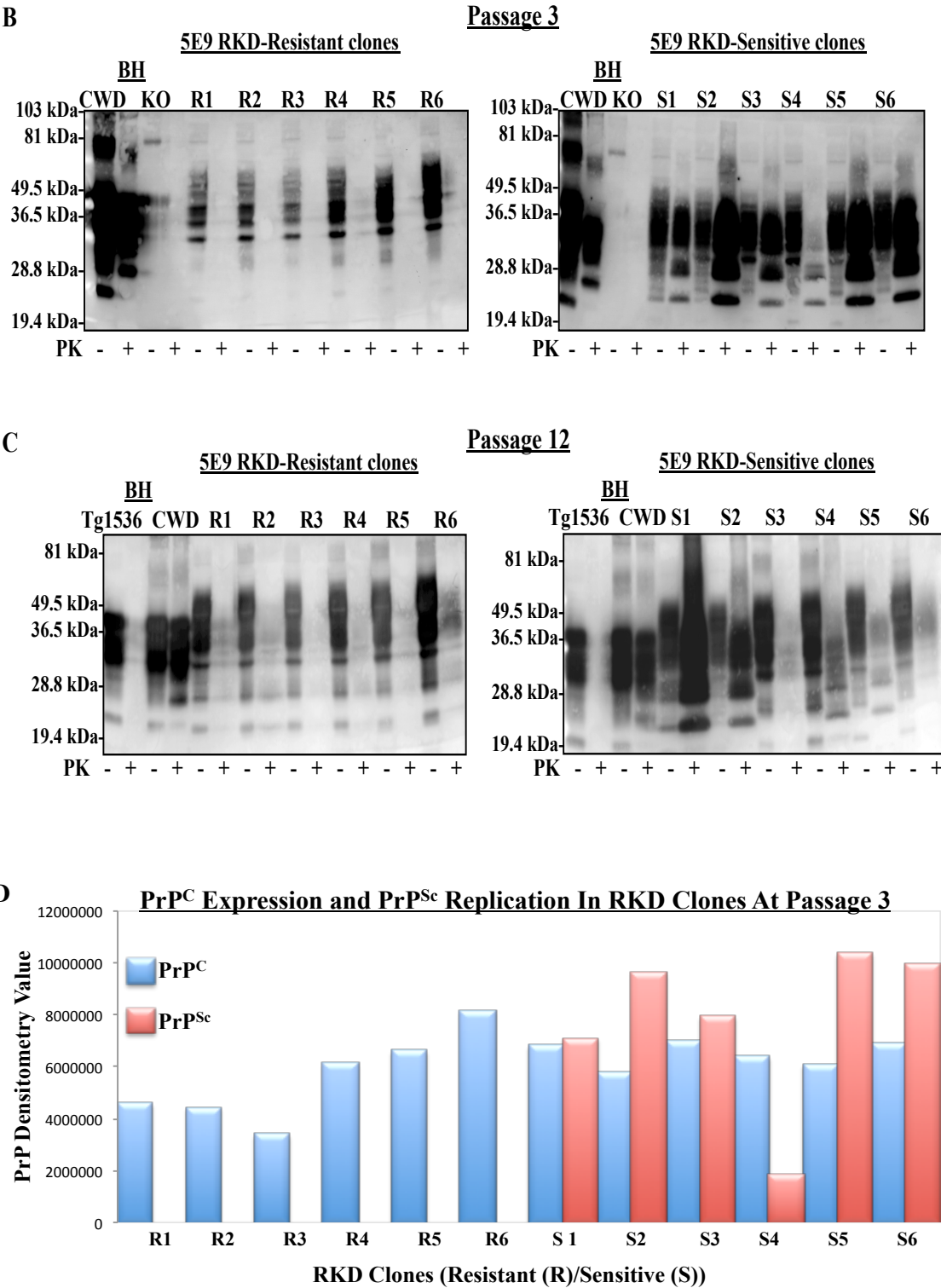


Figure 4.4 Molecular characterizations of RKD subclones.



To increase stringency and remove false positive and false negative data, restrictions were set to eliminate saturated or near background gene signal intensities. Statistical stringency was set by two distinct parameters, which were t-test p-values and fold-cutoff (FC) change. Most stringent of analyses used a t-test p-value of ≤ 0.001 and a FC of ≥ 2.0 (Fig. 4.5B, Tables 4.5 and 4.6), while the least stringent analysis used t-test p-value of ≤ 0.05 and a FC of ≥ 1.5 . The volcano plot exhibited in figure 4.5B graphically represents genes that were either above or below the higher stringency threshold. The y-axis of the volcano plot represents t-test p-values, while the horizontal dotted line spanning the graph represents p-value threshold of 0.001. The line signifies all events (black dots - genes), which were statistically significant and relevant for further analysis. The x-axis of the volcano plot represents FC change, signifying the averaged gene probe intensities of RKD-R gene expression results directly compared to RKD-S gene expression (Fig. 4.5B). In summary, the higher the signal is above red line in either direction, the more significant it is to the overall analysis.

A relationship model to predict mathematical correlation between each RKD clone was established using the principal component analysis (PCA). The PCA is an orthogonal transformation tool used for investigative data analysis and assist in predictive model construction (Jolliffe 2002; Peterson 2002). This procedure is purely mathematical and does not consider biological significance. The differences identified were based of numerical intensities for each individual probe representing the RKD subclones analyzed. The data samples were spatially clustered in two dimensions to demonstrate relationship similarities (Fig. 4.5C). The numbers on the graph represent distinct RKD sub-clones and the colors represents susceptibility phenotype for CWD prions (RKD-S = Red and RKD-

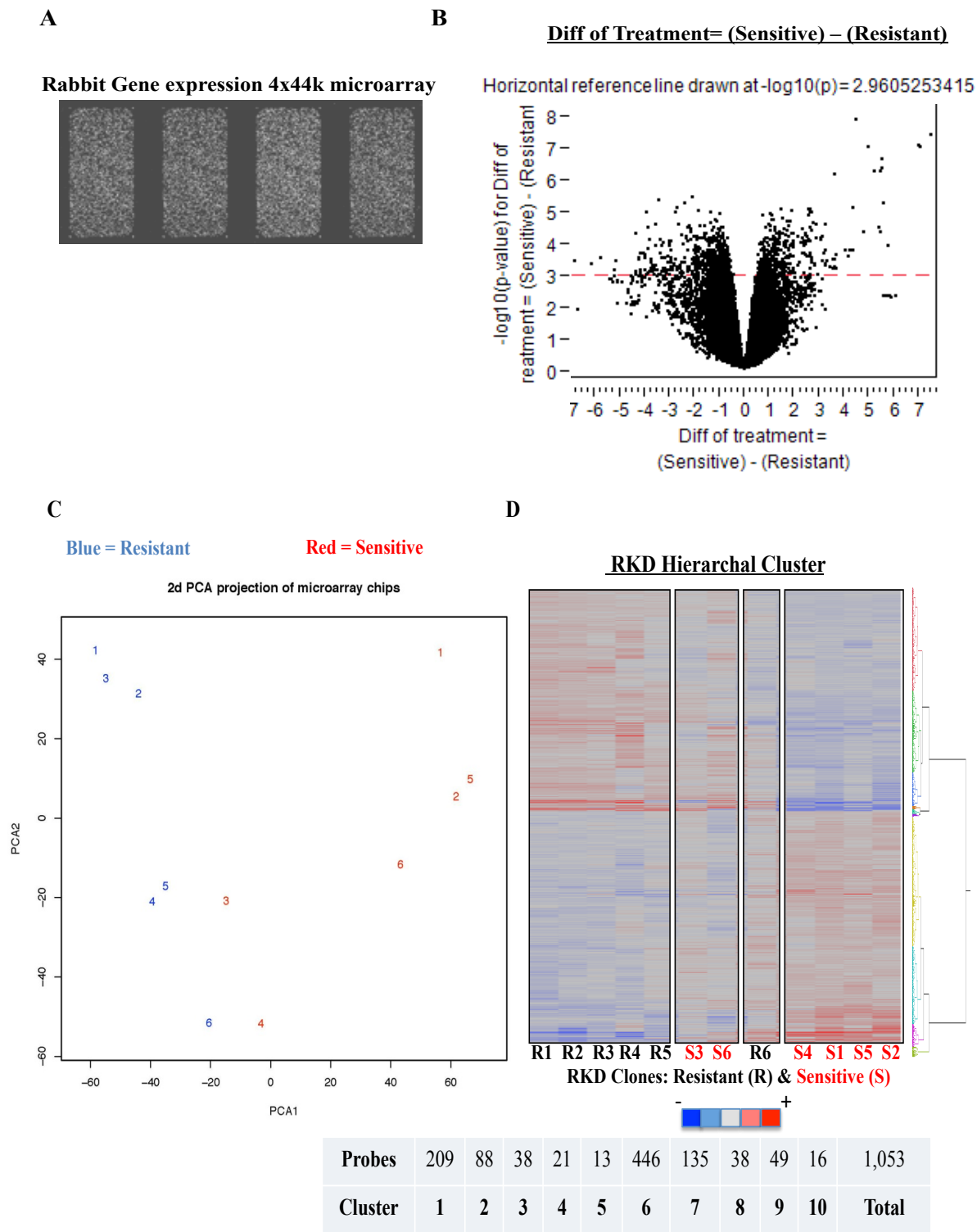
R = Blue) (Fig. 4.5C). The PCA data demonstrates distinct clustering of sensitive and resistant clones (Fig. 4.5C). Spatial distribution of clusters graphically represents variation of gene expression profiles between each clone. The resistant clones cluster into three distinct groups to the left quadrants of the PCA1 x-axis and the four sensitive clones distinctively cluster to the right of the PCA1 x-axis. Thus demarcating a phenotypic difference between the two groups, albeit two of the sensitive clones (RKD-S 3&4) plot closer to the resistant clusters (Fig. 4.5C). The PCA graph gives a global glimpse into the distribution of acquired microarray raw data. Differential distribution of RKD subclones by PCA is first to suggest the possibility for multiple factors/pathways that are involved to cause prion susceptibility in RKD subclonal cells. Bioinformatic analysis of normalized gene intensity data is required to acquire additional detail and significance associated with the PCA findings.

Cluster analysis is a technique utilized to establish phylogenetic relationships between evolutionary conserved genes from various species. Hierarchical cluster analysis algorithm was used to graphically represent RKD normalized microarray data (Fig. 4.5D). The hierarchical cluster data was analyzed by sequentially comparing rows (genes) from each column (RKM clones) side by side. Hypothesis for experimental relationship and significance was determined by analyzing both variables. Ten differential gene clusters were identified using this method (Fig. 4.5D). Gene clustering data exhibited in figure 4.5D was based on a statistical stringency threshold of $p\text{-value} \leq 0.05$ and $FC \geq 1.5$. This analysis provided a more global perspective on the physiological conditions occurring in RKD cells.

Analysis Of Normalized Microarray Data: The hierarchal cluster analysis revealed genes that were associated with various cellular functions. To derive these associated functions, genes from each cluster were systematically annotated and database mined. Database mining revealed specific protein functions associated with endomembrane system trafficking, proteolysis, protein maintenance, protein biosynthesis, cell division and metal ion binding. Moreover, these annotated clusters provide insight to target pathways that could be important prion replication. In particular, the distinct clustering of RKD-S3 and RKD-S6 demonstrate an interesting reflection of phenotypic variation and instability (Fig. 4.5D). These two clones were considered susceptible by primary and secondary CWD prion infection studies but with continuous passages lost detectable PK resistant CerPrP^{Sc} (Fig. 4.4B and Fig. 4.4C). Hierarchal cluster visual analysis of S3 and S6 clearly demonstrates a distinct clustering pattern, which they share with both resistant and sensitive counterparts (Fig. 4.5D). These findings suggest that clones S3 and S6 represent a “quasi-“sensitive species that lacks the full repertoire of host factors required for chronic replication of CWD prions. Subsequent bioinformatic analyses were used to confirm these microarray data findings.

Figure 4.5 Microarray statistical data analysis of differential gene expression in 5E9 RKD CWD prion subclones. **A.** Representative image of the Rabbit Gene expression 4x44k microarray chip **B.** Statistical volcano plot of significantly expressed genes from RKD-R cells subtracted from RKD-S cells with stringency thresholds set to a p-value ≤ 0.001 and FC ≥ 2.0 . The x-axis represents FC and the y-axis represents p-value. The red line on the plot was set for p-value 0.00, all black dots (genes) above the line were statistically significant. **C.** Principal component analysis (PCA) of the 12 RKD clones in two-dimensional schematic. Red numbers represent RKD-S clones and blue numbers represent RKD-R clones. The PCA correlates each mathematical component (RKD Microarray normalized signal intensity) and clusters it in multi-dimensional coordinates to demonstrate the relationship and internal structure of a complex data set. **D.** Heat map of hierarchical gene clustering using the microarray data derived from the 12 RKD clones. A graphical representation of gene expression similarities. Each column represents individual RKD clones, labeled at the bottom of the heat map. The rows represent specific probes (genes). The intensity of red indicates high expression to the sample mean and the blue low expression. Ten clusters were identified, from top to bottom.

Figure 4.5 Microarray statistical data analysis of differential gene expression in 5E9 RKD CWD prion subclones.



Gene List Development and Annotation: Several gene lists were derived from the microarray analyses. The gene selection criteria to develop the lists were based on the following: averaged total gene signal intensities $((R1+R2+R3...R6)/6)$ for each individual gene and statistical thresholds (mentioned earlier). A total of 100 differentially expressed genes were identified using stringent conditions set to t-test p-value ≤ 0.001 and FC of ≥ 2.0 (Table 4.5). RKD-R clones exhibited 32-up and 68-down regulated genes using this threshold parameter (Table 4.5). This statistical stringency leaves no doubt that the genes were differentially expressed, therefore making them primary targets for future validation. These 100 annotated genes are listed in their entirety in tables 4.6 and 4.7. Reduction of statistical stringency to p-values of ≤ 0.05 and FC of ≥ 1.5 resulted in a larger gene list used to gain a global perspective of biological processes (Table 4.5). A total of 1,375 genes were derived using this statistical stringency parameter.

The ongoing rabbit genome-sequencing project made gene annotation of our data challenging. Manual ortholog data mining using multiple database search engines were used to derive the described gene lists. Completing the annotation of these lists required careful extraction and conversion of rabbit gene probes to mouse or human ortholog gene identification names, and symbols. In addition to identifying functional roles of these orthologs, the ortholog conversion enabled the use of gene ontology databases to assess pathway connections and interacting molecules. These databases are currently limited to human and/or mouse annotations.

Table 4.5 Summarization of identified and annotated genes lists by microarray experiments.

Analysis	RKD-R (Resistant) Up Regulated Genes	RKD-S (Sensitive) Up Regulated Genes
Fold Cutoff 2.0 Pval 0.001	32 Genes	68 Genes
Fold Cutoff 1.5 Pval 0.05	664 Genes	711 Genes
FC1.5 Cross referenced to Prion Disease Database (PDDB)	132 Genes	182 Genes

PDDB – The total identified genes from the FC1.5 data subset is cross referenced to the differentially expressed genes identified from in vivo studies following RML infection at 6, 10, 14, 18, 20 and 22 weeks post inoculation.

Functional Correlation Of Gene Data Using Gene Association/Prediction Databases:

Large-scale analysis of microarray data requires access to genomic databases that maintain gene annotation with reference to peer-reviewed literature. In addition, these databases require immense computational power to cross-reference the users gene/probe names against the validated/annotated genes of the database. The databases applied to our microarray analysis include the **P**rotein **A**nalysis **T**hrough **E**volutionary **R**elationships (PANTHER) and the **D**atabase for **A**nnotation, **V**isualization and **I**ntegrated **D**iscovery (DAVID). The PANTHER database functions by applying user's input gene data and cross-referencing it through all data published in scientific journals containing experimental evidence as validating support. Moreover, this database also utilizes evolutionary relationships to predict function (<http://www.pantherdb.org/>). This database has several classification systems that are sub-categorized into the following; Gene families and subfamilies, Gene ontology classes, PANTHER Protein classes and Pathways.

The DAVID database provides users with comprehensive mathematical tools that assist in functional annotation and understand large gene lists derived specifically from transcription profiling experiments (<http://david.abcc.ncifcrf.gov>). This database enables identification of enriched biological themes, gene relationship and simplifies data sets by removing genes that are redundant. In addition, DAVID also cross-references other databases for pathway information, rapid literature searches and structural information. Furthermore, DAVID converts gene identifier between species, a beneficial function to our study. Although the conversion of identifiers comes with a caveat that assumes the

genes have previously been annotated, a hurdle to overcome with the poorly annotated rabbit genome.

Uploading the 1,375 RKD differentially expressed genes into PANTHER database provided the global perspective into the difference of physiological functions between sensitive and resistant cells (Fig. 4.6). Extrapolating the data from PANTHER and DAVID databases establishes biological function associations to analyze by validation in RKD clones. The summaries of the functions are exhibited by percentages of total genes compared to biological parameters and constraints established through respective databases (Fig. 4.6). The molecular functions that associate with differentially expressed RKD gene predominantly participate in binding activity (33%), catalytic activity (30%) or could not be classified (34%) by PANTHER (Fig. 4.6A), while cellular processes were divided between metabolism (39%), cell communication (21%), transport (29%) and unclassified (29%) (Fig. 4.6B). Pathway predictions using PANTHER has enabled the identification of 38 differentially expressed genes associating with protein misfolding diseases such as AD, PD and HD (Fig. 4.6C).

Although simplified, DAVID database analyses provide the most comprehensive insight into cellular physiological differences between RKD clones (Fig. 4.6D). Metabolic processes involved with protein maintenance, intracellular trafficking and plasma membrane delivery of glycosylphosphatidylinositol (GPI)- anchored proteins represented RKD-R down regulated genes. RKD-R and RKD-S gene expression profile have inverse relationship, down-regulated genes in RKD-R were upregulated in RKD-S cells and vice versa. Hence, protein maintenance processes that were down-regulated in RKD-R, dominate the expression profile of the RKD-S cells (Fig. 4.6D). Suggesting that

primary selection of host factors for validation should include protein that regulate homeostasis, intracellular trafficking and lipid raft PrP co-localized proteins. Our in vitro data provides support and allows the opportunity to validate these gene expression interpretations. In contrast, DAVID investigation of RKD-R upregulated genes reveals the enrichment of cell division and DNA replication processes (Fig. 4.6D). Therefore, higher rate of cell division in resistant cells generates unfavorable condition for prion replication. We have not analyzed the rate of cell division between RKD-R and RKD-S cells.

Figure 4.6 Bioinformatic analysis of 1,375 RKD-R differentially expressed genes. **A.** Graphical representation of molecular function percentage representing the complete gene list developed through the PANTHER database. **B.** Clustering percentage of the differentially expressed genes associated to a cellular process developed through the PANTHER database. **C.** PANTHER database pathway prediction clustering graph. Total of 1168 gene IDs were mapped. Classification specificities are based on published literature association predictions. **D.** Graph representing the separation of differentially expressed genes based on positive/negative expression values to demonstrate clustered functionality using the DAVID database.

Figure 4.6 Bioinformatic analysis of the 1,375 RKD-R differentially expressed genes.

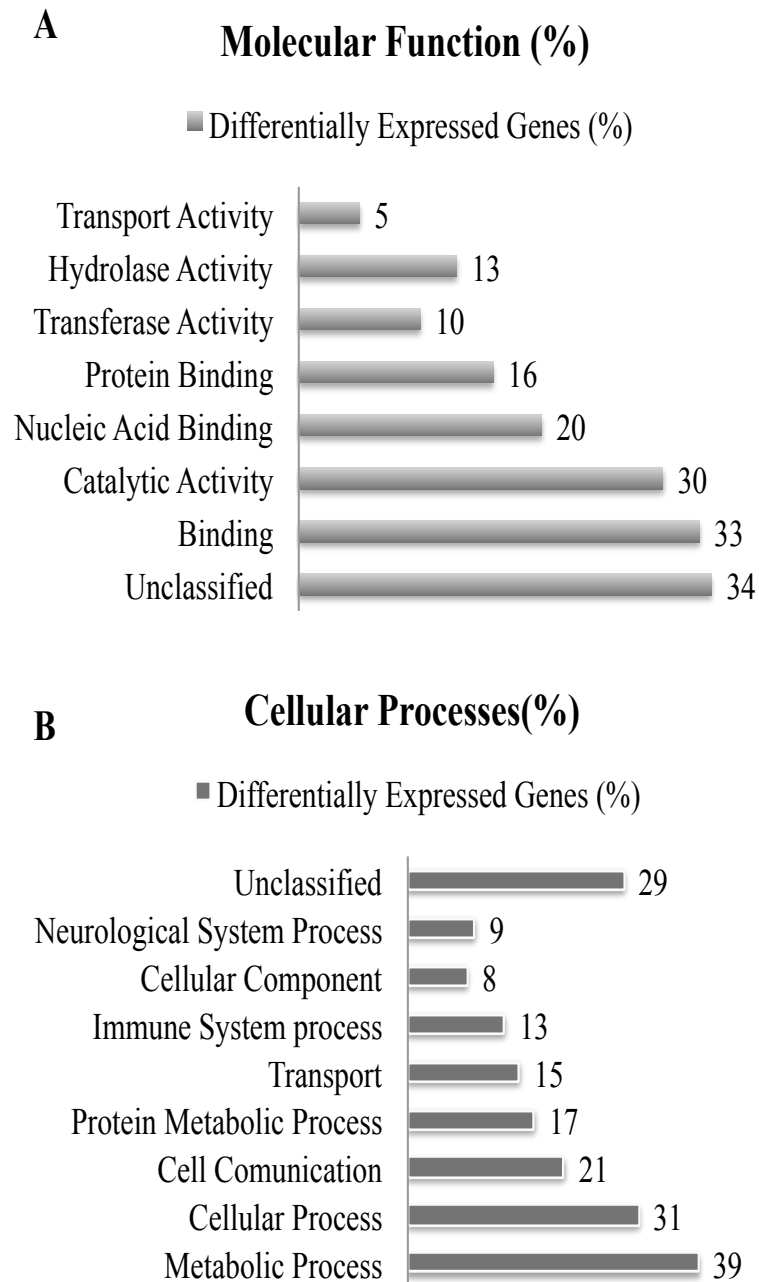


Figure 4.6 Bioinformatic analysis of the 1,375 RKD-R differentially expressed genes.

C

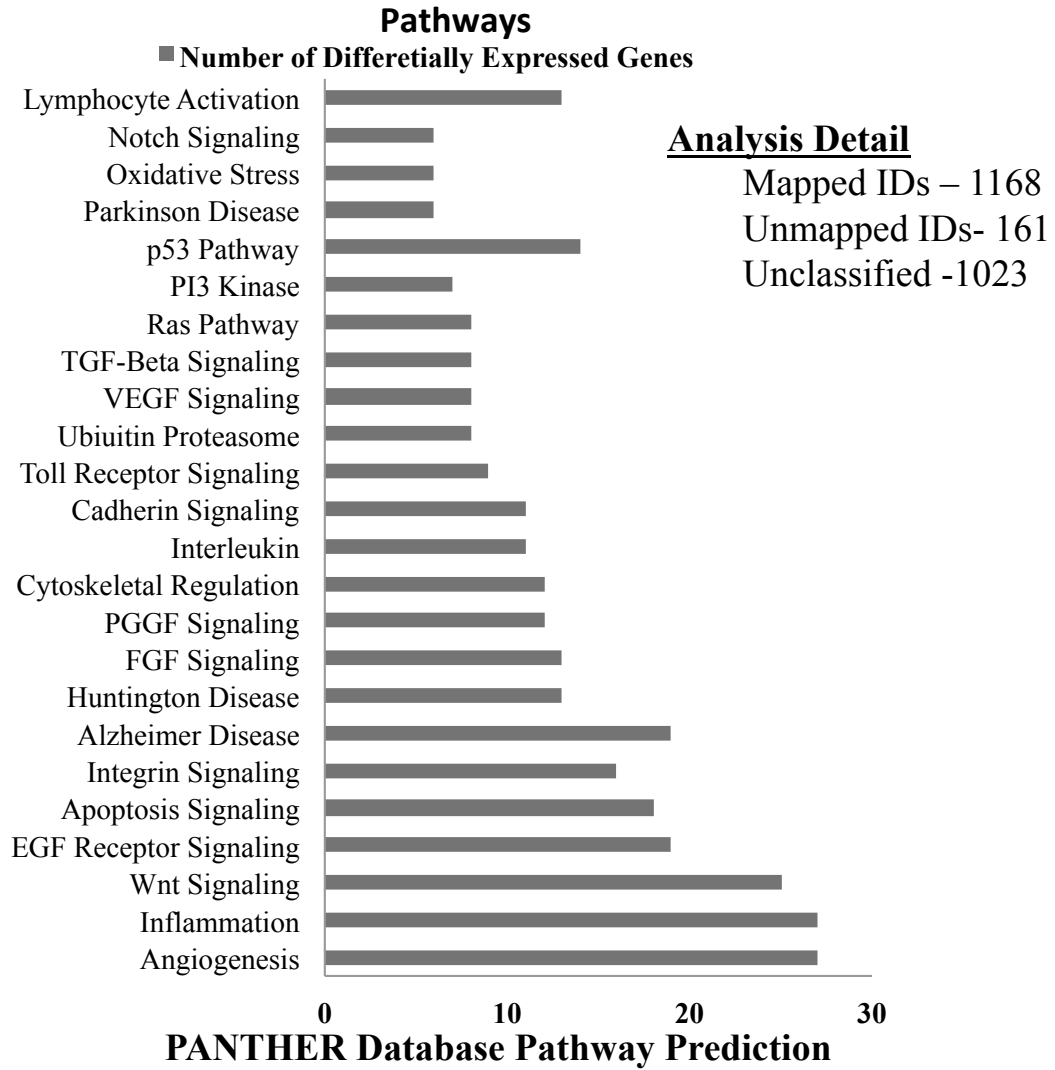
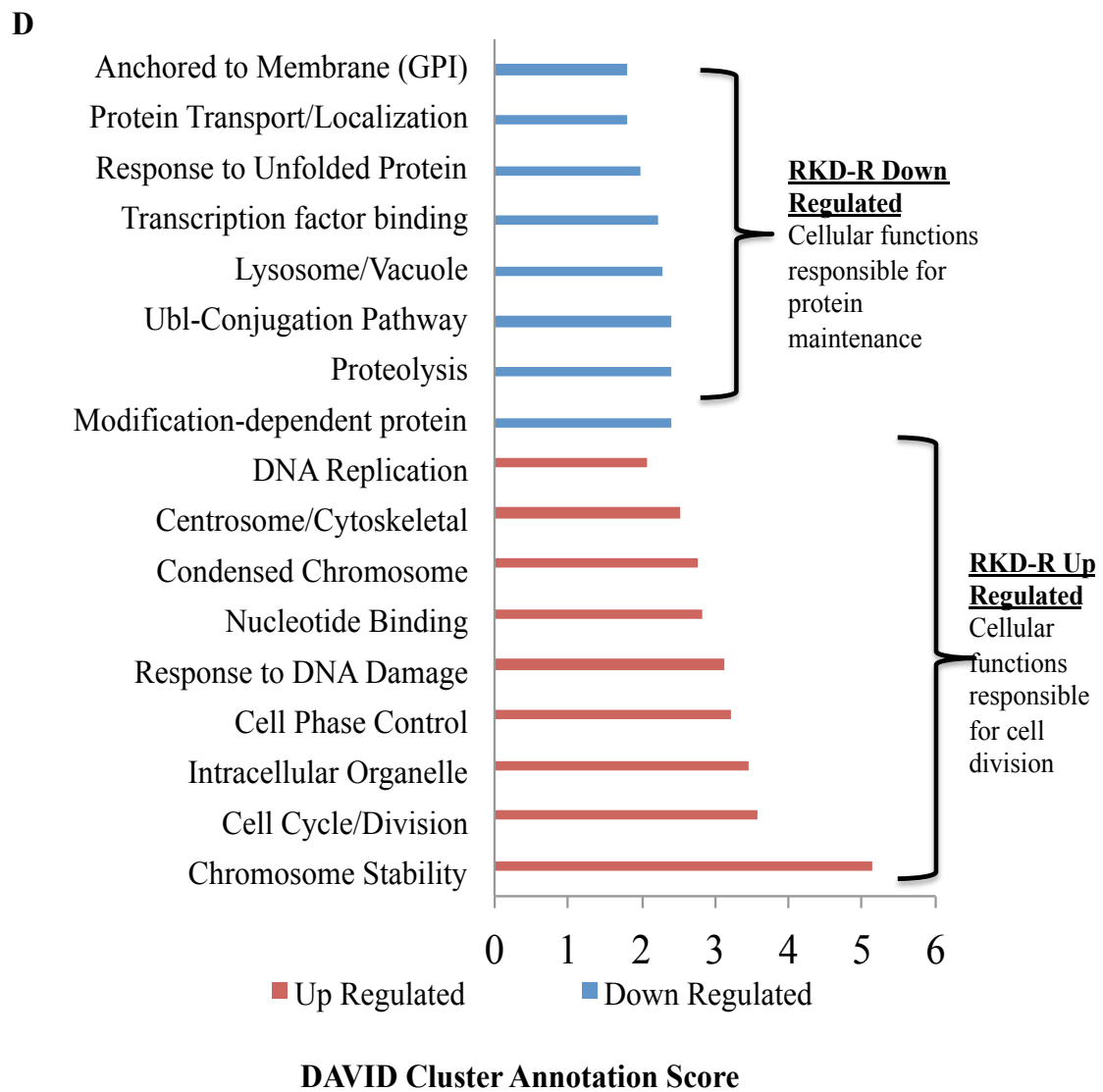


Figure 4.6 Bioinformatic analysis of the 1,375 RKD-R differentially expressed genes.



Section Summary: RKD cells were genetically modified to express Deer PrP^C and HIV-1 Gag, similar to ELK21⁺ cells. Limited dilution cloning was used to derive CWD prion susceptible and resistant RKD clones (Fig. 4.4A). RKD clonal susceptibility to CWD prions was the phenotypic basis used to select cells for transcriptional profiling analyses (Fig. 4.4B). Differential gene expression was assessed using rabbit gene expression microarray chips (Fig. 4.5A). Twelve clones were transcriptionally profiled using microarrays. Transcriptional profiling revealed a significant difference in gene expression between RKD-R and RKD-S clones (Fig. 4.5B,C and D). Continuous passage of CWD prion infected clones subsequently revealed the loss of PK resistant CerPrP^{Sc} material in RKD-S3 and S6 clones, which also exhibited a unique, and distinguishing gene expression profile (Fig. 4.4C and Fig. 4.5D). Averaging signal intensities and applying statistical stringency thresholds led to the development of a dual-parameter based gene lists (Table 4.5). Global characterization of differentially expressed genes was achieved using DAVID and PANTHER bioinformatic databases (Fig. 4.6). These analyses of differentially expressed genes are discussed in the proceeding sections of this thesis.

Discussion

Section I

PrP^C Expression and Clonal Susceptibility Towards PrP^{Sc} Replication: Several studies have demonstrated the primary role of PrP^C as the substrate for PrP^{Sc} conversion and prion disease but few have addressed the underlying factors that allow or inhibit processes at the cellular level. N2a cell culture studies showed that prion susceptibility was a rare event (~0.7% N2a cells accumulate PrP^{Sc}) (Race, Fadness et al. 1987). Additional prion infectivity experiments using N2a cells identified sub-clonal populations that exhibit susceptibility variation (Bosque and Prusiner 2000). These findings suggest that susceptibility in clonal cells does depend on PrP^C expression level in cells. In contrast, in vivo data demonstrates a direct correlation between expression level and PrP^{Sc} accumulation and an inverse relationship for incubation time of disease (Westaway, Miranda et al. 1991). The findings from cell culture studies suggest that additional cofactors are involved to confer cell permissiveness to prion conversion and replication. Ectopic expression of PrP^C in cells cultured from *Prnp*^{0/0} mice do not support prion replication, although ectopic expression of PrP^C in *Prnp*^{0/0} mice replicate prions and succumb to disease (Raeber, Sailer et al. 1999). To extend these findings and identify additional host factors, we chose to use genetically modulated RK13 cells that ectopically express PrP^C.

Our findings suggest that PrP^C expression levels do not correlate with cellular susceptibility to replicating prions (Fig. 4.1 and Fig. 4.4). RKM clonal susceptibility confirms the absolute requirement of PrP^C expression for sustaining prion replication. RK13 cells replicate prions derived from mice, hamster, ovine and cervid (both elk and

deer) but vary in efficiency (Vilette, Andreoletti et al. 2001; Bian, Napier et al. 2010). RKM cells became readily infected with RML prions, while Elk21⁺ and RKD cells require supplemental factors and multiple cloning to identify CWD prion permissive cells (Fig. 4.1, Fig. 4.4 and Chapter 3). This suggests that the efficiency of replicating prions is stochastically rare, that is phenotypically selected through cloning. Clonal selection for CWD prion susceptibility was also shown using genetically modulated N2a cells that ectopically expressed CerPrP^C (Pulford, Reim et al. 2010). Our data also shows that cellular conversion factors required for replicating prions is universally shared in these cells. Without endogenous PrP^C interference, cells may or may not have the supplementary conversion factors. We also show that these conversion factors were partially active in subclones but not sufficient to chronically sustain the replicative process (Fig. 4.4C and Fig. 4.5D). The occurrence of partial susceptibility was demonstrated by RKD clones S3 and S6 (Fig. 4.4). These clones were deemed CWD-prion susceptible at third passage after infection but lost detectable PK resistant CWD-CerPrP^{Sc} by twelfth passage (Fig. 4.4B and C). The loss of prion infectivity in later passages with permissive cell lines is not new, but the distinct transcriptional profile exhibited by these cells revealed a striking difference (Fig. 4.5D). The gene clustering of these two particular clones showed similarities with both sensitive and resistant RKD clones, indicating that the cells partially expressed the repertoire of genes that are required to sustain prion replication but not sufficient enough to maintain it (Fig. 4.4B-C and Fig. 4.5C-D).

Distinguishing Clonal Variation Through PrP^C Cell-Surface Presentation Analysis:

Besides total PrP^C expression, intracellular trafficking and surface presentation

mechanisms may also determine susceptibility in cells. Prion conversion is hypothesized to predominantly occur on the cell surface (Caughey, Race et al. 1989; Caughey and Raymond 1991; Caughey, Raymond et al. 1991; Taraboulos, Raeber et al. 1992; Shyng, Huber et al. 1993; Goold, Rabbanian et al. 2011). Initial pulse-chase labeling experiments and phosphatidylinositol-specific phospholipase C (PIPLC) treatments were used to release PrP^C from the cell surface (Borchelt, Scott et al. 1990). These studies revealed that PrP^C and PrP^{Sc} have differential biogenic stability, and half-life based on their accessibility for degradation. Moreover, the differences between these molecules occurred after post-translational modifications (Borchelt, Scott et al. 1990; Stahl, Borchelt et al. 1990). Topological experiments in ScN2a cells using PIPLC and trypsin protease suggested that PrP^{Sc} was generated from a cell-surface precursor (Caughey and Raymond 1991). Recently, ectopic expression of epitope-tagged PrP in N2a cells lacking endogenous PrP^C revealed rapid PrP^{Sc} conversion mainly occurring at the plasma membrane (Goold, Rabbanian et al. 2011). We hypothesized that prion susceptibility differences were caused by inefficient cell-surface presentation of PrP^C by resistant cells. We used flow cytometry to determine the answer to this question, and discovered similar cell surface presentation of PrP^C. Equal expression of total PrP and similar surface presentation in clonal cells suggests that phenotypic difference is at the transcriptional level.

The Search For Prion Host Factors Using RDA To Transcriptionally Profile Clonal Cells: Transcriptional differences between sensitive and resistant RKM clones were analyzed using RDA. The RDA facilitates the identification of unique transcripts from two nearly identical cDNA pools without the requirement of an annotated starting point

in the genome. RDA was used as a pilot experiment to transcriptionally profile RKM clones. High-throughput molecular tools that are common use for mouse and human genome analysis were still lacking for the rabbit genome. Hence, prior to making large investments into customized gene chips and transcriptional sequencing, we aimed at using experimentally proven and unbiased techniques to identify differences between prion susceptible and resistant clones. RDA does not require an annotated genome to perform the subtractive screening, which was the primary limitation with RKM cells.

As a pilot study, one respective clone from each susceptibility phenotype was selected for analysis. RDA identified transcripts were statistically insignificant ($n=1$). Moreover, subsequent prion infectivity results revealed incomplete resistance by RKM clone 78 (Fig. 4.2C), which led us away from pursuing this approach any further. We concluded that customized microarray expression analysis was a better experimental approach to take. The transcripts that were identified by RDA are listed in Tables 4.2 and 4.4. The genes that are encoded by the identified transcripts represent single targets for elucidating the mechanisms that dictate cellular susceptibility. In addition, three RDA identified transcripts lack characterization data because they were computationally predicted. Basic characterization of these hypothetical proteins was completed using bioinformatic data mining approach (Table 4.3).

Unique Prion Susceptibility Transcripts

Uncharacterized Hypothetical Proteins: Three hypothetical proteins were identified as ORF's in the *Oryctolagus cuniculus* (rabbit) genomic sequences, which was annotated using the GNOMON gene prediction method and supported by EST evidence (Di Palma F. 2009). The predicted proteins range in amino acid length (343-1,295aa) and molecular

weight (~37 – 140-kDa) (Table 4.3). Structural calculation analysis indicates secondary and tertiary structure formation with functional associations in two of the three proteins (Table 4.3), while hypothetical protein LOC100353326 appears lack secondary structure. Roughly 7% of LOC100353326 protein's amino acid sequence is homologous to a human integral membrane transporter protein with an accession number of CAB81951. This integral membrane transporter protein has been associated with anti-apoptotic functions. Interestingly, several studies have implied PrP to have biological functions associated with anti-apoptotic activity (Kurschner and Morgan 1995; Chiarini, Freitas et al. 2002; Zanata, Lopes et al. 2002; Li and Harris 2005). If this hypothetical protein has a functional role in protecting the cell from apoptosis, than it would be reasonable to hypothesize that resistance to cellular toxicity of accumulating PrP^{Sc} enables survival of sensitive cells in an otherwise unfavorable condition. Whereas the resistant cell population lack this anti-apoptotic property and cannot survive PrP^{Sc} accumulating cytotoxicity. In contrast, resistant cells do not die upon prion exposure, suggesting that toxicity from accumulating PrP^{Sc} is exacerbated in cells that are actively replicating the infectious agent. Therefore, susceptible cell must activate protective mechanisms while the prion conversion and accumulation of PrP^{Sc} is occurring. Enhanced anti-apoptotic activity in the permissive clone could be one of several cellular phenotypes that enable prion replication.

LOC100338542 protein (XM_002723594) was the largest of the hypothetical proteins recognized in the study (Table 4.2 and 4.3). Sequence prediction analysis revealed a conserved PAS-domain containing serine/threonine kinase activity. The PAS-domain containing serine/threonine kinases are evolutionary conserved signaling

molecules that are activated in response to stimuli (Rutter, Michnoff et al. 2001). Normal signal detection by PAS-protein domains is through an interaction with an associated cofactor (Ponting and Aravind 1997). In addition, sensory functions of these PAS-proteins regulate metabolic homeostasis (Schlafli, Borter et al. 2009). The relative size and structure of this protein could implicate a very important intracellular function in RK13 cells that should be characterized (Table 4.3). The predicted signaling capabilities of this PAS-domain containing protein could be the intracellular PrP interacting molecule involved in unidentified regulating signaling pathways that control prion replication.

All descriptive records pertaining to hypothetical LOC100338446 protein is nonexistent in NCBI database. Analyzing this protein with various bioinformatic prediction programs has revealed several interesting characteristics, which could be used in future validation studies. The protein, if expressed, would have higher order conformational structure and maintain a molecular weight of 37-kDa (Table 4.3). It would have enzymatic activity regulating some form of homeostatic processes. Similar to LOC100338542, this protein's interactions with PrP could involve the regulation of unidentified signaling cascades regulating PrP conversion (protein homeostasis) or cellular tolerance/survival in response to PrP^{Sc}-induced aggregation toxicity.

Unique Prion Resistant Transcripts

Up Regulation Of Proteolytic Enzymes: The sequence encoding endogenous rabbit retrovirus H (Accession # AF480925) was a product detected in RKM 78 resistant clones (Table 4.4). These viral remnants from the rabbit genome encode retroviral elements *gag*, *pro* and *pol* (Griffiths, Voisset et al. 2002). Retroviral element HIV-1 Gag was shown to enhance prion susceptibility and stabilized chronic infectivity in Elk21⁺ cells (Bian,

Napier et al. 2010). In contrast to Elk21⁺ cells, RKM-78 cells were phenotypically resistant, suggesting that other retroviral elements could have reverse effects on PrP^{Sc} accumulation. Characterization studies of the rabbit endogenous retrovirus H show that it encodes a functional protease, referred to as RERV-H protease (Voisset, Myers et al. 2003). The RERV-H protease is an aspartic protease that cleaves the Gag polypeptide precursor (Voisset, Myers et al. 2003). Other well-characterized eukaryotic aspartic proteases include pepsin, cathepsins and renins (Szecsi 1992). Proteolytic cleavage and processing of PrP molecules have been described and associated with normal and aggregation based toxicity states of the protein (Zhang, Spiess et al. 2003; Luhr, Nordstrom et al. 2004; Yadavalli, Guttman et al. 2004; Dron, Moudjou et al. 2010). These proteases have been described in the context of prion infectivity and resistance. Cathepsins B and L have been shown to degrade prions in GT1-1 neuronal cells (Luhr, Nordstrom et al. 2004). It is therefore reasonable to hypothesize that RERV-H could facilitate resistance within RKM-78 clone using a similar mechanisms.

The mannose-binding protein associated serine protease-3 (MASP-1/3, accession # XM_002716369.1) is another proteolytic enzyme identified in RKM 78 resistant clone (Table 4.4). The mannose-binding protein associated serine protease-3 (MASP-1/3) has a role in complement activation processes (Iwaki, Kanno et al. 2011). Similar to Proteinase K, MASP-1/3 is a serine protease enzyme that could proteolytically digest PrP^C proteins. Upregulation of this protease in resistant cells could interfere in the conversion process by actively interfering in formation of the PrP^C-PrP^{Sc} complex. Rabbit plasma alpha-1-antiprotease S-1, another RDA identified transcript (Table 4.4), protects trypsin (serine protease) from being inactivated by proteolytic inhibitors (Saito and Sinohara 1993). The

abundance of proteolytic enzymes in the resistant clone could signify another cellular mechanism involved in prion sustainability. This mechanism could involve subcellular trafficking of PrP^C to lysosomal compartments where it undergoes rapid degradation by these upregulated proteolytic enzymes. Rapid degradation of the primary PrP substrate for PrP^{Sc} conversion results in a cellular phenotype that confers resistance to prion infectivity. In vivo, these enzymes perform diverse physiological functions but in vitro upregulation simply results in cellular resistance to prions.

Chaperones and PrP^C Folding: The chaperonin-containing TCP-1 subunit gamma (CCT3, accession # XM_002715377) mRNA identified in RKM 78 clone belongs to the molecular chaperone family of proteins called TCP1 ring complex (TRiC) which participate in actin and tubulin folding (Walkley, Demaine et al. 1996). Molecular chaperones are vital to intracellular protein homeostasis. They modulate correct protein folding and/or cause misfolded or dysfunctional proteins to be degraded. Chaperone proteins have previously been implicated with cellular prion replication (Kenward, Hope et al. 1994; Lindquist, Patino et al. 1995; Kenward, Landon et al. 1996; DebBurman, Raymond et al. 1997; Shyu, Harn et al. 2002; Allen, Wegrzyn et al. 2005; Tutar, Song et al. 2006; Lian, Zhang et al. 2007; Loovers, Guinan et al. 2007; Shorter and Lindquist 2008; Guinan and Jones 2009; Wang, Zhou et al. 2011). The distinct expression of this chaperone transcript in resistant cells suggests for the possibility of a selected pathway involved in protein processing which, if carefully regulated would cause attenuation of protein aggregation and toxicity.

Summary: RDA data regarding hypothetical proteins and other recognized proteins were just brief, hypothesis driven predictions that require extensive validation. It is difficult to

elaborate further on these proteins this data is statistical insignificant and resistant cells considered resistant, subsequently replicated RML prions. These were $n = 1$ analyses that would require more RDA screens incorporating various combinations of sensitive and resistant clones. Moreover, additional subtractive hybridization analysis would also be required of the parental RK13 cell line genetically un-modulated to express foreign proteins. The application of microarray gene expression profiling to prion sensitive and resistant clones allowed us to attain statistically confident data that RDA analyses were unable to do. In addition, this high-throughput method also provided a global perspective on cellular functions and pathways occurring amongst the two phenotypically distinct cell populations.

Section II

Gene Annotation And Selection: Microarray gene expression experiments pose a major challenge after completing the initial data acquisition step. This challenge originates from vast amounts of data single gene expression experiment generates. Mining acquired data for meaningful information becomes even more challenging if the expression results of the microarray do not have an annotated genome to work with. This was a major challenge we encountered working with the rabbit gene expression microarray chips. Manual gene annotation was prerequisite to formulating and selecting genes for discussion and future analysis. This was an extremely time consuming process requiring the use of multiple databases to cross-reference microarray gene probe identification numbers with associated Genbank entries, followed by mouse/human ortholog search and conversion. The mouse/human ortholog genes were subsequently used to compile the final version of each list and were used as the basis for downstream bioinformatic

database analyses. Inconsistency in gene nomenclature was another challenge confronted during this phase of research. The existence of multiple names and symbols for single genes makes literature cross-referencing very difficult. For example, during the cross-referencing annotation process of gene list formulation, a microarray rabbit probe id matches a gene in the ensembl genome browser by the name of Ribosomal protein SA (gene symbol *RPSA*). This ortholog information was logged and data-entered into the primary gene list. The issue of multiple gene names reappears when the annotated list is explored for differentially expressed genes that have associations with prion biology. *RPSA* is represented in the ensembl database with the identification of ENSMUSG00000032518, which shows that this gene has multiple nomenclature and is also known as the 67-kDa Laminin Receptor-1 (LAMR1, LAMBR), a protein proposed as a major interactor of PrP (Rieger, Edenhofer et al. 1997; Gauczynski, Peyrin et al. 2001; Hundt, Peyrin et al. 2001; Gauczynski, Nikles et al. 2006; Nikles, Vana et al. 2008; Kolodziejczak, Da Costa Dias et al. 2010). Therefore using *RPSA* gene symbol to scan the annotated gene would not return results indicating importance and the upregulation of 67-kDa Laminin Receptor-1 amongst clonal cells would be overlooked. In actuality, this protein was over-expressed in the CWD prion permissive RKD-S cells (Table 4.10). This issue of multiple gene names/symbols does not emerge when using mouse or human microarrays because the annotations have been well characterized. The preliminary selections of genes for future validation analysis were chosen based on mathematical significance threshold parameters, which enabled us to identify and connect genes in a hypothesis driven prediction analysis (Tables 4.6 and 4.7). The subsequent discussion of

predicted genes associated with prion replication stem from these primary selection criteria.

Cross-Referencing Gene Expression Data To The Prion Disease Databases (PDDDB): To establish a link between the microarray-identified genes and prion disease, we utilized the Prion Disease Database (PDDDB) for comparison analysis. The PDDDB retains documented gene expression profiles from mice of different genetic backgrounds, infected with different mouse-adapted scrapie strains. This systems approach measured gene expression of mouse brains pre- and post- prion infection. Expression was measured using microarray technology over the complete prion disease incubation timeline. The primary time points analyzed and presented in the PDDDB were of 6, 10, 14, 18, 20 and 22 weeks post infection. The 1,375 RKD annotated genes were uploaded and compared into the PDDDB. This scan returned a total of 314 (23%) RKD differentially expressed genes matching annotated genes within PDDDB (Table 4.5). Of these 314 matched genes, 132 were down regulated, while 182 genes were upregulated in RKD-R cells (Table 4.5). Furthermore, of 314 matched genes, 32 genes (10%) have previous publications associated with prions. These genes are presented in tables 4.8 and 4.9.

RKD-R Down Regulated/RKD-S Up Regulated Genes And Vice-Versa: Sixty-eight genes were identified to be significantly down regulated in RKD-R cells (up-regulated in RKD-S cells) using t-test p-values of ≤ 0.001 and FC of ≥ 2.0 (Table 4.6). The chosen genes consequently discussed were selected based on biological relationship to protein misfolding and associational linkage to PrP based of PDDDB cross-reference results. The biological relationships include pathways hypothesized to regulate intracellular protein homeostasis, endocytic trafficking and exocytic transport. Cellular mechanism regulating

metal ion homeostasis and transport were also considered in the rationale for gene selection. DAVID and PANTHER database analyses also demonstrated a clear demarcation of gene expression between the sensitive and resistant RKD clones (Fig. 4.6). Therefore gene selection was partially directed with those data in observance. Cross-reference analysis of genes identified by DAVID database to the high stringency gene list helped identify several interesting gene targets. We chose to specifically target autophagy-related 4a protein (Atg4a), eukaryotic translation initiation factor 2-alpha kinase 2 (eIF2ak2), small heat shock protein 8 (HSPB8), chaperonin containing T-complex polypeptide 1, subunit 6A (CCT6a), cyclophilin peptidyl-prolyl isomerase (Ppil4), Ceruloplasmin (CP), protein C (PROC), alpha-1-Acid glycoprotein (Orm1), protocadherin-alpha 1 (Pcdha1), and adaptor-related protein complex AP-1, sigma 3 (Ap1S3) (Table 4.6 and 4.7). These genes were used as starting points to subsequently analyze the larger gene list containing 1,375 genes. The following discussion assembles and connects the expressed genes to develop a hypothesis driven prediction on the phenotypic characteristics that mediate cellular susceptibility to prions.

Autophagy: The direct translation of autophagy is “self (*auto*)-eating (*phagy-to eat*)”. In the context of cell biology, autophagy is a catabolic process used by cells during stress (Yorimitsu and Klionsky 2005). This mechanism can further be subdivided into three distinct processes, which include macroautophagy, microautophagy and chaperone-mediated autophagy (CMA) (Khalfan and Klionsky 2002; Reggiori and Klionsky 2002; Massey, Kiffin et al. 2004). The mechanisms that dictate the induction of autophagy have not been fully characterized but the basic process of macro- and micro- autophagy entails the engulfment of cytosol by newly-formed double membraned structure called the

autophagosome (Fig. 4.7A) (Horst, Knecht et al. 1999; Klionsky and Ohsumi 1999; Klionsky 2005). The autophagosomes subsequently fuses with lysosomes at which point the autophagosome content is degraded by lysosomal enzymes (Fig. 4.7A). CMA autophagy does not require the formation of autophagosomal structures because the targeted proteins are directly translocated into lysosomes (Massey, Kiffin et al. 2004). Approximately ~30 genes (Atg) have been described to be directly linked to autophagy (Klionsky, Cregg et al. 2003). Autophagy is a tightly regulated process that may be selective or non-selective, and causes deleterious effects if skewed in either direction (Komatsu, Ueno et al. 2007). Moreover, autophagy deregulation is linked to protein aggregation and protein misfolding diseases, making it a primary target mechanism for our differential gene expression analyses (Anglade, Vyas et al. 1997; Anglade, Vyas et al. 1997; Kegel, Kim et al. 2000; Petersen, Larsen et al. 2001; Goldberg 2003; Yu, Cuervo et al. 2005).

Protein Homeostasis, Macroautophagy Induction and CerPrP^{Sc} Replication: The aforementioned predictions made by DAVID led us to initiate the search for genes involved in intracellular protein homeostasis. Autophagy-related 4a protein (Atg4a) and small heat shock protein 8 (HSPB8) were two genes that instantly stood out as possible candidates for further investigation. At the time of selection, there was no prior knowledge of a linking relationship between the two genes and were considered to not be interdependent. Using HSPB8 as the primer in researching functional association to protein misfolding, it was discovered that this particular small heat shock protein has a very unique function that can initiate macroautophagy and/or CMA (Massey, Zhang et al. 2006).

Chaperone proteins are important modulating factors in protein misfolding diseases. HSPB8 was discovered to be significantly upregulated in cells permissive to prion replication (Table 4.6). This protein belongs to the small heat-inducible heat shock chaperone protein family sharing the highly distinctive α -crystallin domain characteristic of other proteins in the family (Chowdary, Raman et al. 2004). Several different names have been used to describe this protein, which include HSPB8, Hsp22, H11 kinase, and E2IG1. This protein is 196aa in length and has a molecular mass of 21.6 kDa (Hu, Chen et al. 2007). Like other small-heat shock proteins, HSPB8 is activated by cellular stress and exhibits protein-folding chaperone activity (Chowdary, Raman et al. 2004). Moreover, HSPB8 has been shown to specifically interact with kinase proteins, causing it to become phosphorylated in the process (Benndorf, Sun et al. 2001). In particular, protein kinase C (PKC), mitogen-activated kinase (MAPK) and eukaryotic translation initiation factor 2- α kinase (eIF2 α) phosphorylate HSPB8, a crucial characteristic to the proceeding discussion. In addition to these physiological functions, HSPB8 exhibits association with several protein misfolding diseases that include distal hereditary motor neuropathy type II (dHMNI), AD, HD and ALS (Fontaine, Sun et al. 2006; Wilhelmus, Boelens et al. 2006; Crippa, Carra et al. 2010; Crippa, Sau et al. 2010; Kwok, Phadwal et al. 2011). Protein misfolding and cellular toxicity associated with HSPB8 is directly linked to the induction of autophagy and containment of protein aggregation (Carra, Seguin et al. 2008; Carra, Brunsting et al. 2009; Carra, Boncoraglio et al. 2010; Crippa, Sau et al. 2010). Autophagy pathway induction by HSPB8 requires a co-chaperone protein called Bcl2-associated athanogene 3 protein (BAG3) (Carra, Seguin et al. 2008).

The Bcl2-associated athanogene (BAG) protein family are co-chaperones functionally attributed to regulating protein quality control with heat shock proteins (Hsc/HSP70) (Takayama and Reed 2001). Three BAG proteins were differentially expressed between the sensitive and resistant RKD cells (Table 4.10). BAG3 protein, the co-chaperone of HSPB8 was up regulated in RKD-S cells while BAG2 and BAG6 were both down regulated (Table 4.10). A molecular link has been made between protein degradation during the aging process and BAG3 expression (Gamerding, Hajieva et al. 2009). During cellular aging, mechanisms that dictate degradation of polyubiquitinated protein gradually switch from proteasomal pathways to macroautophagic degradation processes, shown by the gradual shift in expression ratio levels of BAG1 to BAG3 (Gamerding, Hajieva et al. 2009). In addition to this ratio change, ubiquitin-binding proteins involved in the UPS mechanisms together with higher cathepsin activity were also observed. Interestingly, BAG1 has been described to functionally link Hsc/HSP70 to the proteasome using a unique ubiquitin-like domain (UBL), a domain that is found in one other BAG protein, BAG6 (-1.62-FC in RKD-S, Table 4.10) (Luders, Demand et al. 2000). The down regulation of BAG6 in RKD-S cells provide additional evidence to suggest that the proteasomal mechanisms geared for maintaining proper protein-folding are skewed to cause malfunction. If BAG6 has UPS-related functions (Luders, Demand et al. 2000) and BAG3 induces autophagy specially targeted for protein aggregation (Carra, Seguin et al. 2008), both mechanisms closely related to the prion replication process than BAG2 must also be a crucial component relating to prion cellular susceptibility. Indeed, BAG2 functionally inhibits the chaperone-associated ubiquitin ligase CHIP (Arndt, Daniel et al. 2005). Ubiquitin-ligase CHIP links molecular chaperones to the UPS system

and is vital to the overall protein folding and degradation process in eukaryotic cells (Murata, Minami et al. 2001; Esser, Alberti et al. 2004; Shimura, Schwartz et al. 2004; Esser, Scheffner et al. 2005). Notably, CHIP's main function is to attach ubiquitin-derived signals to chaperone-bound protein clients for one of two reasons; (i) normal conformational regulation of protein folding (Xu, Marcu et al. 2002; Westhoff, Chapple et al. 2005) and more importantly (ii) recognizing aggregation-prone proteins for quality control purposes (Murata, Minami et al. 2001; Shimura, Schwartz et al. 2004). Thus, RKD-S cells down regulate two proteins (BAG2 and BAG6) that strongly associate with targeting proteins for proteasomal degradation and up regulate BAG3, which selectively targets protein degradation by autophagy. Experimental evidence suggests that protein aggregation is correlated with the presences of both HSPB8 and BAG3, and absent of other heat shock proteins, indicating preferential specificity towards aggregation-mediated stress response (Carra, Seguin et al. 2008; Carra, Brunsting et al. 2009; Carra, Boncoraglio et al. 2010; Seidel, Vinet et al. 2012)

The formation of HSPB8-BAG3 complex leads to the phosphorylation of eIF2ak2, which consequently shuts down protein synthesis and initiates autophagy (Fig. 4.7) (Carra, Brunsting et al. 2009). In response to misfolded protein stress, activated eIF2ak2 reduces the influx of nascent proteins into the ER and stimulates upregulation of chaperone proteins (Zhanataev, Lisitsyna et al. 2009). Autophagy initiation by eIF2ak2 is a direct response to misfolded proteins, which include PrP^C-PrP^{Sc} conversion. Moreover, proteasomal dysfunction and ER stress enhances the trafficking of prion protein aggregates, triggering accumulation of PK resistant PrP^{Sc} (Nunziante, Ackermann et al.

2011). The aggregation of the Htt-Poly-(Q) protein in HD also activates the eIF2ak2 autophagy response (Peel, Rao et al. 2001).

DAVID bioinformatic gene analysis uncovered a difference in cell growth and division between the sensitive and resistant RKD cells (Fig. 4.6). The activation of macroautophagy through HSPB8-BAG3 mediated phosphorylation of eIF2ak could provide the explanation to the results obtained from DAVID analysis. If RKD-S cells were preferentially skewed towards eIF2ak-mediated autophagy activation, than the logical side effect would be complete shutdown of protein translation and growth arrest. For that reason, microarray gene expression analysis would filter the cell division genes into the RKD-R group. To extrapolate this beyond the bioinformatic interpretations and put it into the context of prion replication, transient growth arrest mediated by the aforesaid protein-folding stress responses also provides the time required to efficiently convert PrP^C to PrP^{Sc}. Earlier cell culture studies have indicated that cell division strongly influences cellular ability to accumulate PrP^{Sc} (Ghaemmaghami, Phuan et al. 2007).

Looking back at the annotated gene lists, we discovered that both BAG3 (1.54-FC, p-value of ≤ 0.05 and a FC of ≥ 1.5) and eIF2ak2 (2.73-FC, p-value of ≤ 0.001 and a FC of ≥ 2.0) were upregulated in RKD-S cells (Table 4.6 and 4.10). Interestingly, the HSPB8-BAG3 complex initiates the autophagy mechanisms along with stress-induced translational arrest independent from the normal ER stress response other chaperone proteins utilize for dealing with protein misfolding (Carra, Brunsting et al. 2009). The chaperone proteins normally associated to protein misfolding response are the 70-kDa heat shock protein family (HSPA), DNAJ proteins and BAG1 (Cuervo and Dice 1998),

which coincidentally have been down regulated in RKD-S cells (Table 4.10). Indicating a mechanistic shift in the protein maintenance processes.

HSP70 proteins have been shown to significantly reduce α -Synuclein (α -Syn) aggregation, fibril formation and cellular toxicity in both mouse and drosophila PD models (Klucken, Shin et al. 2004; McLean, Klucken et al. 2004; Auluck, Meulener et al. 2005; Dedmon, Christodoulou et al. 2005; Outeiro and Kazantsev 2008; Outeiro, Putcha et al. 2008). Heat-shock 70-kDa protein 12A (HSPA12A, 2.09-FC) and heat-shock 70-kDa protein 2 (HSPA2, 3.89-FC) were upregulated in RKD-R cells (Table 4.10, Fig. 4.7). The upregulation of these proteins could be pertinent to the resistance phenotype, which is based on the described functional characterization studies. Coincidentally, HSPA2 (3.89-FC in RKD-R) is predominantly co-localized to the cell-surface, the primary location predicted for PrP^{Sc} conversion (Goold, Rabbanian et al. 2011), while HSPA12A is cytoplasmic. Overall, HSPA12A and HSPA2 have not been well characterized, therefore it is difficult to speculate further on their exact function in RKD-R cells.

Whereas the abovementioned 70-kDa chaperone proteins were down regulated in RKD-S cells, the reverse was true for the 90-kDa heat shock proteins (HSPB family) (Fig. 4.7 and Table 4.10). Dual upregulation of HSP90B1 (1.6 FC) and HSP90AB1 (1.53 FC) in RKD-S cells also has applicability towards the mechanisms governing cellular permissiveness to prion replication (Table 4.10, Fig. 4.7). Blocking HSP90 from phosphorylating tau in the tauopathy mouse model demonstrated significant reduction of tau aggregate formation (Dickey, Kamal et al. 2007), suggesting that the presence of HSP90 proteins could enhance aggregate formation. In addition to enhancing tau aggregation, HSP90 has also been linked with Rab11a GTPase in recycling and secreting

aggregated α -Syn from cells (Liu, Zhang et al. 2009). Rab GTPase mediated intracellular trafficking and recycling of endosomal, lysosomal, and exosomal vesicles also has relevance to intracellular prion replication (Borchelt, Taraboulos et al. 1992; Fevrier, Vilette et al. 2004; Marijanovic, Caputo et al. 2009).

Additional chaperone like genes differentially expressed in RKD-S cells were the chaperonin containing T-complex polypeptide 1, subunit 6A (CCT6a) and subunit 2 (CCT2a) (Table 4.10 and Fig. 4.7B). The chaperonin protein family separates into two sub-categories, group I and group II. Group I chaperonins are predominantly located in the mitochondria and group II are cytosolic (Mukherjee, Conway de Macario et al. 2010). Both CCT proteins belong to the group II chaperonin family. Each subunit of this complex has an approximate 52-65kDa molecular mass, but becomes 970kDa when formed into the hetero-oligomeric complex (Schwartz, Kittelberger et al. 2000). The primary function of this and other family proteins is to assist proper protein folding and reduce aggregation. Interestingly, an in vivo study analyzing the complete transcription profile of prion-infected mice revealed that CCT6A is one of few chaperone proteins upregulated in the time-course of infection (Sorensen, Medina et al. 2008). In addition, CCT6a and CCT2 have been linked to modulate Htt-mediated polyglutamine expansion, aggregation and cellular toxicity (Kitamura, Kubota et al. 2006; Tam, Geller et al. 2006; Teuling, Bourgonje et al. 2011). CCT6a is upregulated, while CCT2 is down regulated in RKD-S cells. Although, specific roles in prion replication for these proteins have not been determined.

The initial stages of protein misfolding, CMA mechanism is the dominating process by which cells clear aggregate-prone proteins (Cuervo and Dice 1998). CMA

does not rely on autophagosome formation to degrade misfolded proteins, instead HSP/DNAJ/BAG1 complex forms at the membrane of a lysosome that inadvertently interacts with the constitutively active HSPA (70-kDa) chaperone to induce selective protein degradation (Cuervo and Dice 1998). Degradation of misfolded proteins using CMA mediated autophagy is limited to small aggregates and does not have the capacity to break down larger protein aggregate structures (microaggregates) (Ravikumar, Duden et al. 2002). Cellular response to microaggregates is macroautophagy, which HSPB8-BAG3 complex activates. Therefore, the acquired microarray data indicates two divergent mechanisms are occurring within RKD cells. The resistant RKD-R cells are utilizing the UPS and CMA systems very efficiently to disallow the formation of PrP^{Sc} aggregates. This is implied from the overexpressed HSPA, DNAJ and BAG2&6 proteins (Table 4.10). While RKD-S cells are actively shutting-down these systems and inducing macroautophagy in attempt to clear PrP^{Sc} replication and dispersion, which is indicated by the upregulated HSPB8, BAG3, eIF2ak proteins (Table 4.10). Pausing to think about these scenarios and how they relate to the abovementioned experimental evidence, it would seem that these processes are reversed. The initiation of macroautophagy is the exact response a cell would require to efficiently clear large protein aggregates such as the ones formed by PrP^{Sc} aggregates and not the contrary. Macroautophagy studies in AD have shown that autophagosome vacuoles accumulate in dystrophic neurites in the late stages of disease and maintain beta-amyloid (Abeta) proteins (Nixon, Wegiel et al. 2005; Yu, Cuervo et al. 2005). Moreover, targeting mTOR1 (primary inhibitor of autophagy) with inhibitors such rapamycin increases autophagosome formation and the accumulation of Abeta-filled autophagic vacuoles (AVs) (Yu, Cuervo et al. 2005). The buildup of

intracellular Abeta levels in AVs of dystrophic neurites could link autophagy deregulation with promoting Abeta aggregation in AD patients. Additional reports have revealed that deregulating the HSPB8-BAG3 autophagy mechanisms significantly enhances protein aggregation (Carra, Boncoraglio et al. 2010). Thus, it is feasible that the selected RKD-S clones are deregulating these protein homeostatic processes to efficiently replicate and sustain PrP^{Sc} aggregated molecules. But how would this deregulation allow prions to accumulate and infect other cells? Macroautophagy exponentially generating infectious PrP^{Sc} seeds is one hypothesis that could explain these observations. Indeed, others have previously indicated that skewing autophagy is counterproductive and toxic to cells (Nixon, Wegiel et al. 2005; Yu, Cuervo et al. 2005; Heiseke, Aguib et al. 2010; Nunziante, Ackermann et al. 2011). The exposure of PrP^{Sc} aggregate-fibrils to the lysosomal enzymes would induce fragmentation of the fibrils to smaller and more infectious molecules. Previous reports comparing PrP^{Sc} fibril size to infectivity have demonstrated that infectivity and conversion was most efficient with PrP-fibrils 300-600kDa in size or approximately 14-28 PrP molecules (Silveira, Raymond et al. 2005).

Additional evidence to support the autophagy-based PrP^{Sc} replication scenario is the upregulation of lysosomal enzyme cathepsin L1 (CTSL, 2.1-FC) in RKD-S cells. CTSL has previously been associated with various neurodegenerative protein misfolding diseases, which includes TSE (Diedrich, Minnigan et al. 1991; Kegel, Kim et al. 2000; Zhang, Spiess et al. 2003; Brown, Webb et al. 2004; Polyakova, Dear et al. 2009). Prion infectivity studies in N2a cells revealed a significant increase of cathepsins B and L in the ScN2a infected cells as compared to the uninfected counterparts, consequently leading to the hypothesis that lysosomal proteases participate and enable intracellular conversion of

PrP^{Sc} (Zhang, Spiess et al. 2003). In vitro experiments that proteolytically cleaved PrP with Cathepsin S produced N-terminally cleaved protein (PrP₉₄₋₂₃₃) molecule, which readily converted isoform conformation from α -helix to β -sheet rich (Polyakova, Dear et al. 2009). Moreover, the β -sheet rich PrP₉₄₋₂₃₃ molecules formed thioflavin-T positive aggregate species reminiscent of PrP species shown to be highly toxic in mouse models (Shmerling, Hegyi et al. 1998; Baumann, Tolnay et al. 2007). Recently published data analyzing endogenous proteolytic cleavage of PrP^{Sc} in cell culture and tissue demonstrated that both cathepsin B and L were the primary enzymes responsible for cleaving PrP^{Sc} (Dron, Moudjou et al. 2010). Notably, this study utilized RK13 cells for the cell culture portion of the experiments, providing strong support towards the relevance of CTLS over expression in the RKD-S cells.

Cyclophilin Ppil4 is a peptidyl-prolyl isomerase with attributed function of catalyzing the interconversion between *cis* and *trans* isomers of proline (Fischer, Bang et al. 1984; Zeng, Zhou et al. 2001). The Ppil4 gene is upregulated in RKD-S cells determined by high statistical stringency analysis (2.11-FC, Table 4.6). Its selection for functional validation is based on its proposed functions to behave as a chaperone involved in cellular maintenance of protein homeostasis (Fischer and Will 1990). Ppil proteins have been implicated in several signaling pathways but the basic biochemical function of the Cyclophilin enzyme is not fully understood (Davis, Walker et al. 2010). Peptidyl-prolyl *cis-trans* isomerases have previously been described as potential chaperones to PrP^C with associations as a possible factor in GSS (Cohen and Taraboulos 2003). It was experimentally demonstrated that cells treated with Cyclosporin A (CsA), an inhibitor of cyclophilins, induced accumulation of misfolded PrP in aggresomes

(Cohen and Taraboulos 2003). Moreover, cyclophilins associated with prion aggregation to specific cellular compartments designated 'juxta nuclear quality control compartment' (JUNQ) and the 'insoluble protein deposit' compartment (IPOD) (Ben-Gedalya, Lyakhovetsky et al. 2011). These cellular compartments were shown to actively recruit chaperones for quality control purposes. In addition to chaperone activity, human cyclophilins have also been determined as essential interacting partners for the HIV-1 Gag polyprotein during infection, with a suggested role in the un-coating process (Qi, Yang et al. 2008; Schaller, Ocwieja et al. 2011). This HIV-1 Gag interacting function of Ppil4 is especially relevant because all susceptible cell lines described thus far stably co-express HIV-1 Gag (Elk21⁺ & RKD). Therefore, Ppil4 could be the endogenously expressed protein linking HIV-1 Gag with the enhanced susceptibility phenotype exhibited by both RKD-S and Elk21⁺ cells.

Autophagy-related 4a protein (Atg4a) is a cysteine protease protein associated with oxidative stress response and detoxification autophagy pathway (Scherz-Shouval, Shvets et al. 2007). Atg4a is 398 aa in length and is predominantly a cytoplasmic protease responsible for intracellular degradation processes (Marino, Uria et al. 2003). The Atg4a protein is vital for cellular survival under stress conditions, protecting the cell from entering apoptosis (Ohsumi 2001; Marino, Uria et al. 2003; Codogno and Meijer 2005; Scherz-Shouval, Shvets et al. 2007). Besides the direct link with autophagy and overexpression in RKD-S cells, the functions within the autophagy pathway this protein associates with makes it an appropriate to the overall hypothesis driven discussion. Although autophagy is characterized as non-selective self-degradation mechanism, recent studies have shown that certain proteins are highly selected for autophagy-mediated

degradation (Ohsumi and Mizushima 2004; Kim, Rodriguez-Enriquez et al. 2007; Farre, Manjithaya et al. 2008). In both selective and non-selective autophagy processes, there exists two ubiquitin-like protein conjugating systems, which are mediated through either Atg12 or Atg8 proteins (Ohsumi 2001). While Atg12-mediated conjugation is primarily involved in the formation of a multi-protein (Atg12-Atg5-Atg16) complex that guides autophagosome membrane formation, Atg8 conjugation facilitates the progression of non-specific autophagy and vacuole targeted (Vt) autophagy (highly-selective) pathways (Kirisako, Ichimura et al. 2000; Hutchins and Klionsky 2001). Atg4 is vital to the Atg8-conjugating system (Kirisako, Ichimura et al. 2000). As a cysteine protease, Atg4 cleaves Atg8 from the membrane-lipid complex it is bound to (phosphatidylethanolamine (PE)) (Ichimura, Kirisako et al. 2000). This cleavage event allows Atg8 to sequentially go through the multi-step conjugating system to form another membrane integral Atg8-PE complex. Unlike the Atg12 complex, Atg8-PE complex is continuously recycled by a second Atg4 cleavage event which liberates Atg8 to reform new complexes and consequently mediate the specificity of the autophagosome formation and size (Kirisako, Baba et al. 1999). Moreover, Atg8-PE also behaves as a scaffold to enable membrane expansion for larger vesicle formation. Recent studies have provided evidence indicating a direct correlation between the levels of Atg8, size and autophagosomal expansion (Nakatogawa, Ichimura et al. 2007; Xie, Nair et al. 2008; Xie, Nair et al. 2008). Thus, Atg4 over expression in RKD-S cells helps drive selective autophagy that has the potential ability for expanding the autophagosomes to accommodate large CerPrP^{Sc} aggregates.

Recapping the supporting evidence for the hypothesis driven prediction regulating prion susceptibility: The introduction of CWD prions to RKD-S cells causes the upregulation of HSPB8 and BAG3, which forms a co-chaperone complex that phosphorylates eIF2ak (Fig. 4.7B). The activation of eIF2ak causes RKD-S cells to shut down protein translation and become temporarily growth arrested. Concurrently, the second mechanism activated by eIF2ak is the induction of macroautophagy (Fig. 4.7A), which seems to be independent of the UPS and CMA response (Fig 4.7B). This non-canonical response is indicated by the active down regulation of HSPA (70-kDa), DNAJ and BAG (2 & 6) proteins that are normally involved in the classic UPS response (Table 4.10). Selective autophagy in RKD-S cells mediated by the Atg4's release of Atg8-PE complex generates CerPrP^{Sc}-fibril filled autophagosomes that seclude the infectious microaggregates from becoming toxic to the cell. Replication and infectivity of CerPrP^{Sc}-fibrils is ensued when the autophagosome docks and fuses with lysosomes abundantly filled with Cathepsins and other proteases that are upregulated in RKD-S cells. Instead of clearing CerPrP^{Sc}-fibrils, the matured autophagosome-lysosome complex cleaves CerPrP^{Sc}-fibrils into smaller, more infectious molecules that are subsequently released intracellularly and/or exocytosed out to infect neighboring cells (Fig 4.7B). Upregulation of Rab GTPases by RKD-S cells is additional evidence strongly supporting this hypothesis (Table 4.10, Fig 4.8B). In either case, proteolytic digestion and reduction of CerPrP^{Sc} microaggregates releases the cells from growth arrest, which in turn allows RKD-S to divide and exponentially replicate CWD prions.

Figure 4.7 Autophagy and PrP^{Sc} Replication. **A.** Schematic representation of Macroautophagy (Autophagy) induction. Different stimuli induce intracellular autophagy, which range from homeostatic organelle/protein maintenance to stress responses induced by exogenous sources (Infection, Starvation, and Reactive Oxygen Species (ROS)). The multi-step process initiates with cytosolic membrane isolation collecting and sequestering molecules. This progressive cytosolic membrane forms a mature autophagosome containing molecules destined for degradation. Molecule degradation is achieved when the autophagosome docks and fuses with lysosomes, releasing lysosomal proteolytic enzymes to ensue degradation (Klionsky 2005; Nair and Klionsky 2005; Reggiori and Klionsky 2005; Yorimitsu and Klionsky 2005; Moreau, Luo et al. 2010). **B.** Hypothesis driven schematic using differentially expressed RKD genes to predict the intracellular mechanisms regulating prion replication. Significant upregulation of HSPB8, BAG3, eIF2ak, Atg4a (Table 4.6) in the CWD prion permissive RKD-S cells imply the induction autophagy. HSPB8-BAG3 induce the phosphorylation of eIF2ak, which subsequently induces the complete shut down of translation and stimulates autophagy (A non-canonical stimulation irrespective of HSP70 and ubiquitin ligase activation) (Carra, Brunsting et al. 2009). Autophagy induction leads to activation/deactivation of other chaperone proteins involved in stabilizing protein folding (Red color genes indicate upregulation (ex. HSPB8), black color (ex. BAG2) indicate down regulation in RKD-S cells). The continuous stimulation of this process in combination with cell growth arrest (translational shut down) enables PrP^{Sc} infectious seed production enhancing cellular infectivity(Silveira, Raymond et al. 2005; Heiseke, Aguib et al. 2010). Full Gene names and functions are described in table 4.10.

Figure 4.7 Autophagy and PrP^{Sc} Replication.

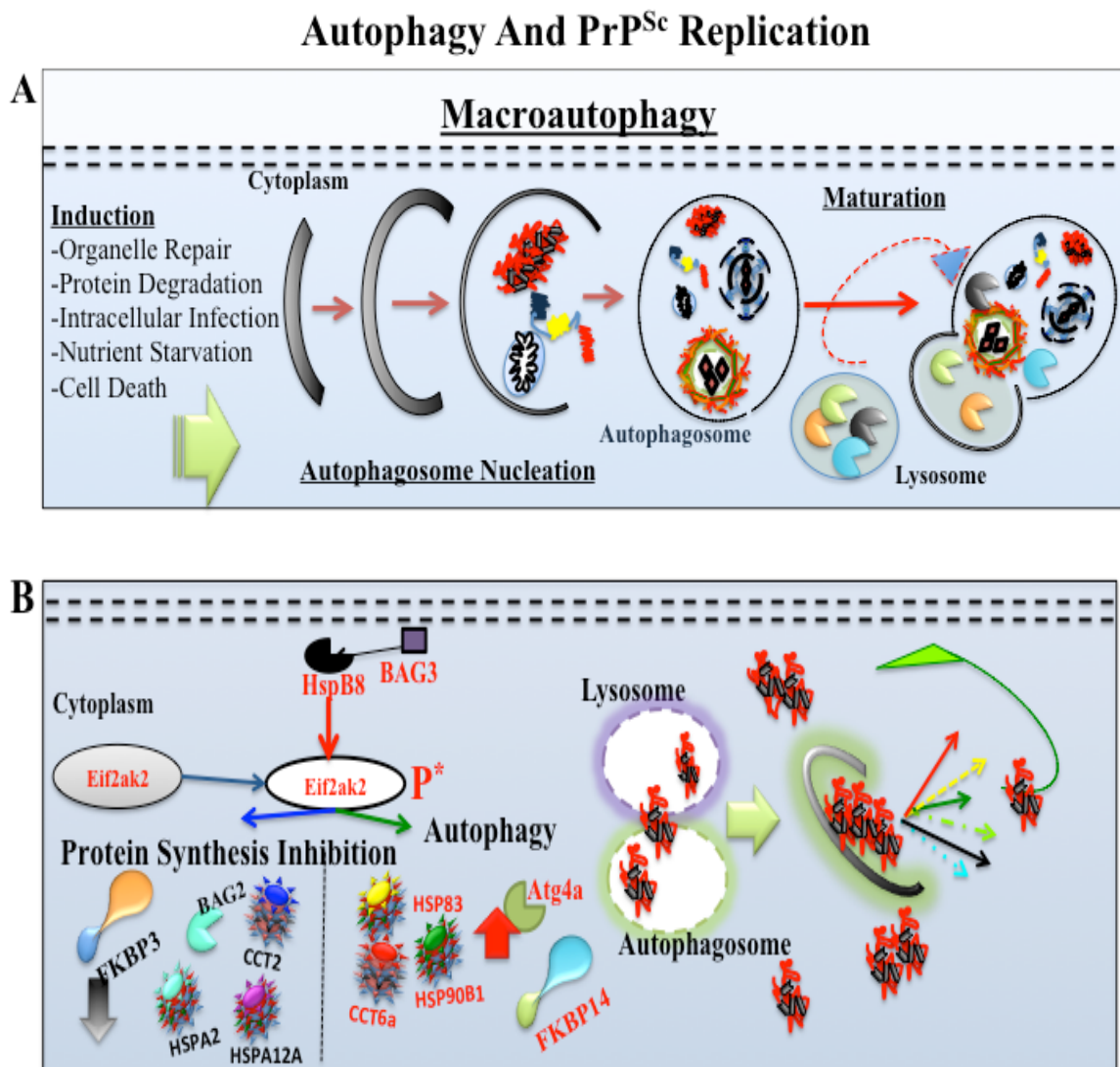


Table 4.6 Differentially down regulated gene expression in RKD-R cells as compared to the RKD-S cells. Robust multichip average (RMA) and quantile normalization methods were used for signal normalization and false-positive signal noise, respectively. Significance and stringency was set to p-value 0.001 and fold change cutoff of 2.0, respectively. Abbreviations, Fold Change (FC), Not Associated (NA), Endoplasmic Reticulum (ER), plasma membrane (PM)

Gene Name	Gene Symbol	FC (-)	Cell Process	Component
Amiloride-sensitive cation channel 2	Accn2	2.57	Cation transport	PM, synapse
Helicase-like transcription factor	Hltf	2.06	Chromatin modification, metabolic process transcription DNA dependent	Nucleus
Autophagy-related 4A	Atg4a	2.78	Autophagy, metabolic transport, protein transport, proteolysis	Cytoplasm
Hepatitis A virus cellular receptor 1	Hvcr1	2.38	Phagocytosis, mycotoxin, nutrient	Cell surface, membrane, phagocytic vesicle
Solute carrier family 25 member 20	Slc25a20	3.0	Carnitine shuttle, transport	Membrane, mitochondrial inner membrane
Interferon gamma receptor 1	Ifngr1	2.52		ER, membrane, postsynaptic density, vesicle
F-box protein 32	Fbxo32	3.55	Muscle atrophy	Nucleus
ABI gene family, member 3 (NESH) binding protein	Abi3bp	2.91	Extracellular matrix organization, positive regulation of cell-substrate adhesion	Extracellular matrix/space, interstitial matrix
RalBP1 associated Eps domain containing protein	Reps1	2.04	NA	Coated pit, plasma membrane
F-box protein 30	Fbxo30	2.43	Protein ubiquitination (computational estimation)	Cellular component
T cell receptor alpha variable 12d-1	Trav12d-1	2.90	NA	NA
BCL2-associated	Bclaf1	2.01	Positive regulation	Cytoplasm, Nucleolus,

transcription factor 1			of Apoptosis	nucleus
Peptidyl-prolyl isomerase (cyclophilin)-like 4	Ppil4	2.11	Protein folding, protein peptidyl-prolyl isomerization	Cellular component, nucleus
ADP-ribosylation factor-like 8B	Arl8b	2.05	Cell cycle/division, chromosome segregation, mitosis	Cytoplasm, cytoskeleton, endosome, lysosome, membrane, midbody, spindle midzone
Docking protein 1	Dok1	3.16	MAPKKK cascade, Ras protein signal transduction, intracellular protein kinase cascade	Cytoplasm
Solute carrier family 6, member 5	Slc6a5	3.46	Amino acid transmembrane transport, glycine transport	Integral to membrane, Membrane
Discoidin, CUB and LCCL domain containing 2	Dcbld2	3.43	Cell adhesion, negative regulation of cell growth	Cell surface, Integral to plasma membrane
RIKEN cDNA 9030625A04 gene	9030625A04Rik	2.31	Biological	Cellular component
Eukaryotic translation initiation factor 2-alpha kinase 2	Eif2ak2	2.73	ER unfolded protein response, phosphorylation, positive regulation of apoptosis, protein autophosphorylation, virus-infected cell apoptosis	Intracellular, nucleus, soluble fraction
Crystallin, beta B2	Crybb2	2.08	Visual perception	NA
Enoyl Coenzyme A hydratase domain containing 1	Echdc1	2.28	Metabolic	Cellular
Protein kinase, cAMP dependent regulatory, type II alpha	Prkar2a	2.63	Phosphorylation, protein, regulation of protein kinase activity	T-tubule, cAMP-dependent protein complex, centrosome, cytoplasm, insoluble/soluble fraction perinuclear region of cytoplasm,

				PM
RIKEN cDNA 1700011H14 gene	170001 1h14Rik	2.17	Biological	Cellular
Relaxin 1	Rln1	21.37	G-protein signaling, regulation of NO mediated signaling	NA
EFR3 homolog A	Efr3a	2.07	Cell-cell adhesion	Cornified envelope, intracellular, Plasma membrane
FYN binding protein	Fyb	3.47	NOT mast cell activation	Cytoplasm, nucleus
Family with sequence similarity 110, member C	Fam110c	2.13	Biological	Cellular-component, cytoplasm, cytoskeleton, microtubule
Hairy/enhancer-of-split related with YRPW motif 2	Hey2	2.54	Notch signaling, negative regulation of transcription	Nucleus
Glia maturation factor, beta	Gmfb	6.11	NA	Intracellular
Splicing factor 3b, subunit 5	Sf3b5	2.00	RNA splicing/processing	U12-type spliceosomal complex, Nucleus
Vanin 3	Vnn3	2.26	Nitrogen compound metabolic process,	Membrane Anchored, extracellular space, PM
Activated leukocyte cell adhesion molecule	Alcam	9.85	Cell adhesion, motor axon guidance	Axon, External side of PM, neuronal cell body
Interferon induced with helicase C domain 1	Ifih1	2.52	Metabolic process, regulation of apoptosis, response to virus	Cytoplasm, intracellular, nucleus
Ribonuclease, RNase A family, 1	Rnase1	9.51	Metabolic	NA
Myelin transcription factor 1-like	Myt1l	3.40	Cell differentiation, nervous system development, DNA-dependent transcriptional regulation	Nucleus
Adenosine deaminase, tRNA-specific 2, TAD2 homolog	Adat2	5.13	tRNA processing	Cellular component
Nuclear receptor	Ncoa7	2.53	Cell wall	Intracellular, nucleus

coactivator 7			macromolecule process, DNA-dependent regulation of transcription	
Ceruloplasmin	Cp	3.23	Copper ion transport, oxidation-reduction process,	Anchored to PM, extracellular region/space
Adenosine deaminase	Ada	2.45	Cell adhesion, negative regulation of apoptosis, inflammatory response	Cell junction, cell surface, cytoplasm, cytoplasmic vesicle, extracellular space, lysosome, membrane,
PPPDE peptidase domain containing	Pppde1	2.19	NA	NA
Monoacylglycerol O-acyltransferase 3	Mogat3	2.29	Glycerol metabolic process, lipid biosynthetic process	ER membrane, membrane
Heat shock protein 8	Hspb8	4.23	Response to stress	Cytoplasm, intracellular, nucleus
2'-5' oligoadenylate synthetase-like 2	Oasl2	7.24	NA	Cellular component
Hypothetical protein LOC73112	311000 3A17Rik	2.39	NA	NA
TNFAIP3 interacting protein 1	Tnip1	2.07	Glycoprotein biosynthetic	Cytoplasm, nucleus
cDNA sequence BC016495	BC016495	2.01	Phosphorylation	Cellular component
Interferon-induced protein with tetratricopeptide repeats 1	Ifit1	6.43	Cellular response to; dsRNA, interferon-alpha/beta, intracellular transport of viral proteins in host cell	Cytoplasm
Eukaryotic release factor 3	Hbs1l	2.09	NA	NA
Sterile alpha motif domain containing 4B	Samd4b	2.04	NA	NA
RAR-related orphan receptor alpha	Rora	2.93	cGMP metabolic process, NO biosynthesis, positive regulation of transcription	Nucleus

			regulation	
Transmembrane protein 89	Tmem89	3.05	NA	Integral to membrane
Myeloblastosis oncogene	Myb	3.79	G1/S transition of mitotic cell cycle, calcium ion transport, chromatin remodeling,	Nucleus
Receptor transporter protein 3	Rtp3	3.78	Protein targeting to membrane	cytoplasm
Family with sequence similarity 126, member B	Fam126b	4.41	NA	Intracellular
Eukaryotic translation initiation factor 4E member 3	Eif4e3	2.11	Regulation of translation	Cytoplasm
human immunodeficiency virus type I enhancer binding protein 2	Hivep2	2.44	Signal transduction, DNA dependent transcription	Intracellular, nucleus, transcription factor complex
Vanin 2	Vnn2	4.10	NA	NA
RAS guanyl releasing protein 1	Rasgrp1	3.17	Cell differentiation, intracellular signal transduction,	Golgi, cytoplasm, ER, PM
CD47 antigen (Rh-related antigen, integrin-associated signal transducer)	CD47	2.02	Cell adhesion, migration, opsonization, cell proliferation, phagocytosis, signal transduction	Extracellular vesicular Exosome, PM
Androgen-induced 1	Aig1	2.03	NA	Integral to membrane
RNA binding motif protein 5	Rbm5	2.41	RNA splicing, positive regulation of apoptosis	Nucleus, spliceosomal complex
Chaperonin containing Tcp1, subunit 6a (zeta)	CCT6a	2.07	Cellular protein metabolic process	Cytoplasm
Ring finger protein 222	RNF222	2.42	NA	Membrane
Zinc finger protein 684	Znf684	2.05	DNA-dependent regulation of	Nucleus

			transcription	
T-cell surface glycoprotein	CD1e	2.63	Antigen processing and presentation	Golgi, early/late endosome, PM, Lysosomal lumen
Nucleus accumbens associated 1, BEN and BTB (POZ) domain containing	Nacc1	2.11	Induction of apoptosis,	Cytoplasm, intracellular membrane bound organelle, nuclear body
Tenascin C	Tnc	2.78	Cell adhesion, positive regulation of cell proliferation and gene expression	Basement membrane, extracellular region/space, proteinaceous extracellular matrix
Cell growth regulator with ring finger domain	Cgrrf1	2.12	Cell cycle arrest	NA

Auxiliary Proteins Correlated To Prion Susceptibility: Differentially expressed proteins that interact with PrP molecules at the cell surface are also important to discuss in the context of prion susceptibility. Although mentioned already, it is important to reiterate that PrP^C-PrP^{Sc} initial interaction and conversion occurs at the cell-surface of the plasma membrane (Stahl, Borchelt et al. 1987; Goold, Rabbanian et al. 2011; Hooper 2011). It is crucial to identify and characterize differentially regulated proteins that interact with PrP in lipid rafts and within intracellular compartments that would involve trafficking to and from the plasma membrane. In the last section of the introductory chapter is a comprehensive list of proteins that have been attributed to interact with PrP^C and/or PrP^{Sc} (Table 1.3). Using that list as reference, both high and low stringency RGD gene lists (Table 4.5) were searched for matching proteins from that list (Table 1.3) or share homologous resemblance to those described proteins. This investigation led to the discovery of genes that have previously been reported on with association to PrP and potentially novel genes. The extrapolated genes are listed in table 4.10.

Proteins At The Cell-Surface PrP^C-PrP^{Sc} Interface

PrP Receptors/Interactors: PrP^C is a glycoprotein tethered to the plasma membrane by a GPI-anchor, which requires interacting proteins for internalization and perhaps signaling (Stahl, Borchelt et al. 1987; Caughey and Raymond 1991; Stefanova, Horejsi et al. 1991; Borchelt, Taraboulos et al. 1992; Taraboulos, Raeber et al. 1992; Shyng, Huber et al. 1993; Shyng, Heuser et al. 1994; Vey, Pilkuhn et al. 1996). Gene list analysis has revealed several proteins previously shown to interact with PrP or co-localize together. These differentially expressed genes include the 37-kDa/67-kDa laminin receptor 1 (Lamr1), apolipoprotein receptors (LRP1 and LRP3), adhesion molecules protocadherin-

Alpha 1 (Pcdha1), cadherin 9 (CDH9), activated leukocyte cell adhesion molecule (ALCAM), integrins (ITGB), glycoproteins (CD36, CD47, ORM1) and metalloproteinases (ADAM & MMP's) (Table 4.10 and Fig. 4.8A).

PrP^C-PrP^{Sc} Complex Stabilization: The 37-kDa/67-kDa laminin receptor 1 (LAMR1) is upregulated in RKD-S cells (Table 4.8, 4.10 and Fig. 4.8A). Several studies have linked direct interaction of LAMR1 with both PrP^C and PrP^{Sc}, acting as internalization receptor (Kolodziejczak, Da Costa Dias et al. 2010; Mbazima, Da Costa Dias et al. 2010). The interaction of PrP with LAMR1 in RKD-S cells could have a multifaceted effect on the cells, which subsequently enables prion replication to ensue. The first and most obvious scenario involves the ability of these proteins to physically interact (Gauczynski, Peyrin et al. 2001). This interaction could stabilize the PrP^C-PrP^{Sc} complex, which would possibly require the participation of other adhesion/receptor proteins (LRP, CDH9, ALCAM) that are also upregulated by RKD-S cells (Fig. 4.8A) (Santuccione, Sytnyk et al. 2005; Gauczynski, Nikles et al. 2006; Taylor and Hooper 2007; Mbazima, Da Costa Dias et al. 2010). Although, stabilization of PrP^C-PrP^{Sc} by these adhesion proteins would not be sufficient to drive the conversion process forward. Coincidentally, RKD-S cells also over express metalloproteinases that have been experimentally validated for their ability to cleave both forms of PrP molecules (Table 4.10, Fig. 4.8A) (Cisse, Sunyach et al. 2005; Taylor, Parkin et al. 2009). Upregulated ADAM-9 has been shown to indirectly induce ectodomain PrP shedding through ADAM10, and therefore could influence the replication process (Cisse, Sunyach et al. 2005). Although, ectodomain shedding process exhibited by ADAM9-10 does not seem to have a direct effect on regulating prion

conversion (Taylor, Parkin et al. 2009). Nonetheless, joint interaction between the described proteins could have the additive effect that is favorable for prion conversion.

In addition, the microarray data indicates that clusterin (CLU) is also upregulated in RKD-S cells. The clusterin (Clu) gene encodes a secreted chaperone protein that is attributed with cellular debris clearance, protein aggregation induction and inhibition of apoptosis (Jones and Jomary 2002; Zhang, Kim et al. 2005; Materia, Cater et al. 2011; Wyatt, Yerbury et al. 2011). Especially relevant to the discussion is clusterin's ability to maintain and stabilize unfolded proteins in a quasi-conformation state without inducing the protein to refold (Yerbury, Poon et al. 2007). Clusterin's interaction with cell surface receptors stimulates internalization and consequent activation of lysosomal degradation processes (Wyatt and Wilson 2010). This characteristic strongly complements the aforementioned discussion on autophagy activation and PrP^{Sc} replication in RKD-S cells. In addition, this protein has been associated with AD, severity of disease, pathology and amyloid plaque formation (DeMattos, O'Dell M et al. 2002; Yerbury, Poon et al. 2007; Nuutinen, Suuronen et al. 2009; Thambisetty, Simmons et al. 2010; Schrijvers, Koudstaal et al. 2011; Schurmann, Wiese et al. 2011; Thambisetty, An et al. 2012). Clusterin exhibits direct interaction with PrP and has previously been linked with reducing the incubation time of prion disease (Kempster, Collins et al. 2004; Xu, Karnaukhova et al. 2008). Thus, it is feasible to hypothesize that the combinatorial interaction between the laminin receptor (LAMR1), adhesion proteins (ALCAM, CDH9, LRP), metalloproteinases (ADAM 1, 8, 9 & MMP/MME) and extracellular chaperone, clusterin (CLU), strongly supports the formation of PrP^C-PrP^{Sc} replicative complex (Fig. 4.8A).

Laminin receptor's capacity for internalization collectively with clusterin's ability to trigger internalization is the second possible mechanism/process in which RKD-S maintain prion susceptibility. In this process, we build onto the predicted cell surface mechanisms. PrP^C-PrP^{Sc} is stabilized by the cell surface proteins, at which point LAMR1 and CLU act out their secondary functions in the conversion process. These processes include subcellular internalization and activation of intracellular chaperones through misfolded stress response mechanisms (Fig. 4.8A-B). Besides internalization, LAMR1 and CLU both exhibit anti-apoptotic survival signaling capacities (Trogakos, Lourda et al. 2009; Vana, Zuber et al. 2009). Thus, at the interface of prion internalization, LAMR1 and CLU trigger additional survival pathways that keep the cell from entering apoptosis. These pathways involve genes that have been upregulated in RKD-S cells (Table 4.10). The genes regulate pathways involved in cellular survival mechanisms, which include ataxin 7 (ATXN7), tumor necrosis factor receptor subfamily member 1B (TNFRSF1B), nuclear factor kappa B subunit -2 (NFKB2), and eIF2ak2 (Table 4.10).

In addition, RKD-S cells recruit other proteins to assist in the process. PDDB cross-referencing enabled the identification of the calcium-dependent, membrane-binding protein, called Copine (Cpne8) (Table 4.8, 4.10 and Fig. 4.8B). The function of Cpne8 remains to be determined, but inferred to participate in membrane trafficking. Copine family of proteins are Ca²⁺-dependent phospholipid-binding proteins involved with membrane trafficking (Tomsig and Creutz 2002). It is probable that Cpne8, LAMBR1 and PrP^C co-localize and form an interaction. The mechanisms of this interaction to assist PrP^{Sc} replication is hard to predict but the upregulation of Cpne8 during the course of prion disease in mice has been reported indicating some sort of connection between these

proteins (Lloyd, Maytham et al. 2010). Consequently, RKD-S cells upregulate, what seems to be the right combination of cell-surface proteins to efficiently stabilize, chaperone and internalize prion molecules.

Ceruloplasmin (CP), upregulated gene in RKD-S cells is not associated with protein homeostasis but could be crucial to prion replication. CP is an alpha-2-glycoprotein that binds 95% of copper in the human serum (Ortel, Takahashi et al. 1984). The primary functions of this protein include iron homeostasis and neuronal survival with profound expression throughout the central nervous system (Klomp, Farhangrazi et al. 1996). Co-localization to lipid rafts and metal ion binding functions similar to PrP^C was the basis for selecting this protein for further analysis (Koschinsky, Chow et al. 1987; Mukhopadhyay, Attieh et al. 1998). CP has been demonstrated to mediate iron and manganese oxidation and transfers it to the plasma transferrin (Tfn) protein (Jursa and Smith 2009), which coincidentally has also been linked to the prion protein internalization mechanisms (Sunyach, Jen et al. 2003). Furthermore, this glycoprotein has been linked with other protein misfolding neurodegenerative disorders such as AD, PD and ALS (Loeffler, LeWitt et al. 1996; Vassiliev, Harris et al. 2005; Squitti, Quattrocchi et al. 2007; Capo, Arciello et al. 2008; Squitti, Quattrocchi et al. 2008; Texel, Xu et al. 2008; Torsdottir, Kristinsson et al. 2010; McNeill and Chinnery 2011; Olivieri, Conti et al. 2011). In addition, CP has been shown to interact with serine proteases and apolipoproteins to induce CP-mediated neuro-aggregation in P19 neuro-embryonic stem cells (Maltais, Desroches et al. 2003; Ducharme, Maltais et al. 2010). In vitro models using ROS in conjunction with CP have shown to induce efficient aggregation of α -Syn (Kim, Choi et al. 2002). This type of activity adds pertinence to the overall phenotype of

the prion sensitive cell. Collectively, RKD-S cells upregulate ApoE proteins (LRP), extracellular proteases (ADAM's & MMP/MME's, Chymase (CMA1-serine protease)) and extracellular chaperones (CLU) concurrently with CP. We hypothesize that these upregulated proteins are needed for optimal PrP^C-PrP^{Sc} conversion (Table 4.10 and Fig. 4.8). Copper chaperone for superoxide dismutase (CCS) is also upregulated by RKD-S cells (Table 4.10 and Fig 4.8B). This protein shares functional similarity to CP through regulation of metal ion homeostasis and copper ion transporting (Fig. 4.8B) (Suazo, Olivares et al. 2008). Co-localization of PrP^C, CCS and CP to the cell surface and cytosolic metal ion transport suggests importance in the global scheme of host modulations that enhance and/or select specific cells sensitive to prion replication.

The cell-surface protein expression in RKD-R cells somewhat differs. RKD-R cells upregulate adhesion proteins and metalloproteases that are different from RKD-S cells (Fig. 4.8A). Unlike RKD-S, RKD-R cells upregulate serine protease enzymes that if activated have the capability to digest PrP^C. Moreover, other RKD-R expressed glycoproteins could indirectly inhibit PrP^{Sc} replication at the cell-surface interphase keeping the cells free from internalizing the infectious agent. For example, alpha-1-Acid glycoprotein (Orm1) is localized to the plasma membrane of RKD-R cells. Orm1 is a 41-45-kDa acute phase plasma-glycoprotein that is prevalent during inflammation (Treuheit, Costello et al. 1992). This protein has been shown to interact with the plasminogen activator inhibitor-1 protein by stabilizing its function in inhibiting plasminogen activation (Fournier, Medjoubi et al. 2000; Boncela, Papiewska et al. 2001). This stabilization of plasminogen activator inhibitor-1 by Orm1 to reduce plasminogen production is indirectly relevant because plasminogen has been hypothesized to be one of

the cofactors associated with PrP^{Sc} conversion (Fischer, Roeckl et al. 2000; Maissen, Roeckl et al. 2001; Ryou, Prusiner et al. 2003; Mays and Ryou 2010; Mays, Yeom et al. 2011). Then, overexpression of Orm1 by RKD-R could inadvertently reduce plasminogen output by the cell, which would destabilize PrP^C-PrP^{Sc} conversion.

An additional glycoprotein expressed by RKD-R cells that could infer resistance is protein C (PROC) (Table 4.7 and Fig. 4.8A). PROC is a predominantly inactive serine protease that is dependent on vitamin K to become active (Clouse and Comp 1986). The protein is 419 aa long and has several function domains that give it both receptor binding and proteolytic properties (Mosnier and Griffin 2006). It was first described in the context of proteolytically inactivating blood coagulation factors V_a and VIII_a (Mammen, Thomas et al. 1960), but recently been associated with cytoprotective properties that include regulatory gene expression functions, anti-inflammatory, anti-apoptotic and endothelial barrier protective functions (Mosnier, Zlokovic et al. 2007). Cytoprotective properties are preformed though the interaction with the endothelial protein c receptor (EPCR) and the protease-activated receptor-1 (PAR-1), causing the activation of downstream regulatory pathways that modulate cellular response to stress (Mosnier, Zlokovic et al. 2007). Activated PROC has been established to upregulate expression of tumor necrosis factor receptor superfamily proteins and bone morphogenic proteins (Riewald, Petrovan et al. 2002), which are also upregulated in RKD-R cells. Furthermore, PROC maintains enzymatic protease similar to PK, a proteolytic enzyme used for digesting PrP^C and biochemically detecting PrP^{Sc}. Over-expression of PROC could bring on the unintentional digestion of PrP^C substrate prior the PrP^{Sc} conformational conversion step, making the cells phenotypically resistant. Ultimately, the pleiotropic functions of

PROC make it an attractive target for validation as a potential resistance factor responsible for inhibiting PrP^C-PrP^{Sc} conversion.

Protocadherin-Alpha 1 (Pcdha1) is a Ca²⁺-dependent cell adhesion molecule upregulated in RKD-R cells (Table 4.7, 4.10 and Fig 4.8A), which is normally expressed in neurons of the central nervous system (CNS) (Yagi and Takeichi 2000). The protocadherin gene family is composed of approximately 60 genes (Nollet, Kools et al. 2000; Yagi and Takeichi 2000). Besides cell adhesion functions, differential expression of protocadherins amongst neurons is hypothesized to provide neuronal identity at the cell surface. Protocadherins have been demonstrated to undergo proteolytic cleavage by both metalloproteinases and γ -secretase (Haas, Frank et al. 2005; Hamsch, Grinevich et al. 2005), enzyme previously linked to protein misfolding diseases (Turner and Nalivaeva 2007; Zhang, Ma et al. 2011). The cadherin proteins concurrently with other cell adhesion proteins have been implicated as probable interacting partners for PrP^C (Gauczynski, Hundt et al. 2001; Aguzzi, Baumann et al. 2008; Malaga-Trillo, Solis et al. 2009). Ultimately, overexpression of this protein in RKD-R clones could have a functional implication towards the resistance.

Activation Of Intracellular Transport: The mechanisms of prion trafficking in relationship to subcellular PrP^{Sc} replication have stimulated great interest in current prion research. Microarray analysis suggests discrete transport mechanisms between RKD-S and RKD-R cells. RKD-R cells upregulate genes that involve caveolae- and clathrin-mediated endocytic transport, whereas RKD-S cells upregulate genes involved in modulating intracellular vesicle docking, fusion and transport (Table 4.10 and Fig. 4.8B). These two scenarios depict the conditions that drastically alter membrane topology and

composition. PrP^C has been shown to utilize both clathrin and/or the caveolin mechanism as vehicles of transport from the surface to the endosomal compartments (Taraboulos, Raeber et al. 1992; Vey, Pilkuhn et al. 1996; Peters, Mironov et al. 2003; Sunyach, Jen et al. 2003; Sarnataro, Caputo et al. 2009). RKD-R cells modulate endocytic pathways that subsequently cause continuous turnover of the plasma membrane. Henceforth, enhanced turnover of the plasma membrane reduces the interaction kinetics between PrP^C and PrP^{Sc} at the cell surface, precluding the occurrence for efficient PrP^{Sc} conversion. This is implied by RKD-R upregulation of caveolin (CAV2, 1.87-FC), flotilins (FLOT1, 2.95-FC), clathrin (CLTC, 1.92-FC), sortilin (SORT1, 1.76-FC), sorting Nexin 17 (AP1B, 1.76-FC), adaptor-related protein complex AP-1, sigma 3 (AP1S3, 2.20-FC) and ras-associated protein 15 (RAB15, 2.02-FC). The aforementioned implications of the plasma membrane as the primary location for PrP^{Sc} conversion makes these differentially expressed genes additional targets for susceptibility assessment (Goold, Rabbanian et al. 2011).

While the plasma membrane is being turned over in RKD-R cells, RKD-S cells are utilizing intracellular vesicle recycling mechanisms to continuously traffic PrP^{Sc} aggregate-fibrils to and from autophagosomal/lysosomal compartments. It is hypothesized that one replicative interphase of PrP^{Sc} is within the transporting vesicles that recycle PrP^C-PrP^{Sc} molecules from the surface (Caughey and Raymond 1991; Goold, Rabbanian et al. 2011). This mechanism could then be linked to the abovementioned autophagy scenario which enable prion replication to proceed. Continuous intracellular transport of PrP^{Sc} molecule to lysosomal degradation compartments induces aggregate-fibril fractionation into smaller and more infectious molecules (Table 4.10 and Fig. 4.8B)

(Silveira, Raymond et al. 2005; Vella, Sharples et al. 2007; Marijanovic, Caputo et al. 2009). The upregulation of RAB (1a, 7, 7a, 7L1, 8b), ADP-ribosylation factors (ARL8B), Ras-like family (RASL12), aminophospholipid transporters (ATP8B1), Exosome components (EXOC5), syntaxins (STX1B) and vesicle transport and docking proteins (VAPA) strongly support the intracellular PrP^{Sc} recycling prediction (Table 4.10 and Fig. 4.8B). These genes specifically associate with intracellular vesicle traffic.

Connecting The Dots: The Collective Mechanisms That Make Cells Prion Susceptible:

Numerous cellular mechanisms/pathways must be activated to enable efficient PrP^{Sc} conversion and prion replication. Starting at the cell surface where the initial PrP^C-PrP^{Sc} contact is made, we hypothesize the conditional presence of protein groups with distinct functions to set off PrP^{Sc} conversion. These cell surface proteins must include PrP-binding receptors with cytoplasmic domains to enable the internalization of PrP^C-PrP^{Sc}. Followed by proteolytic enzymes, which modulate the conversion process, extracellular chaperones for enhanced stability and metal ion binding proteins for dual function that include stabilization and membrane translocation (Fig 4.8A). As the conversion proceeds forward, and becomes internalized, the cell must exponentially increase output of PrP^{Sc} seed. This process is achieved by activating endosome-recycling proteins that induce continuous formation of vesicles. Simultaneously, the cell also activates a very selective protein misfolding response that does not require the recruitment of the proteasome degradation pathways but rather utilizes the already activated lysosomes through macroautophagy-mediated mechanisms. This non-canonical autophagy response transiently arrests cell growth, creating the ideal cytoplasmic conditions to form PrP^{Sc} aggregate-fibrils. Without cell division taking place, the infectious PrP^{Sc}-fibrils grow at

an exponential rate. The cells survive this cytoplasmic stress using two additional mechanisms. First, anti-apoptotic pathways are activated by both cell-surface receptors and intracellular proteins involved in the already activated autophagy pathway. Second, the autophagosome-lysosome fused compartments break apart the large PrP^{Sc} aggregates into smaller less toxic entities. Coincidentally, these smaller less-cytotoxic PrP^{Sc} aggregate molecules are more inclined to reinitiate PrP^{C} - PrP^{Sc} conversion. The break down of the large aggregate fibrils also releases the cell from growth arrest, allowing it to divide. Eventual initiation of cell division releases the infectious PrP^{Sc} molecules into the extracellular space, which subsequently causes neighboring cells to also become infected. Resumed cell division generates additional clones which possess all the proper conversion factors to enable prion replication and survive. These conclusions are inferred entirely from comparing published literature on the topics to the acquired gene expression results. Future validation studies are required to prove or disprove the described hypothesis of cellular mechanisms that dictate prion susceptibility.

Figure 4.8 RKD differentially expressed genes targeted for cell-surface presentation and intracellular transport. **A.** Schematic representation of differentially expressed genes that co-localize to the cell surface of RKD cells. Proteins depicted on the left and labeled in red represent identified genes that were upregulated in PrP^{Sc} sensitive RKD-S cells. Proteins depicted on the right and labeled in black represent identified genes that were up regulated in PrP^{Sc} resistant RKD-R cells. **B.** Schematic depiction of RKD's differentially expressed genes regulating intracellular vesicle transport and recycling. (1) PrP^C-PrP^{Sc} interaction at the cell surface initiates the conversion process. (2) Continuous intracellular transport cycling of PrP^C to and from the surface facilitates intracellular PrP^{Sc} conversion. (3) Endocytic delivery of the PrP^C-PrP^{Sc} complex activates protein-stress response, which consequently induces macroautophagy and chaperone-mediated autophagy, mechanisms that stabilize and enhance prion conversion. (4) Autophagosome transporting large PrP^{Sc} aggregates dock and fuse with lysosomal vacuoles to initiate degradation. Large PrP^{Sc}-aggresomes are fractured to produce smaller, more infectious PrP^{Sc} molecules. (5) The smaller infectious PrP^{Sc} particles are either exocytosed or become intracellular seeding material. Red-labeled genes represent upregulation in RKD-S cells while black-labeled genes represent upregulation in RKD-R cells.

Cell Adhesion/Plasma-Membrane

The diagram illustrates the cell adhesion and signaling pathways at the plasma membrane, comparing RGD-sensitive clones (left) and RGD-resistant clones (right). The extracellular matrix (ECM) is shown at the top, with various adhesion molecules and receptors interacting with it. The cytoplasm is shown at the bottom, with various signaling molecules and pathways.

RGD-Sensitive Clones (Left):

- ECM Interactions:** CMA1, TIMP2, TNC, ALCAM, LRP1, LRP, NEDD9, PrP^{Sc}, ADAM(TS)-1,9, ADAM-8,9, CDH9, and CD36.
- Signaling Pathways:** MMP/MME (16,13,2), CD36, and CDH9. These pathways lead to the activation of RAS, which then activates RAF, MEK, and ERK, resulting in a strong signaling response (indicated by multiple arrows).

RGD-Resistant Clones (Right):

- ECM Interactions:** PrP^{Sc}, PCDH1/(C2), ADAMTS-8,12,17, CD47, LRP3, ITGB(1,4), and PROC.
- Signaling Pathways:** CD47, LRP3, ITGB(1,4), and PROC. These pathways lead to the activation of RAS, which then activates RAF, MEK, and ERK, resulting in a weak or no signaling response (indicated by a single arrow or a crossed-out arrow).

The diagram highlights the differences in the expression and function of these adhesion molecules and signaling pathways between the two clone types.



Table 4.7 Differentially upregulated gene expression in RKD-R cells as compared to the RKD-S cells. Robust multichip average (RMA) and quantile normalization methods were used for signal normalization and false-positive signal noise, respectively. Significance and stringency was set to p-value 0.001 and fold change cutoff of 2.0, respectively. Abbreviations, Fold Change (FC), Not Associated (NA), Endoplasmic Reticulum (ER)

Gene Name	Gene Symbol	FC (+)	Cell Process	Component
Nucleolar protein with MIF4G domain 1	Nom1	2.05	RNA metabolic process	Nucleolus
Sulfatase modifying factor 2	Sumf2	2.01	NA	ER
Orosomucoid 1	Orm1	5.45	Acute-Phase response, regulation of immune system, transport	Extracellular region
Protein-tyrosine sulfotransferase 1	Tpst1	2.38	Metabolic process	Golgi, membrane
BEN domain containing 6	Bend6	2.23	NA	NA
Pro-opiomelanocortin-alpha	Pomc	4.52	Cell-cell signaling, neuropeptide signaling	Cytoplasm, extracellular region, stored secretory granule
Plastin-1	Pls1	3.60	NA	Cytoplasm
Single-stranded DNA binding protein 2	Ssbp2	3.23	DNA dependent transcriptional regulation	Cytoplasm & nucleus
P450 (cytochrome) oxidoreductase	Por	2.03	Internal peptidyl-lysine acetylation, negative regulation of; apoptosis, caspase activity	ER, membrane, microsome, mitochondrion, soluble fraction
Procollagen lysine, 2-oxoglutarate 5-dioxygenase 2	Plod2	2.61	Oxidation-reduction process	ER, Membrane
Cell cycle regulator Mat89Bb homolog	493342 4B01Rik	2.77	Cell cycle	NA
Protocadherin alpha 1	Pcdha1	2.07	NA	Membrane fraction
Centrosomal protein 72	Cep72	2.83	Gamma-tubulin complex	Centrosome, cytoplasm,

			localization, spindle organization	
Bone morphogenetic protein 4	Bmp4	3.28	SMAD protein transduction, activation of MAPKK,	Cytoplasm, extracellular region, membrane bounded vesicles, proteinaceous
Ankyrin3	Ank3	4.79	Establishment of protein organization,	Basolateral plasma membrane, synapse
Thiopurine methyltransferase	Tpmt	2.64	Metabolic process, methylation	Cytoplasm, soluble fraction
Guanine nucleotide binding protein, gamma 10	Gng10	9.96	G-protein coupled receptor signaling	Heterotrimeric G-Protein complex, PM
Adaptor-related protein complex AP-1, sigma 3	Ap1s3	2.20	Endocytosis, intracellular protein transport,	Golgi, coated pits, cytoplasmic vesicle, membrane coat
Protein aurora borealis	672046 3M24R ik	2.01	Cell cycle	NA
Lymphocyte cytosolic protein 1	Lcp1	3.46	Actin filament assembly, intracellular protein transport	Actin cytoskeleton, cell junction, phagocytic cup, PM
Suppressor of cancer cell invasion	Scai	2.25	Negative regulation of; Rho protein signal transduction	Cytoplasm, membrane, nucleus
HEAT repeat containing 5A	Heatr5a	2.12	NA	NA
Tumor necrosis factor receptor superfamily, member 21	Tnfrsf2 1	2.38	Apoptosis, signal transduction	Axon, cytoplasm, membrane
Retinoblastoma binding protein 7	Rbbp7	2.02	DNA replication, negative regulation of cell growth,	ESC/E(Z) complex, NuRD complex, Nucleus
Ubiquitin-conjugating enzyme E2M	Ube2m	2.15	Positive regulation of neuron apoptosis, ubiquitination	NA
Protein C	Proc	5.29	Cellular protein metabolic process, peptidyl-glutamic	Golgi, ER, extracellular, PM

			acid carboxylation, Proteolysis	
Parathyroid hormone 1 receptor	Pthr	2.48	Activation of Phospholipase C activity by GPCR signaling coupled to IP3 second messenger	Basolateral, PM
Discs, large homolog 2	Dlg2	3.16	Neuronal ion channel clustering, receptor clustering	Cytoplasm, membrane fraction, neuronal cell body
Membrane protein, palmitoylated 7	Mpp7	2.24	Positive regulation of protein complex assembly	Adherens junction, membrane, tight junction
Zinc finger protein 397	Zfp397	2.02	Regulation of transcription	Nucleus
Vascular endothelial growth factor C	Vegfc	2.86	Cell differentiation,	Extracellular, membrane
Protocadherin 1	Pcdh1	2.57	Calcium-dependent cell-cell adhesion	Cell-cell junction,

Table 4.8 Prion Disease Database (PDDb) cross-referenced RKD-R down regulated genes associated with published prion literature.

Gene Name	Gene Symb ol	Function
40S ribosomal protein SA/Laminin receptor 1	RPSA/ Lamr1	Cytoplasmic domain, extracellular domain, laminin binding, laminin receptor, translation regulator
Clusterin/Apolipoprotein	CLU	Coiled-coil domain, Ku70 protein binding domain, nuclear localization sequence, protein binding, signal binding, ubiquitin protein ligase binding
Aldolase C	ALDO C	Cytoskeletal protein binding, enzyme, fructose-bisphosphate aldolase, protein binding
Complement Factor B	CFB	Alternative-complement-pathway, C3/C5 convertase, peptidase, serine endopeptidase
Ataxin 7	ATXN 7	Chromatin binding, glutamine repeat domain, nuclear export signal, protein binding
Eukaryotic translation initiation Factor 2-Alpha Kinase 2	EIF2A K2	Phosphotransferase, ATP-binding domain, basic and catalytic domains, coiled-coil domain, dimerization domain, protein binding, protein kinase, protein phosphatase 2A, intrinsic regulator, protein serine/threonine kinase
Copper Chaperone for Superoxide Dismutase	CCS	Copper ion binding, transporter, enzyme, protein binding, superoxide dismutase, copper chaperone, zinc ion binding
Tumor Necrosis Factor Receptor Subfamily Member 1B	TNFR SF1B	Cytoplasmic, cytosolic tail, extracellular and intracellular domains, pre-ligand assembly domain, transmembrane receptor, tyrosine kinase
TATA Box Binding Protein like Protein 1	TBPL 1	Beta-transducin protein family located at the pH resistant lipid raft fraction, plasma membrane
Small Nuclear Ribonucleoprotein Polypeptide N	SNRP N	Protein binding

V-REL Avian Reticuloendotheliosis Viral Oncogene	RELB	Transcription co-repressor, transcription regulator
Protein Kinase C, Zeta Form	PRKC Z	Potassium channel regulator, protein kinase C, protein serine/threonine kinase
Protein Kinase C, Delta	PRKC D	Protein kinase binding, protein kinase C, protein serine/threonine kinase
Polo-like Kinase 3	PLK3	Protein binding, protein kinase , protein serine/threonine kinase
Phospholipase A2, Group II D	PLA2 G2D	Enzyme, phospholipase A2
Nuclear Factor Kappa B Subunit 2	NFKB 2	Transcription co-activator, transcription regulator
Nuclear Factor, Interleukin 3-Regulated	NFIL3	Transcription co-repressor, transcription factor. transcription regulator
Interferon Gamma Receptor 1	IFNG R1	STAT binding domain, transmembrane domain, transmembrane receptor
Immediate-Early Response 3	IER3	Fxfr sequence, nuclear localization sequence, protein binding
Endoglin	ENG	Activin binding, protein binding, cytoplasmic, cytosolic tail, extracellular domain, galactose binding, glycosaminoglycan binding
Copine 8	CPNE 8	Calcium-binding membrane-binding protein

Table 4.9 Prion Disease Database (PDDb) cross-referenced RKD-R up regulated genes associated with published prion literature.

Gene Name	Gene Symbol	Function
TATA Box Binding Protein	TBT	Activation domain, core domain, DNA binding domain, inhibitory DNA-binding domain, p53-binding domain, polyglutamine repeat, transcriptional regulator
Complement Component 4 Binding Protein alpha	C4BPA	Protein Binding
X-Box Binding Protein 1	XPB1	DNA Binding, pXPB(U) degradation motif, transcription factor, transcription regulator
Adenylate Cyclase 3	ADCY3	Calcium/Calmodulin-response adenylate cyclase, protein binding
Myristoylated alanine-rich Protein Kinase C substrate	MARCKS	Protein kinase C substrate
Mitotic Arrest-Deficient 2	MAD2L1	Protein binding, protein homodimerization
Ccto-NOX disulfide-Thiolexchanger 2	ENOX2	Enzyme, protein disulfide oxidoreductase
Amyotrophic Lateral Sclerosis 2 (juvenile) Chromosome region, candidate 2	ALS2CR4	Transmembrane protein 237, protein binding
Apoptosis-inducing Factor Mitochondrion-associated, 3	AIFM3	Caspase activator, enzyme, protein binding, thioredoxin-disulfide reductase
Casein Kinase II Beta	CSNK2B	Acidic loop domain, destruction box, kinase, positive regulatory domain, protein binding, receptor binding, transcription factor binding, zinc-finger domain
Clathrin Heavy Polypeptide	CLTC	Ankyrin binding, clathrin trimerization domain, globular tail domain, heat shock protein binding.

Table 4.10 Extrapolated gene list grouped by functional association. Negative sign in the FC column indicates down regulation of gene expression in the RKD-Resistant clone (Up-regulated in RKD-Sensitive) Abbreviations, Fold Change (FC), Not Associated (NA), Endoplasmic Reticulum (ER), Plasma Membrane (PM)

Protein/Gene Symbol	FC	Function/Class	Localization
Transport/Trafficking-Mechanisms			
ADP-ribosylation factor-like 8B/ARL8B	-2.12	Lysosome motility, Intracellular Protein Transport/GTP-Binding	Late-Endosome, Lysosome Cytoplasm
Ras-associated protein 1A/ RAB1A	-1.60	Endocytic Transport/GTP-binding	Vesicle transport/ER-Golgi
Ras-associated protein 7A/ RAB7A	-1.56	Endocytic Transport/GTP-binding	Late-Endosome, lysosome
Ras-associated protein 7/ RAB7	-1.57	Endocytic Transport/GTP-binding	Late-Endosome, lysosome
Ras-associated protein 8B/ RAB8B	-1.56	Transport/GTPase	Membrane, Cytoplasmic side
Ras-associated protein 7 Like-1/ RAB7L1	-1.52	Transport/GTPase	Membrane, Cytoplasmic side
Caveolin-2/ CAV2	1.87	Caveolae/Scaffold	Lipid Rafts/Vesicle
Flotillin-1/ FLOT1	2.95	Caveolae/Scaffold	Caveolae-Vesicle
Ras-Like Family 12/ RASL12	-1.58	Transport/GTP-binding	Membrane/ Intracellular
Ras-related protein, M-Ras/ MRAS	-1.63	Signaling/GTP-binding	PM
Ras-associated protein 15/ RAB15	2.02	Transport/GTPase	Vesicle-Membrane
Clathrin, Heavy Chain/ CLTC	1.92	Trafficking/ Structural	Cytoplasmic vesicles
Sortilin-1/ SORT1	1.76	Signaling/Sorting Receptor	ER, Endosomes, Lysosomes
Sorting Nexin 17/ AP1B	1.76	Trafficking-Sorting/Receptor-Binding (LRP1)	Endosome, Cytoplasm, Golgi
Adaptor-Related Protein 1, Subunit 3/ AP1S3	2.2	Trafficking-Sorting/Clathrin Binding	Endosomes, Vesicle
ATPase, Aminophospholipid Transporter, Class I, type 8B, member 1/ ATP8B1	-3.56	Aminophospholipid Transport/ATPase	Membrane

Huntingtin/ HTT	1.78	Microtubule-Transport	Cytoplasm
Copine 8/ CPNE8	-1.68	Membrane Trafficking/ Phospholipid Binding	PM
Copine 9/ CPNE9	-1.54	Membrane Trafficking/ Phospholipid Binding	PM
Solute Carrier Family11, Member 2/ DMT1	-2.23	Metal Transport/NEDD4 Proteasome- Degradation	Endosome, Lysosome, Lysosome Membrane
Ceruloplasmin/ CP	-3.37	Ion-Transport/ Metalloprotein	Extracellular Space, PM
Superoxide dismutase copper chaperone/ CCS	-1.69	Ion Transport to SOD	Cytoplasm
ATPase Type 13A3/ ATP13A3	-1.65	Cation Transport	Membrane
Bicaudal D homolog 1/ BICD1	2.29	Transport/Motor Protein Recruitment	ER-Golgi
Exosome Component 8/ EXOSC8	1.87	RNA Degradation	Nucleus, Cytoplasm
Exocyst Component 5/ EXOC5	-1.80	Transport, Exocytic Vesicle Docking	Cytoplasm
Exosome Component 3/ Exosc3	1.58	RNA Degradation	Nucleus, Cytoplasm
TNFAIP3 interacting protein 3/ TNIP3	-3.41	HIV-1 Matrix Protein Interaction (GAG)/Virion Incorporation	Intracellular, Nucleus, Cytoplasm
TNFAIP3 interacting protein/ TNIP	-2.07	HIV-1 Matrix Protein Interaction (GAG)/Virion Incorporation	Intracellular, Nucleus, Cytoplasm
Syntaxin 1B/ STX1B	-1.69	Vesicle Transport/Docking	Membrane
VAMP (vesicle- associated membrane protein)-associated protein A, 33kDa/ VAPA	-1.59	Vesicle Transport/ Membrane Fusion	ER Membrane, Vesicles
Chromatin- modifying protein 2a/ CHMP2A	1.51	ESCRT- III/Degradation of Surface receptor	Late Endosome Membrane

proteins/MVB formation/HIV-1 Gag (p6)			
Cell Adhesion/Plasma-Membrane			
67-kDa Laminin receptor 1/ LAMR1/RPSA	-1.89	Cell Adhesion/Signaling Receptor	PM, Cytoplasm
Tenascin –C/ TNC	-2.8	Extracellular Matrix/Neurite Outgrowth	Extracellular Space
Neural precursor cell expressed, developmentally down-regulated 9/ NEDD9	-2.11	Docking/ Tyr-Kinase Signaling Focal Adhesion	Cytoplasm, Golgi, Projection
Integrin, beta 1/ ITGB1	1.78	Collagen Receptor/Focal Adhesion	Membrane
Integrin, beta 4/ ITGB4	1.7	Laminin Receptor	Membrane
RAS p21 protein activator/ RASA1	1.62	GTPase-Activating	Cytoplasm
A Disintegrin and Metalloproteinase with Thrombospondin Motifs 8/ ADAMTS8	2.37	Metalloproteinase /COMP Degradation	Extracellular Space
Motifs 12/ ADAMTS12	1.83		
Motifs 17/ ADAMTS17	1.77		
Low density lipoprotein receptor-related protein 1/ LRP1	-1.81	Endocytic Receptor/APP Regulation/Signaling	Membrane, Coated-Pits
Matrix Metallopeptidase 16/ MMP16	-1.52	Extracellular matrix Endopeptidase	Extracellular Space, Cell-Surface
Matrix Metallopeptidase 13/ MMP13	-3.17	Collagen Degradation	
Matrix Metallopeptidase 2/ MMP2	-2.5	Extracellular matrix Endopeptidase/ Interacts with TIMP2	
A Disintegrin and	-3.3	Metalloproteinase/Extrav	

Metalloproteinase Domain 8/ ADAM8		asation	
Motifs 1/ ADAMTS1	-2.78	Metalloproteinase/ Proteoglycan cleavage	
A Disintegrin and Metalloproteinase Domain 9/ ADAM9	-1.8	Metalloproteinase/Zinc Protease, cell-cell interaction	
Motifs 9/ ADAMTS9	-2.56	Metalloproteinase/ Cleaves Aggregating Proteoglycans	
Membrane Metallo-Endopeptidase/ MME	-6.45	Thermolysin/ Elastase Activity	Cell Membrane
Tissue inhibitor of metalloproteinases 2/ TIMP2	-2.11	Inactivation of MMP (1,2,3,7,8,9,10,13,14,15,16,19)	Secreted
Protein C/ PROC	5.3	Serine Protease	ER, Golgi, PM, Extracellular
Low density lipoprotein receptor-related protein 3/ LRP3	3.64	Predicted Receptor	Membrane, Coated-Pits
Chymase-1/ CMA1	-2.14	EM Degradation/ Protease	Secreted
Activated leukocyte cell adhesion molecule/ ALCAM	-2.75	Adhesion/Neurite extension	Membrane
Glycoprotein IIIb/ CD36	-2.54	Thrombospondin Receptor/Adhesion/Fatty Acid Transport	Membrane
CD47 glycoprotein/ CD47	-2.02	Adhesion/ Membrane Transport	Membrane
Cadherin-9/ CDH9	-1.70	Ca ²⁺ dependent Adhesion	Membrane
Protocadherin 1/ PCDH1	2.58	Adhesion	Cell Junction, Membrane
Protocadherin alpha subfamily C, 2/ PCDHAC2	2.07	Ca ²⁺ dependent Adhesion	Membrane
Tetraspanin-29/ CD9	1.87	Adhesion/ Transmembrane Glycoprotein	Membrane
Plastin-1/ PLS1	3.60	Actin-Binding	Cytoplasm
Lipoma-preferred partner/ LPP	-1.66	Adhesion/ Scaffolding Protein	Cytoplasm, Membrane, Cell Junction

Ubiquitin-Proteasome Pathway/Protein Degradation/Apoptosis			
Cathepsin L1/ CTSL	-2.1	Protein Degradation /Cysteine Proteinase	Lysosome
Palmitoyl-protein hydrolase 1/ PPT1	-1.62	Lipid-modified Protein Degradation	Lysosome
Programmed cell death 2/ PDCD2	1.59	DNA-Binding Regulatory/ Survival	Nucleus
Apoptosis-inducing factor, mitochondrion-associated, 3/ AIFM3	2.76	Caspase-dependent Apoptosis	Mitochondrion
Neural precursor cell expressed, developmentally down-regulated 4/ NEDD4	-1.86	E3-Ubiquitin Ligase/Receptor Internalization and Degradation	Cytoplasm, Membrane, Endosome, Exosome
Ataxin 7-Like/ ATXN7L1	-1.78	NA	NA
Ataxin 7/ ATXN7	-1.72	Histone Modification	Cytoplasm, Nucleus
Ubiquitin-conjugating enzyme E2H/ UBE2H	-1.59	Ubiquitin Acceptor/ Misfolded Protein Degradation UPS	Cytoplasm, Nucleus,
Ubiquitin protein ligase E3A/ UBE3A	-1.6	E3-Ubiquitin Acceptor/ UPS	Cytoplasm,
Ubiquitin specific peptidase 18/ USP18	-3.84	Deubiquitinating protease	Cytoplasm, Nucleus
Ubiquitin specific peptidase 4/ USP4	-1.52	Deubiquitinating protease/ER Quality Control	Cytoplasm, ER
Ubiquitin-conjugating enzyme E2M/ UBE2M	2.15	Ubiquitin Acceptor- NEDD8/UPS	Cytoplasm
Proteasome (prosome, macropain) 26S subunit, non-ATPase, 5/ PSMD5	1.55	Chaperone/26s Proteasome/UPS	Proteasome Complex
Proteasome (prosome, macropain) 26S	1.51	Chaperone/26s Proteasome/UPS	Proteasome Complex

subunit, ATPase, 6/ PSMC6			
Ubiquitin specific peptidase 5 (isopeptidase T)/ USP5	1.64	Ubiquitin thiolesterase activity/ positive regulation ubiquitin- dependent protein catabolic process UPS	Cytoplasm
BCL2-associated transcription factor 1/ BCLAF1	-2.00	Death-promoting transcriptional repressor	Cytoplasm, Nucleus
CASP8 and FADD- like apoptosis regulator/ CFLAR	-1.69	Apoptosis Regulation/ TNFRSF-triggered apoptosis	Cytoplasm
TP53 apoptosis effector/ PERP	-1.97	TP53-dependent apoptotic pathway	Membrane, Golgi
F-box protein 32/ FBXO32	-3.76	Ubiquitin-protein ligase activity/UPS	Ubiquitin ligase complex
F-box protein 10/ FBXO10	1.55	Ubiquitin-protein ligase activity/UPS	Ubiquitin ligase complex
F-box protein 48/ FBXO48	-2.13	NA	NA
F-box protein 21/ FBXO21	1.68	Ubiquitin-protein ligase activity/UPS	Ubiquitin ligase complex
F-box protein 42/ FBXO42	-1.52	Ubiquitin-protein ligase activity/UPS	Ubiquitin ligase complex
Ring-Finger Protein 139/RFN139	-1.50	E3-ubiquitin ligase/ negative regulator of Growth	ER Membrane
Ring-Finger Protein 4/RFN4	1.56	E3-ubiquitin ligase/Protein degradation	Cytoplasm
Ring-Finger Protein 217/RFN217	-1.95	E3-ubiquitin ligase/Protein degradation	Membrane
Ring-Finger Protein 123/RFN123	-1.88	E3-ubiquitin ligase/ proteasome-mediated degradation of CDKN1B	Cytoplasm
Chaperone/Protein Homeostasis			
Clusterin/ CLU	-1.67	Extracellular Chaperone/Stress- Induced Aggregation	PM, ER, Vesicle, Cytoplasm
HtrA serine peptidase 4/ HTRA4	-1.78	Chaperone Serine Protease	Extracellular

Chaperonin containing T-complex subunit 6/ CCT6A	-2.01	Molecular Chaperone/ Actin/Tubulin	Cytoplasm
BCL2-associated athanogene 3/ BAG3	-1.54	Inhibits HSP70/Anti-Apoptotic	Cytoplasm
Heat shock 22kDa protein 8/ HSPB8	-3.78	Chaperone/ Binds BAG3 (Cofactor)/ Macroautophagy	Cytoplasm
Heat shock protein 90kDa beta (Grp94), member 1/ HSP90B1	-1.6	Chaperone/ ERAD/ Process & Transport	ER
Heat shock protein 90kDa alpha (cytosolic), class B member 1/ HSP90AB1 (HSP83)	-1.53	Protein Maturation Chaperone	Cytoplasm
Chaperonin containing T-complex subunit 2 (beta)/ CCT2	1.77	Molecular Chaperone/ Actin/Tubulin	Cytoplasm
Protein phosphatase 4, regulatory subunit 1/ PPP4R1	1.89	Protein Phosphorylation/ Signaling	NA
J-domain-containing protein disulfide isomerase-like protein/ DNAJC10	1.78	Protein Folding /Co-Chaperone with HSPA5	ER, Secreted
Heat shock 70kDa protein 12A/ HSPA12A	2.09	Chaperone/UPS	Cytoplasm
Heat shock 70kDa protein 2/ HSPA2	3.89	Chaperone	Cell-Surface, Mitochondrion
BCL2-associated athanogene 2/ BAG2	1.68	Inhibits HSP70/Anti-Apoptotic	Cytoplasm
BCL2-associated athanogene 6/ BAG6	1.62	Apoptotic Chaperone/Interacts with HSPA2 and AIFM1	Cytoplasm/BAT3 Complex
FK506-binding	-1.82	Accelerates protein	ER

protein 14/FKBP14		folding/ peptidyl-prolyl cis-trans isomerase	
FK506-binding protein 3,25kDa/FKBP3	1.71	Accelerates protein folding/ peptidyl-prolyl cis-trans isomerase	Membrane
Signaling/Transcription Activation Pathway			
Lipopolysaccharide -induced TNF factor/ LITAF	-1.83	Apoptosis, Signaling	Lysosome, Golgi, Membrane
Frizzled family receptor 6/ FZD6	-1.81	Wnt-Signaling	Membrane
Amyloid beta precursor protein binding protein 1, 59kDa/ NAE1(APPBP1)	1.62	Cell-Surface Signaling/ Apoptosis	Membrane
Interferon regulatory factor 7/ IRF7	-4.83	Transcriptional activator	Cytoplasm
Eukaryotic translation initiation factor 2C, 3/ EIF2C3	-1.58	RNA-mediated gene silencing (RNAi)	Cytoplasm
Eukaryotic translation initiation factor 2- alpha kinase 3/ EIF2AK3	-1.50	Phosphorylates/ unfolded protein response (UPR)	ER
Eukaryotic translation initiation factor 2- alpha kinase 2/ EIF2AK2	-3.92	Autophosphorylated protein serine/threonine kinase, Autophagy Induction	Cytoplasm
Protein kinase C, delta/ PRKCD	-1.81	Protein serine/threonine kinase	Cytoplasm, Membrane
Protein kinase C, zeta/ PRKCZ	-1.95	Protein serine/threonine kinase	Cytoplasm, Membrane
p38/ CRK	-1.60	Adapter-protein	Cytoplasm, PM
Casein kinase II beta subunit/ CSNK2B	1.86	Protein serine/threonine kinase	Cytoplasm, Nucleus
Cyclin-dependent kinase 8/ CDK8	1.72	Protein serine/threonine kinase/ Transcription	Nucleus Cytoplasm
Cyclin-dependent	1.53	Activation	

kinase 16/ CDK16		Transport Exocytosis	
Cyclin-dependent kinase-like 2 (CDC2-related kinase)/ CDKL2	1.50		
Mitogen-activated protein kinase 12/ MAPK12	1.76		
Mitogen-activated protein kinase-activated protein kinase 3/ MAPKAPK3	-1.68		
Mitogen-activated protein kinase 1 interacting protein 1-like/ MAPK1IP1L	-1.54		
Mitogen-activated protein kinase-activated protein kinase 5/ MAP3K5	- 1.81	Phosphorylates and activates MAP2K4 and MAP2K6/Apoptosis Induction	
Protein kinase, cAMP-dependent, regulatory, type II, alpha/ Prkar2a	-2.62	Binds Anchoring Proteins/Regulates protein transport	Cytoplasm, Membrane
A kinase (PRKA) anchor protein 12/ AKAP12	-2.04		
A kinase (PRKA) anchor protein 13/ AKAP13	-1.66	Anchoring protein/ subcellular compartmentation of PKA and PKC	Cytoplasm
A kinase (PRKA) anchor protein 11/ AKAP11	1.67		
Autophagy-Related Genes			
Programmed cell death 6 interacting protein/ PDCD6IP	-1.98	Cell Death Inhibitor/HIV-1 Budding/Apoptosis-Autophagy Adhesion	Cytoplasm
Polo-like kinase 4/ PLK4	2.34	Serine/threonine-protein kinase/ Cell Division	Cytoplasm, Nucleus, Membrane
Kinase 3/ PLK3	-1.61	Regulation	
SNF-related serine/threonine-	-1.55	Serine/threonine-protein kinase / mediator of	Nucleus

protein kinase/ SNRK		neuronal Apoptosis	
Functional spliceosome-associated protein 79/ THOC5	2.07	Nuclear export of HSP70 mRNA	Nucleus, Cytoplasm
Myosin, heavy chain 10/ Myh10	1.65	Motor Protein	Cytoplasm
Ubiquitin-like modifier activating enzyme 2/ UBA2	1.6	E1 ligase / Ubiquitin mediated proteolysis	Nucleus
Vimentin/ Vim	-1.81	Intermediate filament/Lysosomal Transport	Cytoplasm
F-box protein 30/ FBXO30	-2.45	Ubiquitin-protein ligase activity/UPS	Ubiquitin ligase complex
Autophagy-related cysteine Endopeptidase/ ATG4a	-2.78	Cysteine protease required for autophagy	Cytoplasm
Apurinic-apyrimidinic (AP) endonuclease 1/ Apex1	1.56	Cellular response to oxidative stress/ endodeoxyribonuclease	Nucleus, Cytoplasm
Microtubule associated monooxygenase, calponin and LIM domain/ Mical1	-1.63	Cytoskeletal regulator that connects NEDD9 to intermediate filaments	Cytoplasm
TATA element modulatory factor 1/ Tmfl	-1.77	STAT3 degradation/ RAB6-dependent retrograde transport process/Inhibits TBP	ER, Golgi, Cytoplasm, Nucleus
Ataxia telangiectasia and Rad3 related/ ATR	1.56	Serine/threonine protein kinase/ Activated by DNA damage	Nucleus
Transformation/transcription domain-associated protein/ TRRAP	1.59	Adapter protein/ Transcription factor	Nucleus
BCL2-antagonist/killer 1/ BAK1	2.13	Apoptosis Regulator	Mitochondrion
Disks large	1.55	Guanylate kinase	Cytoplasm, PM

homolog 3/ Dlg3		activity/ negative regulation of cell proliferation	
Syntrophin, alpha 1/ SNTA1	1.74	Adapter protein/ Regulation of secretory granules	Cytoplasm, PM, Vesicles, Cell Junction
Syntrophin, beta 2/ SNTB2	1.5		
Ras-associated protein 1A/ RAB1A	-1.6	Transport/GTPase	ER, Golgi
Sequestosome 1/ SQSTM1	-1.75	Adapter protein binds ubiquitin, Regulation of Signaling cascades through ubiquitination	Cytoplasm, Late endosome, Nucleus
Karyopherin alpha 1/ KPNA1	-1.52	Nuclear protein import adapter protein	Cytoplasm, Nucleus

Chapter 5

Discussion & Future Directions

Prion Infectivity Using Different Cell Culture Models: In these studies, we utilized cell culture models to characterize prion strain diversity and initiated the search for endogenous host factors that confer prion susceptibility. Three different cell lines were genetically modulated to ectopically express heterologous PrP^C, which were used for infection studies with species specific PrP^{Sc}. These cell lines included the HEK293A, N2a and RK13 cells. Several heterologous PrP^C's were chosen for ectopic expression in the cells. These expressed proteins included cervid (elk/deer), hamster and mouse. Prion infections used infectious isolates derived from the respective species to keep the PrP^C primary sequence equivalent to the prion isolate.

The cell culture infection experiments recapitulated *in vivo* results demonstrating prion species-barrier and interfering effect of endogenously expressed PrP^C. N2a cells demonstrated resistance towards replicating CWD and hamster-adapted TME prions. No inhibition for replicating mouse-adapted RML scrapie prions was showed notwithstanding the cells over-expressed the ectopic PrP^C transgene. Endogenous expression of PrP^C in N2a cells appeared to interfere with the co-expressed heterologous PrP^C for the cellular host factors that mediate the replicating process, which is reminiscent of the initial *in vivo* studies exhibiting the interfering effect (Telling, Scott et al. 1994; Telling, Scott et al. 1995). We hypothesized that prion replication was inhibited as a result of endogenous interference of mouse PrP^C. Recent studies have demonstrated N2a capacity to replicate heterologous CWD prions. Isolation of N2a cells lacking endogenous PrP^C expression permitted transient CWD prion replication (Pulford, Reim et

al. 2010). Several steps were taken to identify CWD prion susceptible N2a cells. First, these cells were sorted five individual times to identify a population of N2a cells that do not express detectable PrP levels. Second, the sorted cells were genetically modulated to ectopically express cervid PrP. These methods allowed the identification of cells with the capacity to convert and replicate CWD prions. It is not surprising that the abrogation of endogenous PrP resulted in heterologous replication of prions because these cells have been well established to generally be permissive towards prions. This method, closely recapitulates the in vivo PrP interference data (Telling, Scott et al. 1995), except for N2a's inability to sustain CWD prion infectivity (personal communication with Dr. Zabel). Together, this data suggests that N2a cells express and maintain the host conversion factors that are required for prion replication.

The inability to sustain detectable levels of PK resistant CerPrP^{Sc} in N2a cells led us to try RK13 cells next. These cells do not express endogenous PrP^C and have previously been shown to replicate ovine derived prions (Vilette, Andreoletti et al. 2001). Initial experiments demonstrated inefficient CWD prion replication using these cells. To enhance RK13 cells we exploited previously published evidence suggesting retroviral elements enhance scrapie infection (Leblanc, Alais et al. 2006). RK13 cells were genetically modulated to co-express HIV-1 Gag and cervid (elk/deer) PrP^C. This modification permitted the cells to replicate both elk and deer CWD-prions. In addition to replicating CWD-prions, RK13 cells readily replicated mouse-adapted RML-prions, and demonstrated the capacity to replicate SHa HY-prions but not DY-prions. Unlike N2a cells, the interference of endogenous PrP^C were not an issue with RK13 cells, but other similarities could be drawn. Similar to CWD prion replicating N2a cells (Pulford, Reim

et al. 2010), our RK13 cells lost prion infectivity with certain strains upon continuous passage. RKE cells not expressing HIV-1 Gag eventually lost CWD prion infectivity and RK13 cells expressing SHaPrP lost infectivity with HY with irrespective of HIV-1 Gag expression. It would be interesting to test the effects HIV-1 Gag would have on N2a cells that lack endogenous PrP because the neuronal origins of N2a cells enhanced with Gag could lead to new cell line considerably more prion susceptible than any characterized cell line we currently have to work with.

We reasoned that ectopic expression of PrP^C in other cells lacking endogenous expression of PrP would also enable them to replicate prions. HEK293 cells were used in similar infectivity experiment to follow up the proposed hypothesis. Unlike RK13 cells, HEK293 cells did not exhibit the capacity to replicate prions. The lack of detectable PK resistant PrP^{Sc} material in 293 cells provided supplementary evidence to support the hypothesis that PrP^C expression alone is not sufficient to sustain prion infectivity. Moreover, cells derived from *Prnp*^{0/0} mice genetically modulated to ectopically express PrP^C exhibited similar prion susceptibility outcomes (Raeber, Sailer et al. 1999). Similarly, PrP^C expression levels in cells known for their susceptibility do not automatically confer prion susceptibility. Beyond that, cellular susceptibility to prions in general is a rare event, which in some, not most cases requires extensive cellular cloning to identify the single cell with “all the conversion tools” to efficiently replicate prions without inducing apoptosis (Butler, Scott et al. 1988; Race, Caughey et al. 1988; Bosque and Prusiner 2000; Bian, Napier et al. 2010).

Our RK13 characterization studies led us to discover that single cell cloning is crucial to sustaining chronic infectivity. Incidentally, the abovementioned work using

N2a cells exhibited evidence suggesting significant variation in prion susceptible N2a cells (Bosque and Prusiner 2000). This phenotypic variation towards prion susceptibility could be used as a cellular tool to identify host factors responsible for the modulating effects. Conforming these observations to our cell culture system, we identified 78 RK13 (RKM) clones that differentially expressed Mouse PrP^C. Several methods were used to characterize these clones for total PrP^C expression. Mouse-adapted RML-prions infection revealed diverse susceptibility amongst individual clones. Similar expression of PrP^C in conjunction with differential susceptibility led us to formulate the working hypothesis for subsequent experiments, which states that, while expression of PrP^C is required for infectivity, it is not sufficient to render the cell permissive. Therefore, endogenous host factors are necessary to sustained prion replication.

Transcriptional Differences Amongst PrP^{Sc} Susceptible And Resistant Clones: Two experimental approaches were used to identify differences in the molecular basis for susceptibility amongst clonal cells. Both methods relied on transcriptional difference between cell lines to help elucidate the protein and/or pathways that enable prion replication. RDA was used as a pilot approach to analyze two phenotypically distinct clones sensitive or resistant to RML prions. We were able to isolate several unique transcripts. The isolated transcripts encoded hypothetical and/or poorly annotated proteins. Furthermore, subsequent analysis of the two clones revealed phenotypic reversion. The resistant clone exhibited permissiveness to prions, which led us towards a newer and quicker microarray method. The lack of throughput, statistical insignificance and experimental setback led us to abandon this approach.

We utilized high-throughput microarray genome analysis as the second experimental to identify transcriptional differences between clones. Clonal cells that were susceptible and/or resistant to CWD-prion were characterized prior to microarray profiling. As part of our experimental design, we isolated the RNA for transcriptional analysis from uninfected clones. Previously studies have showed that the transcription stability of cells pre- and post- prion infection were not altered (Julius, Hutter et al. 2008). Therefore, transcriptional differences that dictate clonal susceptibility are constitutively active. In the time course of the study, two clones deemed susceptible lost detectable CerPrP^{Sc} implying an incomplete molecular phenotype for susceptibility. This was subsequently confirmed with microarray results.

Microarray transcriptional profiling revealed significant difference between susceptible and resistant clones. Two distinct criteria were set to identify unique transcripts, which include FC differences and statistical t-test p-value stringency cut-off. The derivation of gene lists for prediction based analyses required the use of mathematical confinements to set selection stringency. The most stringent mathematical confinements utilized t-test p-value of ≤ 0.001 and FC of ≥ 2.0 . These values generated a list consisting of 100 differentially regulated genes, listed in tables 4.6 and 4.7. Stringency reduction to the p-value of ≤ 0.05 and FC of ≥ 1.5 generated a gene lists consisting of 1,375 differentially expressed genes. Both lists enabled us to gain insight into the global perspective of the cellular physiology.

The primary difficulty with the microarray analysis was gene annotation. The rabbit genome is poorly annotated, which required manual conversion of each rabbit gene to the mouse/human ortholog. Subsequently, the second challenge of microarray analysis

is acquiring meaningful information from the derived gene lists. The annotated rabbit gene lists were bioinformatically analyzed using three different databases. These databases include the Prion Disease Database (PDDB), Database for Annotation, Visualization and Integrated Discovery (DAVID) and Protein ANalysis THrough Evolutionary Relationships (PANTHER). Using PDDB, we identified 314 genes that matched *in vivo* longitudinal gene expression studies characterizing prion pathogenesis. In addition, a handful of matched genes have experimental evidence that functionally connects them to prion disease. These genes are listed in tables 4.8 and 4.9. Unlike PDDB that is designed to deal with prion disease associations only, DAVID and PANTHER are designed to deal with large-scale transcriptional microarray data sets. Gene pathway association and function analyses by DAVID and PANTHER databases reveal metabolic pathways involved in protein homeostasis and cell division as primary targets for subsequent validation.

The Phenotype Of A PrP^{Sc} Susceptible Cell: The gene expression data indicate that prion sensitivity in RKD cells stem from pathways that regulate protein homeostasis. These pathways include differentially regulated genes that partake in protein folding, degradation, trafficking and cellular compartmentalization sorting. On the other hand, cellular resistance amongst RKD clones is indicated by accelerated cell division. Experimental precedence to both of these observations has been established but it is highly possible that a combination of these attributes concurrently with prion strains dictates the outcome of susceptibility (Ghaemmaghami, Phuan et al. 2007; Nunziante, Ackermann et al. 2011). *In vivo*, prions preferentially propagate in post-mitotic neurons of the CNS. It is intuitive that continuous cell division would eventually cause prions to

dilute out beyond detectability, however cells in culture growing at various rates maintain the ability to replicate prions (Butler, Scott et al. 1988; Race, Caughey et al. 1988; Bosque and Prusiner 2000; Ghaemmaghami, Phuan et al. 2007; Nunziante, Ackermann et al. 2011). Both exogenous and endogenous factors dictate susceptibility. Therefore, cellular capacity to chronically sustain detectable PrP^{Sc} depends on a highly interrelated balancing act between cellular mechanisms that maintain protein synthesis, protein degradation, cell division and compatibility of the infecting prion strain. Our microarray results suggest that CWD prion resistant clones upregulate gene clusters that modulate and promote cell division. We have not experimentally addressed cell division rate differences between the sensitive and resistant clones. Earlier studies have shown that cell division actively dilutes detectable levels of PK resistant PrP^{Sc}, reducing the total amount by half after each division (Race, Fadness et al. 1987). Moreover, systematic analysis comparing cell division to prion replication kinetics revealed direct evidence for steady-state reduction of prion levels in rapidly dividing cells (Ghaemmaghami, Phuan et al. 2007). Interestingly, the steady-state reduction of prions by cell division was not absolute indicating that other cellular mechanisms were undertaking the task to sustaining low-levels of prions.

Our sensitive cells upregulate proteins that control mechanisms responsible for protein. Careful analysis of the gene lists revealed macroautophagy as one of the prevalent pathway activated in susceptible cells. This upregulated autophagy pathway does not rely on the classical stress response proteins. The genes upregulated by RKD-S cells activate a selective non-canonical pathway specific to aggregation-prone proteins. Moreover, this pathway has a secondary function that transiently arrests cell growth.

Aggregated protein response and growth arrest makes this pathway pertinent to the global phenotype of the prion sensitive cell. In addition to autophagy activation, other chaperone proteins were also upregulated by sensitive cells. It is likely that a skewed stress response in susceptible cells is mediating the overall PrP^{Sc} conversion process. To support this hypothesis, recently published findings indicate that proteasomal dysfunction and endoplasmic reticulum stress in prion infected cells leads to enhanced accumulation of PrP^{Sc} (Nunziante, Ackermann et al. 2011). By inducing ER stress and impairing proteasomal regulatory pathways in cells, significant increase of misfolded protein fractions were observed. Furthermore, the accumulated PrP^{Sc} was efficiently trafficked to the plasma membrane using intracellular vesicle transport mechanisms. These studies imply that ER environment together with protein quality control mechanisms tightly modulate PrP maturation and PrP^{Sc} formation (Nunziante, Ackermann et al. 2011). Understanding the cellular mechanisms that render cells susceptible to prion replication could be used to explore mechanisms that govern other protein misfolding proteinopathies.

Prion Propagation Under Cell Free Conditions: Several in vitro assays have been described, which use purified components to catalyze PrP^C to PrP^{Sc} conversion and propagate infectious prions (Kocisko, Priola et al. 1995; Saborio, Permanne et al. 2001; Wong, Xiong et al. 2001; Deleault, Geoghegan et al. 2005; Atarashi, Moore et al. 2007; Deleault, Harris et al. 2007; Abid, Morales et al. 2010; Kim, Cali et al. 2010; Wang, Wang et al. 2010). These assays rely on using PrP^C substrate that has been purified from brain tissue or generated recombinantly in bacteria combined with PrP^{Sc} to seed the converting reaction. The CFCA was first to show that PrP^C could be converted to PrP^{Sc} in

the absence of cellular factors but the reaction required a 50-fold molar excess PrP^{Sc} , which makes it highly inefficient (Kocisko, Come et al. 1994). Mammalian prions have also been generated using recombinant SHaPrP ($\text{rPrP}^{\text{PMCA}}$) in a seeded PMCA reaction using 263K hamster purified PrP27-30 (Kim, Cali et al. 2010). The infectivity of these prions was confirmed by bioassay, which resulted in variable attack rates, and long incubation times, suggesting low prion titer. Although infectious prions can be generated without additional cofactors, the low infectivity titers suggest that the process is inefficient. Therefore suggesting that even in a cell free system, prions require additional cofactors to accelerate the conversion process.

This in vitro prion conversion data compliments our prion cell culture system because it demonstrates de novo generation of infectious prions is rare event requiring cofactors. Therefore, supplementing cofactors into the prion conversion reaction may accelerate or enhance the process. This is supported by findings that show how additional cofactors can be applied to enhance PrP^{Sc} conversion efficiency (Abid, Morales et al. 2010; Kim, Cali et al. 2010; Wang, Wang et al. 2010). PMCA was crucial in identifying cofactor components that accelerate prion conversion. RNA molecules were first to show enhancement of prion conversion by PMCA (Deleault, Lucassen et al. 2003). Subsequent studies using an overnight rapid shaking incubation assay demonstrated that optimal prion amplification could be achieved using polyanions that include RNA and HSPG's (Deleault, Geoghegan et al. 2005). RNA length (>4kb) and not the source was the important determinant of enhancing amplification. Several conclusions were made from this data (Deleault, Geoghegan et al. 2005). First, adoption of a supporting structure in 3D space was the probable mechanisms that regulated polyanions enhancement of

PrP^{Sc} conversion in vitro. Second, the structure or scaffold that was forming by these polyanions in 3D space was of specific length/size. Finally, once the amplified fibrils reached a certain size in the scaffolded structure, disaggregation would occur causing the fibrils to break and generate smaller, more infectious particle to drive the amplification reaction forward (Deleault, Geoghegan et al. 2005;Silveira, Raymond et al. 2005). Upregulation of cell-surface proteins in RK13 susceptible cells coincide with these hypothesis driven predictions. The upregulated receptor, adhesion, enzyme and chaperone proteins discussed in Chapter 4, were predicted to execute scaffolding and stabilization functions in the PrP^C-PrP^{Sc} conversion process. The polyanion-enhancing component data was applied towards successfully generating unseeded de novo infectious prions (rPrP-res) with bacterially expressed rPrP, anion-phospholipids, and RNA using PMCA (Wang, Wang et al. 2010). Like rPrP^{PMCA}, rPrP-res ability to cause prion disease was confirmed by bioassay.

The generation of de novo prions using rPrP with the addition of lipids and RNA molecules suggest that different molecules may help without specificity to enhance prion conversion. Therefore, it is probable that within the confinements of a susceptible cell, several molecules of different composition, work together to allow prion accumulation to occur. Our predicted cofactor data supports this hypothesis. The scenario our susceptible RK13 cells reveal requires the combination of extra- and intracellular components to become activated for prions to accumulate. The intracellular recycling proteins combined with overly activated macroautophagy would provide plenty of anion-phospholipids and cytoplasmic RNA molecules to enhance PrP^{Sc} conversion (Figs. 4.7 and 4.8). Investigation for cellular components that mediate prion replication activity led to several

interesting discoveries, which helps provide experimental evidence to support our data (Abid, Morales et al. 2010). To address species-specificity of cellular prion conversion factors, brain homogenates from various species, including *Prnp*^{0/0} mice, was used in PMCA to show efficient prion amplification (Abid, Morales et al. 2010). This finding indicates that prion conversion factors are not species specific, because extracts from every species used in the experiment efficiently amplified SHa-PrP^{Sc}. The PMCA data is analogous to our system, which uses rabbit cells to replicate CWD, HY and RML prions, again demonstrating the lack of species-specificity. Secondly, extracts derived from various tissue sources (heart, liver, kidney, heart, muscle and brain) were applied to PMCA experiments demonstrating efficient conversion irrespective of tissue source (Abid, Morales et al. 2010). Another similarity can be drawn to our data, we use cells that are of kidney epithelial origin and not neuronal origin.

Lastly, it is the third and fourth PMCA experiment of this report that provides experimental evidence to support our predicted prion susceptibility cofactor data (Abid, Morales et al. 2010). Using cellular fractions for PMCA, it was shown that lipid rafts were the dominant conversion factors that achieved successful amplification. This can be correlated to our prediction because every mechanism described in our hypothesis driven prediction has association with membranes and perhaps lipid rafts. At cell surface, where the initial PrP^C-PrP^{Sc} interaction occurs, the upregulated proteins described in Chapter 4 localize to lipid rafts, which also happen to be one of the criterion for selecting the molecules from the 1,375 gene list. Once internalized, the upregulated intracellular recycling proteins have all been predicted to regulate membrane formed vesicles to dock, fuse and trafficking molecules intracellularly. Concurrently, the primary indication of

macroautophagy activation is the formation of autophagosomes, which require intracellular double-layered membrane formation to enclose the molecules destined for degradation. The described processes that occur in susceptible cells require lipid membranes.

The chemical nature of conversion factors was determined using sequential inactivation of molecule classes (proteins, nucleic acids, HSPG...etc.) in supplemental extracts used for PMCA (Abid, Morales et al. 2010). The results of these experiments revealed that inactivation of single molecule classes did not inhibit prion replication. This implies that the composition of converting cofactors cannot be specified to individual molecules. It is more probable that various molecule classes work together to positively enhance prion conversion. Our gene expression data supports the described PMCA data. The mechanisms that enhance prion replication in susceptible cells are complex, and are likely to use various pathways and proteins. Beyond the predicted process hypothesized to regulate prion susceptibility, other physiological factors should also be considered. These factors should include pH conditions that are inside and outside the cell, temperature fluctuations, and the presence of ROS. Any one of those factors alone or combined could have affect cells capacity to replicate and sustain prions.

Cellular Aneuploidy: This study is not without caveats that must be addressed in future experiments. One such caveat is the genetic composition of transformed cells. Transformed cells tend to be aneuploidy, which have considerable variation in chromosomal number. Approaches to circumvent and validate this drawback would be to increase the n-value of samples analyzed. Moreover, It will be crucial to identify clonal populations that exhibit susceptibility phenotypes to prion strains from different species.

The use of next-generation sequencing technology for transcriptome analysis could help validate the findings and consolidate identified host factors. Consequently, any endogenous protein that is deemed a cofactor in prion replication will have to be functionally validated both in vitro and in vivo to demonstrate its role in the process. Consequently, the aneuploid genetic composition will become irrelevant if the protein is validated.

Future Direction

Secondary Confirmation Of Target Gene Expression: The first approach towards taking this data forward is secondary confirmation of the genes identified in the microarray experiments. Genes listed in table 4.10 are the ideal targets for preliminary validation. Table 4.10 represent carefully selected genes involved in pathways relevant to protein homeostasis. These experiments should include quantitative real-time PCR (qRT-PCR) assay to confirm the differential expression of genes discussed in chapter 4. The measuring expression levels of target genes would have to be achieved in susceptible, resistant and un-transfected parent cell line. Furthermore, the qRT-PCR analysis could be done at several time points of infection. This mode of validation has the potential to be used in both animal tissues and cell culture models. A different approach to validate possible target genes is through western immunoblotting. This method would indicate that the cell is making the target protein. Although, this form of analysis would require a specific antibody for the protein in question, which is not always available. Both approaches provide rapid results to support or negate the microarray results.

Cell-Culture Based Experiments: Following secondary confirmation, cell culture based analyses can be used to assess predicted host factor capacity to modulate prion infectivity. For example, PrP^{Sc}-resistant clones could be genetically modulated to over-express genes associated with PrP^{Sc} susceptibility. These might include the macroautophagy genes such as HSPB8, BAG3 and/or eIF2ak or vesicular transport genes such as the Rab genes. Preceding the infectivity experiments, all transfected genes would have to be assessed for stable expression. These genetically modified PrP^{Sc} resistant cells would then be infected with PrP^{Sc} and assessed for susceptibility using the standard PK resistance western-immuno blotting readout. Inversely, inhibitors of these pathways could be applied to PrP^{Sc} susceptible cells in an attempt to cure cells of infectivity. In addition to inhibitors, gene-silencing approaches using siRNA techniques can also be applied to cure PrP^{Sc} infected cells. Co-immuno precipitation (co-IP) is an approach, which can be used to ascertain physical interactions between target genes and PrP molecules. Co-localization studies using light microscopy can be applied to determine cellular processes that are modulating replication. This combination of assays would be beneficial for identifying cellular sites for PrP^{Sc} replication.

It will be imperative to produce additional cell lines with similar PrP^{Sc} phenotypes from other species. RK13 cellular permissiveness towards replicating prions is a characteristic, which can be applied towards generating sensitive cell line (Vilette, Andreoletti et al. 2001; Bian, Napier et al. 2010). In initial attempts to develop such a cell line, we utilized the Cre-Lox recombination system to selectively interchange species specific PrP^C ORF in a clonally selected RK13 cell. The Cre-Lox site-specific recombination system is originally derived from bacteriophage P1, which utilizes the

Cre-recombinase enzyme to remove stretches of DNA flanked by recognition sequences (loxP) in an enzyme-mediated cleavage and ligation mechanism (Sauer 1987). We engineered a PrP^C expression vector with flanking loxP sites. This construct is referred to as the floxed-PrP^C ORF (Fig. 5.1A). The construct allows selective deletion of PrP^C from cells through the use of Cre-recombinase. The floxed-Mouse-PrP^C was cloned into pIRESpuro expression vector and stably transfected into RK13 cells (floxed-RKM cells). The proper positioning of loxP sites and expression of murine PrP^C was verified using adeno-viral vector carrying the Cre-recombinase transgene at the multiplicity of infection (MOI) of 15. The cells were kept in minimally supplemented media to reduce the growth rate for 8 days. Lysate samples were collected for analysis at designated time points (Fig. 5.1B). This proof-of-principle experiment validates normal expression and processing of loxP-flanked PrP^C (Fig. 5.1B).

Clones of floxed-murine PrP^C cells were derived by limited dilution cloning technique. Clones were infected with mouse-adapted RML and at third passage assessed using the mSCA. Floxed-RKM-11D4 clone was chosen for further studies as the most sensitive PrP^{Sc} clone. Infected (RML) and uninfected cells were treated with the Ad-Cre viral vector (MOI 15) and the kinetics of prion reduction was measured over a 72h time frame (Fig. 5.1C). Western blot results revealed reduction of PrP^{Sc} in the RML infected 11D4 cells as the expression of PrP^C is reduced (Fig. 5.1C). The data implies that PrP^{Sc} persistence in RK13 cells goes beyond PrP^C deletion.

Figure 5.1 Generating a prion permissive susceptible cell line. **A.** Schematic representation of the PrP^C ORF with the addition of Lox-p (floxed) and restriction endonuclease sites for versatile cloning into various expression and/or transgenic vectors. The red (BsiWI, NheI, BglII, FseI) and blue (HindIII, AflII, EcoRI, Sall) boxes represent restriction sites for down stream cloning strategies. The green box represents the addition of the Kozak consensus sequence for initiation of the translation process. **B.** RK13 cells expressing the floxed-mouse PrP^C ORF expression vector (RKM Floxed), pIRESpuromouse PrP^C (RKM7, clonally selected and described in Chapter 3) or pIRESpuromouse vector only control (RKV) were transduced with the Adeno viral vector carrying the Cre-recombinase (Ad-Cre) trans gene at the MOI of 15. Cell lysates were collected at designated time points represented by numerical values on the blot (in hours). PrP^C expression was detected by western blotting using mAb 6H4. Actin expression is used for total protein control Pan-Actin mAb-5. **C.** Time course (72h) assessment of PrP^C and PrP^{Sc} reduction in RKM, RKV, 11D4 (Single cell RKM-floxed clone) and 11D4-RML (Chronically infected with mouse adapted RML scrapie) post Adeno virus transduction (Ad-Cre (Cre-recombinase), MOI of 15). PrP was detected by western blotting using mAb 6H4.

[illegible]

High-Throughput Analysis: Next-generation sequencing technology can be used to profile the transcriptome quantitatively with incredible accuracy. Although, microarray gene expression profiling is very informative, it is not without limitations. Microarray limitations are both technical and biological in type. Transcriptional sequencing drastically bypasses both types of limitations. Transcriptional sequence output designates numerical frequency of each transcript within each clone, which can subsequently be averaged and correlated to other analyzed samples. Transcriptional screening can be complemented with the use of protein array experiment for additional validation purposes.

Other biochemical approaches that can be used to identify and validate the cellular host factors would include the *in vitro* conversion assays discussed in the introduction. Particularly the use of protein misfolding cyclical amplification (PMCA) and the real-time quaking induced conversion assay (RT-QuIC). Using PMCA, subcellular fractions purified from cells could be used to identify infectious cellular compartments. Subsequently, amplified fractions would become subject to proteomic analysis for comparison using tandem mass spectrometry to elucidate composition of these fractions. Moreover, the RT-QuIC assay can be used to measure the kinetics of prion replication from these identified sub-cellular fractions.

In conclusion, high throughput experiments using prion cell culture models will provide greater insight into the mechanism that drive neurodegenerative disease at the cellular level. Ultimately, PrP^{Sc} modulating host factors identified at in cells would have to be applied and validated *in vivo*.

Copyright © Vadim Khaychuk 2012

References

- Abid, K., R. Morales, et al. (2010). "Cellular factors implicated in prion replication." FEBS Lett **584**(11): 2409-2414.
- Abid, K., R. Morales, et al. (2010). "Cellular factors implicated in prion replication." FEBS letters **584**(11): 2409-2414.
- Abramoff, M. D., Magalhaes, P.J., Ram, S.J. (2004). "Image Processing with ImageJ." Biophotonics International **11**(7): 36-42.
- Adjou, K. T., S. Simoneau, et al. (2003). "A novel generation of heparan sulfate mimetics for the treatment of prion diseases." J Gen Virol **84**(Pt 9): 2595-2603.
- Adler, V., B. Zeiler, et al. (2003). "Small, highly structured RNAs participate in the conversion of human recombinant PrP(Sen) to PrP(Res) in vitro." Journal of molecular biology **332**(1): 47-57.
- Agrimi, U., R. Nonno, et al. (2008). "Prion protein amino acid determinants of differential susceptibility and molecular feature of prion strains in mice and voles." PLoS pathogens **4**(7): e1000113.
- Aguib, Y., A. Heiseke, et al. (2009). "Autophagy induction by trehalose counteracts cellular prion infection." Autophagy **5**(3): 361-369.
- Aguzzi, A., F. Baumann, et al. (2008). "The prion's elusive reason for being." Annu Rev Neurosci **31**: 439-477.
- Aguzzi, A. and A. M. Calella (2009). "Prions: protein aggregation and infectious diseases." Physiol Rev **89**(4): 1105-1152.
- Alexeeva, E. I., S. I. Valieva, et al. (2011). "Efficacy and safety of repeat courses of rituximab treatment in patients with severe refractory juvenile idiopathic arthritis." Clinical rheumatology **30**(9): 1163-1172.
- Allen, K. D., R. D. Wegrzyn, et al. (2005). "Hsp70 chaperones as modulators of prion life cycle: novel effects of Ssa and Ssb on the *Saccharomyces cerevisiae* prion [PSI+]." Genetics **169**(3): 1227-1242.
- Almeida, L. M., U. Basu, et al. (2011). "Gene expression in the medulla following oral infection of cattle with bovine spongiform encephalopathy." Journal of toxicology and environmental health. Part A **74**(2-4): 110-126.

- Alper, T., W. A. Cramp, et al. (1967). "Does the agent of scrapie replicate without nucleic acid?" Nature **214**: 764-766.
- Alper, T., W. A. Cramp, et al. (1967). "Does the agent of scrapie replicate without nucleic acid?" Nature **214**(5090): 764-766.
- Alper, T., D. A. Haig, et al. (1966). "The exceptionally small size of the scrapie agent." Biochem. Biophys. Res. Commun. **22**: 278-284.
- Angers, R. C., H. E. Kang, et al. (2010). "Prion strain mutation determined by prion protein conformational compatibility and primary structure." Science **328**(5982): 1154-1158.
- Angers, R. C., T. S. Seward, et al. (2009). "Chronic wasting disease prions in elk antler velvet." Emerging Infectious Diseases **15**(5): 696-703.
- Anglade, P., S. Vyas, et al. (1997). "Apoptosis in dopaminergic neurons of the human substantia nigra during normal aging." Histology and histopathology **12**(3): 603-610.
- Anglade, P., S. Vyas, et al. (1997). "Apoptosis and autophagy in nigral neurons of patients with Parkinson's disease." Histology and histopathology **12**(1): 25-31.
- Archer, F., C. Bachelin, et al. (2004). "Cultured peripheral neuroglial cells are highly permissive to sheep prion infection." J Virol **78**(1): 482-490.
- Arima, K., N. Nishida, et al. (2005). "Biological and biochemical characteristics of prion strains conserved in persistently infected cell cultures." J Virol **79**(11): 7104-7112.
- Arjona, A., L. Simarro, et al. (2004). "Two Creutzfeldt-Jakob disease agents reproduce prion protein-independent identities in cell cultures." Proc Natl Acad Sci U S A **101**(23): 8768-8773.
- Arndt, V., C. Daniel, et al. (2005). "BAG-2 acts as an inhibitor of the chaperone-associated ubiquitin ligase CHIP." Molecular biology of the cell **16**(12): 5891-5900.
- Asante, E. A., J. M. Linehan, et al. (2002). "BSE prions propagate as either variant CJD-like or sporadic CJD-like prion strains in transgenic mice expressing human prion protein." Embo J **21**(23): 6358-6366.
- Atarashi, R., R. A. Moore, et al. (2007). "Ultrasensitive detection of scrapie prion protein using seeded conversion of recombinant prion protein." Nat Methods **4**(8): 645-650.

- Atarashi, R., J. M. Wilham, et al. (2008). "Simplified ultrasensitive prion detection by recombinant PrP conversion with shaking." Nat Methods **5**(3): 211-212.
- Auluck, P. K., M. C. Meulener, et al. (2005). "Mechanisms of Suppression of {alpha}-Synuclein Neurotoxicity by Geldanamycin in Drosophila." J Biol Chem **280**(4): 2873-2878.
- Bahmanyar, S., E. S. Williams, et al. (1985). "Amyloid plaques in spongiform encephalopathy of mule deer." J. Comp. Pathol. **95**: 1-5.
- Baker, C. A. and L. Manuelidis (2003). "Unique inflammatory RNA profiles of microglia in Creutzfeldt-Jakob disease." Proceedings of the National Academy of Sciences of the United States of America **100**(2): 675-679.
- Baker, C. A., D. Martin, et al. (2002). "Microglia from Creutzfeldt-Jakob disease-infected brains are infectious and show specific mRNA activation profiles." J Virol **76**(21): 10905-10913.
- Balducci, C., M. Beeg, et al. (2010). "Synthetic amyloid-beta oligomers impair long-term memory independently of cellular prion protein." Proceedings of the National Academy of Sciences of the United States of America **107**(5): 2295-2300.
- Balla, S., V. Thapar, et al. (2006). "Minimotif Miner: a tool for investigating protein function." Nature methods **3**(3): 175-177.
- Ballerini, C., P. Gourdain, et al. (2006). "Functional implication of cellular prion protein in antigen-driven interactions between T cells and dendritic cells." Journal of immunology **176**(12): 7254-7262.
- Baloui, H., Y. von Boxberg, et al. (2004). "Cellular prion protein/laminin receptor: distribution in adult central nervous system and characterization of an isoform associated with a subtype of cortical neurons." Eur J Neurosci **20**(10): 2605-2616.
- Baron, G. S., A. C. Magalhaes, et al. (2006). "Mouse-adapted scrapie infection of SN56 cells: greater efficiency with microsome-associated versus purified PrP-res." J Virol **80**(5): 2106-2117.
- Baron, T., A. Bencsik, et al. (2007). "Phenotypic similarity of transmissible mink encephalopathy in cattle and L-type bovine spongiform encephalopathy in a mouse model." Emerging Infectious Diseases **13**(12): 1887-1894.
- Basler, K., B. Oesch, et al. (1986). "Scrapie and cellular PrP isoforms are encoded by the same chromosomal gene." Cell **46**(3): 417-428.
- Baumann, F., M. Tolnay, et al. (2007). "Lethal recessive myelin toxicity of prion protein lacking its central domain." Embo J **26**(2): 538-547.

- Baylis, M. and W. Goldmann (2004). "The genetics of scrapie in sheep and goats." Current molecular medicine **4**(4): 385-396.
- Baylis, M., W. Goldmann, et al. (2002). "Scrapie epidemic in a fully PrP-genotyped sheep flock." J Gen Virol **83**(Pt 11): 2907-2914.
- Bazan, J. F., R. J. Fletterick, et al. (1987). "Predicted secondary structure and membrane topology of the scrapie prion protein." Protein Engineering **1**(2): 125-135.
- Ben-Gedalya, T., R. Lyakhovetsky, et al. (2011). "Cyclosporin-A-induced prion protein aggregates are dynamic quality-control cellular compartments." Journal of cell science **124**(Pt 11): 1891-1902.
- Benestad, S. L., J. N. Arsac, et al. (2008). "Atypical/Nor98 scrapie: properties of the agent, genetics, and epidemiology." Veterinary research **39**(4): 19.
- Benestad, S. L., P. Sarradin, et al. (2003). "Cases of scrapie with unusual features in Norway and designation of a new type, Nor98." The Veterinary record **153**(7): 202-208.
- Benndorf, R., X. Sun, et al. (2001). "HSP22, a new member of the small heat shock protein superfamily, interacts with mimic of phosphorylated HSP27 ((3D)HSP27)." J Biol Chem **276**(29): 26753-26761.
- Beranger, F., A. Mange, et al. (2002). "Stimulation of PrP(C) retrograde transport toward the endoplasmic reticulum increases accumulation of PrP(Sc) in prion-infected cells." J Biol Chem **277**(41): 38972-38977.
- Beringue, V., K. T. Adjou, et al. (2000). "Opposite effects of dextran sulfate 500, the polyene antibiotic MS-8209, and Congo red on accumulation of the protease-resistant isoform of PrP in the spleens of mice inoculated intraperitoneally with the scrapie agent." J Virol **74**(12): 5432-5440.
- Bessen, R. A., D. A. Kocisko, et al. (1995). "Non-genetic propagation of strain-specific properties of scrapie prion protein." Nature **375**(6533): 698-700.
- Bessen, R. A. and R. F. Marsh (1992). "Biochemical and physical properties of the prion protein from two strains of the transmissible mink encephalopathy agent." J. Virol. **66**: 2096-2101.
- Bessen, R. A. and R. F. Marsh (1992). "Identification of two biologically distinct strains of transmissible mink encephalopathy in hamsters." J. Gen. Virol. **73**: 329-334.
- Bessen, R. A., H. Shearin, et al. (2010). "Prion shedding from olfactory neurons into nasal secretions." PLoS Pathog **6**(4): e1000837.

- Biacabe, A. G., J. L. Laplanche, et al. (2004). "Distinct molecular phenotypes in bovine prion diseases." EMBO Rep **5**(1): 110-115.
- Biacabe, A. G., E. Morignat, et al. (2008). "Atypical bovine spongiform encephalopathies, France, 2001-2007." Emerging Infectious Diseases **14**(2): 298-300.
- Bian, J., D. Napier, et al. (2010). "Cell-based quantification of chronic wasting disease prions." J Virol **84**(16): 8322-8326.
- Birkett, C. R., R. M. Hennion, et al. (2001). "Scrapie strains maintain biological phenotypes on propagation in a cell line in culture." Embo J **20**(13): 3351-3358.
- Blindauer, C. A. and O. I. Leszczyszyn (2010). "Metallothioneins: unparalleled diversity in structures and functions for metal ion homeostasis and more." Natural product reports **27**(5): 720-741.
- Bolstad, B. M., R. A. Irizarry, et al. (2003). "A comparison of normalization methods for high density oligonucleotide array data based on variance and bias." Bioinformatics **19**(2): 185-193.
- Boncela, J., I. Papiewska, et al. (2001). "Acute phase protein alpha 1-acid glycoprotein interacts with plasminogen activator inhibitor type 1 and stabilizes its inhibitory activity." J Biol Chem **276**(38): 35305-35311.
- Booth, S., C. Bowman, et al. (2004). "Identification of central nervous system genes involved in the host response to the scrapie agent during preclinical and clinical infection." The Journal of general virology **85**(Pt 11): 3459-3471.
- Borchelt, D. R., M. Scott, et al. (1990). "Scrapie and cellular prion proteins differ in their kinetics of synthesis and topology in cultured cells." The Journal of cell biology **110**(3): 743-752.
- Borchelt, D. R., A. Taraboulos, et al. (1992). "Evidence for synthesis of scrapie prion proteins in the endocytic pathway." J. Biol. Chem. **267**: 16188-16199.
- Bosque, P. J. and S. B. Prusiner (2000). "Cultured cell sublines highly susceptible to prion infection." J Virol **74**(9): 4377-4386.
- Bragason, B. T. and A. Palsdottir (2005). "Interaction of PrP with NRAGE, a protein involved in neuronal apoptosis." Molecular and cellular neurosciences **29**(2): 232-244.
- Brazier, M. W., P. Davies, et al. (2008). "Manganese binding to the prion protein." J Biol Chem **283**(19): 12831-12839.

- Bredt, D. S. and S. H. Snyder (1994). "Nitric oxide: a physiologic messenger molecule." Annual review of biochemistry **63**: 175-195.
- Brown, A. R., S. Rebus, et al. (2005). "Gene expression profiling of the preclinical scrapie-infected hippocampus." Biochemical and biophysical research communications **334**(1): 86-95.
- Brown, A. R., J. Webb, et al. (2004). "Identification of up-regulated genes by array analysis in scrapie-infected mouse brains." Neuropathology and applied neurobiology **30**(5): 555-567.
- Brown, D. R. (1998). "Prion protein-overexpressing cells show altered response to a neurotoxic prion protein peptide." J Neurosci Res **54**(3): 331-340.
- Brown, D. R. (1999). "Prion protein expression aids cellular uptake and veratridine-induced release of copper." J Neurosci Res **58**(5): 717-725.
- Brown, D. R. (2000). "Altered toxicity of the prion protein peptide PrP106-126 carrying the Ala(117)-->Val mutation." Biochem J **346 Pt 3**: 785-791.
- Brown, D. R., R. S. Nicholas, et al. (2002). "Lack of prion protein expression results in a neuronal phenotype sensitive to stress." Journal of neuroscience research **67**(2): 211-224.
- Brown, P., L. G. Goldfarb, et al. (1991). "The new biology of spongiform encephalopathy: infectious amyloidoses with a genetic twist." Lancet **337**: 1019-1022.
- Browning, S., C. A. Baker, et al. (2011). "Abrogation of complex glycosylation by Swainsonine results in strain- and cell-specific inhibition of prion replication." J Biol Chem.
- Browning, S. R., G. L. Mason, et al. (2004). "Transmission of prions from mule deer and elk with chronic wasting disease to transgenic mice expressing cervid PrP." J Virol **78**(23): 13345-13350.
- Bruce, M. E. and A. G. Dickinson (1979). Biological stability of different classes of scrapie agent. Slow Transmissible Diseases of the Nervous System, Vol. 2. S. B. Prusiner and W. J. Hadlow. New York, Academic Press: 71-86.
- Bruce, M. E., P. A. McBride, et al. (1989). "Precise targeting of the pathology of the sialoglycoprotein, PrP, and vacuolar degeneration in mouse scrapie." Neuroscience letters **102**(1): 1-6.

- Bruce, M. E., P. A. McBride, et al. (1989). "Precise targeting of the pathology of the sialoglycoprotein, PrP, and vacuolar degeneration in mouse scrapie." Neurosci. Lett. **102**: 1-6.
- Bruce, M. E., R. G. Will, et al. (1997). "Transmissions to mice indicate that 'new variant' CJD is caused by the BSE agent." Nature **389**: 498-501.
- Bruce, M. E., R. G. Will, et al. (1997). "Transmissions to mice indicate that 'new variant' CJD is caused by the BSE agent." Nature **389**(6650): 498-501.
- Büeler, H., A. Aguzzi, et al. (1993). "Mice devoid of PrP are resistant to scrapie." Cell **73**: 1339-1347.
- Büeler, H., M. Fischer, et al. (1992). "Normal development and behaviour of mice lacking the neuronal cell-surface PrP protein." Nature **356**: 577-582.
- Bueler, H., M. Fischer, et al. (1992). "Normal development and behaviour of mice lacking the neuronal cell-surface PrP protein." Nature **356**(6370): 577-582.
- Burger, D. and G. R. Hartsough (1965). "Encephalopathy of mink. II. Experimental natural transmission." J. Infect. Dis. **115**: 393-399.
- Buschmann, A., A. G. Biacabe, et al. (2004). "Atypical scrapie cases in Germany and France are identified by discrepant reaction patterns in BSE rapid tests." Journal of virological methods **117**(1): 27-36.
- Buschmann, A., A. Gretzschel, et al. (2006). "Atypical BSE in Germany--proof of transmissibility and biochemical characterization." Veterinary microbiology **117**(2-4): 103-116.
- Butler, D. A., M. R. Scott, et al. (1988). "Scrapie-infected murine neuroblastoma cells produce protease-resistant prion proteins." J Virol **62**(5): 1558-1564.
- Butler, D. A., M. R. D. Scott, et al. (1988). "Scrapie-infected murine neuroblastoma cells produce protease-resistant prion proteins." J. Virol. **62**: 1558-1564.
- Camasses, A., A. Bogdanova, et al. (2003). "The CCT chaperonin promotes activation of the anaphase-promoting complex through the generation of functional Cdc20." Molecular cell **12**(1): 87-100.
- Campbell, S. M., S. M. Crowe, et al. (2001). "Lipid rafts and HIV-1: from viral entry to assembly of progeny virions." Journal of clinical virology : the official publication of the Pan American Society for Clinical Virology **22**(3): 217-227.
- Capecchi, M. R. (1989). "The new mouse genetics: altering the genome by gene targeting." Trends Genet. **5**: 70-76.

- Capo, C. R., M. Arciello, et al. (2008). "Features of ceruloplasmin in the cerebrospinal fluid of Alzheimer's disease patients." Biomaterials : an international journal on the role of metal ions in biology, biochemistry, and medicine **21**(3): 367-372.
- Carlson, G. A., C. Ebeling, et al. (1994). "Prion isolate specified allotypic interactions between the cellular and scrapie prion proteins in congenic and transgenic mice." Proceedings of the National Academy of Sciences of the United States of America **91**(12): 5690-5694.
- Carra, S., A. Boncoraglio, et al. (2010). "Identification of the Drosophila ortholog of HSPB8: implication of HSPB8 loss of function in protein folding diseases." J Biol Chem **285**(48): 37811-37822.
- Carra, S., J. F. Brunsting, et al. (2009). "HspB8 participates in protein quality control by a non-chaperone-like mechanism that requires eIF2{alpha} phosphorylation." J Biol Chem **284**(9): 5523-5532.
- Carra, S., S. J. Seguin, et al. (2008). "HspB8 chaperone activity toward poly(Q)-containing proteins depends on its association with Bag3, a stimulator of macroautophagy." J Biol Chem **283**(3): 1437-1444.
- Casalone, C., G. Zanusso, et al. (2004). "Identification of a second bovine amyloidotic spongiform encephalopathy: molecular similarities with sporadic Creutzfeldt-Jakob disease." Proc Natl Acad Sci U S A **101**(9): 3065-3070.
- Castellino, F. J. and S. G. McCance (1997). "The kringle domains of human plasminogen." Ciba Foundation symposium **212**: 46-60; discussion 60-45.
- Castilla, J., P. Saa, et al. (2005). "In vitro generation of infectious scrapie prions." Cell **121**(2): 195-206.
- Castilla, J., P. Saa, et al. (2006). "Protein misfolding cyclic amplification for diagnosis and prion propagation studies." Methods Enzymol **412**: 3-21.
- Caughey, B., R. E. Race, et al. (1989). "Prion protein biosynthesis in scrapie-infected and uninfected neuroblastoma cells." J. Virol. **63**: 175-181.
- Caughey, B. and G. J. Raymond (1991). "The scrapie-associated form of PrP is made from a cell surface precursor that is both protease- and phospholipase-sensitive." J. Biol. Chem. **266**: 18217-18223.
- Caughey, B. and G. J. Raymond (1993). "Sulfated polyanion inhibition of scrapie-associated PrP accumulation in cultured cells." J. Virol. **67**: 643-650.

- Caughey, B., G. J. Raymond, et al. (1991). "N-terminal truncation of the scrapie-associated form of PrP by lysosomal protease(s): implications regarding the site of conversion of PrP to the protease-resistant state." J. Virol. **65**: 6597-6603.
- Chakrabarti, O. and R. S. Hegde (2009). "Functional depletion of mahogunin by cytosolically exposed prion protein contributes to neurodegeneration." Cell **137**(6): 1136-1147.
- Cheng, F., J. Lindqvist, et al. (2006). "Copper-dependent co-internalization of the prion protein and glypican-1." J Neurochem **98**(5): 1445-1457.
- Chiarini, L. B., A. R. Freitas, et al. (2002). "Cellular prion protein transduces neuroprotective signals." Embo J **21**(13): 3317-3326.
- Chiesa, R., P. Piccardo, et al. (1998). "Neurological illness in transgenic mice expressing a prion protein with an insertional mutation." Neuron **21**(6): 1339-1351.
- Chowdary, T. K., B. Raman, et al. (2004). "Mammalian Hsp22 is a heat-inducible small heat-shock protein with chaperone-like activity." The Biochemical journal **381**(Pt 2): 379-387.
- Churchill, G. A. (2002). "Fundamentals of experimental design for cDNA microarrays." Nature genetics **32 Suppl**: 490-495.
- Cimarelli, A. and J. L. Darlix (2002). "Assembling the human immunodeficiency virus type 1." Cellular and molecular life sciences : CMLS **59**(7): 1166-1184.
- Cisse, M. A., C. Sunyach, et al. (2005). "The disintegrin ADAM9 indirectly contributes to the physiological processing of cellular prion by modulating ADAM10 activity." J Biol Chem **280**(49): 40624-40631.
- Clarke, M. C. and D. A. Haig (1970). "Evidence for the multiplication of scrapie agent in cell culture." Nature **225**: 100-101.
- Clewley, J. P., C. M. Kelly, et al. (2009). "Prevalence of disease related prion protein in anonymous tonsil specimens in Britain: cross sectional opportunistic survey." BMJ **338**: b1442.
- Cloucard, C., P. Beaudry, et al. (1995). "Different allelic effects of the codons 136 and 171 of the prion protein gene in sheep with natural scrapie." J Gen Virol **76 (Pt 8)**: 2097-2101.
- Clouse, L. H. and P. C. Comp (1986). "The regulation of hemostasis: the protein C system." The New England journal of medicine **314**(20): 1298-1304.

- Codogno, P. and A. J. Meijer (2005). "Autophagy and signaling: their role in cell survival and cell death." Cell death and differentiation **12 Suppl 2**: 1509-1518.
- Cohen, E. and A. Taraboulos (2003). "Scrapie-like prion protein accumulates in aggregates of cyclosporin A-treated cells." Embo J **22**(3): 404-417.
- Coitinho, A. S., R. Roesler, et al. (2003). "Cellular prion protein ablation impairs behavior as a function of age." NeuroReport **14**(10): 1375-1379.
- Collinge, J. (1996). "New diagnostic tests for prion diseases." N Engl J Med **335**(13): 963-965.
- Collinge, J. (1999). "Variant Creutzfeldt-Jakob disease." Lancet **354**(9175): 317-323.
- Collinge, J. (2001). "Prion diseases of humans and animals: their causes and molecular basis." Annu Rev Neurosci **24**: 519-550.
- Collinge, J. and A. R. Clarke (2007). "A general model of prion strains and their pathogenicity." Science **318**(5852): 930-936.
- Collinge, J., M. S. Palmer, et al. (1995). "Unaltered susceptibility to BSE in transgenic mice expressing human prion protein." Nature **378**(6559): 779-783.
- Collinge, J., M. S. Palmer, et al. (1995). "Unaltered susceptibility to BSE in transgenic mice expressing human prion protein." Nature **378**: 779-783.
- Collinge, J., K. C. Sidle, et al. (1996). "Molecular analysis of prion strain variation and the aetiology of 'new variant' CJD." Nature **383**(6602): 685-690.
- Collinge, J., K. C. L. Sidle, et al. (1996). "Molecular analysis of prion strain variation and the aetiology of 'new variant' CJD." Nature **383**: 685-690.
- Collinge, J., M. A. Whittington, et al. (1994). "Prion protein is necessary for normal synaptic function." Nature **370**(6487): 295-297.
- Come, J. H., P. E. Fraser, et al. (1993). "A kinetic model for amyloid formation in the prion diseases: importance of seeding." Proc Natl Acad Sci U S A **90**(13): 5959-5963.
- Cordeiro, Y., F. Machado, et al. (2001). "DNA converts cellular prion protein into the beta-sheet conformation and inhibits prion peptide aggregation." J Biol Chem **276**(52): 49400-49409.
- Cordeiro, Y. and J. L. Silva (2005). "The hypothesis of the catalytic action of nucleic acid on the conversion of prion protein." Protein Pept Lett **12**(3): 251-255.

- Courageot, M. P., N. Daude, et al. (2008). "A cell line infectible by prion strains from different species." J Gen Virol **89**(Pt 1): 341-347.
- Creutzfeldt, H. G. (1920). "Über eine eigenartige herdförmige Erkrankung des Zentralnervensystems." Z. Gesamte Neurol. Psychiatrie **57**: 1-18.
- Crippa, V., S. Carra, et al. (2010). "A role of small heat shock protein B8 (HspB8) in the autophagic removal of misfolded proteins responsible for neurodegenerative diseases." Autophagy **6**(7): 958-960.
- Crippa, V., D. Sau, et al. (2010). "The small heat shock protein B8 (HspB8) promotes autophagic removal of misfolded proteins involved in amyotrophic lateral sclerosis (ALS)." Human molecular genetics **19**(17): 3440-3456.
- Croes, E. A., G. Roks, et al. (2002). "Creutzfeldt-Jakob disease 38 years after diagnostic use of human growth hormone." Journal of neurology, neurosurgery, and psychiatry **72**(6): 792-793.
- Cronier, S., H. Laude, et al. (2004). "Prions can infect primary cultured neurons and astrocytes and promote neuronal cell death." Proceedings of the National Academy of Sciences of the United States of America **101**(33): 12271-12276.
- Cuervo, A. M. and J. F. Dice (1998). "Lysosomes, a meeting point of proteins, chaperones, and proteases." Journal of molecular medicine **76**(1): 6-12.
- Cuillé, J. and P. L. Chelle (1939). "Experimental transmission of trembling to the goat." C.R. Seances Acad. Sci. **208**: 1058-1060.
- Cunningham, A. A., G. A. H. Wells, et al. (1993). "Transmissible spongiform encephalopathy in greater kudu (*Tragelaphus strepsiceros*)." Vet. Rec. **132**: 68.
- Dandoy-Dron, F., F. Guillo, et al. (1998). "Gene expression in scrapie. Cloning of a new scrapie-responsive gene and the identification of increased levels of seven other mRNA transcripts." The Journal of biological chemistry **273**(13): 7691-7697.
- Davies, D. R. (1990). "The structure and function of the aspartic proteinases." Annual review of biophysics and biophysical chemistry **19**: 189-215.
- Davies, J. P., P. D. Cotter, et al. (1997). "Cloning and mapping of human Rab7 and Rab9 cDNA sequences and identification of a Rab9 pseudogene." Genomics **41**(1): 131-134.
- Davis, T. L., J. R. Walker, et al. (2010). "Structural and biochemical characterization of the human cyclophilin family of peptidyl-prolyl isomerases." PLoS biology **8**(7): e1000439.

- Dawson, M., L. J. Hoinville, et al. (1998). "Guidance on the use of PrP genotyping as an aid to the control of clinical scrapie. Scrapie Information Group." The Veterinary record **142**(23): 623-625.
- de Almeida, C. J., L. B. Chiarini, et al. (2005). "The cellular prion protein modulates phagocytosis and inflammatory response." Journal of leukocyte biology **77**(2): 238-246.
- DeArmond, S. J. and S. B. Prusiner (1996). Transgenetics and neuropathology of prion diseases. Prions Prions Prions. S. B. Prusiner. Berlin, Springer-Verlag: 125-146.
- DeArmond, S. J., Y. Qiu, et al. (1996). "Abnormal plasma membrane properties and functions in prion-infected cell lines." Cold Spring Harb Symp Quant Biol **61**: 531-540.
- DeBurman, S. K., G. J. Raymond, et al. (1997). "Chaperone-supervised conversion of prion protein to its protease-resistant form." Proc. Natl. Acad. Sci. USA **94**: 13938-13943.
- Dedmon, M. M., J. Christodoulou, et al. (2005). "Heat shock protein 70 inhibits alpha-synuclein fibril formation via preferential binding to prefibrillar species." J Biol Chem **280**(15): 14733-14740.
- Deleault, N. R., J. C. Geoghegan, et al. (2005). "Protease-resistant prion protein amplification reconstituted with partially purified substrates and synthetic polyanions." The Journal of biological chemistry **280**(29): 26873-26879.
- Deleault, N. R., J. C. Geoghegan, et al. (2005). "Protease-resistant prion protein amplification reconstituted with partially purified substrates and synthetic polyanions." J Biol Chem **280**(29): 26873-26879.
- Deleault, N. R., B. T. Harris, et al. (2007). "Formation of native prions from minimal components in vitro." Proceedings of the National Academy of Sciences of the United States of America **104**(23): 9741-9746.
- Deleault, N. R., R. W. Lucassen, et al. (2003). "RNA molecules stimulate prion protein conversion." Nature **425**(6959): 717-720.
- Della-Bianca, V., F. Rossi, et al. (2001). "Neurotrophin p75 receptor is involved in neuronal damage by prion peptide-(106-126)." J Biol Chem **276**(42): 38929-38933.
- DeMattos, R. B., A. O'Dell M, et al. (2002). "Clusterin promotes amyloid plaque formation and is critical for neuritic toxicity in a mouse model of Alzheimer's disease." Proceedings of the National Academy of Sciences of the United States of America **99**(16): 10843-10848.

- Demirov, D. G. and E. O. Freed (2004). "Retrovirus budding." Virus research **106**(2): 87-102.
- Dephoure, N., C. Zhou, et al. (2008). "A quantitative atlas of mitotic phosphorylation." Proceedings of the National Academy of Sciences of the United States of America **105**(31): 10762-10767.
- Derrington, E., C. Gabus, et al. (2002). "PrPC has nucleic acid chaperoning properties similar to the nucleocapsid protein of HIV-1." Comptes rendus biologies **325**(1): 17-23.
- Di Palma F., H. D., Young S., Gnerre S., Johnson J., Lander E.S., Lindblad-Toh K. (2009). "Genome Sequence of *Oryctolagus cuniculus* (European rabbit)." Genome **52**(1): 1-10.
- Dickey, C. A., A. Kamal, et al. (2007). "The high-affinity HSP90-CHIP complex recognizes and selectively degrades phosphorylated tau client proteins." The Journal of clinical investigation **117**(3): 648-658.
- Diedrich, J. F., H. Minnigan, et al. (1991). "Neuropathological changes in scrapie and Alzheimer's disease are associated with increased expression of apolipoprotein E and cathepsin D in astrocytes." J. Virol. **65**: 4759-4768.
- Dlakic, W. M., E. Grigg, et al. (2007). "Prion infection of muscle cells in vitro." J Virol **81**(9): 4615-4624.
- Doh-ura, K., S. Perryman, et al. (1995). "Identification of differentially expressed genes in scrapie-infected mouse neuroblastoma cells." Microb. Pathog. **18**: 1-9.
- Doms, R. W. and J. P. Moore (2000). "HIV-1 membrane fusion: targets of opportunity." The Journal of cell biology **151**(2): F9-14.
- Dong, C. F., S. Shi, et al. (2008). "The N-terminus of PrP is responsible for interacting with tubulin and fCJD related PrP mutants possess stronger inhibitive effect on microtubule assembly in vitro." Archives of biochemistry and biophysics **470**(1): 83-92.
- Dong, C. F., X. F. Wang, et al. (2008). "Molecular interaction between prion protein and GFAP both in native and recombinant forms in vitro." Med Microbiol Immunol **197**(4): 361-368.
- Donne, D. G., J. H. Viles, et al. (1997). "Structure of the recombinant full-length hamster prion protein PrP(29-231): the N terminus is highly flexible." Proceedings of the National Academy of Sciences of the United States of America **94**(25): 13452-13457.

- Dron, M., M. Moudjou, et al. (2010). "Endogenous proteolytic cleavage of disease-associated prion protein to produce C2 fragments is strongly cell- and tissue-dependent." J Biol Chem **285**(14): 10252-10264.
- Ducharme, P., D. Maltais, et al. (2010). "Ceruloplasmin-induced aggregation of P19 neurons involves a serine protease activity and is accompanied by reelin cleavage." Neuroscience **167**(3): 633-643.
- Ducrot, C., M. Arnold, et al. (2008). "Review on the epidemiology and dynamics of BSE epidemics." Veterinary research **39**(4): 15.
- Duguid, J. R., C. W. Bohmont, et al. (1989). "Changes in brain gene expression shared by scrapie and Alzheimer disease." Proceedings of the National Academy of Sciences of the United States of America **86**(18): 7260-7264.
- Duguid, J. R., R. G. Rohwer, et al. (1988). "Isolation of cDNAs of scrapie-modulated RNAs by subtractive hybridization of a cDNA library." Proceedings of the National Academy of Sciences of the United States of America **85**(15): 5738-5742.
- Duguid, J. R., R. G. Rohwer, et al. (1988). "Isolation of cDNAs of scrapie-modulated RNAs by subtractive hybridization of a cDNA library." Proc. Natl. Acad. Sci. USA **85**: 5738-5742.
- Dulbecco, R. and M. Vogt (1953). "Some problems of animal virology as studied by the plaque technique." Cold Spring Harbor Symposia on Quantitative Biology **18**: 273-279.
- Eckroade, R. J., G. M. ZuRhein, et al. (1973). "Transmissible mink encephalopathy in carnivores: clinical, light and electron microscopic studies in raccons, skunks and ferrets." Journal of wildlife diseases **9**(3): 229-240.
- Ellis, V., M. Daniels, et al. (2002). "Plasminogen activation is stimulated by prion protein and regulated in a copper-dependent manner." Biochemistry **41**(22): 6891-6896.
- Eloit, M., K. Adjou, et al. (2005). "BSE agent signatures in a goat." The Veterinary record **156**(16): 523-524.
- Emanuelsson, O., H. Nielsen, et al. (2000). "Predicting subcellular localization of proteins based on their N-terminal amino acid sequence." Journal of molecular biology **300**(4): 1005-1016.
- Enari, M., E. Flechsig, et al. (2001). "Scrapie prion protein accumulation by scrapie-infected neuroblastoma cells abrogated by exposure to a prion protein antibody." Proc Natl Acad Sci U S A **98**(16): 9295-9299.

- Esser, C., S. Alberti, et al. (2004). "Cooperation of molecular chaperones with the ubiquitin/proteasome system." Biochimica et biophysica acta **1695**(1-3): 171-188.
- Esser, C., M. Scheffner, et al. (2005). "The chaperone-associated ubiquitin ligase CHIP is able to target p53 for proteasomal degradation." J Biol Chem **280**(29): 27443-27448.
- Everest, S. J., L. Thorne, et al. (2006). "Atypical prion protein in sheep brain collected during the British scrapie-surveillance programme." J Gen Virol **87**(Pt 2): 471-477.
- Everest, S. J., L. T. Thorne, et al. (2006). "No abnormal prion protein detected in the milk of cattle infected with the bovine spongiform encephalopathy agent." J Gen Virol **87**(Pt 8): 2433-2441.
- Farre, J. C., R. Manjithaya, et al. (2008). "PpAtg30 tags peroxisomes for turnover by selective autophagy." Developmental cell **14**(3): 365-376.
- Fasano, C., V. Campana, et al. (2006). "Prions: protein only or something more? Overview of potential prion cofactors." J Mol Neurosci **29**(3): 195-214.
- Fernandez-Funez, P., S. Casas-Tinto, et al. (2009). "In vivo generation of neurotoxic prion protein: role for hsp70 in accumulation of misfolded isoforms." PLoS Genet **5**(6): e1000507.
- Fevrier, B., D. Vilette, et al. (2004). "Cells release prions in association with exosomes." Proceedings of the National Academy of Sciences of the United States of America **101**(26): 9683-9688.
- Filali, H., I. Martin-Burriel, et al. (2011). "Gene expression profiling and association with prion-related lesions in the medulla oblongata of symptomatic natural scrapie animals." PLoS One **6**(5): e19909.
- Fischer, B. E. and H. Will (1990). "Effects of intact fibrin and partially plasmin-degraded fibrin on kinetic properties of one-chain tissue-type plasminogen activator." Biochimica et biophysica acta **1041**(1): 48-54.
- Fischer, G., H. Bang, et al. (1984). "[Determination of enzymatic catalysis for the cis-trans-isomerization of peptide binding in proline-containing peptides]." Biomedica biochimica acta **43**(10): 1101-1111.
- Fischer, M., T. Rulicke, et al. (1996). "Prion protein (PrP) with amino-proximal deletions restoring susceptibility of PrP knockout mice to scrapie." Embo J **15**(6): 1255-1264.

- Fischer, M. B., C. Roeckl, et al. (2000). "Binding of disease-associated prion protein to plasminogen." Nature **408**(6811): 479-483.
- Follet, J., C. Lemaire-Vieille, et al. (2002). "PrP expression and replication by Schwann cells: implications in prion spreading." J Virol **76**(5): 2434-2439.
- Fontaine, J. M., X. Sun, et al. (2006). "Abnormal small heat shock protein interactions involving neuropathy-associated HSP22 (HSPB8) mutants." FASEB journal : official publication of the Federation of American Societies for Experimental Biology **20**(12): 2168-2170.
- Forsgren, M., B. Raden, et al. (1987). "Molecular cloning and characterization of a full-length cDNA clone for human plasminogen." Febs Letters **213**(2): 254-260.
- Foster, J. D., M. Wilson, et al. (1996). "Immunolocalisation of the prion protein (PrP) in the brains of sheep with scrapie." Vet. Rec. **139**: 512-515.
- Fournier, T., N. N. Medjoubi, et al. (2000). "Alpha-1-acid glycoprotein." Biochimica et biophysica acta **1482**(1-2): 157-171.
- Gains, M. J., K. A. Roth, et al. (2006). "Prion protein protects against ethanol-induced Bax-mediated cell death in vivo." NeuroReport **17**(9): 903-906.
- Gajdusek, D. C., C. J. Gibbs, Jr., et al. (1966). "Experimental transmission of a kuru-like syndrome to chimpanzees." Nature **209**: 794-796.
- Gamerding, M., P. Hajieva, et al. (2009). "Protein quality control during aging involves recruitment of the macroautophagy pathway by BAG3." The EMBO journal **28**(7): 889-901.
- Gauczynski, S., C. Hundt, et al. (2001). "Interaction of prion proteins with cell surface receptors, molecular chaperones, and other molecules." Advances in protein chemistry **57**: 229-272.
- Gauczynski, S., D. Nikles, et al. (2006). "The 37-kDa/67-kDa laminin receptor acts as a receptor for infectious prions and is inhibited by polysulfated glycanes." The Journal of infectious diseases **194**(5): 702-709.
- Gauczynski, S., J. M. Peyrin, et al. (2001). "The 37-kDa/67-kDa laminin receptor acts as the cell-surface receptor for the cellular prion protein." The EMBO journal **20**(21): 5863-5875.
- Gauczynski, S., J. M. Peyrin, et al. (2001). "The 37-kDa/67-kDa laminin receptor acts as the cell-surface receptor for the cellular prion protein." Embo J **20**(21): 5863-5875.

- Geoghegan, J. C., P. A. Valdes, et al. (2007). "Selective incorporation of polyanionic molecules into hamster prions." J Biol Chem **282**(50): 36341-36353.
- Gerhard, D. S., L. Wagner, et al. (2004). "The status, quality, and expansion of the NIH full-length cDNA project: the Mammalian Gene Collection (MGC)." Genome research **14**(10B): 2121-2127.
- Ghaemmaghami, S., P. W. Phuan, et al. (2007). "Cell division modulates prion accumulation in cultured cells." Proceedings of the National Academy of Sciences of the United States of America **104**(46): 17971-17976.
- Gibbs, C. J., Jr. and C. L. Bolis (1997). "Normal isoform of amyloid protein (PrP) in brains of spawning salmon." Molecular psychiatry **2**(2): 146-147.
- Gilch, S., K. F. Winklhofer, et al. (2001). "Intracellular re-routing of prion protein prevents propagation of PrP(Sc) and delays onset of prion disease." Embo J **20**(15): 3957-3966.
- Giorgi, A., L. Di Francesco, et al. (2009). "Proteomic profiling of PrP27-30-enriched preparations extracted from the brain of hamsters with experimental scrapie." Proteomics **9**(15): 3802-3814.
- Giri, R. K., R. Young, et al. (2006). "Prion infection of mouse neurospheres." Proc Natl Acad Sci U S A **103**(10): 3875-3880.
- Glatzel, M., K. Stoeck, et al. (2005). "Human prion diseases: molecular and clinical aspects." Arch Neurol **62**(4): 545-552.
- Goldberg, A. L. (2003). "Protein degradation and protection against misfolded or damaged proteins." Nature **426**(6968): 895-899.
- Gomes, M. P., Y. Cordeiro, et al. (2008). "The peculiar interaction between mammalian prion protein and RNA." Prion **2**(2): 64-66.
- Gomes, M. P., T. A. Millen, et al. (2008). "Prion protein complexed to N2a cellular RNAs through its N-terminal domain forms aggregates and is toxic to murine neuroblastoma cells." J Biol Chem **283**(28): 19616-19625.
- Goold, R., S. Rabbanian, et al. (2011). "Rapid cell-surface prion protein conversion revealed using a novel cell system." Nature communications **2**: 281.
- Gossert, A. D., S. Bonjour, et al. (2005). "Prion protein NMR structures of elk and of mouse/elk hybrids." Proc Natl Acad Sci U S A **102**(3): 646-650.

- Gossner, A. G., J. D. Foster, et al. (2011). "Gene expression analysis in distinct regions of the central nervous system during the development of SSBP/1 sheep scrapie." Veterinary microbiology **147**(1-2): 42-48.
- Gottlinger, H. G. (2001). "The HIV-1 assembly machine." AIDS **15 Suppl 5**: S13-20.
- Gottlinger, H. G., T. Dorfman, et al. (1991). "Effect of mutations affecting the p6 gag protein on human immunodeficiency virus particle release." Proceedings of the National Academy of Sciences of the United States of America **88**(8): 3195-3199.
- Graham, F. L., J. Smiley, et al. (1977). "Characteristics of a human cell line transformed by DNA from human adenovirus type 5." J Gen Virol **36**(1): 59-74.
- Graham, J. F., S. Agarwal, et al. (2010). "Low density subcellular fractions enhance disease-specific prion protein misfolding." J Biol Chem **285**(13): 9868-9880.
- Graner, E., A. F. Mercadante, et al. (2000). "Cellular prion protein binds laminin and mediates neuritogenesis." Brain Res Mol Brain Res **76**(1): 85-92.
- Green, K. M., S. R. Browning, et al. (2008). "The elk PRNP codon 132 polymorphism controls cervid and scrapie prion propagation." J Gen Virol **89**(Pt 2): 598-608.
- Green, K. M., J. Castilla, et al. (2008). "Accelerated high fidelity prion amplification within and across prion species barriers." PLoS pathogens **4**(8): e1000139.
- Greenwood, A. D., M. Horsch, et al. (2005). "Cell line dependent RNA expression profiles of prion-infected mouse neuronal cells." J Mol Biol **349**(3): 487-500.
- Greenwood, A. D., M. Horsch, et al. (2005). "Cell line dependent RNA expression profiles of prion-infected mouse neuronal cells." Journal of molecular biology **349**(3): 487-500.
- Griffith, J. S. (1967). "Self-replication and scrapie." Nature **215**: 1043-1044.
- Griffiths, D. J., P. J. Venables, et al. (1997). "A novel exogenous retrovirus sequence identified in humans." J Virol **71**(4): 2866-2872.
- Griffiths, D. J., C. Voisset, et al. (2002). "Novel endogenous retrovirus in rabbits previously reported as human retrovirus 5." J Virol **76**(14): 7094-7102.
- Griffiths, H. H., I. J. Whitehouse, et al. (2011). "Prion protein interacts with BACE1 protein and differentially regulates its activity toward wild type and Swedish mutant amyloid precursor protein." J Biol Chem **286**(38): 33489-33500.
- Grimwood, J., L. A. Gordon, et al. (2004). "The DNA sequence and biology of human chromosome 19." Nature **428**(6982): 529-535.

- Guinan, E. and G. W. Jones (2009). "Influence of Hsp70 chaperone machinery on yeast prion propagation." Protein Pept Lett **16**(6): 583-586.
- Guiroy, D. C., R. F. Marsh, et al. (1993). "Immunolocalization of scrapie amyloid in non-congophilic, non-birefringent deposits in golden Syrian hamsters with experimental transmissible mink encephalopathy." Neuroscience letters **155**(1): 112-115.
- Guo, M., T. Huang, et al. (2008). "PrPC interacts with tetraspanin-7 through bovine PrP154-182 containing alpha-helix 1." Biochemical and biophysical research communications **365**(1): 154-157.
- Haas, I. G., M. Frank, et al. (2005). "Presenilin-dependent processing and nuclear function of gamma-protocadherins." J Biol Chem **280**(10): 9313-9319.
- Hager, G., H. Pawelzik, et al. (1998). "A peptide derived from a neurite outgrowth-promoting domain on the gamma 1 chain of laminin modulates the electrical properties of neocortical neurons." Neuroscience **86**(4): 1145-1154.
- Hajj, G. N., M. H. Lopes, et al. (2007). "Cellular prion protein interaction with vitronectin supports axonal growth and is compensated by integrins." J Cell Sci **120**(Pt 11): 1915-1926.
- Hajj, G. N., T. G. Santos, et al. (2009). "Developmental expression of prion protein and its ligands stress-inducible protein 1 and vitronectin." J Comp Neurol **517**(3): 371-384.
- Hambsch, B., V. Grinevich, et al. (2005). "{gamma}-Protocadherins, presenilin-mediated release of C-terminal fragment promotes locus expression." J Biol Chem **280**(16): 15888-15897.
- Han, J., J. Zhang, et al. (2006). "Study on interaction between microtubule associated protein tau and prion protein." Sci China C Life Sci **49**(5): 473-479.
- Haraguchi, T., S. Fisher, et al. (1989). "Asparagine-linked glycosylation of the scrapie and cellular prion proteins." Archives of biochemistry and biophysics **274**(1): 1-13.
- Harris, D. A. (2003). "Trafficking, turnover and membrane topology of PrP." Brit. Med. Bul **66**: 71-85.
- Harris, D. A., M. T. Huber, et al. (1993). "Processing of a cellular prion protein: identification of N- and C-terminal cleavage sites." Biochemistry **32**(4): 1009-1016.

- Harris, D. A., P. Lele, et al. (1993). "Localization of the mRNA for a chicken prion protein by in situ hybridization." Proceedings of the National Academy of Sciences of the United States of America **90**(9): 4309-4313.
- Harris, D. A., A. Lesko, et al. (1993). "The N-terminal extracellular domain of a glycolipid-anchored prion protein is essential for efficient endocytosis." Mol. Biol. Cell **4** [Suppl.]: 436a.
- Hartsough, G. R. and D. Burger (1965). "Encephalopathy of mink. I. Epizootiologic and clinical observations." J. Infect. Dis. **115**: 387-392.
- Hay, B., S. B. Prusiner, et al. (1987). "Evidence for a secretory form of the cellular prion protein." Biochemistry **26**(25): 8110-8115.
- Hegde, R. S., J. A. Mastrianni, et al. (1998). "A transmembrane form of the prion protein in neurodegenerative disease." Science **279**(5352): 827-834.
- Heiseke, A., Y. Aguib, et al. (2010). "Autophagy, prion infection and their mutual interactions." Current issues in molecular biology **12**(2): 87-97.
- Hill, A. F., M. Antoniou, et al. (1999). "Protease-resistant prion protein produced in vitro lacks detectable infectivity." J. Gen. Virol. **80**: 11-14.
- Hill, J. and L. H. Phylip (1997). "Bacterial aspartic proteinases." Febs Letters **409**(3): 357-360.
- Hockenbery, D., G. Nunez, et al. (1990). "Bcl-2 is an inner mitochondrial membrane protein that blocks programmed cell death." Nature **348**(6299): 334-336.
- Holscher, C., U. C. Bach, et al. (2001). "Prion protein contains a second endoplasmic reticulum targeting signal sequence located at its C terminus." J Biol Chem **276**(16): 13388-13394.
- Hooper, N. M. (2005). "Roles of proteolysis and lipid rafts in the processing of the amyloid precursor protein and prion protein." Biochemical Society transactions **33**(Pt 2): 335-338.
- Hooper, N. M. (2011). "Glypican-1 facilitates prion conversion in lipid rafts." J Neurochem **116**(5): 721-725.
- Hope, J., L. J. Reekie, et al. (1988). "Fibrils from brains of cows with new cattle disease contain scrapie-associated protein." Nature **336**(6197): 390-392.
- Hornshaw, M. P., J. R. McDermott, et al. (1995). "Copper binding to the N-terminal tandem repeat regions of mammalian and avian prion protein." Biochem Biophys Res Commun **207**(2): 621-629.

- Horst, M., E. C. Knecht, et al. (1999). "Import into and degradation of cytosolic proteins by isolated yeast vacuoles." Molecular biology of the cell **10**(9): 2879-2889.
- Hoshino, S., K. Inoue, et al. (2003). "Prions prevent brain damage after experimental brain injury: a preliminary report." Acta neurochirurgica. Supplement **86**: 297-299.
- Hsiao, K. K., M. Scott, et al. (1990). "Spontaneous neurodegeneration in transgenic mice with mutant prion protein." Science **250**(4987): 1587-1590.
- Hu, Z., L. Chen, et al. (2007). "Structure, function, property, and role in neurologic diseases and other diseases of the sHsp22." Journal of neuroscience research **85**(10): 2071-2079.
- Hundt, C., J. M. Peyrin, et al. (2001). "Identification of interaction domains of the prion protein with its 37-kDa/67-kDa laminin receptor." The EMBO journal **20**(21): 5876-5886.
- Hunter, N., J. D. Foster, et al. (1996). "Natural scrapie in a closed flock of Cheviot sheep occurs only in specific PrP genotypes." Archives of virology **141**(5): 809-824.
- Hunter, N., W. Goldmann, et al. (2000). "Sheep and goats: natural and experimental TSEs and factors influencing incidence of disease." Arch Virol Suppl(16): 181-188.
- Hutchins, M. U. and D. J. Klionsky (2001). "Vacuolar localization of oligomeric alpha-mannosidase requires the cytoplasm to vacuole targeting and autophagy pathway components in *Saccharomyces cerevisiae*." J Biol Chem **276**(23): 20491-20498.
- Ichimura, Y., T. Kirisako, et al. (2000). "A ubiquitin-like system mediates protein lipidation." Nature **408**(6811): 488-492.
- Iwaki, D., K. Kanno, et al. (2011). "The role of mannose-binding lectin-associated serine protease-3 in activation of the alternative complement pathway." Journal of immunology **187**(7): 3751-3758.
- Iwamaru, Y., T. Takenouchi, et al. (2007). "Microglial cell line established from prion protein-overexpressing mice is susceptible to various murine prion strains." J Virol **81**(3): 1524-1527.
- Jacobs, J. G., J. P. Langeveld, et al. (2007). "Molecular discrimination of atypical bovine spongiform encephalopathy strains from a geographical region spanning a wide area in Europe." Journal of clinical microbiology **45**(6): 1821-1829.

- Jakob, A. (1921). "Über eine der multiplen Sklerose klinisch nahestehende Erkrankung des Zentralnervensystems (spastische Pseudosklerose) mit bemerkenswertem anatomischem Befunde. Mitteilung eines vierten Falles." Med. Klin. **17**: 372-376.
- James, T. L., H. Liu, et al. (1997). "Solution structure of a 142-residue recombinant prion protein corresponding to the infectious fragment of the scrapie isoform." Proceedings of the National Academy of Sciences of the United States of America **94**(19): 10086-10091.
- Jarrett, J. T. and P. T. Lansbury, Jr. (1993). "Seeding "one-dimensional crystallization" of amyloid: a pathogenic mechanism in Alzheimer's disease and scrapie?" Cell **73**: 1055-1058.
- Jeffrey, M. and L. Gonzalez (2007). "Classical sheep transmissible spongiform encephalopathies: pathogenesis, pathological phenotypes and clinical disease." Neuropathology and applied neurobiology **33**(4): 373-394.
- Jin, T., Y. Gu, et al. (2000). "The chaperone protein BiP binds to a mutant prion protein and mediates its degradation by the proteasome." J Biol Chem **275**(49): 38699-38704.
- Job, J. C., F. Maillard, et al. (1992). "Epidemiologic survey of patients treated with growth hormone in France in the period 1959-1990: preliminary results." Hormone research **38 Suppl 1**: 35-43.
- Jolliffe, I. T. (2002). Principal Component Analysis.
- Jones, S. E. and C. Jomary (2002). "Clusterin." The international journal of biochemistry & cell biology **34**(5): 427-431.
- Julius, C., G. Hutter, et al. (2008). "Transcriptional stability of cultured cells upon prion infection." J Mol Biol **375**(5): 1222-1233.
- Jursa, T. and D. R. Smith (2009). "Ceruloplasmin alters the tissue disposition and neurotoxicity of manganese, but not its loading onto transferrin." Toxicological sciences : an official journal of the Society of Toxicology **107**(1): 182-193.
- Kaneko, K., L. Zulianello, et al. (1997). "Evidence for protein X binding to a discontinuous epitope on the cellular prion protein during scrapie prion propagation." Proceedings of the National Academy of Sciences of the United States of America **94**(19): 10069-10074.
- Kanu, N., Y. Imokawa, et al. (2002). "Transfer of scrapie prion infectivity by cell contact in culture." Curr Biol **12**(7): 523-530.

- Kegel, K. B., M. Kim, et al. (2000). "Huntingtin expression stimulates endosomal-lysosomal activity, endosome tubulation, and autophagy." The Journal of neuroscience : the official journal of the Society for Neuroscience **20**(19): 7268-7278.
- Kempster, S., M. E. Collins, et al. (2004). "Clusterin shortens the incubation and alters the histopathology of bovine spongiform encephalopathy in mice." NeuroReport **15**(11): 1735-1738.
- Kenward, N., J. Hope, et al. (1994). "Expression of polyubiquitin and heat-shock protein 70 genes increases in the later stages of disease progression in scrapie-infected mouse brain." J. Neurochem. **62**: 1870-1877.
- Kenward, N., M. Landon, et al. (1996). "Heat shock proteins, molecular chaperones and the prion encephalopathies." Cell Stress Chaperones **1**(1): 18-22.
- Kerr, M. K. and G. A. Churchill (2007). "Statistical design and the analysis of gene expression microarray data." Genetical research **89**(5-6): 509-514.
- Keshet, G. I., O. Bar-Peled, et al. (2000). "The cellular prion protein colocalizes with the dystroglycan complex in the brain." J Neurochem **75**(5): 1889-1897.
- Keshet, G. I., H. Ovadia, et al. (1999). "Scrapie-infected mice and PrP knockout mice share abnormal localization and activity of neuronal nitric oxide synthase." Journal of Neurochemistry **72**(3): 1224-1231.
- Kessels, H. W., L. N. Nguyen, et al. (2010). "The prion protein as a receptor for amyloid-beta." Nature **466**(7308): E3-4; discussion E4-5.
- Khalfan, W. A. and D. J. Klionsky (2002). "Molecular machinery required for autophagy and the cytoplasm to vacuole targeting (Cvt) pathway in *S. cerevisiae*." Current opinion in cell biology **14**(4): 468-475.
- Khaniya, B., L. Almeida, et al. (2009). "Microarray analysis of differentially expressed genes from Peyer's patches of cattle orally challenged with bovine spongiform encephalopathy." Journal of toxicology and environmental health. Part A **72**(17-18): 1008-1013.
- Kim, I., S. Rodriguez-Enriquez, et al. (2007). "Selective degradation of mitochondria by mitophagy." Archives of biochemistry and biophysics **462**(2): 245-253.
- Kim, J. I., I. Cali, et al. (2010). "Mammalian prions generated from bacterially expressed prion protein in the absence of any mammalian cofactors." J Biol Chem **285**(19): 14083-14087.

- Kim, J. I., I. Cali, et al. (2010). "Mammalian prions generated from bacterially expressed prion protein in the absence of any mammalian cofactors." The Journal of biological chemistry **285**(19): 14083-14087.
- Kim, K., S. O. Zakharkin, et al. (2010). "Expectations, validity, and reality in gene expression profiling." Journal of clinical epidemiology **63**(9): 950-959.
- Kim, K. S., S. Y. Choi, et al. (2002). "The ceruloplasmin and hydrogen peroxide system induces alpha-synuclein aggregation in vitro." Biochimie **84**(7): 625-631.
- Kimberlin, R. H. and C. A. Walker (1986). "Suppression of scrapie infection in mice by heteropolyanion 23, dextran sulfate, and some other polyanions." Antimicrobial agents and chemotherapy **30**(3): 409-413.
- King, D. J., J. G. Safar, et al. (2007). "Thioaptamer interactions with prion proteins: sequence-specific and non-specific binding sites." J Mol Biol **369**(4): 1001-1014.
- Kirisako, T., M. Baba, et al. (1999). "Formation process of autophagosome is traced with Apg8/Aut7p in yeast." The Journal of cell biology **147**(2): 435-446.
- Kirisako, T., Y. Ichimura, et al. (2000). "The reversible modification regulates the membrane-binding state of Apg8/Aut7 essential for autophagy and the cytoplasm to vacuole targeting pathway." The Journal of cell biology **151**(2): 263-276.
- Kirkwood, J. K., A. A. Cunningham, et al. (1993). "Spongiform encephalopathy in a herd of greater kudu (*Tragelaphus strepsiceros*): epidemiological observations." Vet. Rec. **133**: 360-364.
- Kitamura, A., H. Kubota, et al. (2006). "Cytosolic chaperonin prevents polyglutamine toxicity with altering the aggregation state." Nature cell biology **8**(10): 1163-1170.
- Klamt, F., F. Dal-Pizzol, et al. (2001). "Imbalance of antioxidant defense in mice lacking cellular prion protein." Free radical biology & medicine **30**(10): 1137-1144.
- Klein, M. A., P. S. Kaeser, et al. (2001). "Complement facilitates early prion pathogenesis." Nat Med **7**(4): 488-492.
- Klionsky, D. J. (2005). "The molecular machinery of autophagy: unanswered questions." Journal of cell science **118**(Pt 1): 7-18.
- Klionsky, D. J., J. M. Cregg, et al. (2003). "A unified nomenclature for yeast autophagy-related genes." Developmental cell **5**(4): 539-545.
- Klionsky, D. J. and Y. Ohsumi (1999). "Vacuolar import of proteins and organelles from the cytoplasm." Annual review of cell and developmental biology **15**: 1-32.

- Klohn, P. C., L. Stoltze, et al. (2003). "A quantitative, highly sensitive cell-based infectivity assay for mouse scrapie prions." Proceedings of the National Academy of Sciences of the United States of America **100**(20): 11666-11671.
- Klomp, L. W., Z. S. Farhangrazi, et al. (1996). "Ceruloplasmin gene expression in the murine central nervous system." The Journal of clinical investigation **98**(1): 207-215.
- Klucken, J., Y. Shin, et al. (2004). "Hsp70 Reduces alpha-Synuclein Aggregation and Toxicity." J Biol Chem **279**(24): 25497-25502.
- Kobzik, L., M. B. Reid, et al. (1994). "Nitric oxide in skeletal muscle." Nature **372**(6506): 546-548.
- Kocisko, D. A., J. H. Come, et al. (1994). "Cell-free formation of protease-resistant prion protein." Nature **370**(6489): 471-474.
- Kocisko, D. A., S. A. Priola, et al. (1995). "Species specificity in the cell-free conversion of prion protein to protease-resistant forms: a model for the scrapie species barrier." Proceedings of the National Academy of Sciences of the United States of America **92**(9): 3923-3927.
- Kocisko, D. A., S. A. Priola, et al. (1995). "Species specificity in the cell-free conversion of prion protein to protease-resistant forms: a model for the scrapie species barrier." Proc. Natl. Acad. Sci. USA **92**: 3923-3927.
- Kolodziejczak, D., B. Da Costa Dias, et al. (2010). "Prion interaction with the 37-kDa/67-kDa laminin receptor on enterocytes as a cellular model for intestinal uptake of prions." Journal of molecular biology **402**(2): 293-300.
- Kolodziejczak, D., B. Da Costa Dias, et al. (2010). "Prion interaction with the 37-kDa/67-kDa laminin receptor on enterocytes as a cellular model for intestinal uptake of prions." J Mol Biol **402**(2): 293-300.
- Komatsu, M., T. Ueno, et al. (2007). "Constitutive autophagy: vital role in clearance of unfavorable proteins in neurons." Cell death and differentiation **14**(5): 887-894.
- Kong, Q., M. Zheng, et al. (2008). "Evaluation of the human transmission risk of an atypical bovine spongiform encephalopathy prion strain." J Virol **82**(7): 3697-3701.
- Konold, T., A. Davis, et al. (2007). "Clinical findings in two cases of atypical scrapie in sheep: a case report." BMC veterinary research **3**: 2.
- Koschinsky, M. L., B. K. Chow, et al. (1987). "Isolation and characterization of a processed gene for human ceruloplasmin." Biochemistry **26**(24): 7760-7767.

- Kretzschmar, H. A., L. E. Stowring, et al. (1986). "Molecular cloning of a human prion protein cDNA." DNA **5**(4): 315-324.
- Kretzschmar, H. A., L. E. Stowring, et al. (1986). "Molecular cloning of a human prion protein cDNA." DNA **5**: 315-324.
- Kubota, H., G. Hynes, et al. (1994). "Identification of six Tcp-1-related genes encoding divergent subunits of the TCP-1-containing chaperonin." Curr. Biol. **4**: 89-99.
- Kubota, H., G. Hynes, et al. (1995). "The chaperonin containing t-complex polypeptide 1 (TCP-1). Multisubunit machinery assisting in protein folding and assembly in the eukaryotic cytosol." European journal of biochemistry / FEBS **230**(1): 3-16.
- Kuczius, T. and M. H. Groschup (1999). "Differences in proteinase K resistance and neuronal deposition of abnormal prion proteins characterize bovine spongiform encephalopathy (BSE) and scrapie strains." Molecular medicine **5**(6): 406-418.
- Kurschner, C. and J. I. Morgan (1995). "The cellular prion protein (PrP) selectively binds to Bcl-2 in the yeast two-hybrid system." Mol. Brain Res. **30**: 165-168.
- Kurschner, C. and J. I. Morgan (1995). "The cellular prion protein (PrP) selectively binds to Bcl-2 in the yeast two-hybrid system." Brain Res Mol Brain Res **30**(1): 165-168.
- Kurt, T. D., M. R. Perrott, et al. (2007). "Efficient in vitro amplification of chronic wasting disease PrPRES." J Virol **81**(17): 9605-9608.
- Kwok, A. S., K. Phadwal, et al. (2011). "HspB8 mutation causing hereditary distal motor neuropathy impairs lysosomal delivery of autophagosomes." Journal of Neurochemistry **119**(6): 1155-1161.
- Ladogana, A., P. Casaccia, et al. (1992). "Sulphate polyanions prolong the incubation period of scrapie-infected hamsters." J. Gen. Virol. **73**: 661-665.
- LaFauci, G., R. I. Carp, et al. (2006). "Passage of chronic wasting disease prion into transgenic mice expressing Rocky Mountain elk (*Cervus elaphus nelsoni*) PrPC." J Gen Virol **87**(Pt 12): 3773-3780.
- Lauren, J., D. A. Gimbel, et al. (2009). "Cellular prion protein mediates impairment of synaptic plasticity by amyloid-beta oligomers." Nature **457**(7233): 1128-1132.
- Lawson, V. A. (2008). "Quantitative bioassay of surface-bound prion infectivity." Methods Mol Biol **459**: 265-273.

- Le Dur, A., V. Beringue, et al. (2005). "A newly identified type of scrapie agent can naturally infect sheep with resistant PrP genotypes." Proceedings of the National Academy of Sciences of the United States of America **102**(44): 16031-16036.
- Leblanc, P., S. Alais, et al. (2006). "Retrovirus infection strongly enhances scrapie infectivity release in cell culture." The EMBO journal **25**(12): 2674-2685.
- Leblanc, P., D. Baas, et al. (2004). "Analysis of the interactions between HIV-1 and the cellular prion protein in a human cell line." Journal of molecular biology **337**(4): 1035-1051.
- Lechauve, C., H. Rezaei, et al. (2009). "Neuroglobin and prion cellular localization: investigation of a potential interaction." J Mol Biol **388**(5): 968-977.
- Lee, K. S., R. Linden, et al. (2003). "Towards cellular receptors for prions." Reviews in medical virology **13**(6): 399-408.
- Li, A. and D. A. Harris (2005). "Mammalian prion protein suppresses Bax-induced cell death in yeast." J Biol Chem **280**(17): 17430-17434.
- Li, X. L., C. F. Dong, et al. (2009). "Manganese-induced changes of the biochemical characteristics of the recombinant wild-type and mutant PrPs." Medical microbiology and immunology **198**(4): 239-245.
- Lian, H. Y., H. Zhang, et al. (2007). "Hsp40 interacts directly with the native state of the yeast prion protein Ure2 and inhibits formation of amyloid-like fibrils." J Biol Chem **282**(16): 11931-11940.
- Liao, Y. C., R. V. Lebo, et al. (1986). "Human prion protein cDNA: molecular cloning, chromosomal mapping, and biological implications." Science **233**(4761): 364-367.
- Liesi, P., A. Narvanen, et al. (1989). "Identification of a neurite outgrowth-promoting domain of laminin using synthetic peptides." Febs Letters **244**(1): 141-148.
- Lima, L. M., Y. Cordeiro, et al. (2006). "Structural insights into the interaction between prion protein and nucleic acid." Biochemistry **45**(30): 9180-9187.
- Lin, D. T., J. Jodoin, et al. (2008). "Cytosolic prion protein is the predominant anti-Bax prion protein form: exclusion of transmembrane and secreted prion protein forms in the anti-Bax function." Biochimica et biophysica acta **1783**(10): 2001-2012.
- Lin, K., V. A. Simossis, et al. (2005). "A simple and fast secondary structure prediction method using hidden neural networks." Bioinformatics **21**(2): 152-159.

- Lindquist, S., M. M. Patino, et al. (1995). "The role of Hsp104 in stress tolerance and [PSI⁺] propagation in *Saccharomyces cerevisiae*." Cold Spring Harb. Symp. Quant. Biol. **60**: 451-460.
- Lisitsyn Iu, P. (1992). "[From public health to social medicine]." Gigiena i sanitariia(4): 35-39.
- Lisitsyn, N. and M. Wigler (1993). "Cloning the differences between two complex genomes." Science **259**(5097): 946-951.
- Lisitsyn, N. A., F. S. Leach, et al. (1994). "Detection of genetic loss in tumors by representational difference analysis." Cold Spring Harbor Symposia on Quantitative Biology **59**: 585-587.
- Lisitsyn, N. A., M. V. Rosenberg, et al. (1993). "A method for isolation of sequences missing in one of two related genomes." Molekuliarnaia genetika, mikrobiologiia i virusologiia(3): 26-29.
- Lisitsyn, V. I. (2010). "[The analysis of mortality according the personalized data base of deceased population]." Problemy sotsial'noi gigieny, zdravookhraneniia i istorii meditsiny / NII sotsial'noi gigieny, ekonomiki i upravleniia zdravookhraneniem im. N.A. Semashko RAMN ; AO "Assotsiatsiia 'Meditsinskaia literatura'.(6): 11-14.
- Liu, J., J. P. Zhang, et al. (2009). "Rab11a and HSP90 regulate recycling of extracellular alpha-synuclein." The Journal of neuroscience : the official journal of the Society for Neuroscience **29**(5): 1480-1485.
- Liu, J., Zhang,J., Zhou,R. and Jin,C. (2000). "Molecular cloning and preliminary study on biological function of a novel gene overexpressed in human hepatocellular carcinoma." Unpublished.
- Liu, L., D. Jiang, et al. (2011). "Copper redox cycling in the prion protein depends critically on binding mode." Journal of the American Chemical Society **133**(31): 12229-12237.
- Lloyd, S. E., E. G. Maytham, et al. (2010). "A Copine family member, Cpne8, is a candidate quantitative trait gene for prion disease incubation time in mouse." Neurogenetics **11**(2): 185-191.
- Loeffler, D. A., P. A. LeWitt, et al. (1996). "Increased regional brain concentrations of ceruloplasmin in neurodegenerative disorders." Brain research **738**(2): 265-274.
- Loovers, H. M., E. Guinan, et al. (2007). "Importance of the Hsp70 ATPase domain in yeast prion propagation." Genetics **175**(2): 621-630.

- Lopez, C. D., C. S. Yost, et al. (1990). "Unusual topogenic sequence directs prion protein biogenesis." Science **248**: 226-229.
- Lopez, C. D., C. S. Yost, et al. (1990). "Unusual topogenic sequence directs prion protein biogenesis." Science **248**(4952): 226-229.
- Luders, J., J. Demand, et al. (2000). "The ubiquitin-related BAG-1 provides a link between the molecular chaperones Hsc70/Hsp70 and the proteasome." J Biol Chem **275**(7): 4613-4617.
- Luhken, G., A. Buschmann, et al. (2007). "Epidemiological and genetical differences between classical and atypical scrapie cases." Veterinary research **38**(1): 65-80.
- Luhr, K. M., E. K. Nordstrom, et al. (2004). "Cathepsin B and L are involved in degradation of prions in GT1-1 neuronal cells." NeuroReport **15**(10): 1663-1667.
- Luo, K., S. Li, et al. (2010). "Real-time visualization of prion transport in single live cells using quantum dots." Biochem Biophys Res Commun **394**(3): 493-497.
- Lysek, D. A. and K. Wuthrich (2004). "Prion protein interaction with the C-terminal SH3 domain of Grb2 studied using NMR and optical spectroscopy." Biochemistry **43**(32): 10393-10399.
- M'Fadyean, J. (1918). "Scrapie." J. Comp. Pathol. **31**: 102-131.
- M'Gowan, J. P. (1914). Investigation into the Disease of Sheep Called "Scrapie".
Edinburgh, William Blackwood and Sons.
- Ma, J. and S. Lindquist (2001). "Wild-type PrP and a mutant associated with prion disease are subject to retrograde transport and proteasome degradation." Proc Natl Acad Sci U S A **98**(26): 14955-14960.
- Ma, J. and S. Lindquist (2001). "Wild-type PrP and a mutant associated with prion disease are subject to retrograde transport and proteasome degradation." Proceedings of the National Academy of Sciences of the United States of America **98**(26): 14955-14960.
- Ma, J., R. Wollmann, et al. (2002). "Neurotoxicity and neurodegeneration when PrP accumulates in the cytosol." Science **298**(5599): 1781-1785.
- Maas, E., M. Geissen, et al. (2007). "Scrapie infection of prion protein-deficient cell line upon ectopic expression of mutant prion proteins." J Biol Chem **282**(26): 18702-18710.

- Mabbott, N. A., M. E. Bruce, et al. (2001). "Temporary depletion of complement component C3 or genetic deficiency of C1q significantly delays onset of scrapie." Nature medicine **7**(4): 485-487.
- Mahal, S. P., C. A. Baker, et al. (2007). "Prion strain discrimination in cell culture: the cell panel assay." Proc Natl Acad Sci U S A **104**(52): 20908-20913.
- Mahal, S. P., S. Browning, et al. (2010). "Transfer of a prion strain to different hosts leads to emergence of strain variants." Proc Natl Acad Sci U S A **107**(52): 22653-22658.
- Mahal, S. P., C. A. Demczyk, et al. (2008). "Assaying prions in cell culture: the standard scrapie cell assay (SSCA) and the scrapie cell assay in end point format (SCEPA)." Methods in molecular biology **459**: 49-68.
- Maissen, M., C. Roeckl, et al. (2001). "Plasminogen binds to disease-associated prion protein of multiple species." Lancet **357**(9273): 2026-2028.
- Malaga-Trillo, E., G. P. Solis, et al. (2009). "Regulation of embryonic cell adhesion by the prion protein." PLoS biology **7**(3): e55.
- Malaga-Trillo, E., G. P. Solis, et al. (2009). "Regulation of embryonic cell adhesion by the prion protein." PLoS Biol **7**(3): e55.
- Mallucci, G., A. Dickinson, et al. (2003). "Depleting neuronal PrP in prion infection prevents disease and reverses spongiosis." Science **302**(5646): 871-874.
- Mallucci, G. R., S. Ratte, et al. (2002). "Post-natal knockout of prion protein alters hippocampal CA1 properties, but does not result in neurodegeneration." The EMBO journal **21**(3): 202-210.
- Mallucci, G. R., S. Ratte, et al. (2002). "Post-natal knockout of prion protein alters hippocampal CA1 properties, but does not result in neurodegeneration." Embo J **21**(3): 202-210.
- Mallucci, G. R., M. D. White, et al. (2007). "Targeting cellular prion protein reverses early cognitive deficits and neurophysiological dysfunction in prion-infected mice." Neuron **53**(3): 325-335.
- Maltais, D., D. Desroches, et al. (2003). "The blue copper ceruloplasmin induces aggregation of newly differentiated neurons: a potential modulator of nervous system organization." Neuroscience **121**(1): 73-82.
- Mammen, E. F., W. R. Thomas, et al. (1960). "Activation of purified prothrombin to autoprothrombin I or autoprothrombin II (platelet cofactor II or autoprothrombin II-A)." Thrombosis et diathesis haemorrhagica **5**: 218-249.

- Mange, A., F. Beranger, et al. (2004). "Alpha- and beta- cleavages of the amino-terminus of the cellular prion protein." Biology of the cell / under the auspices of the European Cell Biology Organization **96**(2): 125-132.
- Manson, J. C., J. Hope, et al. (1995). "PrP gene dosage and long term potentiation." Neurodegeneration : a journal for neurodegenerative disorders, neuroprotection, and neuroregeneration **4**(1): 113-114.
- Marijanovic, Z., A. Caputo, et al. (2009). "Identification of an intracellular site of prion conversion." PLoS Pathog **5**(5): e1000426.
- Marino, G., J. A. Uria, et al. (2003). "Human autophagins, a family of cysteine proteinases potentially implicated in cell degradation by autophagy." J Biol Chem **278**(6): 3671-3678.
- Markovits, P., V. Mutel, et al. (1985). "Effects of in vitro infection of mouse glial and neuroblastoma cells with the scrapie agent." Ann. Recherches Vet. **16**(1): 111-119.
- Marques, A. F., Y. Cordeiro, et al. (2009). "Enhanced prion protein stability coupled to DNA recognition and milieu acidification." Biophys Chem **141**(2-3): 135-139.
- Marsh, R. F., R. A. Bessen, et al. (1991). "Epidemiological and experimental studies on a new incident of transmissible mink encephalopathy." J. Gen. Virol. **72**: 589-594.
- Martin, D. P., V. Anantharam, et al. (2011). "Infectious prion protein alters manganese transport and neurotoxicity in a cell culture model of prion disease." Neurotoxicology **32**(5): 554-562.
- Martínez-Lage, J. F., M. Poza, et al. (1994). "Accidental transmission of Creutzfeldt-Jakob disease by dural cadaveric grafts." J. Neurol. Neurosurg. Psychiatry **57**: 1091-1094.
- Martins, V. R., E. Graner, et al. (1997). "Complementary hydrophathy identifies a cellular prion protein receptor." Nat. Med. **3**: 1376-1382.
- Massey, A., R. Kiffin, et al. (2004). "Pathophysiology of chaperone-mediated autophagy." The international journal of biochemistry & cell biology **36**(12): 2420-2434.
- Massey, A. C., C. Zhang, et al. (2006). "Chaperone-mediated autophagy in aging and disease." Current topics in developmental biology **73**: 205-235.
- Mastrianni, J. A., S. Capellari, et al. (2001). "Inherited prion disease caused by the V210I mutation: transmission to transgenic mice." Neurology **57**(12): 2198-2205.

- Materia, S., M. A. Cater, et al. (2011). "Clusterin (apolipoprotein J), a molecular chaperone that facilitates degradation of the copper-ATPases ATP7A and ATP7B." J Biol Chem **286**(12): 10073-10083.
- Matsushita, M., S. Thiel, et al. (2000). "Proteolytic activities of two types of mannose-binding lectin-associated serine protease." Journal of immunology **165**(5): 2637-2642.
- Matthews, L., P. G. Coen, et al. (2001). "Population dynamics of a scrapie outbreak." Archives of virology **146**(6): 1173-1186.
- Mays, C. E. and C. Ryou (2010). "Plasminogen stimulates propagation of protease-resistant prion protein in vitro." FASEB J **24**(12): 5102-5112.
- Mays, C. E., J. Yeom, et al. (2011). "In vitro amplification of misfolded prion protein using lysate of cultured cells." PLoS One **6**(3): e18047.
- Mbazima, V., B. Da Costa Dias, et al. (2010). "Interactions between PrP(c) and other ligands with the 37-kDa/67-kDa laminin receptor." Frontiers in bioscience : a journal and virtual library **15**: 1150-1163.
- McLean, P. J., J. Klucken, et al. (2004). "Geldanamycin induces Hsp70 and prevents alpha-synuclein aggregation and toxicity in vitro." Biochemical and biophysical research communications **321**(3): 665-669.
- McNeill, A. and P. F. Chinnery (2011). "Neurodegeneration with brain iron accumulation." Handbook of clinical neurology / edited by P.J. Vinken and G.W. Bruyn **100**: 161-172.
- Mead, S. (2006). "Prion disease genetics." Eur J Hum Genet **14**(3): 273-281.
- Mead, S., M. Poulter, et al. (2009). "Genetic risk factors for variant Creutzfeldt-Jakob disease: a genome-wide association study." Lancet neurology **8**(1): 57-66.
- Meade-White, K., B. Race, et al. (2007). "Resistance to chronic wasting disease in transgenic mice expressing a naturally occurring allelic variant of deer prion protein." J Virol **81**(9): 4533-4539.
- Medina, S., A. Hatherall, et al. (2009). "Quantitative reverse-transcription polymerase chain reaction analysis of Alzheimer's-associated genes in mouse scrapie." Journal of toxicology and environmental health. Part A **72**(17-18): 1075-1082.
- Meggio, F., A. Negro, et al. (2000). "Bovine prion protein as a modulator of protein kinase CK2." Biochem J **352 Pt 1**: 191-196.

- Mei, G. Y., Y. Li, et al. (2009). "[Molecular interaction between PrP protein and the signal protein 14-3-3 beta]." Bing du xue bao = Chinese journal of virology / [bian ji, Bing du xue bao bian ji wei yuan hui] **25**(3): 208-212.
- Mi, T., J. C. Merlin, et al. (2012). "Minimotif Miner 3.0: database expansion and significantly improved reduction of false-positive predictions from consensus sequences." Nucleic acids research **40**(Database issue): D252-260.
- Milhabet, O., D. Casanova, et al. (2006). "Neural stem cell model for prion propagation." Stem Cells **24**(10): 2284-2291.
- Milhabet, O., H. E. McMahon, et al. (2000). "Prion infection impairs the cellular response to oxidative stress." Proc Natl Acad Sci U S A **97**(25): 13937-13942.
- Mishra, R. S., S. Basu, et al. (2004). "Protease-resistant human prion protein and ferritin are cotransported across Caco-2 epithelial cells: implications for species barrier in prion uptake from the intestine." The Journal of neuroscience : the official journal of the Society for Neuroscience **24**(50): 11280-11290.
- Mitrova, E. and G. Belay (1999). "Creutzfeldt-Jakob disease risk in Slovak recipients of human pituitary growth hormone." Bratislavske lekarske listy **100**(4): 187-191.
- Moreau, K., S. Luo, et al. (2010). "Cytoprotective roles for autophagy." Current opinion in cell biology **22**(2): 206-211.
- Mosnier, L. O. and J. H. Griffin (2006). "Protein C anticoagulant activity in relation to anti-inflammatory and anti-apoptotic activities." Frontiers in bioscience : a journal and virtual library **11**: 2381-2399.
- Mosnier, L. O., B. V. Zlokovic, et al. (2007). "The cytoprotective protein C pathway." Blood **109**(8): 3161-3172.
- Mouillet-Richard, S., M. Ermonval, et al. (2000). "Signal transduction through prion protein." Science **289**(5486): 1925-1928.
- Mukherjee, K., E. Conway de Macario, et al. (2010). "Chaperonin genes on the rise: new divergent classes and intense duplication in human and other vertebrate genomes." BMC evolutionary biology **10**: 64.
- Mukhopadhyay, C. K., Z. K. Attieh, et al. (1998). "Role of ceruloplasmin in cellular iron uptake." Science **279**(5351): 714-717.
- Munoz, S., B. Rivas-Santiago, et al. (2009). "Mycobacterium tuberculosis entry into mast cells through cholesterol-rich membrane microdomains." Scandinavian journal of immunology **70**(3): 256-263.

- Murata, S., Y. Minami, et al. (2001). "CHIP is a chaperone-dependent E3 ligase that ubiquitylates unfolded protein." EMBO reports **2**(12): 1133-1138.
- Murayama, Y., M. Yoshioka, et al. (2007). "Efficient in vitro amplification of a mouse-adapted scrapie prion protein." Neurosci Lett **413**(3): 270-273.
- Musinova, Y. R., O. M. Lisitsyna, et al. (2011). "Nucleolar localization/retention signal is responsible for transient accumulation of histone H2B in the nucleolus through electrostatic interactions." Biochimica et biophysica acta **1813**(1): 27-38.
- Nair, U. and D. J. Klionsky (2005). "Molecular mechanisms and regulation of specific and nonspecific autophagy pathways in yeast." J Biol Chem **280**(51): 41785-41788.
- Nakatogawa, H., Y. Ichimura, et al. (2007). "Atg8, a ubiquitin-like protein required for autophagosome formation, mediates membrane tethering and hemifusion." Cell **130**(1): 165-178.
- Narindrasorasak, S., D. E. Lowery, et al. (1992). "Characterization of high affinity binding between laminin and Alzheimer's disease amyloid precursor proteins." Laboratory investigation; a journal of technical methods and pathology **67**(5): 643-652.
- Nazor, K. E., F. Kuhn, et al. (2005). "Immunodetection of disease-associated mutant PrP, which accelerates disease in GSS transgenic mice." The EMBO journal **24**(13): 2472-2480.
- Negro, A., F. Meggio, et al. (2000). "Susceptibility of the prion protein to enzymic phosphorylation." Biochem Biophys Res Commun **271**(2): 337-341.
- Nichols, T. A., B. Pulford, et al. (2009). "Detection of protease-resistant cervid prion protein in water from a CWD-endemic area." Prion **3**(3): 171-183.
- Nicholson, E. M., B. W. Brunelle, et al. (2008). "Identification of a heritable polymorphism in bovine PRNP associated with genetic transmissible spongiform encephalopathy: evidence of heritable BSE." PLoS One **3**(8): e2912.
- Nico, P. B., F. de-Paris, et al. (2005). "Altered behavioural response to acute stress in mice lacking cellular prion protein." Behavioural brain research **162**(2): 173-181.
- Nielsen, P. J. (1991). "Primary structure of a human protein kinase regulator protein." Biochimica et biophysica acta **1088**(3): 425-428.
- Nieznanski, K. (2010). "Interactions of prion protein with intracellular proteins: so many partners and no consequences?" Cell Mol Neurobiol **30**(5): 653-666.

- Nieznanski, K., H. Nieznanska, et al. (2005). "Direct interaction between prion protein and tubulin." Biochem Biophys Res Commun **334**(2): 403-411.
- Nieznanski, K., Z. A. Podlubnaya, et al. (2006). "Prion protein inhibits microtubule assembly by inducing tubulin oligomerization." Biochem Biophys Res Commun **349**(1): 391-399.
- Nikles, D., K. Vana, et al. (2008). "Subcellular localization of prion proteins and the 37 kDa/67 kDa laminin receptor fused to fluorescent proteins." Biochim Biophys Acta **1782**(5): 335-340.
- Nishida, N., D. A. Harris, et al. (2000). "Successful transmission of three mouse-adapted scrapie strains to murine neuroblastoma cell lines overexpressing wild-type mouse prion protein." J Virol **74**(1): 320-325.
- Nishida, N., S. Katamine, et al. (2005). "Reciprocal interference between specific CJD and scrapie agents in neural cell cultures." Science **310**(5747): 493-496.
- Nixon, R. A., J. Wegiel, et al. (2005). "Extensive involvement of autophagy in Alzheimer disease: an immuno-electron microscopy study." Journal of neuropathology and experimental neurology **64**(2): 113-122.
- Nollet, F., P. Kools, et al. (2000). "Phylogenetic analysis of the cadherin superfamily allows identification of six major subfamilies besides several solitary members." Journal of molecular biology **299**(3): 551-572.
- Novakofski, J., M. S. Brewer, et al. (2005). "Prion biology relevant to bovine spongiform encephalopathy." Journal of animal science **83**(6): 1455-1476.
- Nunziante, M., K. Ackermann, et al. (2011). "Proteasomal dysfunction and endoplasmic reticulum stress enhance trafficking of prion protein aggregates through the secretory pathway and increase accumulation of pathologic prion protein." J Biol Chem **286**(39): 33942-33953.
- Nuutinen, T., T. Suuronen, et al. (2009). "Clusterin: a forgotten player in Alzheimer's disease." Brain research reviews **61**(2): 89-104.
- Oesch, B., D. B. Teplow, et al. (1990). "Identification of cellular proteins binding to the scrapie prion protein." Biochemistry **29**(24): 5848-5855.
- Oesch, B., D. Westaway, et al. (1985). "A cellular gene encodes scrapie PrP 27-30 protein." Cell **40**: 735-746.
- Ohsumi, Y. (2001). "Molecular dissection of autophagy: two ubiquitin-like systems." Nature reviews. Molecular cell biology **2**(3): 211-216.

- Ohsumi, Y. and N. Mizushima (2004). "Two ubiquitin-like conjugation systems essential for autophagy." Seminars in cell & developmental biology **15**(2): 231-236.
- Oleksiak, M. F., G. A. Churchill, et al. (2002). "Variation in gene expression within and among natural populations." Nature genetics **32**(2): 261-266.
- Olivieri, S., A. Conti, et al. (2011). "Cerulein oxidation, a feature of Parkinson's disease CSF, inhibits ferroxidase activity and promotes cellular iron retention." The Journal of neuroscience : the official journal of the Society for Neuroscience **31**(50): 18568-18577.
- Orge, L., A. Galo, et al. (2004). "Identification of putative atypical scrapie in sheep in Portugal." J Gen Virol **85**(Pt 11): 3487-3491.
- Orru, C. D., J. M. Wilham, et al. (2009). "Human variant Creutzfeldt-Jakob disease and sheep scrapie PrP(res) detection using seeded conversion of recombinant prion protein." Protein engineering, design & selection : PEDS **22**(8): 515-521.
- Ortel, T. L., N. Takahashi, et al. (1984). "Structural model of human ceruloplasmin based on internal triplication, hydrophilic/hydrophobic character, and secondary structure of domains." Proceedings of the National Academy of Sciences of the United States of America **81**(15): 4761-4765.
- Osiecka, K. M., H. Nieznanska, et al. (2009). "Prion protein region 23-32 interacts with tubulin and inhibits microtubule assembly." Proteins **77**(2): 279-296.
- Ota, T., Y. Suzuki, et al. (2004). "Complete sequencing and characterization of 21,243 full-length human cDNAs." Nature genetics **36**(1): 40-45.
- Ott, D. E. (1997). "Cellular proteins in HIV virions." Reviews in medical virology **7**(3): 167-180.
- Outeiro, T. F. and A. Kazantsev (2008). "Drug Targeting of alpha-Synuclein Oligomerization in Synucleinopathies." Perspectives in medicinal chemistry **2**: 41-49.
- Outeiro, T. F., P. Putcha, et al. (2008). "Formation of toxic oligomeric alpha-synuclein species in living cells." PLoS One **3**(4): e1867.
- Pan, T., B. S. Wong, et al. (2002). "Cell-surface prion protein interacts with glycosaminoglycans." Biochem J **368**(Pt 1): 81-90.
- Panelli, S., F. Strozzi, et al. (2011). "Analysis of gene expression in white blood cells of cattle orally challenged with bovine amyloidotic spongiform encephalopathy." Journal of toxicology and environmental health. Part A **74**(2-4): 96-102.

- Panigaj, M., A. Brouckova, et al. (2010). "Underestimation of the expression of cellular prion protein on human red blood cells." Transfusion.
- Paquet, S., N. Daude, et al. (2007). "PrP^c does not mediate internalization of PrP^{Sc} but is required at an early stage for de novo prion infection of RoV cells." J Virol **81**(19): 10786-10791.
- Paquet, S., E. Sabuncu, et al. (2004). "Prion infection of epithelial RoV cells is a polarized event." J Virol **78**(13): 7148-7152.
- Parkin, E. T., N. T. Watt, et al. (2007). "Cellular prion protein regulates beta-secretase cleavage of the Alzheimer's amyloid precursor protein." Proceedings of the National Academy of Sciences of the United States of America **104**(26): 11062-11067.
- Parkin, E. T., N. T. Watt, et al. (2004). "Dual mechanisms for shedding of the cellular prion protein." J Biol Chem **279**(12): 11170-11178.
- Patnaik, A., V. Chau, et al. (2000). "Ubiquitin is part of the retrovirus budding machinery." Proceedings of the National Academy of Sciences of the United States of America **97**(24): 13069-13074.
- Pattison, I. H. (1965). Experiments with scrapie with special reference to the nature of the agent and the pathology of the disease. Slow, Latent and Temperate Virus Infections, NINDB Monograph 2. D. C. Gajdusek, C. J. Gibbs, Jr. and M. P. Alpers. Washington, D.C., U.S. Government Printing: 249-257.
- Pattison, I. H. and G. C. Millson (1961). "Further experimental observations on scrapie." J. Comp. Pathol. **71**: 350-359.
- Pattison, I. H. and G. C. Millson (1961). "Scrapie produced experimentally in goats with special reference to the clinical syndrome." J. Comp. Pathol. **71**: 101-108.
- Pauly, P. C. and D. A. Harris (1998). "Copper stimulates endocytosis of the prion protein." J. Biol. Chem. **273**: 33107-33110.
- Pauly, P. C. and D. A. Harris (1998). "Copper stimulates endocytosis of the prion protein." J Biol Chem **273**(50): 33107-33110.
- Pearson, G. R., J. M. Wyatt, et al. (1992). "Feline spongiform encephalopathy: fibril and PrP studies." Vet. Rec. **131**: 307-310.
- Peden, A. H., M. W. Head, et al. (2004). "Preclinical vCJD after blood transfusion in a PRNP codon 129 heterozygous patient." Lancet **364**(9433): 527-529.

- Peel, A. L., R. V. Rao, et al. (2001). "Double-stranded RNA-dependent protein kinase, PKR, binds preferentially to Huntington's disease (HD) transcripts and is activated in HD tissue." Human molecular genetics **10**(15): 1531-1538.
- Pelchen-Matthews, A., G. Raposo, et al. (2004). "Endosomes, exosomes and Trojan viruses." Trends in microbiology **12**(7): 310-316.
- Peretz, D., M. R. Scott, et al. (2001). "Strain-specified relative conformational stability of the scrapie prion protein." Protein science : a publication of the Protein Society **10**(4): 854-863.
- Peters, P. J., A. Mironov, Jr., et al. (2003). "Trafficking of prion proteins through a caveolae-mediated endosomal pathway." J Cell Biol **162**(4): 703-717.
- Petersen, A., K. E. Larsen, et al. (2001). "Expanded CAG repeats in exon 1 of the Huntington's disease gene stimulate dopamine-mediated striatal neuron autophagy and degeneration." Human molecular genetics **10**(12): 1243-1254.
- Peterson, L. E. (2002). "CLUSFAVOR 5.0: hierarchical cluster and principal-component analysis of microarray-based transcriptional profiles." Genome biology **3**(7): SOFTWARE0002.
- Piro, J. R., B. T. Harris, et al. (2011). "In situ photodegradation of incorporated polyanion does not alter prion infectivity." PLoS Pathog **7**(2): e1002001.
- Pizarro-Cerda, J. and P. Cossart (2006). "Bacterial adhesion and entry into host cells." Cell **124**(4): 715-727.
- Polyakova, O., D. Dear, et al. (2009). "Proteolysis of prion protein by cathepsin S generates a soluble beta-structured intermediate oligomeric form, with potential implications for neurotoxic mechanisms." Eur Biophys J **38**(2): 209-218.
- Ponting, C. P. and L. Aravind (1997). "PAS: a multifunctional domain family comes to light." Current biology : CB **7**(11): R674-677.
- Potempa, J., W. Watorek, et al. (1986). "The inactivation of human plasma alpha 1-proteinase inhibitor by proteinases from *Staphylococcus aureus*." J Biol Chem **261**(30): 14330-14334.
- Priola, S. A., B. Caughey, et al. (1994). "Heterologous PrP molecules interfere with accumulation of protease-resistant PrP in scrapie-infected murine neuroblastoma cells." J. Virol. **68**: 4873-4878.
- Prusiner, S. B. (1982). "Novel proteinaceous infectious particles cause scrapie." Science **216**: 136-144.

- Prusiner, S. B., D. C. Bolton, et al. (1982). "Further purification and characterization of scrapie prions." Biochemistry **21**: 6942-6950.
- Prusiner, S. B., D. F. Groth, et al. (1984). "Purification and structural studies of a major scrapie prion protein." Cell **38**: 127-134.
- Prusiner, S. B., D. F. Groth, et al. (1980). "Gel electrophoresis and glass permeation chromatography of the hamster scrapie agent after enzymatic digestion and detergent extraction." Biochemistry **19**: 4892-4898.
- Pulford, B., N. Reim, et al. (2010). "Liposome-siRNA-peptide complexes cross the blood-brain barrier and significantly decrease PrP on neuronal cells and PrP in infected cell cultures." PLoS One **5**(6): e11085.
- Pushie, M. J., I. J. Pickering, et al. (2011). "Prion protein expression level alters regional copper, iron and zinc content in the mouse brain." Metallomics : integrated biometal science **3**(2): 206-214.
- Qi, M., R. Yang, et al. (2008). "Cyclophilin A-dependent restriction of human immunodeficiency virus type 1 capsid mutants for infection of nondividing cells." J Virol **82**(24): 12001-12008.
- Race, R. E., B. Caughey, et al. (1988). "Analyses of frequency of infection, specific infectivity, and prion protein biosynthesis in scrapie-infected neuroblastoma cell clones." J Virol **62**(8): 2845-2849.
- Race, R. E., B. Caughey, et al. (1988). "Analyses of frequency of infection, specific infectivity, and prion protein biosynthesis in scrapie-infected neuroblastoma cell clones." J. Virol. **62**: 2845-2849.
- Race, R. E., L. H. Fadness, et al. (1987). "Characterization of scrapie infection in mouse neuroblastoma cells." J. Gen. Virol. **68**: 1391-1399.
- Raeber, A. J., A. Sailer, et al. (1999). "Ectopic expression of prion protein (PrP) in T lymphocytes or hepatocytes of PrP knockout mice is insufficient to sustain prion replication." Proceedings of the National Academy of Sciences of the United States of America **96**(7): 3987-3992.
- Raeber, A. J., A. Sailer, et al. (1999). "Ectopic expression of prion protein (PrP) in T lymphocytes or hepatocytes of PrP knockout mice is insufficient to sustain prion replication." Proc. Natl. Acad. Sci. USA **96**(7): 3987-3992.
- Rajasekaran, S., S. Balla, et al. (2009). "Minimotif miner 2nd release: a database and web system for motif search." Nucleic acids research **37**(Database issue): D185-190.

- Rambold, A. S., M. Miesbauer, et al. (2006). "Association of Bcl-2 with misfolded prion protein is linked to the toxic potential of cytosolic PrP." Mol Biol Cell **17**(8): 3356-3368.
- Ramljak, S., A. R. Asif, et al. (2008). "Physiological role of the cellular prion protein (PrP^c): protein profiling study in two cell culture systems." J Proteome Res **7**(7): 2681-2695.
- Ravikumar, B., R. Duden, et al. (2002). "Aggregate-prone proteins with polyglutamine and polyalanine expansions are degraded by autophagy." Human molecular genetics **11**(9): 1107-1117.
- Raymond, G. J., E. A. Olsen, et al. (2006). "Inhibition of protease-resistant prion protein formation in a transformed deer cell line infected with chronic wasting disease." J Virol **80**(2): 596-604.
- Reggiori, F. and D. J. Klionsky (2002). "Autophagy in the eukaryotic cell." Eukaryotic cell **1**(1): 11-21.
- Reggiori, F. and D. J. Klionsky (2005). "Autophagosomes: biogenesis from scratch?" Current opinion in cell biology **17**(4): 415-422.
- Resenberger, U. K., K. F. Winklhofer, et al. (2011). "Cellular Prion Protein Mediates Toxic Signaling of Amyloid Beta." Neuro-degenerative diseases.
- Richt, J. A. and S. M. Hall (2008). "BSE case associated with prion protein gene mutation." PLoS Pathog **4**(9): e1000156.
- Rieger, R., F. Edenhofer, et al. (1997). "The human 37-kDa laminin receptor precursor interacts with the prion protein in eukaryotic cells." Nature medicine **3**(12): 1383-1388.
- Riek, R., S. Hornemann, et al. (1996). "NMR structure of the mouse prion protein domain PrP(121-321)." Nature **382**(6587): 180-182.
- Riemer, C., S. Neidhold, et al. (2004). "Gene expression profiling of scrapie-infected brain tissue." Biochemical and biophysical research communications **323**(2): 556-564.
- Riewald, M., R. J. Petrovan, et al. (2002). "Activation of endothelial cell protease activated receptor 1 by the protein C pathway." Science **296**(5574): 1880-1882.
- Robinson, M. M., W. J. Hadlow, et al. (1994). "Experimental infection of mink with bovine spongiform encephalopathy." J. Gen. Virol. **75**: 2151-2155.

- Rogers, M., F. Yehiely, et al. (1993). "Conversion of truncated and elongated prion proteins into the scrapie isoform in cultured cells." Proceedings of the National Academy of Sciences of the United States of America **90**(8): 3182-3186.
- Roucou, X., Q. Guo, et al. (2003). "Cytosolic prion protein is not toxic and protects against Bax-mediated cell death in human primary neurons." J Biol Chem **278**(42): 40877-40881.
- Rubenstein, R., R. I. Carp, et al. (1984). "In vitro replication of scrapie agent in a neuronal model: infection of PC12 cells." J. Gen. Virol. **65**: 2191-2198.
- Rutter, J., C. H. Michnoff, et al. (2001). "PAS kinase: an evolutionarily conserved PAS domain-regulated serine/threonine kinase." Proceedings of the National Academy of Sciences of the United States of America **98**(16): 8991-8996.
- Ryou, C., S. B. Prusiner, et al. (2003). "Cooperative binding of dominant-negative prion protein to kringle domains." J Mol Biol **329**(2): 323-333.
- Saborio, G. P., B. Permanne, et al. (2001). "Sensitive detection of pathological prion protein by cyclic amplification of protein misfolding." Nature **411**(6839): 810-813.
- Safar, J., F. E. Cohen, et al. (2000). "Quantitative traits of prion strains are enciphered in the conformation of the prion protein." Archives of virology. Supplementum(16): 227-235.
- Safar, J., H. Wille, et al. (1998). "Eight prion strains have PrP(Sc) molecules with different conformations." Nature medicine **4**(10): 1157-1165.
- Sailer, A., H. Bueler, et al. (1994). "No propagation of prions in mice devoid of PrP." Cell **77**(7): 967-968.
- Saito, A. and H. Sinohara (1993). "Rabbit plasma alpha-1-antiproteinase S-1: cloning, sequencing, expression, and proteinase inhibitory properties of recombinant protein." Journal of biochemistry **113**(4): 456-461.
- Salehi, A. H., S. Xanthoudakis, et al. (2002). "NRAGE, a p75 neurotrophin receptor-interacting protein, induces caspase activation and cell death through a JNK-dependent mitochondrial pathway." J Biol Chem **277**(50): 48043-48050.
- Salmona, M., R. Capobianco, et al. (2005). "Role of plasminogen in propagation of scrapie." J Virol **79**(17): 11225-11230.
- Sandberg, M. K., H. Al-Doujaily, et al. (2010). "Chronic wasting disease prions are not transmissible to transgenic mice overexpressing human prion protein." J Gen Virol **91**(Pt 10): 2651-2657.

- Santuccione, A., V. Sytnyk, et al. (2005). "Prion protein recruits its neuronal receptor NCAM to lipid rafts to activate p59^{fyn} and to enhance neurite outgrowth." The Journal of cell biology **169**(2): 341-354.
- Sarnataro, D., A. Caputo, et al. (2009). "Lipid rafts and clathrin cooperate in the internalization of PrP in epithelial FRT cells." PLoS One **4**(6): e5829.
- Satoh, J., S. Obayashi, et al. (2009). "Protein microarray analysis identifies human cellular prion protein interactors." Neuropathol Appl Neurobiol **35**(1): 16-35.
- Satoh, J., H. Onoue, et al. (2005). "The 14-3-3 protein forms a molecular complex with heat shock protein Hsp60 and cellular prion protein." J Neuropathol Exp Neurol **64**(10): 858-868.
- Satoh, J. and T. Yamamura (2004). "Gene expression profile following stable expression of the cellular prion protein." Cell Mol Neurobiol **24**(6): 793-814.
- Satoh, J. and T. Yamamura (2004). "Gene expression profile following stable expression of the cellular prion protein." Cellular and molecular neurobiology **24**(6): 793-814.
- Sauer, B. (1987). "Functional expression of the cre-lox site-specific recombination system in the yeast *Saccharomyces cerevisiae*." Molecular and cellular biology **7**(6): 2087-2096.
- Sayer, N. M., M. Cubin, et al. (2004). "Structural determinants of conformationally selective, prion-binding aptamers." J Biol Chem **279**(13): 13102-13109.
- Schaller, T., K. E. Ocwieja, et al. (2011). "HIV-1 Capsid-Cyclophilin Interactions Determine Nuclear Import Pathway, Integration Targeting and Replication Efficiency." PLoS pathogens **7**(12): e1002439.
- Schätzl, H. M., L. Laszlo, et al. (1997). "A hypothalamic neuronal cell line persistently infected with scrapie prions exhibits apoptosis." J. Virol. **71**: 8821-8831.
- Scherz-Shouval, R., E. Shvets, et al. (2007). "Reactive oxygen species are essential for autophagy and specifically regulate the activity of Atg4." The EMBO journal **26**(7): 1749-1760.
- Schlaefli, P., E. Bortner, et al. (2009). "The PAS-domain kinase PASKIN: a new sensor in energy homeostasis." Cellular and molecular life sciences : CMLS **66**(5): 876-883.
- Schmitt-Ulms, G., G. Legname, et al. (2001). "Binding of neural cell adhesion molecules (N-CAMs) to the cellular prion protein." Journal of molecular biology **314**(5): 1209-1225.

- Schmitt-Ulms, G., G. Legname, et al. (2001). "Binding of neural cell adhesion molecules (N-CAMs) to the cellular prion protein." J Mol Biol **314**(5): 1209-1225.
- Schneider, B., M. Pietri, et al. (2011). "Understanding the neurospecificity of Prion protein signaling." Front Biosci **16**: 169-186.
- Schrijvers, E. M., P. J. Koudstaal, et al. (2011). "Plasma clusterin and the risk of Alzheimer disease." JAMA : the journal of the American Medical Association **305**(13): 1322-1326.
- Schubert, U., D. E. Ott, et al. (2000). "Proteasome inhibition interferes with gag polyprotein processing, release, and maturation of HIV-1 and HIV-2." Proceedings of the National Academy of Sciences of the United States of America **97**(24): 13057-13062.
- Schurmann, B., B. Wiese, et al. (2011). "Association of the Alzheimer's disease clusterin risk allele with plasma clusterin concentration." Journal of Alzheimer's disease : JAD **25**(3): 421-424.
- Schwartz, G. J., A. M. Kittelberger, et al. (2000). "Cloning of rabbit Cct6 and the distribution of the Cct complex in mammalian tissues." Experimental nephrology **8**(3): 152-160.
- Scott, M., D. Foster, et al. (1989). "Transgenic mice expressing hamster prion protein produce species-specific scrapie infectivity and amyloid plaques." Cell **59**(5): 847-857.
- Scott, M., D. Groth, et al. (1993). "Propagation of prions with artificial properties in transgenic mice expressing chimeric PrP genes." Cell **73**: 979-988.
- Scott, M. R., R. Will, et al. (1999). "Compelling transgenic evidence for transmission of bovine spongiform encephalopathy prions to humans." Proc. Natl. Acad. Sci. USA **26**.
- Seidel, K., J. Vinet, et al. (2012). "The HSPB8-BAG3 chaperone complex is upregulated in astrocytes in the human brain affected by protein aggregation diseases." Neuropathology and applied neurobiology **38**(1): 39-53.
- Sekiya, S., F. Nishikawa, et al. (2005). "In vitro selection of RNA aptamers against cellular and abnormal isoform of mouse prion protein." Nucleic Acids Symp Ser (Oxf)(49): 361-362.
- Shi, Q. and X. P. Dong (2011). "(Ctm) PrP and ER stress: A neurotoxic mechanism of some special PrP mutants." Prion **5**(3).

- Shimura, H., D. Schwartz, et al. (2004). "CHIP-Hsc70 complex ubiquitinates phosphorylated tau and enhances cell survival." J Biol Chem **279**(6): 4869-4876.
- Shmakov, A. N., J. Bode, et al. (2000). "Diverse patterns of expression of the 67-kD laminin receptor in human small intestinal mucosa: potential binding sites for prion proteins?" J Pathol **191**(3): 318-322.
- Shmerling, D., I. Hegyi, et al. (1998). "Expression of amino-terminally truncated PrP in the mouse leading to ataxia and specific cerebellar lesions." Cell **93**(2): 203-214.
- Shorter, J. (2011). "The mammalian disaggregase machinery: Hsp110 synergizes with Hsp70 and Hsp40 to catalyze protein disaggregation and reactivation in a cell-free system." PLoS One **6**(10): e26319.
- Shorter, J. and S. Lindquist (2008). "Hsp104, Hsp70 and Hsp40 interplay regulates formation, growth and elimination of Sup35 prions." The EMBO journal **27**(20): 2712-2724.
- Shyng, S.-L., J. E. Heuser, et al. (1994). "A glycolipid-anchored prion protein is endocytosed via clathrin-coated pits." J. Cell Biol. **125**: 1239-1250.
- Shyng, S.-L., M. T. Huber, et al. (1993). "A prion protein cycles between the cell surface and an endocytic compartment in cultured neuroblastoma cells." J. Biol. Chem. **21**: 15922-15928.
- Shyng, S.-L., S. Lehmann, et al. (1995). "Sulfated glycans stimulate endocytosis of the cellular isoform of the prion protein, PrP^C, in cultured cells." J. Biol. Chem. **270**: 30221-30229.
- Shyng, S. L., J. E. Heuser, et al. (1994). "A glycolipid-anchored prion protein is endocytosed via clathrin-coated pits." The Journal of cell biology **125**(6): 1239-1250.
- Shyng, S. L., M. T. Huber, et al. (1993). "A prion protein cycles between the cell surface and an endocytic compartment in cultured neuroblastoma cells." J Biol Chem **268**(21): 15922-15928.
- Shyng, S. L., K. L. Moulder, et al. (1995). "The N-terminal domain of a glycolipid-anchored prion protein is essential for its endocytosis via clathrin-coated pits." J Biol Chem **270**(24): 14793-14800.
- Shyu, W. C., H. J. Harn, et al. (2002). "Molecular modulation of expression of prion protein by heat shock." Mol Neurobiol **26**(1): 1-12.
- Silva, J. L., L. M. Lima, et al. (2008). "Intriguing nucleic-acid-binding features of mammalian prion protein." Trends Biochem Sci **33**(3): 132-140.

- Silva, J. L., T. C. Vieira, et al. (2011). "Experimental approaches to the interaction of the prion protein with nucleic acids and glycosaminoglycans: Modulators of the pathogenic conversion." Methods **53**(3): 306-317.
- Silveira, J. R., G. J. Raymond, et al. (2005). "The most infectious prion protein particles." Nature **437**(7056): 257-261.
- Silverstein, R. L., L. L. Leung, et al. (1984). "Complex formation of platelet thrombospondin with plasminogen. Modulation of activation by tissue activator." The Journal of clinical investigation **74**(5): 1625-1633.
- Simon, R. (2009). "Analysis of DNA microarray expression data." Best practice & research. Clinical haematology **22**(2): 271-282.
- Simonic, T., S. Duga, et al. (2000). "cDNA cloning of turtle prion protein." Febs Letters **469**(1): 33-38.
- Singh, A., Q. Kong, et al. (2009). "Prion protein (PrP) knock-out mice show altered iron metabolism: a functional role for PrP in iron uptake and transport." PLoS One **4**(7): e6115.
- Singh, A., M. L. Mohan, et al. (2009). "Prion protein modulates cellular iron uptake: a novel function with implications for prion disease pathogenesis." PLoS One **4**(2): e4468.
- Sivashankari, S. and P. Shanmughavel (2006). "Functional annotation of hypothetical proteins - A review." Bioinformatics **1**(8): 335-338.
- Skinner, P. J., H. Abbassi, et al. (2006). "Gene expression alterations in brains of mice infected with three strains of scrapie." BMC Genomics **7**: 114.
- Smyth, G. K., Y. H. Yang, et al. (2003). "Statistical issues in cDNA microarray data analysis." Methods in molecular biology **224**: 111-136.
- Snow, A. D., R. Kisilevsky, et al. (1989). "Sulfated glycosaminoglycans in amyloid plaques of prion diseases." Acta Neuropathol. **77**: 337-342.
- Solforosi, L., J. R. Criado, et al. (2004). "Cross-linking cellular prion protein triggers neuronal apoptosis in vivo." Science **303**(5663): 1514-1516.
- Solis, G. P., E. Malaga-Trillo, et al. (2010). "Cellular roles of the prion protein in association with reggie/flotillin microdomains." Front Biosci **15**: 1075-1085.
- Sorensen, G., S. Medina, et al. (2008). "Comprehensive transcriptional profiling of prion infection in mouse models reveals networks of responsive genes." BMC Genomics **9**: 114.

- Soto, C., L. Anderes, et al. (2005). "Pre-symptomatic detection of prions by cyclic amplification of protein misfolding." FEBS letters **579**(3): 638-642.
- Sparkes, R. S., M. Simon, et al. (1986). "Assignment of the human and mouse prion protein genes to homologous chromosomes." Proceedings of the National Academy of Sciences of the United States of America **83**(19): 7358-7362.
- Spielhauser, C. and H. M. Schatzl (2001). "PrPC directly interacts with proteins involved in signaling pathways." J Biol Chem **276**(48): 44604-44612.
- Squitti, R., C. C. Quattrocchi, et al. (2007). "Ceruloplasmin (2-D PAGE) Pattern and Copper Content in Serum and Brain of Alzheimer Disease Patients." Biomarker insights **1**: 205-213.
- Squitti, R., C. C. Quattrocchi, et al. (2008). "Ceruloplasmin fragmentation is implicated in 'free' copper deregulation of Alzheimer's disease." Prion **2**(1): 23-27.
- Stahl, N., D. R. Borchelt, et al. (1987). "Scrapie prion protein contains a phosphatidylinositol glycolipid." Cell **51**: 229-240.
- Stahl, N., D. R. Borchelt, et al. (1990). "Differential release of cellular and scrapie prion proteins from cellular membranes by phosphatidylinositol-specific phospholipase C." Biochemistry **29**(22): 5405-5412.
- Staubach, S. and F. G. Hanisch (2011). "Lipid rafts: signaling and sorting platforms of cells and their roles in cancer." Expert review of proteomics **8**(2): 263-277.
- Stefanova, I., V. Horejsi, et al. (1991). "GPI-anchored cell-surface molecules complexed to protein tyrosine kinases." Science **254**(5034): 1016-1019.
- Stellato, F., A. Spevacek, et al. (2011). "Zinc modulates copper coordination mode in prion protein octa-repeat subdomains." European biophysics journal : EBJ **40**(11): 1259-1270.
- Stewart, R. S., B. Drisaldi, et al. (2001). "A transmembrane form of the prion protein contains an uncleaved signal peptide and is retained in the endoplasmic Reticulum." Molecular biology of the cell **12**(4): 881-889.
- Stewart, R. S. and D. A. Harris (2005). "A transmembrane form of the prion protein is localized in the Golgi apparatus of neurons." J Biol Chem **280**(16): 15855-15864.
- Stewart, R. S., P. Piccardo, et al. (2005). "Neurodegenerative illness in transgenic mice expressing a transmembrane form of the prion protein." The Journal of neuroscience : the official journal of the Society for Neuroscience **25**(13): 3469-3477.

- Stockel, J. and F. U. Hartl (2001). "Chaperonin-mediated de novo generation of prion protein aggregates." J Mol Biol **313**(4): 861-872.
- Stockel, J., J. Safar, et al. (1998). "Prion protein selectively binds copper(II) ions." Biochemistry **37**(20): 7185-7193.
- Stover, C. M., N. J. Lynch, et al. (2003). "Murine serine proteases MASP-1 and MASP-3, components of the lectin pathway activation complex of complement, are encoded by a single structural gene." Genes and immunity **4**(5): 374-384.
- Strack, B., A. Calistri, et al. (2000). "A role for ubiquitin ligase recruitment in retrovirus release." Proceedings of the National Academy of Sciences of the United States of America **97**(24): 13063-13068.
- Strom, A., S. Diecke, et al. (2006). "Identification of prion protein binding proteins by combined use of far-Western immunoblotting, two dimensional gel electrophoresis and mass spectrometry." Proteomics **6**(1): 26-34.
- Strumbo, B., S. Ronchi, et al. (2001). "Molecular cloning of the cDNA coding for *Xenopus laevis* prion protein." Febs Letters **508**(2): 170-174.
- Suazo, M., F. Olivares, et al. (2008). "CCS and SOD1 mRNA are reduced after copper supplementation in peripheral mononuclear cells of individuals with high serum ceruloplasmin concentration." The Journal of nutritional biochemistry **19**(4): 269-274.
- Sugaya, M., K. Nakamura, et al. (2002). "Expression of cellular prion-related protein by murine Langerhans cells and keratinocytes." J Dermatol Sci **28**(2): 126-134.
- Sun, G., M. Guo, et al. (2005). "Bovine PrPC directly interacts with alphaB-crystalline." FEBS letters **579**(24): 5419-5424.
- Sunkesula, S. R., X. Luo, et al. (2010). "Iron content of ferritin modulates its uptake by intestinal epithelium: implications for co-transport of prions." Molecular brain **3**: 14.
- Sunyach, C., A. Jen, et al. (2003). "The mechanism of internalization of glycosylphosphatidylinositol-anchored prion protein." Embo J **22**(14): 3591-3601.
- Supattapone, S., N. R. Deleault, et al. (2008). "Amplification of purified prions in vitro." Methods in molecular biology **459**: 117-130.
- Szelesi, P. B. (1992). "The aspartic proteases." Scandinavian journal of clinical and laboratory investigation. Supplementum **210**: 5-22.

- Takahashi, H., T. Iwata, et al. (1999). "Increased levels of epsilon and gamma isoforms of 14-3-3 proteins in cerebrospinal fluid in patients with Creutzfeldt-Jakob disease." Clinical and diagnostic laboratory immunology **6**(6): 983-985.
- Takayama, S. and J. C. Reed (2001). "Molecular chaperone targeting and regulation by BAG family proteins." Nature cell biology **3**(10): E237-241.
- Tam, S., R. Geller, et al. (2006). "The chaperonin TRiC controls polyglutamine aggregation and toxicity through subunit-specific interactions." Nature cell biology **8**(10): 1155-1162.
- Tamguney, G., K. Giles, et al. (2006). "Transmission of elk and deer prions to transgenic mice." J Virol **80**(18): 9104-9114.
- Tanaka, M., S. R. Collins, et al. (2006). "The physical basis of how prion conformations determine strain phenotypes." Nature **442**(7102): 585-589.
- Taraboulos, A., A. J. Raeber, et al. (1992). "Synthesis and trafficking of prion proteins in cultured cells." Molecular biology of the cell **3**(8): 851-863.
- Taraboulos, A., A. J. Raeber, et al. (1992). "Synthesis and trafficking of prion proteins in cultured cells." Mol. Biol. Cell **3**: 851-863.
- Taraboulos, A., A. J. Raeber, et al. (1992). "Synthesis and trafficking of prion proteins in cultured cells." Mol Biol Cell **3**(8): 851-863.
- Taraboulos, A., D. Serban, et al. (1990). "Scrapie prion proteins accumulate in the cytoplasm of persistently infected cultured cells." J. Cell Biol. **110**: 2117-2132.
- Tashiro, K., G. C. Sephel, et al. (1989). "A synthetic peptide containing the IKVAV sequence from the A chain of laminin mediates cell attachment, migration, and neurite outgrowth." J Biol Chem **264**(27): 16174-16182.
- Taylor, D. R. and N. M. Hooper (2007). "The low-density lipoprotein receptor-related protein 1 (LRP1) mediates the endocytosis of the cellular prion protein." The Biochemical journal **402**(1): 17-23.
- Taylor, D. R., E. T. Parkin, et al. (2009). "Role of ADAMs in the ectodomain shedding and conformational conversion of the prion protein." J Biol Chem **284**(34): 22590-22600.
- Taylor, D. R., I. J. Whitehouse, et al. (2009). "Glypican-1 mediates both prion protein lipid raft association and disease isoform formation." PLoS Pathog **5**(11): e1000666.

- Telling, G. C. (2011). "Transgenic mouse models and prion strains." Topics in current chemistry **305**: 79-99.
- Telling, G. C., T. Haga, et al. (1996). "Interactions between wild-type and mutant prion proteins modulate neurodegeneration in transgenic mice." Genes & development **10**(14): 1736-1750.
- Telling, G. C., P. Parchi, et al. (1996). "Evidence for the conformation of the pathologic isoform of the prion protein enciphering and propagating prion diversity." Science **274**(5295): 2079-2082.
- Telling, G. C., M. Scott, et al. (1994). "Transmission of Creutzfeldt-Jakob disease from humans to transgenic mice expressing chimeric human-mouse prion protein." Proceedings of the National Academy of Sciences of the United States of America **91**(21): 9936-9940.
- Telling, G. C., M. Scott, et al. (1995). "Prion propagation in mice expressing human and chimeric PrP transgenes implicates the interaction of cellular PrP with another protein." Cell **83**(1): 79-90.
- Teuling, E., A. Bourgonje, et al. (2011). "Modifiers of mutant huntingtin aggregation: functional conservation of C. elegans-modifiers of polyglutamine aggregation." PLoS currents **3**: RRN1255.
- Texel, S. J., X. Xu, et al. (2008). "Ceruloplasmin in neurodegenerative diseases." Biochemical Society transactions **36**(Pt 6): 1277-1281.
- Thambisetty, M., Y. An, et al. (2012). "Plasma clusterin concentration is associated with longitudinal brain atrophy in mild cognitive impairment." Neuroimage **59**(1): 212-217.
- Thambisetty, M., A. Simmons, et al. (2010). "Association of plasma clusterin concentration with severity, pathology, and progression in Alzheimer disease." Archives of general psychiatry **67**(7): 739-748.
- Thorne, L. and L. A. Terry (2008). "In vitro amplification of PrPSc derived from the brain and blood of sheep infected with scrapie." J Gen Virol **89**(Pt 12): 3177-3184.
- Tobler, I., T. Deboer, et al. (1997). "Sleep and sleep regulation in normal and prion protein-deficient mice." The Journal of neuroscience : the official journal of the Society for Neuroscience **17**(5): 1869-1879.
- Tobler, I., S. E. Gaus, et al. (1996). "Altered circadian activity rhythms and sleep in mice devoid of prion protein." Nature **380**(6575): 639-642.

- Tofoleanu, F. and N. V. Buchete (2012). "Molecular Interactions of Alzheimer's Abeta Protofilaments with Lipid Membranes." Journal of molecular biology.
- Tomaselli, K. J. and L. F. Reichardt (1988). "Peripheral motoneuron interactions with laminin and Schwann cell-derived neurite-promoting molecules: developmental regulation of laminin receptor function." Journal of neuroscience research **21**(2-4): 275-285.
- Tomoo, K., T. M. Yao, et al. (2005). "Possible role of each repeat structure of the microtubule-binding domain of the tau protein in in vitro aggregation." Journal of biochemistry **138**(4): 413-423.
- Tomsig, J. L. and C. E. Creutz (2002). "Copines: a ubiquitous family of Ca(2+)-dependent phospholipid-binding proteins." Cellular and molecular life sciences : CMLS **59**(9): 1467-1477.
- Torsdottir, G., J. Kristinsson, et al. (2010). "Case-control studies on ceruloplasmin and superoxide dismutase (SOD1) in neurodegenerative diseases: a short review." Journal of the neurological sciences **299**(1-2): 51-54.
- Travis, J. and G. Salvesen (1983). "Control of coagulation and fibrinolysis by plasma proteinase inhibitors." Behring Institute Mitteilungen(73): 56-65.
- Treuheit, M. J., C. E. Costello, et al. (1992). "Analysis of the five glycosylation sites of human alpha 1-acid glycoprotein." The Biochemical journal **283** (Pt 1): 105-112.
- Trougakos, I. P., M. Lourda, et al. (2009). "Intracellular clusterin inhibits mitochondrial apoptosis by suppressing p53-activating stress signals and stabilizing the cytosolic Ku70-Bax protein complex." Clinical cancer research : an official journal of the American Association for Cancer Research **15**(1): 48-59.
- Turk, E., D. B. Teplow, et al. (1988). "Purification and properties of the cellular and scrapie hamster prion proteins." European journal of biochemistry / FEBS **176**(1): 21-30.
- Turner, A. J. and N. N. Nalivaeva (2007). "New insights into the roles of metalloproteinases in neurodegeneration and neuroprotection." International review of neurobiology **82**: 113-135.
- Tutar, Y., Y. Song, et al. (2006). "Primate chaperones Hsc70 (constitutive) and Hsp70 (induced) differ functionally in supporting growth and prion propagation in *Saccharomyces cerevisiae*." Genetics **172**(2): 851-861.
- van Keulen, L. J., A. Bossers, et al. (2008). "TSE pathogenesis in cattle and sheep." Veterinary research **39**(4): 24.

- Vana, K., C. Zuber, et al. (2007). "Novel aspects of prions, their receptor molecules, and innovative approaches for TSE therapy." Cellular and molecular neurobiology **27**(1): 107-128.
- Vana, K., C. Zuber, et al. (2009). "LRP/LR as an alternative promising target in therapy of prion diseases, Alzheimer's disease and cancer." Infectious disorders drug targets **9**(1): 69-80.
- Vana, K., C. Zuber, et al. (2009). "LRP/LR as an alternative promising target in therapy of prion diseases, Alzheimer's disease and cancer." Infect Disord Drug Targets **9**(1): 69-80.
- Vassiliev, V., Z. L. Harris, et al. (2005). "Ceruleplasmin in neurodegenerative diseases." Brain research. Brain research reviews **49**(3): 633-640.
- Vella, L. J., R. A. Sharples, et al. (2007). "Packaging of prions into exosomes is associated with a novel pathway of PrP processing." The Journal of pathology **211**(5): 582-590.
- Vey, M., S. Pilkuhn, et al. (1996). "Subcellular colocalization of the cellular and scrapie prion proteins in caveolae-like membranous domains." Proc Natl Acad Sci U S A **93**(25): 14945-14949.
- Vey, M., S. Pilkuhn, et al. (1996). "Subcellular colocalization of the cellular and scrapie prion proteins in caveolae-like membranous domains." Proceedings of the National Academy of Sciences of the United States of America **93**(25): 14945-14949.
- Vilette, D., O. Andreoletti, et al. (2001). "Ex vivo propagation of infectious sheep scrapie agent in heterologous epithelial cells expressing ovine prion protein." Proceedings of the National Academy of Sciences of the United States of America **98**(7): 4055-4059.
- Vilette, D., O. Andreoletti, et al. (2001). "Ex vivo propagation of infectious sheep scrapie agent in heterologous epithelial cells expressing ovine prion protein." Proc Natl Acad Sci U S A **98**(7): 4055-4059.
- Vincent, B., E. Paitel, et al. (2001). "The disintegrins ADAM10 and TACE contribute to the constitutive and phorbol ester-regulated normal cleavage of the cellular prion protein." J Biol Chem **276**(41): 37743-37746.
- Vinnik, L. F. and A. S. Lisitsyn (1993). "[The methodology for studying the health of servicemen]." Voenno-meditsinskii zhurnal(2): 9-12.
- Voisset, C., R. E. Myers, et al. (2003). "Rabbit endogenous retrovirus-H encodes a functional protease." J Gen Virol **84**(Pt 1): 215-225.

- Vorberg, I., A. Buschmann, et al. (1999). "A novel epitope for the specific detection of exogenous prion proteins in transgenic mice and transfected murine cell lines." Virology **255**(1): 26-31.
- Vorberg, I., A. Raines, et al. (2004). "Acute formation of protease-resistant prion protein does not always lead to persistent scrapie infection in vitro." J Biol Chem **279**(28): 29218-29225.
- Wadsworth, J. D., A. F. Hill, et al. (1999). "Strain-specific prion-protein conformation determined by metal ions." Nature cell biology **1**(1): 55-59.
- Wadsworth, J. D., A. F. Hill, et al. (1999). "Strain-specific prion-protein conformation determined by metal ions." Nat Cell Biol **1**(1): 55-59.
- Walkley, N. A., A. G. Demaine, et al. (1996). "Cloning, structure and mRNA expression of human Cctg, which encodes the chaperonin subunit CCT gamma." The Biochemical journal **313** (Pt 2): 381-389.
- Wang, F., X. Wang, et al. (2010). "Generating a prion with bacterially expressed recombinant prion protein." Science **327**(5969): 1132-1135.
- Wang, G. H., X. M. Zhou, et al. (2011). "Hsp70 binds to PrPC in the process of PrPC release via exosomes from THP-1 monocytes." Cell biology international **35**(6): 553-558.
- Wang, X. F., C. F. Dong, et al. (2008). "Human tau protein forms complex with PrP and some GSS- and fCJD-related PrP mutants possess stronger binding activities with tau in vitro." Molecular and cellular biochemistry **310**(1-2): 49-55.
- Weiss, S., D. Proske, et al. (1997). "RNA aptamers specifically interact with the prion protein PrP." J Virol **71**(11): 8790-8797.
- Weissmann, C. (1991). "A 'unified theory' of prion propagation." Nature **352**(6337): 679-683.
- Weissmann, C., M. Fischer, et al. (1998). "The use of transgenic mice in the investigation of transmissible spongiform encephalopathies." Revue scientifique et technique **17**(1): 278-290.
- Wells, G. A., A. C. Scott, et al. (1987). "A novel progressive spongiform encephalopathy in cattle." The Veterinary record **121**(18): 419-420.
- Westaway, D., P. A. Goodman, et al. (1987). "Distinct prion proteins in short and long scrapie incubation period mice." Cell **51**: 651-662.

- Westaway, D., C. A. Mirenda, et al. (1991). "Paradoxical shortening of scrapie incubation times by expression of prion protein transgenes derived from long incubation period mice." Neuron **7**: 59-68.
- Westaway, D., C. A. Mirenda, et al. (1991). "Paradoxical shortening of scrapie incubation times by expression of prion protein transgenes derived from long incubation period mice." Neuron **7**(1): 59-68.
- Westaway, D. and S. B. Prusiner (1986). "Conservation of the cellular gene encoding the scrapie prion protein." Nucleic Acids Res **14**(5): 2035-2044.
- Westaway, D., V. Zuliani, et al. (1994). "Homozygosity for prion protein alleles encoding glutamine-171 renders sheep susceptible to natural scrapie." Genes Dev. **8**: 959-969.
- Westhoff, B., J. P. Chapple, et al. (2005). "HSJ1 is a neuronal shuttling factor for the sorting of chaperone clients to the proteasome." Current biology : CB **15**(11): 1058-1064.
- Wietgreffe, S., M. Zupancic, et al. (1985). "Cloning of a gene whose expression is increased in scrapie and in senile plaques in human brain." Science **230**(4730): 1177-1179.
- Wilham, J. M., C. D. Orru, et al. (2010). "Rapid end-point quantitation of prion seeding activity with sensitivity comparable to bioassays." PLoS Pathog **6**(12): e1001217.
- Wilhelmus, M. M., W. C. Boelens, et al. (2006). "Small heat shock protein HspB8: its distribution in Alzheimer's disease brains and its inhibition of amyloid-beta protein aggregation and cerebrovascular amyloid-beta toxicity." Acta Neuropathol (Berl) **111**(2): 139-149.
- Wilkins, S., A. A. Choglay, et al. (2010). "The binding of the molecular chaperone Hsc70 to the prion protein PrP is modulated by pH and copper." Int J Biochem Cell Biol **42**(7): 1226-1232.
- Williams, E. S. and S. Young (1980). "Chronic wasting disease of captive mule deer: a spongiform encephalopathy." Journal of wildlife diseases **16**(1): 89-98.
- Wilson, D. R., R. D. Anderson, et al. (1950). "Studies in scrapie." J. Comp. Pathol. **60**: 267-282.
- Wlodawer, A. and A. Gustchina (2000). "Structural and biochemical studies of retroviral proteases." Biochimica et biophysica acta **1477**(1-2): 16-34.

- Wong, B. S., T. Liu, et al. (2001). "Increased levels of oxidative stress markers detected in the brains of mice devoid of prion protein." Journal of Neurochemistry **76**(2): 565-572.
- Wong, C., L. W. Xiong, et al. (2001). "Sulfated glycans and elevated temperature stimulate PrP(Sc)-dependent cell-free formation of protease-resistant prion protein." Embo J **20**(3): 377-386.
- Woolhouse, M. E., L. Matthews, et al. (1999). "Population dynamics of scrapie in a sheep flock." Philosophical transactions of the Royal Society of London. Series B, Biological sciences **354**(1384): 751-756.
- Wyatt, A. R. and M. R. Wilson (2010). "Identification of human plasma proteins as major clients for the extracellular chaperone clusterin." J Biol Chem **285**(6): 3532-3539.
- Wyatt, A. R., J. J. Yerbury, et al. (2011). "Clusterin facilitates in vivo clearance of extracellular misfolded proteins." Cellular and molecular life sciences : CMLS **68**(23): 3919-3931.
- Xiang, W., O. Windl, et al. (2005). "Cerebral gene expression profiles in sporadic Creutzfeldt-Jakob disease." Annals of neurology **58**(2): 242-257.
- Xiang, W., O. Windl, et al. (2004). "Identification of differentially expressed genes in scrapie-infected mouse brains by using global gene expression technology." Journal of virology **78**(20): 11051-11060.
- Xiao, B., S. J. Smerdon, et al. (1995). "Structure of a 14-3-3 protein and implications for coordination of multiple signalling pathways." Nature **376**(6536): 188-191.
- Xie, Z., U. Nair, et al. (2008). "Atg8 controls phagophore expansion during autophagosome formation." Molecular biology of the cell **19**(8): 3290-3298.
- Xie, Z., U. Nair, et al. (2008). "Dissecting autophagosome formation: the missing pieces." Autophagy **4**(7): 920-922.
- Xu, F., E. Karnaukhova, et al. (2008). "Human cellular prion protein interacts directly with clusterin protein." Biochim Biophys Acta **1782**(11): 615-620.
- Xu, W., M. Marcu, et al. (2002). "Chaperone-dependent E3 ubiquitin ligase CHIP mediates a degradative pathway for c-ErbB2/Neu." Proceedings of the National Academy of Sciences of the United States of America **99**(20): 12847-12852.
- Yadavalli, R., R. P. Guttman, et al. (2004). "Calpain-dependent endoproteolytic cleavage of PrPSc modulates scrapie prion propagation." J Biol Chem **279**(21): 21948-21956.

- Yagi, T. and M. Takeichi (2000). "Cadherin superfamily genes: functions, genomic organization, and neurologic diversity." Genes & development **14**(10): 1169-1180.
- Yedidia, Y., L. Horonchik, et al. (2001). "Proteasomes and ubiquitin are involved in the turnover of the wild-type prion protein." Embo J **20**(19): 5383-5391.
- Yehiely, F., P. Bamborough, et al. (1997). "Identification of candidate proteins binding to prion protein." Neurobiol. Dis. **3**: 339-355.
- Yerbury, J. J., S. Poon, et al. (2007). "The extracellular chaperone clusterin influences amyloid formation and toxicity by interacting with prefibrillar structures." FASEB journal : official publication of the Federation of American Societies for Experimental Biology **21**(10): 2312-2322.
- Yorimitsu, T. and D. J. Klionsky (2005). "Autophagy: molecular machinery for self-eating." Cell death and differentiation **12 Suppl 2**: 1542-1552.
- Yost, C. S., C. D. Lopez, et al. (1990). "Non-hydrophobic extracytoplasmic determinant of stop transfer in the prion protein." Nature **343**(6259): 669-672.
- Younan, N. D., M. Klewpatinond, et al. (2011). "Copper(II)-induced secondary structure changes and reduced folding stability of the prion protein." Journal of molecular biology **410**(3): 369-382.
- Yu, W. H., A. M. Cuervo, et al. (2005). "Macroautophagy--a novel Beta-amyloid peptide-generating pathway activated in Alzheimer's disease." The Journal of cell biology **171**(1): 87-98.
- Yu, X. F., Z. Matsuda, et al. (1995). "Role of the C terminus Gag protein in human immunodeficiency virus type 1 virion assembly and maturation." J Gen Virol **76 (Pt 12)**: 3171-3179.
- Zafar, S., N. von Ahsen, et al. (2011). "Proteomics approach to identify the interacting partners of cellular prion protein and characterization of Rab7a interaction in neuronal cells." Journal of proteome research **10**(7): 3123-3135.
- Zanata, S. M., M. H. Lopes, et al. (2002). "Stress-inducible protein 1 is a cell surface ligand for cellular prion that triggers neuroprotection." Embo J **21**(13): 3307-3316.
- Zeng, L., Z. Zhou, et al. (2001). "Molecular cloning, structure and expression of a novel nuclear RNA-binding cyclophilin-like gene (PPIL4) from human fetal brain." Cytogenetics and cell genetics **95**(1-2): 43-47.

- Zhanataev, A. K., T. A. Lisitsyna, et al. (2009). "Effect of afobazole on DNA damage in patients with systemic lupus erythematosus." Bulletin of experimental biology and medicine **148**(4): 602-605.
- Zhang, H., J. K. Kim, et al. (2005). "Clusterin inhibits apoptosis by interacting with activated Bax." Nature cell biology **7**(9): 909-915.
- Zhang, H., Q. Ma, et al. (2011). "Proteolytic processing of Alzheimer's beta-amyloid precursor protein." Journal of Neurochemistry.
- Zhang, Y., E. Spiess, et al. (2003). "Up-regulation of cathepsin B and cathepsin L activities in scrapie-infected mouse Neuro2a cells." J Gen Virol **84**(Pt 8): 2279-2283.
- Zhu, F., P. Davies, et al. (2008). "Raman optical activity and circular dichroism reveal dramatic differences in the influence of divalent copper and manganese ions on prion protein folding." Biochemistry **47**(8): 2510-2517.
- Zuber, C., S. Knackmuss, et al. (2008). "Single chain Fv antibodies directed against the 37 kDa/67 kDa laminin receptor as therapeutic tools in prion diseases." Mol Immunol **45**(1): 144-151.
- Zuber, C., G. Mitteregger, et al. (2008). "Delivery of single-chain antibodies (scFvs) directed against the 37/67 kDa laminin receptor into mice via recombinant adeno-associated viral vectors for prion disease gene therapy." J Gen Virol **89**(Pt 8): 2055-2061.
- Zwanzig, R., A. Szabo, et al. (1992). "Levinthal's paradox." Proceedings of the National Academy of Sciences of the United States of America **89**(1): 20-22.

Vita
Vadim Khaychuk

Date and Place of Birth

July 28, 1982 Kiev, Ukraine

Education

Undergraduate

Rochester Institute of Technology (RIT), BS in Biotechnology, May 2005

Graduate

University of Rochester School of Medicine and Dentistry, Rochester, New York
2nd year student in the Interdepartmental Graduate Program in Microbiology and Immunology

University of Kentucky, College of Medicine, Lexington, Kentucky
Microbiology, Immunology and Molecular Genetics Graduate Program

Language

Fluent in the English and Russian language

Grant Funding

NIH Training Grant 1T32 DA022738: “*Therapeutic Strategies for Neurodegeneration*”

Honors and Awards

Dean’s List, Rochester Institute of Technology, Fall 2001 – Spring 2003
GEBS Summer Scholar at University of Rochester, Summer 2004

Scientific & Educational Activities

September 2006 – Present Member of Immunology Seminar committee

September 2005 – Present Immunology Journal Club, University of Rochester,
Department of Microbiology and Immunology

Publications

Charles E. Mays, Jihyun Yeom, Hae-Eun Kang, Jifeng Bian, **Vadim Khaychuk**, Younghwan Kim, Jason C. Bartz, Glenn C. Telling, Chongsuk Ryou. *In Vitro* Amplification of Misfolded Prion Protein Using Lysate of Cultured Cells. *PloS one*, 6(3): e18047 2011

Bian, Jifeng, Dana Napier, **Vadim Khaychuk**, Catherine Graham and Glenn Telling. Cell-Based Quantification of Chronic Wasting Disease Prions. *J. Virol.*, 84 (16): 8322-8326. Epub, Jun 2, 2010

Poster Presentations

Khaychuk, Vadim, Jifeng Bian, Dana Napier, Rachel Angers, Catherine Graham and Glenn Telling. Cell-Based Quantification of Chronic Wasting Disease Prions. PRION 2010 Salzburg, Austria, September 2010

Khaychuk, Vadim, Wuertzer, Charles A. Sullivan, Mark and Federoff, Howard J. Immuno-Therapeutics for Transmissible Spongiform Encephalopathies (TSE). Department of Aging and Developmental Biology, University of Rochester Medical Center, Rochester, NY14642, United States.

Khaychuk, Vadim, Gantress, Jennifer, Guselnikov, Sergei V, Taranin Alexander V and Robert, Jacques. Expression of FCR-Like Genes during Metamorphosis of the Amphibian *Xenopus*. Eastern Great Lakes Molecular Evolution Meeting, University of Toronto 2005.